

8623

Structure-function Studies on Successive Purine Salvage Pathway Enzymes - Hypoxanthine Guanine Phosphoribosyltransferase and Adenylosuccinate Synthetase

JNCASR
572.7 P04



A Thesis Submitted for the Award of the Degree of
Doctor of Philosophy

By
R. Jayalakshmi



**Molecular Biology and Genetics Unit
Jawaharlal Nehru Centre for Advanced Scientific Research
(A Deemed University)
Bangalore - 560064
INDIA
January, 2004**

Declaration

I hereby declare that this thesis entitled “Structure-function studies on successive purine salvage pathway enzymes - hypoxanthine guanine phosphoribosyl-transferase and adenylosuccinate synthetase.” is an authentic record of research work carried out by me under the supervision of Prof. Hemalatha Balaram at the Molecular Biology and Genetics Unit, Jawaharlal Nehru Centre for Advanced Scientific Research, Bangalore, India and that this work has not been submitted elsewhere for the award for any other degree.

In keeping with the general practice of reporting scientific observations, due acknowledgement has been made wherever the work described has been based on the findings of other investigators. Any omission, which might have occurred by oversight or misjudgement, is regretted.


R. Jayalakshmi

Bangalore

Date: 8th January, 2004

572.7

P04



Hemalatha Balaram

Certificate

This is to certify that the work described in this thesis entitled "Structure-function studies on successive purine salvage pathway enzymes - hypoxanthine guanine phosphoribosyltransferase and adenylosuccinate synthetase." is the result of investigations carried out by Ms. R. Jayalakshmi in the Molecular Biology and Genetics Unit, Jawaharlal Nehru Centre for Advanced Scientific Research, Bangalore, India under my supervision, and that the results presented in this thesis have not previously formed the basis for the award of any other diploma, degree or fellowship.

Hemalatha Balaram

Hemalatha Balaram

Bangalore

Date: 8 January, 2004

Acknowledgements

I am indebted to my supervisor, Prof Hemalatha Balaram for her constant guidance and encouragement. Her amazing patience, even in the face of extreme provocation and, the intellectual freedom she allowed ensured that working in the laboratory was always a pleasure. I take this opportunity to express my gratitude to her.

The fruitful collaboration with Prof.M.R.N.Murthy, MBU, IISc., and his students, Isai and Gayathri, for solving the crystal structure of PfAdSS, has been a rewarding experience.

I take this opportunity to thank Prof. Dipankar Chaterji, who has taken an active interest in my work, for his encouragement and advice. I also thank all the faculty at MBGU, JNCASR for their support and help.

I have had the pleasure of the association of many people during the course of my work. Sumathy initiated the random mutagenesis experiments in the laboratory and created the HGPRT library used. The truncated clone of PfAdSS generated by her also laid the foundation for the work on this enzyme. Ranjith and Chetan have assisted in many of the experiments that form a part of this thesis. Summer students - Suja, Meenakshi and Preethi have also contributed to this effort. Sudarshan in Prof. Balaram's lab, IISc was involved in the preliminary hanging drop crystallisation attempts on PfAdSS.

My labmates, Sujay, Pattu, Selvi, Sonali, Chetan, Ranjith, Bimba, Deepak, Shivshankar, Sumathy and Shubra have been forever supportive and helpful. Special thanks are due to Sonali for painstakingly proof reading this entire thesis. Selvi and Chetan have also been of immense help during the writing of this thesis.

John Thomas saved me from the nightmares associated with thesis writing on MS-Word by introducing me to \LaTeX and instructing me on its use. Vinod has generously allowed the use of his computer for running Molscript that has been used to generate many of the illustrations in this thesis.

All my friends have made my stay an enjoyable experience. Thanks are due to Swami, Vaidhya, John, Gautam, Sudhee, Kavith, Lakshmi, Deepak, Vinod, Ashish, Arpita, Pushpa, Smitha and Raghavendra with whom I have shared many fun-filled times.

Computer lab personnel, especially Rajesh and Sheetal, and, the library and administrative staff at JNCASR have been of great help throughout.

CSIR and JNCASR are acknowledged for providing the fellowship.

I thank my parents for all the support and understanding during the course of my PhD.

Summary

Plasmodium falciparum, being an intra-erythrocytic parasite, has evolved a unique set of biochemical pathways to adapt to the specific milieu that it resides in. This makes the biochemistry of the parasite different from the human host. The lack of the *de novo* purine nucleotide biosynthetic pathway is one such difference. The parasite depends exclusively on the salvage of preformed purine bases from the host to meet its requirement for adenine and guanine nucleotides. Hypoxanthine, the major purine base available to the parasite, is converted to IMP by the enzyme hypoxanthine guanine phosphoribosyltransferase (HGPRT). IMP serves as a precursor for both AMP and GMP. Conversion to AMP, proceeding in two steps, involves the enzymes adenylosuccinate synthetase (AdSS) and adenylosuccinate lyase. Conversion to GMP is mediated by inosine monophosphate dehydrogenase and GMP synthetase. The enzymes, HGPRT and AdSS form the subject of this Ph.D. thesis.

The first chapter provides an introduction to the malaria parasite and its biochemistry, with specific emphasis on nucleotide metabolism. The purine salvage pathway is discussed in detail and existing literature on the individual enzymes summarised. Hypoxanthine guanine phosphoribosyltransferases are described in detail and the substrate specificity problem defined. The chapter also presents an overview of the available literature on adenylosuccinate synthetase.

HGPRT catalyses the phosphoribosylation of 6-oxopurine bases to their corre-

sponding nucleotides. Phosphoribosylpyrophosphate (PRPP) serves as the source of the phosphoribosyl group. The substrate specificity of HGPRT varies with the source of the enzyme. Human HGPRT can catalyse the phosphoribosylation of the purine bases, hypoxanthine and guanine. HGPRT from *Plasmodium falciparum* (PfHGPRT), and many other parasites can take up, in addition, xanthine as a substrate. Despite the availability of high-resolution structures of many HGPRTs, the basis for xanthine specificity has remained elusive. The second chapter describes the directed evolution approach adopted here to address this problem of substrate specificity. Random mutagenesis followed by selection for xanthine activity led to the identification of a mutation, F36L, that confers xanthine activity on the human enzyme. The activities of this mutant on hypoxanthine and guanine are not significantly affected. Residue F36 modulates substrate specificity even though it lies far from the active site of the enzyme. Site-directed mutants constructed to introduce a cavity or charge at this position indicated that mutation at this position in the hydrophobic core of the protein also alters protein stability. The gain of xanthine activity could be attributed to a reduction in the activation energies for xanthine phosphoribosylation by the mutant as compared to the wildtype enzyme. This reduction is probably due to minor reorganization in the protein around the mutation, leading in turn to alterations in the vicinity of the active site. Examination of the crystal structure of human HGPRT in complex with a transition state analog, immucillin-GP, indicated that such reorganization in the mutant can offset potentially destabilising interactions that the protein would make if the substrate were xanthine.

Chapter three deals with the effect of a similar mutation on the *P. falciparum* enzyme. F36 of the human HGPRT corresponds to L44 in the *P. falciparum* sequence. The effect of mutation of this residue to Phe in the *P. falciparum* enzyme was also examined. The L44F mutant of PfHGPRT was found to be temperature sensitive as judged by loss of activity and secondary structure with increase in temperature. Temperature dependent activity measurements on the L44F

mutant and the wildtype enzyme also led to the identification of the active form of PfHGPRT as a metastable state. PfHGPRT on purification from recombinant expression systems is inactive. This is also the case with the L44F mutant. Stable activity can be obtained on incubation of the purified enzymes with the substrates, PRPP and hypoxanthine. The purine base xanthine is not as effective in activating the enzyme. Activity measurements at different temperatures indicated that the enzymes respond differently to the purine bases, hypoxanthine and xanthine. Activity on xanthine starts to drop at temperatures 10°C lower than on hypoxanthine. Differences between the response to the two purine bases were also apparent when the unfolding of the enzymes was monitored by far-UV CD. Both hypoxanthine and xanthine, in the presence of PRPP, destabilised the enzyme to denaturation at higher temperatures. Destabilisation was greater in the presence of xanthine as compared to hypoxanthine. This effect is more pronounced in the L44F mutant. Destabilisation of the *P. falciparum* enzyme under conditions used for activation indicates that the active form of the enzyme is metastable. Xanthine can also activate the enzyme but to a lesser extent and destabilises it further indicating that in a folding landscape, the protein-PRPP-xanthine complex can be placed higher than the protein-PRPP-hypoxanthine complex. The protein-PRPP-hypoxanthine complex itself is higher than the purified inactive protein on the folding landscape.

The remaining sections of the thesis are centered on *P. falciparum* adenylosuccinate synthetase (PfAdSS). AdSS catalyses the condensation of IMP with aspartate in a magnesium requiring reaction accompanied by the hydrolysis of GTP to GDP. The enzyme is important in both the *de novo* and salvage pathways for purine nucleotide biosynthesis. This enzyme gains additional importance in context of the A/T rich *P. falciparum* genome, as it is involved in the regulation of ATP/GTP ratios in the cell. Chapter four describes the cloning, purification and kinetic characterization of this enzyme. *P. falciparum* adenylosuccinate synthetase was cloned and shown to be functional by its ability to complement AdSS deficiency in an AdSS deficient strain of *E. coli*, H1238. The functional complementation studies were carried out

Summary

with a N-terminal truncated clone of AdSS in addition to the full-length clone. The full length clone was found to complement AdSS deficiency only in the presence of casein hydrolysate in the medium while the truncated clone complemented even in the absence of casein hydrolysate. Since H1238 is a strain that can produce but not degrade the AdSS inhibitor, guanosine tetraphosphate (ppGpp) under conditions of amino acid starvation, the functional complementation results indicate that ppGpp inhibits the full-length PfAdSS protein but not the truncated protein. It is interesting to note that ppGpp, an effector of the stringent response in prokaryotes, affects the activity of *P. falciparum* AdSS.

PfAdSS was hyper-expressed and the conditions for obtaining stable activity of the enzyme after purification were standardized. Detailed kinetic characterization of PfAdSS allowed the identification of properties unique to the parasite enzyme. All AdSS in literature have a random sequential mechanism. Each of the substrates, IMP, GTP and aspartate, can bind to the enzyme independently. Catalysis, however, proceeds only after all substrates bind to the enzyme. Kinetic studies show that in contrast to all other AdSS, PfAdSS has an ordered mechanism. Competitive inhibitors of GTP inhibit IMP uncompetitively and competitive inhibitors of aspartate show uncompetitive inhibition with both IMP and GTP. This indicates that the order of substrate binding in PfAdSS is IMP, GTP and finally aspartate. Inhibition studies with end products of the reaction and the purine salvage pathway indicate that PfAdSS is similar to the acidic mammalian isozyme rather than the basic isozyme.

During the course of efforts to stabilise the activity of purified PfAdSS, it was observed that EDTA is essential for maintaining stable activity of the recombinant protein. This indicated the role of metal ions in the inactivation of the enzyme in the absence of EDTA. The effect of two metal ions, Cu^{2+} (redox active) and Mn^{2+} (not redox active) on the enzyme were therefore, examined. Cu^{2+} and not Mn^{2+} was found to inactivate the enzyme. Inactivation was accompanied by the formation of disulphide bonded dimers. AdSS is active as a non-covalently linked homodimer

with the active site at the interface. Inactivation by the cysteine modifying agent, iodoacetate, was also accompanied by the destabilisation of the dimers as seen on gel filtration. The substrate IMP could protect the protein from inactivation by both Cu^{2+} and iodoacetate. These observations implicated interface cysteines in the inactivation process. Two Cys residues, C328 and C368 were identified, based on sequence comparison with other AdSS for which structural data was available, to lie at the dimer interface of the protein. Three Cys to Ser mutants, C328S, C368S and C328S C368S were constructed with a view to obtain mutants that are stable to oxidation. The mutants were partially protected against inactivation by iodoacetate indicating that both C328 and C368 were involved in the loss of activity on treatment with iodoacetate. Surprisingly, the dimer interface in C328S and the double mutant was destabilised as judged by gel filtration. In addition, the aspartate K_m of the double mutant was considerably lower than that of the wildtype. Mass spectral (LC-ESI-MS) analysis of tryptic digests of the active, wildtype AdSS showed that C328 is modified to a sulphenic acid. These results implicate a cysteine thiolate or a sulphenic acid in the maintenance of PfAdSS dimer integrity. These studies are described in Chapter 5 of the thesis.

The crystal structure of PfAdSS was solved in collaboration with Prof. M.R.N. Murthy, Molecular Biophysics Unit, Indian Institute of Science, to a resolution of 2. The final chapter of the thesis presents the crystal structure of PfAdSS, with 6-phosphoryl IMP, GDP, hadacidin and Mg^{2+} in the active site. The asymmetric unit is a monomer with a crystallographic axis of symmetry coinciding with the molecular 2-fold axis of symmetry. The dimer interface of PfAdSS is unusual in having a preponderance of positive charges. In addition, C328 at the interface, showed the presence of extra electron density attached to the sulphur indicating that it is modified in the crystal. The density was greater than the single oxygen observed on mass spectrometry, probably indicating further oxidation during crystallisation. This is in agreement with the mutagenesis studies, which highlight the importance of C328 at the interface.

Summary

Comparison of PfAdSS with similarly ligated complexes of other AdSS also gives a plausible explanation for the ordered binding of substrates. AdSS undergoes considerable loop organization in response to IMP binding. In PfAdSS, one such loop, the switch loop, is positioned further towards the GTP pocket making H-bonds with the ribose hydroxyls. These H-bonds are not seen in other AdSS. Examination of the structure also identifies additional H-bonds within the protein that serve to produce additional movement of this loop. Since this loop is known to be organized in response to IMP binding, it could explain the ordered binding of GTP. Additional H-bonding between Thr307 and GTP may account for the ordered binding of aspartate. Thr307 is in a loop that in other AdSS responds to aspartate binding. Ordering of this loop after GTP binding probably facilitates aspartate binding.

List of Publications

1. Cloning and characterization of the *Plasmodium falciparum* adenylosuccinate synthetase gene. Sumathy, K., **Jayalakshmi, R.**, Shivayogi, M.S. and Balaram, H. *Current Science*. (2000) 78, 101-105.
2. Expression, purification and characterization of *Plasmodium falciparum* adenylosuccinate synthetase. **Jayalakshmi, R.**, Sumathy, K and Balaram, H. *Protein Expression and Purification*, (2002) 25:65-72.
3. Perspectives in drug design against malaria. Priyaranjan Pattanaik, **Jayalakshmi, R.**, Balaram, H. *Current Topics in Medicinal Chemistry*, 2002, 2(5):483-505. (Review)
4. Crystal Structure of fully ligated Adenylosuccinate synthetase from *Plasmodium falciparum*. Eaazhisai, K., **Jayalakshmi, R.**, Gayathri, P., Anand, R.P., Sumathy, K. Balaram, H., Murthy, M. R. N. *Journal of Molecular Biology*. (2003), In press
5. Unique kinetic mechanism of *Plasmodium falciparum* adenylosuccinate synthetase. **Jayalakshmi, R.**, Anand, R.P., Balaram, H. (Manuscript under preparation).
6. *Plasmodium falciparum* adenylosuccinate synthetase: Role of interface cysteines in enzyme activity. **Jayalakshmi, R.**, Anand, R.P, Balaram, H.. (Manuscript under preparation).
7. The active form of *Plasmodium falciparum* HGPRT is metastable. **Jayalakshmi, R.**, Anand, R.P, Balaram, H. (Manuscript under preparation).
8. Altered specificity variant of human HGPRT: Insights into the substrate specificity problem. **Jayalakshmi, R.**, Anand, R.P, Sumathy, K., Balaram, H. (Manuscript under preparation).

List of Abbreviations

ADA	Adenosine deaminase
ADS	Adenylosuccinate
APRT	Adenine phosphoribosyltransferase
AdSS	Adenylosuccinate synthetase
DHFR-TS	Dihydrofolate reductase-thymidylate synthase
DHODH	Dihydroorotate dehydrogenase
DTT	Dithiothreitol
GMPS	Guanosine monophosphate synthetase
HDA	Hadacidin
HGPRT	Hypoxanthine guanine phosphoribosyltransferase
IAA	Iodoacetate
IMO	6-phosphoryl-IMP
IMPDH	Inosine monophosphate dehydrogenase
IPTG	Isopropyl thio- β -D-galactopyranoside
LB plot	Lineweaver-Burk plot
LBHB	Low barrier hydrogen bonds
LDH	Lactate dehydrogenase
OPRT	Orotate phosphoribosyltransferase
PEI	Polyethyleneimine
PMSF	Phenylmethyl-sulfonyl fluoride
PNP	Purine nucleoside phosphorylase
PPi	Inorganic pyrophosphate
PRPP	α -D-Phosphoribosyl pyrophosphate
PRT	phosphoribosyltransferase
PfAdSS	<i>P. falciparum</i> AdSS
PfHGPRT	<i>P. falciparum</i> HGPRT

Contents

Declaration	i
Certificate	iii
Acknowledgements	v
Summary	vii
List of Publications	xiii
List of Abbreviations	xv
1 Introduction	1
1.1 Malaria: General Introduction	1
1.1.1 The Life cycle of Plasmodium	2
1.1.2 The <i>Plasmodium falciparum</i> genome	5
1.1.3 Currently used antimalarials	7
1.2 Parasite metabolism as a target for antimalarials	9
1.2.1 Energy metabolism	9
1.2.2 Hemoglobin degradation	11
1.2.3 Fatty acid biosynthesis	12
1.2.4 Nucleotide metabolism	12
1.3 Phosphoribosyltransferases (PRTases)	20

1.3.1	6-oxopurine phosphoribosyltransferases	23
1.3.2	Kinetic mechanism of HGPRTs	24
1.3.3	Substrate binding	25
1.3.4	The HGPRT reaction	27
1.3.5	The HGPRT reaction mechanism	29
1.4	Adenylosuccinate synthetase (AdSS)	31
1.4.1	Isozymes	31
1.4.2	AdSS Kinetics and Mechanism	32
1.4.3	Structure of AdSS and catalysis	34
1.5	Inhibitors and substrate analogs of HGPRT and AdSS	36
1.5.1	HGPRT	36
1.5.2	AdSS	38
1.5.3	Subversive substrates	39
2	Xanthine active mutant of human HGPRT	41
2.1	Introduction	41
2.1.1	Purine recognition in HGPRTs	42
2.1.2	Altered specificity mutants of HGPRTs	44
2.1.3	Random mutagenesis and directed evolution	46
2.2	Materials and Methods	49
2.2.1	Random mutagenesis and screening	50
2.2.2	Construction of single mutants	50
2.2.3	Site-directed mutagenesis	51
2.2.4	Functional complementation	52
2.2.5	Protein expression and purification	53
2.2.6	Enzyme assays and kinetics	55
2.2.7	Temperature stability	56
2.2.8	Structure analysis	56

2.3	Results	56
2.3.1	Screening for xanthine active mutants of human HGPRT . . .	56
2.3.2	Functional complementation of site-directed mutants	57
2.3.3	Enzyme purification	59
2.3.4	Kinetics	60
2.3.5	Temperature stability	61
2.3.6	Activation energy for the reactions	63
2.4	Discussion	63
2.4.1	Kinetics	63
2.4.2	Activation energies and xanthine activity	65
2.4.3	Structural basis for xanthine activity	66
3	The nature of the active form of PfHGPRT	71
3.1	Introduction	71
3.2	Materials and Methods	73
3.2.1	Site-directed mutagenesis	73
3.2.2	Functional complementation	74
3.2.3	Determination of <i>in vivo</i> stability.	75
3.2.4	Enzyme purification	75
3.2.5	Gel filtration	76
3.2.6	Enzyme activation	77
3.2.7	Enzyme assays and kinetics	78
3.2.8	Circular dichroism	78
3.2.9	Paper chromatography	78
3.2.10	Temperature stability and activity	79
3.3	Results	79
3.3.1	Site-directed mutagenesis and functional complementation .	79
3.3.2	Mutation of L44 to F in chimeric HGPRTs	82

3.3.3	Protein expression and <i>in vivo</i> stability	83
3.3.4	Protein purification	84
3.3.5	Oligomerization	84
3.3.6	Activation and kinetic characterization	86
3.3.7	Temperature stability	88
3.3.8	Effect of substrates on thermal stability	89
3.3.9	Activation of PfHGPRT: Product formation	91
3.3.10	Activation by products	93
3.4	Discussion	95
3.4.1	Core mutations and protein stability	95
3.4.2	Activation of PfHGPRT	96
3.4.3	The active form of PfHGPRT is metastable	97
4	PfAdSS: Purification and kinetics	101
4.1	Introduction	101
4.1.1	Sequence comparison	102
4.1.2	Kinetics	102
4.1.3	Oligomerization	105
4.1.4	Regulation of AdSS activity	105
4.2	Materials and Methods	107
4.2.1	<i>Plasmodium falciparum</i> culture and RNA isolation	108
4.2.2	Cloning of full-length AdSS	108
4.2.3	Functional complementation	109
4.2.4	Protein expression	109
4.2.5	Protein purification	110
4.2.6	Western blotting	110
4.2.7	Analytical gel filtration	111
4.2.8	Enzyme assays and kinetics	111

4.2.9	Kinetic data analysis	112
4.3	Results	112
4.3.1	Cloning of PfAdSS	112
4.3.2	Functional complementation	113
4.3.3	Hyper-expression of PfAdSS in <i>E.coli</i>	115
4.3.4	Purification of recombinant PfAdSS and stabilisation of activity	115
4.3.5	Oligomerization	117
4.3.6	Kinetic characterization	119
4.3.7	Inhibition studies	119
4.4	Discussion	122
4.4.1	Protein Stability	125
4.4.2	Kinetic characterization	125
4.4.3	Regulation of PfAdSS	128
5	Interface cysteines in PfAdSS	131
5.1	Introduction	131
5.1.1	Metal catalysed oxidation systems	131
5.1.2	Improving protein stability	133
5.1.3	Oxidized cysteines in proteins	133
5.1.4	Protein-protein interactions	135
5.1.5	The AdSS dimer interface	136
5.2	Materials and Methods	139
5.2.1	Enzyme assays	139
5.2.2	Fluorescence	139
5.2.3	Cysteine modification	140
5.2.4	Size-exclusion chromatography	140
5.2.5	Site-directed mutagenesis.	141
5.2.6	Protein expression, purification and enzyme assays	142

5.3	Results	143
5.3.1	Effect of metal ions on PfAdSS	143
5.3.2	Effect of cysteine modifying agents on activity	145
5.3.3	Rationale for generation of cysteine mutants	145
5.3.4	Expression and purification of interface cysteine mutants of AdSS	147
5.3.5	Kinetic characterization cysteine mutants	148
5.3.6	Oligomeric status	148
5.3.7	Stability	149
5.3.8	Effect of iodoacetate treatment on the mutants	150
5.3.9	Oxidation of C328	152
5.4	Discussion	152
5.4.1	Metal catalysed inactivation of PfAdSS	152
5.4.2	Kinetic properties of interface mutants	153
5.4.3	Importance of C328 and C368 in PfAdSS	154
5.4.4	Is a charged cysteine necessary for maintaining dimer integrity?	154
6	PfAdSS: Structure & Function	159
6.1	Introduction	159
6.1.1	Structure of <i>E. coli</i> and mouse AdSS	159
6.2	Materials and Methods	163
6.2.1	Structure analysis	163
6.3	Results and Discussion	163
6.3.1	Protein crystallisation	163
6.3.2	Structure of <i>P. falciparum</i> AdSS	165
6.3.3	Dimer interface	168
6.3.4	Active site pocket	173

6.3.5	Conformation of dynamic loops: Implication for an ordered mechanism	178
6.4	Conclusion	182
A	Column calibration and mass spectrometry	185
	References	187

List of Figures

1.1	Life cycle of <i>Plasmodium falciparum</i>	2
1.2	Functional profiles of proteins expressed in <i>P. falciparum</i>	5
1.3	Purine salvage pathway in <i>P. falciparum</i>	16
1.4	Stage specific expression profiles of PfHGPRT and PfAdSS	19
1.5	Structures of different PRTs	21
1.6	The HGPRT reaction	23
1.7	Sequence alignment of HGPRTs from different species	24
1.8	The ordered kinetic mechanism of HGPRTs.	25
1.9	Flexible loops in HGPRTs	26
1.10	Proposed reaction mechanisms for the HGPRT catalysed reaction . .	29
1.11	The reaction catalysed by adenylosuccinate synthetase.	33
1.12	Structures of hadacidin and aspartate	35
2.1	Purine contacts in HGPRT	42
2.2	Schematic representation of the single mutant construction	51
2.3	Sequencing chromatogram confirming incorporation of F36K and F36G mutations	53
2.4	Purification profile of F36L human HGPRT	54
2.5	Growth of S ϕ 609 transformed with different HGPRTs on minimal medium plates	57
2.6	Sequencing chromatogram showing mutations in xanthine active human HGPRT	58

List of Figures

2.7	Functional complementation of single mutants	58
2.8	SDS-PAGE of purified human wildtype and mutant HGPRTs.	59
2.9	Xanthine activity of F36L.	61
2.10	Temperature stability of human wildtype and F36L HGPRTs	62
2.11	Stability of mutant human HGPRTs to temperature	62
2.12	Arrhenius plot for wildtype and F36L human HGPRTs.	64
2.13	Comparison of k_{cat} with activation energy for phosphoribosylation by HGPRT	66
2.14	Superposition of structures of human HGPRT in complex with GMP and ImmucillinGP.	67
2.15	Contacts of F36 with Loop IV	68
3.1	Sequence alignment of human and <i>P. falciparum</i> HGPRTs	72
3.2	Superposition of human and <i>P. falciparum</i> HGPRTs	72
3.3	L44F: Sequencing chromatogram	74
3.4	Purification profile of L44F.	77
3.5	Functional complementation by L44F	80
3.6	Effect of temperature on complementation by P2A and L44F.	81
3.7	Substrate specificity of L44F mutants of chimeric HGPRTs	82
3.8	<i>In vivo</i> stability of P2A and L44F.	83
3.9	SDS-PAGE profile of L44F and P2A	85
3.10	Gel filtration profiles of P2A and L44F.	85
3.11	Concentration dependence of P2A and L44F activity	86
3.12	Activation of L44F and wildtype PfHGPRTs	87
3.13	Temperature stability of wildtype and mutant PfHGPRTs.	88
3.14	Activity of L44F and P2A at different temperatures.	89
3.15	Denaturation of P2A and L44F with temperature	90
3.16	Effect of substrates on stability of P2A and L44F.	90
3.17	Effect of activation temperature on activity	93

3.18	Product formation and rate of activation	94
3.19	Activation of WTPfHGPRT by products of the reaction	94
3.20	Effect of temperature on activation of WTPfHGPRT by IMP.	95
3.21	Proposed energy landscape for PfHGPRT	99
4.1	Alignment of AdSS from different species	103
4.2	Effect of IPTG and hadacidin on complementation	114
4.3	Functional complementation in <i>E. coli</i> H1238 by full-length and truncated AdSS	114
4.4	SDS-PAGE analysis of PfAdSS induction in BL21(DE3)	115
4.5	SDS-PAGE analysis of recombinant PfAdSS	116
4.6	Stabilization of AdSS activity by EDTA	117
4.7	Analytical gel filtration of PfAdSS	118
4.8	Lineweaver-Burk plots of the inhibition of PfAdSS	120
4.9	Inhibition of PfAdSS by GDP	121
4.10	Substrate inhibition of PfAdSS	122
5.1	Subunit complementation in <i>E. coli</i> AdSS.	137
5.2	Alignment of <i>P. falciparum</i> , <i>E. coli</i> and mouse AdSS	138
5.3	Sequencing chromatograms confirming incorporation of mutations	142
5.4	Purification of C368S	143
5.5	Effect of metal ions on activity of PfAdSS	144
5.6	Effect of Cu ²⁺ ions on properties of PfAdSS	145
5.7	Effect of cysteine modifying agents on activity of PfAdSS	146
5.8	Gel filtration profile of WTPfAdSS after iodoacetate modification	146
5.9	SDS-PAGE profiles mutant PfAdSS	147
5.10	Gel filtration profile of wildtype and mutant PfAdSS	149
5.11	Equilibrium unfolding of wildtype and mutant PfAdSS	150
5.12	Effect of iodoacetate treatment on oligomerization of PfAdSS mutants	151

List of Figures

6.1	Structures of AMP, PIMP, GDP and hadacidin	162
6.2	Crystal of PfAdSS grown in the presence of IMP and GTP	164
6.3	Ribbon representation of the PfAdSS monomer	166
6.4	The PfAdSS dimer	167
6.5	Superposition of PfAdSS and <i>E. coli</i> and mouse AdSS	168
6.6	Topology diagram of PfAdSS	169
6.7	Interface residues in <i>P. falciparum</i> and mouse AdSS.	171
6.8	Electron density around C328 and C368 in PfAdSS	172
6.9	Activity of dissolved crystals of PfAdSS	172
6.10	C328 environment in the PfAdSS crystal structure	173
6.11	$2F_o - F_c$ map corresponding to the bound ligands	174
6.12	phosphoryl-IMP contacts in PfAdSS	175
6.13	GDP contacts in PfAdSS	176
6.14	Mg ²⁺ co-ordination	177
6.15	Hadacidin binding in PfAdSS	178
6.16	Superposition of ligated and unligated mouse AdSS	179
6.17	Superposition of Switch, Asp and GTP loops of Pf and mouse AdSS	181
6.18	Sequence alignment showing 4 residue deletion in PfAdSS	182
A.1	Gel filtration column calibration curved	185
A.2	LC-MS analysis of tryptic digests of wildtype PfAdSS	186

List of Tables

1.1	Inhibitors of purine salvage pathway enzymes	17
2.1	Substrate specificity of human HGPRT mutants as determined by functional complementation in the <i>E. coli</i> strain S ϕ 609	59
2.2	Kinetic parameters of human wildtype and mutant HGPRTs.	60
2.3	Activation energy for the HGPRT catalysed reactions	64
2.4	Comparison of F36 . . contacts in 1BZY and 1HMP.	68
3.1	Kinetic parameters of wildtype and mutant PfHGPRTs.	87
3.2	Melting temperatures of P2A and L44F	91
3.3	Product formation during activation of WTPfHGPRT at 4°C.	92
4.1	Purification table of recombinant PfAdSS.	116
4.2	Summary of AdSS inhibition kinetics	127
4.3	Kinetic constants for AdSS from different species	128
4.4	Inhibition constants for AdSS from different species	129
5.1	Kinetic parameters of wildtype and mutant PfAdSS.	148
5.2	Effect of iodoacetate treatment on activity of PfAdSS	151
6.1	Data collection and refinement statistics of PfAdSS complex	165
6.2	Dynamic loops in AdSS	179

Erratum

1. The reference “Markham GD and Reed GH (1977) Adenylosuccinate synthetase from *Azotobacter vinelandii*: purification, properties and steady-state kinetics. Arch. Biochem. Biophys. 184: 24-35.” is missing from the reference list.
2. Page 18, line 5
 - . “product of the enzyme, inosine” should read “product of the enzyme, hypoxanthine”
3. Addition to legend to Fig. 3.8b: The unlabelled lanes correspond to wildtype PfhGPRT used as a marker.
4. Page 107, line 14 :
 - . “ affected by AMP concentrations” should read “affected by IMP concentration.”
5. Section 4.3.7, page 119 to 122.
 - . All references to Fig. 5.1 should be to Fig. 4.8
6. Legend to Fig. 6.8:
 - . “around C328 (a-c) and C368 (c)” should read “ around C328 (a-c) and C368(d).
7. The grey sphere in Fig. 6.12, 6.13 and 6.14 indicates Mg²⁺.

Chapter 1

Introduction

This chapter gives a general introduction to malaria. This is followed by a detailed description of nucleotide metabolism in the parasite. The enzymes that form the subject of the studies reported in this thesis, hypoxanthine guanine phosphoribosyltransferase and adenylosuccinate synthetase, are considered in detail.

1.1 Malaria: General Introduction

Plasmodium falciparum, the causative agent of malaria, is one of the world's most pathogenic microbes. The annual morbidity of malaria is close to 500 million, and the mortality, predominantly among young children, between 1-2 million (WHO,1999). The discovery of the insecticidal effects of DDT along with the antimalarial chloroquine led to efforts to eradicate the disease. Indeed, in the latter half of the 20th century the combination of potent insecticides and cheap drugs offered the possibility of global eradication. Malaria, however, remains one of the largest global health care problems of the 21st century, eradication plans having been defeated by such diverse factors as insecticide resistance and environmental impact, drug resistance, and insufficient investment in the discovery of new drugs.

Malaria is one of the oldest diseases known to man. Documentation dating back to 2500 BC describes tertian and quartan fevers accompanied by splenomegaly (Sherman, 1998). The etiology of the disease however, was

elucidated only in the early 20th century. The work of Laveran in 1880, identifying the causative agent of malaria as *Plasmodium* won him the Nobel Prize in 1907. Sir Ronald Ross working on the suggestions of Patrick Manson, established in 1897 that the malaria parasite is transmitted by the *Anopheles* mosquito. This work won him the Nobel Prize in 1902, 5 years before Laveran whose work formed the starting point of Ross' work. The tissue stages of the malaria parasite in primates and humans were discovered much later in 1948 establishing the complete life cycle of the malaria parasite (Sherman, 1998).

1.1.1 The Life cycle of Plasmodium

Malaria in humans is caused by four species of *Plasmodium*: *P. falciparum*, *P. vivax*, *P. ovale* and *P. malariae*. Of these, *P. falciparum* malaria is the most lethal due to the cerebral complications associated with the disease. The life cycle of all species of human malaria parasites is essentially the same (Sherman, 1998) (Figure 1.1). It comprises an exogenous sexual phase (sporogony) with

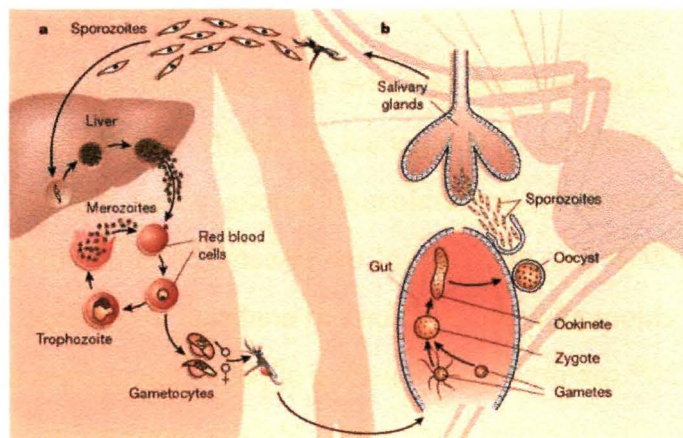


Figure 1.1: Life cycle of *Plasmodium falciparum*) Human stages b) Mosquito stages. Figure taken from Wirth, D.F. (2002)

multiplication in certain *Anopheles* mosquitoes and an endogenous asexual phase (schizogony) with multiplication in the vertebrate host. Gametocytes of the parasite in the circulation of individuals infected with malaria are ingested by the mosquito vector during a blood meal. The temperature change in the mosquito gut induces

gametogenesis, which is quickly followed by fertilization. The resultant zygote undergoes meiotic division and transforms into the ookinete. The ookinete then moves from the midgut to a site between the midgut epithelium and the hemolymph and develops into an oocyst. The oocyst ruptures to release fully formed sporozoites into the hemolymph which migrate to the salivary glands of the mosquito. These sporozoites are injected into the vertebrate host initiating the asexual phases of the life cycle.

Within 30 min of injection the sporozoites are carried to the liver where they pass through a layer of liver epithelium to invade the hepatocytes. The parasite then undergoes a series of asexual cycles called pre-erythrocytic shizogony. The resultant merozoites are released into circulation and invade erythrocytes in the blood. On entry into the erythrocyte, the merozoites transform into the ring form within a membrane-lined cavity called the parasitophorous vacuole. The appearance as a ring is due to the presence of a large food vacuole that is involved in the degradation of hemeoglobin, with the elongated nucleus occupying the perimeter. Modification of the RBC membrane by parasite proteins begins at this stage. The ring develops into a rounded trophozoite, the most active feeding and growth stage of the parasite. The trophozoite stage is characterized by the accumulation of the hemozoin pigment in the food vacuole. The parasite then undergoes a series of nuclear divisions along with an intense synthesis of molecules required for the next round of erythrocyte invasion. About 16 nuclei are generated and these move into merozoite buds formed at the periphery of the schizont. Merozoites then pinch off from the residual body of the cytoplasm and are released into the circulation by a protease mediated rupture of the membranes surrounding the parasite. These merozoites can now establish fresh infections. During the erythrocytic stages some merozoites enter the RBC to develop into gametocytes. Commitment of merozoites to development into gametocytes occurs before the invasion of the erythrocyte. The gametocytes are taken up by mosquitoes during a blood meal to initiate a fresh cycle of sexual development (Sherman, 1998, Bannister & Mitchell, 2003).

The only human malaria parasite associated with cerebral complications is *P. falciparum*. A central feature of falciparum malaria is the sequestration of parasitised erythrocytes within the microvasculature of the major organs of the body, predominantly the brain, heart, lungs and submucosa of the small intestine. Rosetting which is the binding of uninfected RBCs to infected RBCs, has been found to be higher in parasites isolated from cases of cerebral malaria (Chen et al., 2000). In the brain, vascular obstruction can lead to ischaemia and hemorrhages. These obstructions are thought to be the reason for the coma associated with malaria. Production of proinflammatory cytokines (TNF α), upregulation of endothelial cell adhesion molecules have also been implicated in the development of cerebral malaria (Medana et al., 2001). Studies in African children has suggested that metabolic acidosis associated with respiratory failure may be the cause for death. Associations between the clinical features of malaria and fatal outcomes have been described, but causality has not been established (Newton et al., 1998). It is likely that multiple mechanisms are involved in the induction of cerebral complications and both the presence of parasitised erythrocytes in the central nervous system and sequestration and immunopathological processes contribute to the pathogenesis of cerebral malaria.

The life cycle highlights an extraordinary feature of *Plasmodium* biology: The ability of this small, predominantly haploid, but genomically complicated eukaryote to change its gene expression patterns to efficiently exploit dramatically different environments; the hepatocyte and erythrocyte in the human host and, the midgut, the “vasculature” and the salivary glands of the mosquito (Fig. 1.1), (Bannister&Mitchell, 2003). In addition, being a predominantly intracellular parasite, it has also done away with many biochemical pathways, deriving many metabolites from the host . Understanding parasite biology and biochemistry therefore, becomes a challenge. The sequencing of the genomes of *Plasmodium falciparum* (Gardner et al., 2002, Gardner et al., 2001, Hall et al., 2002, Hyman et al., 2002), and its two hosts, human (Lander et al., 2001, Venter et al., 2001)

and *Anopheles gambiae* (Holt et al., 2002) has made available an enormous body of information that will allow a detailed investigation of the biology of the parasite. These genomes along with the tools of proteomics that have developed over the last few years are already revolutionizing the study of the parasite (Hoffman et al., 2002). The *Plasmodium* genome therefore, merits at least a brief discussion.

1.1.2 The *Plasmodium falciparum* genome

The nuclear genome of the *Plasmodium falciparum* is 22.8 Mb. The parasite also has a 35 kb apicoplast genome (Wilson et al., 1996) and a 6 kb mitochondrial genome (Suplick et al., 1988). The nuclear genome is organized into 14 chromosomes ranging in size from 0.643 Mb to 3.29 Mb (Triglia et al., 1992). About 52 % of the genome comprises of coding regions, with the number of predicted genes being 5268. Of these, 60 % are annotated as hypothetical proteins with no obvious homology with any sequenced functional protein to date (Gardner et al., 2002). Proteomic analysis of expression during different stages of the *P. falciparum* life cycle has led to the identification of 2415 expressed proteins (46 % of the total annotated genes), 51 % of which are annotated as hypothetical (Florens et al., 2002, Lasonder et al., 2002). Figure 1.2 shows the functional profiles of proteins expressed and detected by the proteome analysis. Also of interest in this analysis

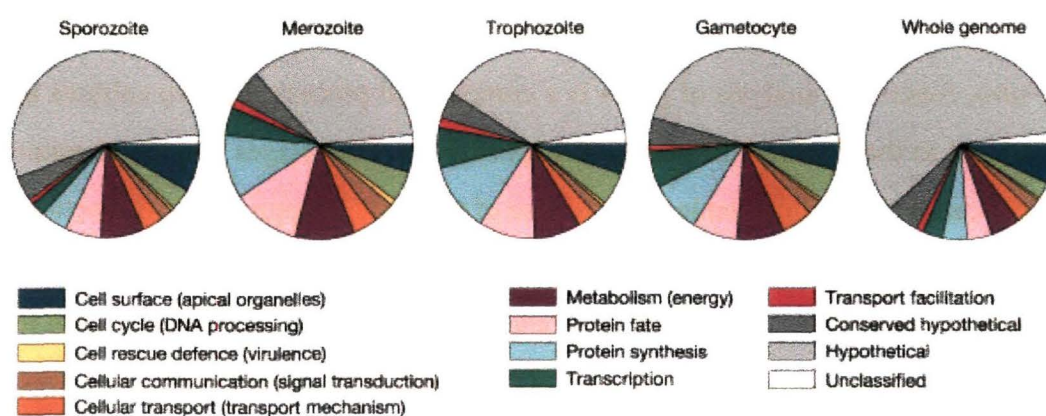


Figure 1.2: Functional profiles of proteins expressed in *P. falciparum*. Proteins identified in each stage are plotted as a function of their broad functional classification. Figure is taken from Florens et al., 2002

is the identification of metabolic pathways that vary with different stages of the parasite life cycle. For example, the intraerythrocytic stages of the parasite express the enzymes of the glycolytic pathway, the only pathway for energy metabolism in these stages. However, the gametocyte and sporozoite preparations were found to express enzymes of the mitochondrial TCA cycle also, indicating a variation in the energy metabolism. Interestingly, the stages of the parasite that express the TCA cycle enzymes are also the stages that are susceptible to drugs that disrupt mitochondrial function (Florens et al., 2002).

An expression profiling of the entire malarial genome has also been carried out using 25 bp oligonucleotides covering both strands of the *P. falciparum* genome at a frequency of about one oligonucleotide every 150 bp of the sequence (Le Roch et al., 2003, Bozdech et al., 2003). The expression analysis has been carried out on all the erythrocytic stages including the gametocytes and on the sporozoite. The expression patterns, along with the mass spectrometric analysis of the proteome, allow the identification of stage specific expression patterns. The agreement between the proteome and transcriptome analysis has been found to be good. Stage specific expression profiling will aid the identification of the functions of the numerous hypothetical proteins. Such profiling has also helped in reinterpretation of existing data.

Even though *P. falciparum* is a unicellular organism that can easily be cultured *in vitro*, functional analysis of genes is a complicated process. *In vitro* cultures are restricted to the erythrocytic stages; the sporozoites, liver stages and the mosquito stages cannot be maintained in culture. One of the popular approaches to functional characterization is the creation of knockouts. Methods for stable transfection of malaria parasites have been established and many different vectors constructed for transgene expression (Gardiner et al., 2003, Waters et al., 1997, Waterkeyn et al., 1999). The validity of these methods has also been established with knock out studies on many genes (de Koning-Ward et al., 2000). However, all these studies are on non-essential proteins, for example the knob associated histidine rich protein

(KAHRP) which has a role to play in adherence (Crabb et al., 1997). As the intraerythrocytic stages of the parasite are haploid, knocking out essential genes is lethal and therefore, not possible limiting the use of this popular tool.

RNA interference (RNAi) is an emerging technique that has proved to be useful for functional genomic screening (Hannon, 2002). RNAi acts post-transcriptionally and results in the specific degradation of target mRNA leading to decreased synthesis of specific proteins. This method that has been extensively used to study gene expression in a diverse range of organisms (*Caenorhabditis elegans*, *Drosophila melanogaster*, fungi, plants and vertebrate cell lines) (Hannon, 2002, Plasterk & Ketting, 2000) has now been applied to the malaria parasite. Dihydroorotate dehydrogenase, a target for currently used antimalarials has been used to demonstrate the validity of the RNAi approach in cultured malaria parasites (McRobert & McConkey, 2002). Other genes whose functions have been explored and their essentiality established using this approach are the cysteine proteases, falcipain 1 and 2 (Malahotra, P et al., 2002), chorismate synthase and PP1, a serine/threonine protein phosphatase (Kumar et al., 2002). All these data in combination with the new tools being developed for functional analysis will aid in understanding parasite biology and in validating new drug and vaccine targets.

1.1.3 Currently used antimalarials

The drug armoury against malaria is limited. The quinoline family of drugs, originating from quinine, the oldest of the antimalarials, remain the cheapest and most accessible drugs against malaria. Chloroquine continues to be the most widely used drug worldwide for the treatment of non-complicated malaria, despite extensive drug resistance. Amodiaquine, also belonging to the quinoline family, has greater efficacy than chloroquine in resistant strains and is used as the second line of attack against the disease. Other drugs of the same genre include halofantrine and mefloquine (Wellems & Plowe, 2001). Except in parts of South-East Asia, quinine remains the final line of attack, despite its severe side effects in complicated,

multidrug resistant malaria, as relatively little resistance against this drug has developed (Meshnick, 1997).

Artemisinins, semi-synthetic derivatives of the plant extract artemisinin, are used in both uncomplicated and severe malaria (Price, 2000). The most commonly used derivatives are artemether, artether and artesunate, which are metabolised into dihydroartemisinin which itself is now used as a drug (White & Olliaro, 1998). Despite their high potency and ability to reduce circulating parasitemia rapidly, these drugs have a very short half-life and are generally used in combination with mefloquine (Ridley, 2002).

Most other drugs in use target pyrimidine biosynthesis, either directly or indirectly. Pyrimethamine, a competitive inhibitor of dihydrofolate reductase (DHFR), in combination with sulfadoxine, an inhibitor of dihydropteroate synthase, is a single dose treatment for the disease. However, resistance develops rapidly. Proguanil and chlorproguanil are metabolised by human CYP2C19 and CYP3A4 to the active metabolites cycloguanil and chlorcycloguanil, which inhibit parasite DHFR (Giao & de Vries, 2001).

Atavaquone, a hydroxynaphthoquinone, inhibits mitochondrial electron transport (Srivatsava et al., 1997). Since, a major function of the electron transport pathway is to provide reducing equivalents to dihydroorotate dehydrogenase, it indirectly inhibits pyrimidine biosynthesis. It is usually administered in combination with proguanil (Malarone) (Wilairatana et al., 2002). However, resistance is making treatment redundant faster than the rate at which newer drugs can be developed. Older drugs that were displaced by the availability of cheaper drugs like chloroquine are therefore receiving renewed attention. One such drug is pyronaridine, an acridine based drug synthesised in China in the 1970s and in use in both the oral and parenteral forms for the treatment of chloroquine-resistant *P. falciparum* malaria (Chen & Zheng, 1992), is being pursued by the WHO. The mode of action of this drug is not known.

The rapid emergence of drug resistance against the limited armory of drugs available against the parasite necessitates the identification of new drug targets and drugs (Hyde, 2002). A rational approach to this goal would be the identification of players in metabolic pathways in the parasite and their characterization with the aim of knowledge based drug design. The availability of the genome sequence of both the parasite and the human host should aid this process. The next section identifies some potential metabolic pathways that can be targeted for therapeutic intervention. Nucleotide metabolism, due to its relevance to the studies described in this thesis is dealt with in some detail.

1.2 Parasite metabolism as a target for antimalarials

The erythrocyte, the host cell for the symptomatic stages of malaria infection, is a unique milieu. In addition to protecting the parasite from host defenses, it also offers a singular set of metabolic precursors for the parasite. The mature human erythrocyte is also transcriptionally silent and lacks many of the metabolic pathways operative in human tissues. During the course of adaptation, the malaria parasite has done away with many metabolic pathways and also acquired some which make it metabolically distinct from the host. The challenge therefore is to identify and target these differences. The availability of the parasite genome along with its transcriptome and proteome should greatly aid this process. Once these targets are identified, validated and characterized, rational drug design may be attempted. This section highlights the major metabolic differences between the human host and the parasite, with a focus on nucleotide metabolism. This list is not a comprehensive one and represents only some of the metabolic pathways that have generated interest in the recent years.

1.2.1 Energy metabolism

The intraerythrocytic stages of the parasite derive their entire ATP pools by glycolysis. A 30-100 fold increase in glycolytic flux has been documented in the

infected erythrocyte when compared to the uninfected erythrocyte (Roth, 1990). All the enzymes involved in glycolysis are present in the parasite genome (Bahl et al., 2002). The erythrocytic stages of the parasite have only a single rudimentary mitochondrion that does not play a role in the energy metabolism of the parasite. Proteome analysis also corroborates this observation, with the TCA cycle enzymes not being detected in the parasite erythrocytic stages (Florens et al., 2002). The enzymes for the TCA cycle are indeed present in the genome and are expressed in the gametocyte and sporozoite stages of the parasite (Bahl et al., 2002, Florens et al., 2002). These stages also have cristate mitochondria and are susceptible to drugs that target this organelle (Lanners, 1991). A recent study in the mouse malaria parasite *P. berghei*, has demonstrated increased oxygen consumption on addition of TCA cycle intermediates in the intraerythrocytic stages raising the possibility of oxidative phosphorylation occurring in the parasite. Efforts to reproduce these observations in *P. falciparum*, were however, unsuccessful (Sergio et al., 2000). Antiamoebic, zervamicin and efrapeptins, fungal metabolites which are uncouplers of oxidative phosphorylation, have also been shown to have antiparasitic activity in *P. falciparum* cultures (Nagaraj et al., 2001). In view of these studies, the enzymes involved in energy metabolism, especially those of the glycolytic pathway are good targets against the erythrocytic stages.

Only three enzymes of the glycolytic pathway, aldolase (Kim et al., 1998), triosephosphate isomerase (TIM) (Velankar et al., 1997) and lactate dehydrogenase (LDH) (Dunn et al., 1996), have been characterized in detail with crystal structures solved. The crystal structures allow the identification of features unique to the parasite enzyme. Inhibition of these enzymes has been shown to be lethal to the parasite, though no candidate drugs have been identified. Parasite LDH differs from the human counterpart in its ability to accept the synthetic molecule, 3-acetylpyridine adenine dinucleotide, as a cofactor. This property has been exploited in a diagnostic assay for malaria infection (Basco et al., 1995). LDH has also been crystallised with the antimalarial, chloroquine providing a starting template

for inhibitor design (Read et al., 1999).

1.2.2 Hemoglobin degradation

The intraerythrocytic malaria parasite does not carry out any amino acid biosynthesis. The amino acid requirement is met through the degradation of hemoglobin taken up from the host erythrocyte. The parasite is auxotrophic for amino acids that are absent or infrequently represented in hemoglobin (Rosenthal & Meshnick, 1998). Hemoglobin is taken up from the erythrocyte cytoplasm via a cytotostomic pathway and degradation takes place in the food vacuole, an acidic lysosome like organelle within the parasite. Many classes of proteases, aspartyl, thiol and metallo proteases- have been implicated in this apparently ordered process. Plasmepsins, 10 of which have been identified in the *P. falciparum* genome, are aspartic proteases involved in the initial steps of hemoglobin degradation (Banerjee et al., 2002). Of these Plasmepsin I and II are relatively well studied with the crystal structure of Plasmepsin II determined (Silva et al., 1996). Use of the crystal structure has also led to identification of a few small non-peptidyl compounds that inhibit plasmepsin II activity with sub-nanomolar K_i s (Silva et al., 1996). Three thiol proteases, falcipain 1 (Salas et al., 1995), 2 (Shenai et al., 2000) and 3 (Sijwali et al., 2001) constitute the second major class of proteases involved in hemoglobinolysis. Falcipain 2 is characterized as the principal trophozoite cysteine protease that is responsible for more than 90 % of total trophozoite soluble thiol protease activity (Shenai et al., 2000). Apart from hemoglobin degradation falcipain 2 can participate in degradation of erythrocyte cytoskeleton. Falcilysin, a metalloprotease and some aminopeptidase activities complete the hemoglobin degradation process. Hemoglobinolysis is one of the most promising targets against malaria.

1.2.3 Fatty acid biosynthesis

Fatty acid biosynthesis in the parasite takes place in a specialized organelle called the apicoplast. This alga-derived organelle enclosed by four membranes has a 35 kb genome encoding rRNA and tRNA genes in addition to many proteins (Wilson & Williamson, 1997). Many nuclear encoded proteins have also been found to have plastid targeting signals (Foth et al., 2003). The plastid is thought to play a role in fatty acid and heme biosynthesis (McFadden & Roos, 1999). The nuclear encoded plastid proteins are plant-like, indicative of a transfer of genes from the plastid to the nucleus during evolution. One of the established functions of this organelle is fatty acid biosynthesis, which differs from the pathway operative in the human host. In *P. falciparum*, independent enzymes catalyse individual steps of fatty acid biosynthesis (Type I) in contrast to the human host where all these activities are resident on one single large polypeptide (Type II). Triclosan, an inhibitor of Type I fatty acid biosynthesis has antiparasitic Activity (McLeod et al., 2001, Surolia & Surolia, 2001). All enzymes of this pathway are therefore potential drug targets.

1.2.4 Nucleotide metabolism

Human erythrocytes have very limited nucleotide requirements and therefore, lack the complete nucleotide biosynthetic pathway. However, the rapidly dividing parasite has a dramatically increased nucleotide requirement that has to be met through parasite-encoded pathways. Purine nucleotides, in most protozoan parasites, are derived through the salvage of preformed host bases, while pyrimidine nucleotides are synthesised through the *de novo* biosynthetic pathway (Sherman, 1979). Flux through both of these pathways is essential with little or no means of bypass. The two pathways therefore, present a range of essential enzymes that can be targeted for therapeutic intervention. In addition, nucleotide metabolism in the parasite includes the transcriptional and replicative machinery. Another aspect of the above processes is the regulation of gene expression, at the level of both

transcription and translation. These mechanisms are also of paramount importance to the parasite, which undergoes a series of differentiation events through multiple stages during its intra-erythrocytic cycle.

Pyrimidine biosynthesis

The malaria parasite derives its entire pyrimidine nucleotide pool via the *de novo* biosynthetic pathway. The salvage enzymes are absent in the parasite (Gero et al., 1984). This pathway, which includes the enzyme thymidylate synthase (TS)-dihydrofolate reductase (DHFR), connecting up to folate biosynthesis, is by far the best exploited clinically. A number of drugs routinely used for antimalarial therapy directly or indirectly target enzymes of the pathway. The only enzymes of the pathway that have been extensively studied are dihydroorotate dehydrogenase (DHODH) and TS-DHFR. Many antimalarial drugs in use target folate metabolism. These include pyrimethamine and proguanil which target DHFR and sulphadoxine which inhibits folate biosynthesis (Hitchings, 1971). Resistance to these drugs is however rampant, with a number of mutations contributing to resistance characterized (Warhurst et al., 1998).

Thymidylate synthase in the parasite is metabolically linked to DHFR, a proven target for antimalarial chemotherapy, with the two activities residing in the same bifunctional polypeptide. The PfDHFR-TS polypeptide is 608 amino acids of which the first 221 constitute the DHFR domain. The C-terminal 288 amino acids comprising the TS domain are linked to the DHFR domain by an 88 amino acid junction region. The structures of PfDHFR-TS and two mutants that are resistant to both pyrimethamine and cycloguanil have been solved recently (Yuvaniyama et al., 2003). These structures have led to an understanding of the mechanisms of resistance and will aid the design of new inhibitors. TS is a highly conserved protein and selective inhibitors may be hard to come by. Since partial inhibition of TS is sufficient to produce fatal nucleotide imbalances in the parasite (Yoshioka et al., 1987), an alternative strategy suggested is the combination of an effective

TS inhibitor and a nucleoside that can be utilized by the host (Rathod et al., 1989). Anti-TS drugs include 5-fluoropyrimidines but these lead to host toxicity due to their incorporation into the host nucleotide pool (Parker et al., 1990). N⁵-N¹⁰-methylene tetrahydrofolate analogs, which inhibit TS without being metabolized into the nucleotide pool, are attractive alternatives. Use in combination with thymidine selectively inhibits parasite growth through inhibition of TS with reduced host toxicity (Jiang et al., 2000). Such analogs need to be explored further. The crystal structures of PFDHFR-TS have also identified a unique junction that links up the two activities in this bifunctional protein. Inhibitors targeting this region would interfere with inter-domain interactions leading to species specific inhibition of dTMP synthesis.

The parasite is also capable of biosynthesising folate and this forms the basis of sulpha drugs used in combination with pyrimithamine. These act on the enzyme dihydropteroate synthase, but as in the case of DHFR, resistance readily develops in the field (Triglia et al., 1997). Other enzymes of the pathway remain relatively uncharacterized and should be pursued in view of the proven efficacy of inhibition of the pathway.

The shikimate pathway provides the pABA precursor for folate biosynthesis. Glyphosate, a specific inhibitor of chorismate synthase, is antiparasitic, establishing the importance of this pathway for the parasite (Roberts et al., 1998). In the absence of evidence for aromatic amino acid biosynthesis, the primary role of this pathway seems to be the supply of pABA for folate metabolism. This pathway, which localizes to the cytosol (Fitzpatrick et al., 2001), is an important target in view of its absence in the host. Though the inhibition studies indicate that the shikimate pathway is operative in the parasite, only chorismate synthase has been found in the parasite genome. Genes with obvious homology to other enzymes of the pathway are absent in the genome. The presence of significantly divergent genes performing these functions cannot be ruled out.

DHODH is a mitochondrial enzyme in the parasite and its activity is closely linked to the mitochondrial electron transport chain. The enzyme purified from *P. berghii* (Krungkrai et al., 1991) and *P. falciparum* (Krungkrai et al., 1995) has an iron-sulphur redox active cluster, does not bind flavin nucleotides and uses ubiquinone as an electron sink. Inhibitors of the electron transport chain, like the clinically used drug atovaquone, exert their antiparasitic activity by indirectly inhibiting this enzyme (Ittarat et al., 1994). The *P. falciparum* gene has a long leader sequence that presumably plays a role in mitochondrial targeting. The enzyme, also has a 42 amino acid insertion not present in any other DHODH, the functional role of which is not clear. Structural information on the enzyme is lacking.

The first three enzymes of the pyrimidine biosynthetic pathway are monofunctional enzymes in *Plasmodium*, but are a single trifunctional protein in higher eukaryotes (Krungkrai et al., 1990). The first step, the glutamate dependent synthesis of carbamoyl phosphate requires, a series of reactions which are catalysed by distinct domains of the enzyme, carbamoyl phosphate synthetase (Flores et al., 1994). The *P. falciparum* enzyme has unusually large insertions between these domains. The function of these large domains has not been determined, and might even have an additional uncharacterized activity. The unusually long ORF that results, in fact among the largest known in *P. falciparum*, has been utilized for the design of enzyme specific phosphorothioated ribozymes, which have antimalarial activity *in vitro* due to their ability to specifically cleave carbamoyl phosphate synthetase mRNA (Flores et al., 1997). The other enzymes of the pathway, aspartate transcarbamoylase, dihydroorotase, OPRT, UMP kinases and cytidylate synthase remain largely uncharacterized in spite of inhibition studies that illustrate their importance to parasite survival (Seymour et al., 1994).

Purine nucleotide metabolism

Unlike pyrimidine nucleotide biosynthesis, the parasite relies exclusively on the salvage of preformed host purine bases to meet its requirement of purine nucleotides.

Table 1.1: Inhibitors of purine salvage pathway enzymes that kill the parasite

Enzyme	Inhibitor	Reference
Adenosine deaminase	6-thioguanosine	Queen et al., 1990
Purine nucleoside phosphorylase	Immucillin H	Kicska et al., 2002b
Hypoxanthine guanine phosphoribosyltransferase	6-thioguanine	Queen et al., 1990
Adenylosuccinate synthetase	Hadacidin	Webster et al., 1984
IMP dehydrogenase	Bredinin	Webster & Whaun, 1982
GMP synthetase	Psicofuranine	McConkey, 2000

Toxoplasma gondii (Schumacher et al., 2000), the structure of the latter having been solved by crystallography (Sinha et al., 2000). However, the enzyme activity has not been detected in *P. falciparum* (Reyes et al., 1982) and a sequence with significant homology to known AKs from other species is not present in the genome (Bahl et al., 2003). The other bypass mechanism involves the conversion of adenine to AMP by adenine phosphoribosyltransferase (APRT). Adenine levels in the parasite are low as adenosine is not a substrate for either host or parasite PNPs (Kicska, et al., 2002a, 2002b) and because the high levels of adenosine deaminase keep the levels of adenosine in the parasite negligible. Low levels of APRT have been detected in the parasite (Queen et al., 1989) and the cloning of the *P. falciparum* APRT by functional complementation in APRT deficient mouse cells has been reported (Pollack et al., 1985). However, no sequence information is available in the nucleotide database and a putative enzyme sequence could not be found in the genome by homology searches. The evidence for the existence of this enzyme in the parasite remains ambiguous. The other two enzymes indicated, AMP deaminase and GMP reductase, are either present in insignificant levels or absent in the intra-erythrocytic parasite (Reyes et al., 1982).

Most of the enzymes involved in the primary pathway for salvage remain poorly characterized. The parasite purine nucleoside phosphorylase has been cloned and

the recombinant enzyme purified from *E. coli* (Kicska, 2002a). A transition state analog of this enzyme based on the mechanism of homologs from other species has been shown to kill the parasite in culture. However, complete elimination of the parasite requires the inhibition of the host enzyme also (Kicska et al., 2002b). This is because the product of the enzyme, inosine, can freely diffuse across membranes. The parasite can therefore survive on host derived inosine even in the absence of a parasite encoded PNP. PNP however, remains of interest as mode of directing subversive substrates into the purine salvage pathway. Another enzyme, catalysing the formation of hypoxanthine from inosine, a purine nucleoside hydrolase has generated interest in other protozoan parasites, as this enzyme is absent in the human host (Versees et al., 2001). The enzyme has not been reported in *P. falciparum* and simple homology searches do not show the presence in the genome.

In spite of the proven efficacy of nucleotide metabolism in therapy, not only in *Plasmodium*, but also in many other parasitic and bacterial diseases, studies on most enzymes of the pathway remain superficial, with little more than gene sequence information existing in most cases. The only enzyme of the purine salvage pathway that has been extensively characterized is HGPRT. With regard to adenylosuccinate synthetase, the activity of the enzyme has been measured in parasite lyses (Reyes et al., 1982) and inhibition of parasite growth by the AdSS inhibitor, hadacidin, documented (Webster et al., 1984). The remaining enzymes of the pathway, adenylosuccinate lyase, inosine monophosphate dehydrogenase and GMP synthetase have little more than sequence information available. The availability of large libraries of a variety of molecules that can potentially inhibit enzymes involved in nucleotide metabolism, generated for testing against various cancers, should provide additional impetus to studies on the enzymes of this pathway. Since HGPRT and AdSS form the basis of this study, the properties of these enzymes are discussed in some detail.

1.2. Parasite metabolism as a target for antimalarials

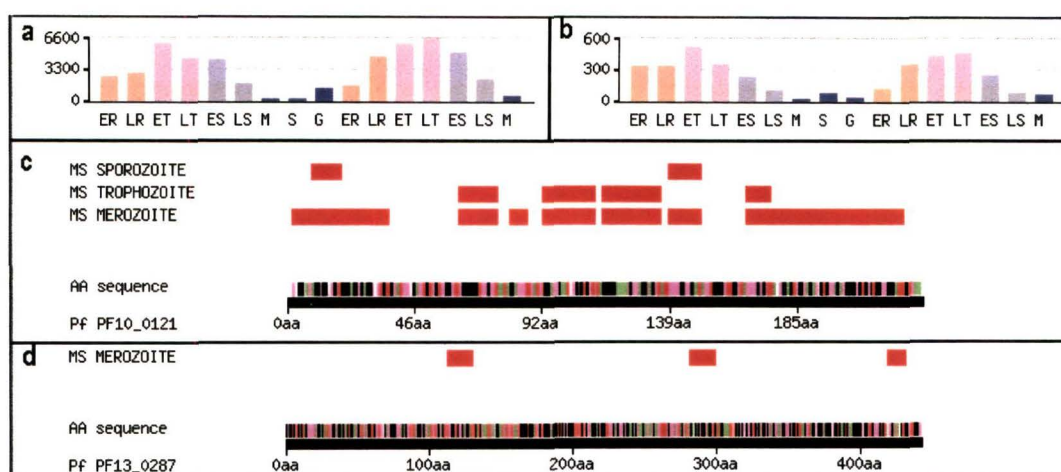


Figure 1.4: Stage specific expression profiles of PfHGPRT and PfAdSS. (a) and (b) show the levels of HGPRT and AdSS RNA in the parasite, respectively. (c) and (d) show the peptide fragments of HGPRT and AdSS detected in a proteome wide analysis of *P. falciparum*. Red bars indicate peptide fragments detected in the analysis. These expression profiles are taken from PlasmodB. (Bahl et al., 2003).

Expression and inhibition studies on the parasite

As mentioned earlier in this section, the publication of the *P. falciparum* genome has been followed by the proteome and transcriptome of the parasite. The stage specific expression profiles of *P. falciparum* HGPRT (PfHGPRT) and *P. falciparum* AdSS (PfAdSS) genes as detected by 25 residue oligonucleotide arrays is shown in Fig.4.4. Both these genes, being house keeping genes are expressed in all the parasite stages. The expression levels of HGPRT seem to be higher than AdSS. The proteome analysis detects peptides corresponding to HGPRT in all stages of the life cycle. Peptides corresponding to AdSS are however, detected only in the merozoites. (Fig. 4.4). The absence of detection in the mass spectrometric analysis is not conclusive evidence for the lack of expression. Western blot analysis with PfAdSS antibodies in our laboratory show that this enzyme is expressed in the intraerythrocytic stages of the parasite.

Many different inhibitors of HGPRT have been shown to kill the parasite in culture. These include 6-mercaptopurine ($IC_{50}=6.2 \mu M$) and 6-thioguanine

($IC_{50}=18 \mu M$) (Queen et al., 1990). 2-deoxycoformycin an inhibitor of adenosine deaminase leads to the depletion of hypoxanthine pools. This compound has been shown to dramatically reduce parasitemia in *P. knowlesi* infected rhesus monkeys indicating the importance of hypoxanthine in the parasites' purine metabolism (Luebke et al.,1991). Hypoxanthine depletion by the addition of xanthine oxidase also kills *P. falciparum* in culture (Berman et al.,1991). Hadacidin, a specific inhibitor of AdSS has also been shown to have antiparasitic activity (Webster et al., 1984). These studies demonstrate the importance of these two enzymes for the survival of the parasite.

Recent immunological investigations using native antigen fractions from rodent parasite *P. yoelii* have shown that parasite HGPRT is capable of activating the immune system through Th1 CD4⁺ T-cells (Makobongo et al., 2003). When extended to *P. falciparum* , the recombinant HGXPRT could activate T-cells *in vitro* and immunization of normal mice with recombinant HGXPRT reduced parasite growth following challenge. This observation qualifies HGXPRT as a vaccine candidate and further emphasizes its importance in parasite survival.

1.3 Phosphoribosyltransferases (PRTases)

PRTases catalyse the displacement of pyrophosphate from PRPP by a nitrogen containing nucleophile such as ammonia or purine or pyrimidine bases. The reaction results in an inversion of configuration at the anomeric carbon of PRPP. These enzymes belong to the PRT family of proteins that also comprises some regulatory proteins in addition to the PRTases (Sinha & Smith,2001). All members of this family contain a 13 residue motif consisting of 4 hydrophobic residues, 2 acidic residues and 7 of variable character. This motif constitutes the PRPP binding loop in PRPP binding proteins and the level of sequence homology beyond this motif is low.

In spite of the low sequence level similarity within this family, PRT proteins

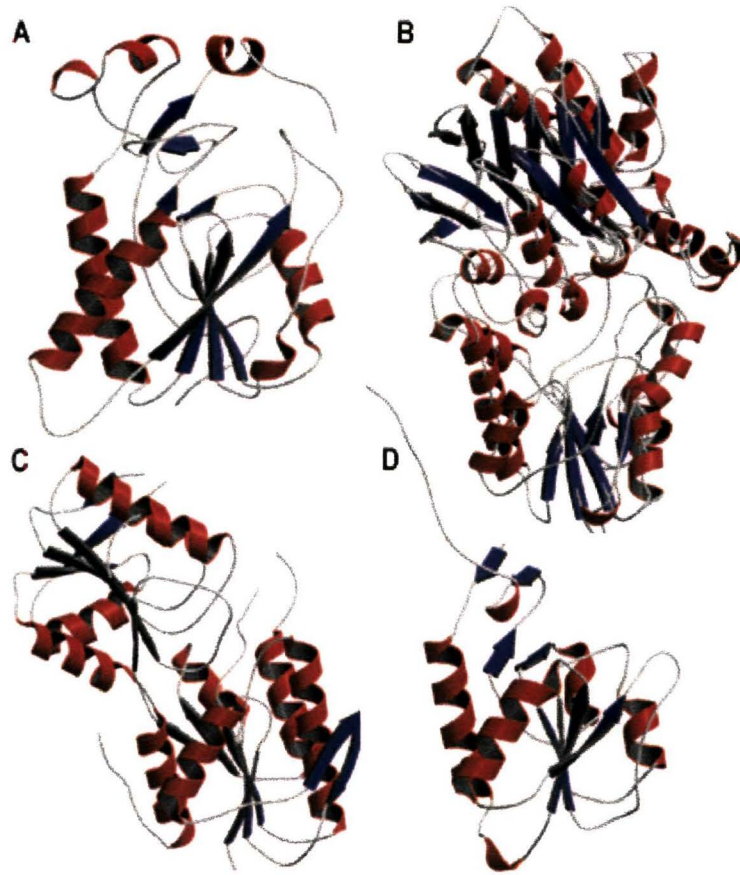


Figure 1.5: Structures of different PRTs. a) PfHGPRT(1CJB)(Shi et al., 1999a) b) *E. coli* GPATase(1ECC) (Krahn et al., 1997) c) *Bacillus subtilis* PRPP synthetase(1IBS)(Eriksen et al., 2000) d) *E. coli*XPRT(1NUL)(Vos et al., 1997). Only monomers are represented.

have a common structure (Fig. 1.5). The structure comprises a core consisting of 4-5 β -strands sandwiched between layers of α -helices, two on one side and at least one on the other. At the C-terminal edge of the core β -sheet is a second domain or subdomain known as the hood, formed by the N and C terminus of the protein (Sinha & Smith,2001). A pyrophosphate loop, conformationally conserved across the family is also involved in PRPP binding. A rare non-proline cis peptide bond between the 1st and 2nd residues of this loop may have an important role in PRPP binding and product release (Heroux et al., 1999a). Another structural feature common to this class of proteins is a flexible loop that closes over the bound PRPP in the PRTases (Sinha & Smith, 2001, Craig & Eakin, 2000). This loop is found to

be ordered only in the presence of Mg^{2+} -PRPP. The conformational response of the flexible loop to PRPP binding is used by these proteins for a variety of processes including catalysis (Ozturk et al., 1995), signalling and co-operativity. The most remarkable of these is the case of glutamine PRPP aminotransferase (GPAT) where the movement of the loop activates a second catalytic domain (the hood) leading to the production of the nucleophile, ammonia (Bera et al., 2000). The hood domain varies considerably with the enzyme (Fig. 1.5). In GPATase (Smith et al., 1994) and PRPP synthetase (Eriksen, et al., 2000) it forms a separate domain and is a subdomain in most PRTases (Craig & Eakin, 2000). The hood domain is involved in recognition of the base. In GPATase, the hood is catalytic and generates the nucleophile, ammonia.

Another class of PRTases, named the type II PRTases do not have the motif characteristic of the PRT family of proteins. Only one representative structure, that of quinolinc acid phosphoribosyltransferase exists (Sharma et al., 1998). The fold consists of an N terminal open-faced β -sandwich domain and a C terminal incomplete $\alpha - \beta$ barrel domain. The PRTases involved in histidine and tryptophan biosynthesis do not show sequence homology to either of the above class of enzymes. The structure of anthranilate phosphoribosyltransferase involved in tryptophan biosynthesis shows it to be different in its fold from both the above PRTase families (Kim et al., 2002). Designated a Type III PRTase, this enzyme is similar to the pyrimidine nucleoside phosphorylase II family of proteins. It is a two-domain protein, one domain being entirely helical and the other comprising a β -sheet surrounded by 8 helices. In all these three classes of PRTases, a metal ion mediates PRPP binding. The type I and III families also share the pyrophosphate binding motif. Catalyzing identical reactions these three classes of PRTases are an example of convergent evolution of similar catalytic roles.

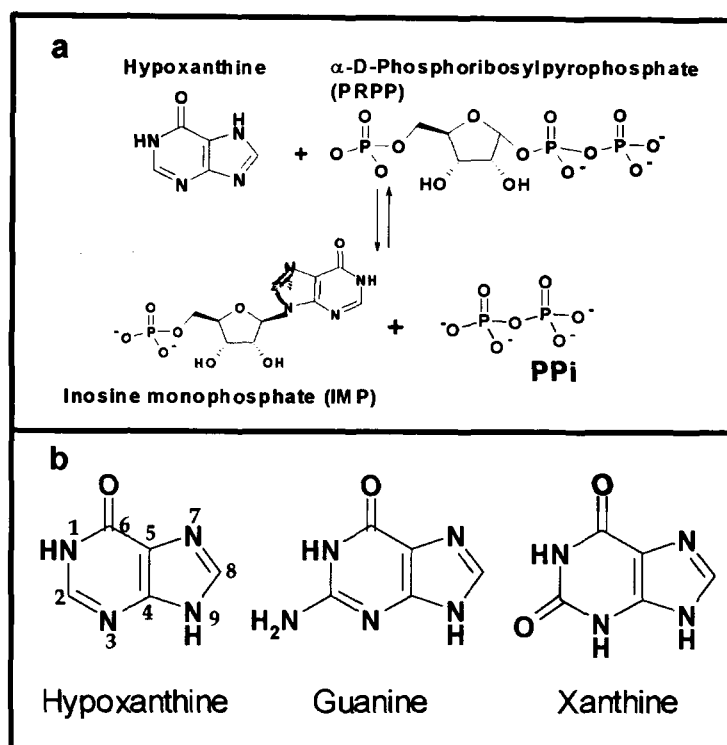


Figure 1.6: a) The reaction catalysed by HGPRT shown for the purine base hypoxanthine. b) The purine base substrates for HGPRTs.

1.3.1 6-oxopurine phosphoribosyltransferases

As the name suggests, these enzymes catalyse the phosphoribosylation of 6-oxopurine bases to their respective mononucleotides in a Mg^{2+} dependent reaction (Fig. 1.6a). The purine base (Fig. 1.6b) specificity of these enzymes varies with the species they are derived from. The human enzyme is a HGPRT, i.e. it takes up the purine bases hypoxanthine and guanine as substrates. The enzyme from many parasitic protozoa including *P. falciparum* is a HGXPRT, taking up the base, xanthine as a substrate in addition (Queen et al., 1988). *E. coli* has two enzymes, HPRT with weak activity on guanine (Guddat et al., 2002) and a GXPRT (Vos et al., 1997). The enzyme from the parasite *Giardia* is unique in being a GPRT (Sommer et al., 1996). In addition to these enzymes which take up 6-oxopurines as substrates, many organisms also have an adenine phosphoribosyltransferase for the salvage of adenine (Craig & Eakin, 2000). The length of the purine phosphoribosyltransferases

<i>P. falciparum</i>	-----MPIP	NNPAGENAF	DPVFKDDDG	YDLDSFMIPA	HYKKYLT EVL	VPNGVTKNRI	EKLAYDIKRV	64
<i>T. gondii</i>	GSHM	ASKPIE	DY-GKKGRI	EPMYIPDNTF	YNADDFLVPP	HCKPYIDKIL	LPGGLVKDRV	69
Human	-----	-----MATRSP	GVVISDDEPG	YDLDLFCIPN	HYAEDLERVF	IPHGLIMDRT	ERLARDVMKE	56
<i>T. foetus</i>	-----	-----	-----MTET	FMDDL ERLV	YNQDDIQKRI	RELAELTEF	34	
<i>T. cruzi</i>	-----	-----	-----MP	REYEFABKIL	FTEEEIRTRI	MEVAKRIADD	32	
<i>G. lamblia</i>	-----	-----MICSV	TGKPVKDVLS	TFFKDRNDVL	ESEVKKPHLI	ATFEECKALA	ADTARRMNEY	55
<i>E. coli</i>	-----	-----	-----	-----	-----MSEKYI	VTWMLQIHA	RKLASRLMPS	26
<i>P. falciparum</i>	YNN-----	-EPHILCLLK	GSRGFFTALL	KHLSRIHNYS	AVETSKPLFG	EHYVRVKSYS	NDQSTGTLEI	126
<i>T. gondii</i>	YFGE-----	-ELHIICILK	GSRGFFNLLI	DYLATIQKYS	GRESSVPPFF	EHYVRLKSYQ	NDNSTGQLTV	132
Human	MGGH-----	-HIVALCVLK	GGYKFPADLI	DIKALNRNS	--DRSIP-MT	VPFIRLKSVC	NDQSTGDIKV	116
<i>T. foetus</i>	YEDK-----	-NPMVICVLT	GAVFFYDILL	KHLDFQ----	-----LE	PDYIICSSYS	GTKSTGNLTI	85
<i>T. cruzi</i>	YKGGLRPYV	NPLVLSVLK	GSPFMTADLC	RALSDFN----	-----VPVR	MEPICVSSYG	EGVTSSGQVR	93
<i>G. lamblia</i>	YKDVA-----	EPVTLVALLT	GAYLYASLLT	VHLTFP----	-----YT	LHFVKVSSYK	GTRQES-VVF	107
<i>E. coli</i>	EQWKG-----	-----IIAVSR	GGLVPGALLA	RELGIR----	-----H	VDTVCISSYD	HDNQRELKVL	74
<i>P. falciparum</i>	VS-EDLSCLK	GKHLVIVEDI	IDTGKTLVKF	CEYLKKEFIK	TVAIACLFIK	RT-PLWNGFK	ADPVGFSIPD	194
<i>T. gondii</i>	LS-DDLSIFR	DKHVLIVEDI	VATGFTLTFE	GERLKAVGPK	SMRIATLVEK	RT-DRSNSLK	GDFVGFSTED	200
Human	IGGDDLSTLT	GKNVLIVEDI	IDTGKTMQTL	LSLVRQYNPK	MVKVASLLVK	RT-PRSVGYK	PDFVGFEPD	185
<i>T. foetus</i>	SK-DLKTNIE	GRHVLVVEDI	IDTGLTMYQL	LNNLQMRKPA	SLKVCTLCDK	DIGKKAYDVP	IDYCGFVVEN	154
<i>T. cruzi</i>	MLLDTRHSIE	GHEVLIVEDI	VDTALTLNLY	YHMYFTRRPA	SLKTVVLLDK	RE-GRRVPPS	ADYVYVANIPN	162
<i>G. lamblia</i>	DEE DLKQLKE	KREVVLIIDEY	VDSGHTIFS I	QEQIKHAKIC	SCFVKDVAI	KKHSALADT K	MFYGYTFMPK	177
<i>E. coli</i>	KR----AEGD	GEGFIVIDDL	VDTGGTAVAI	REMYPKAHFV	TIFAKPAG--	-----RPLV	DDYVVDIPQD	132
<i>P. falciparum</i>	-HFVVGYSLD	YNEIFRDLDH	CCLVNDEGKK	KYKATSL---	-----	-----	231	
<i>T. gondii</i>	-VWIVGCCYD	FNEMFRDFDH	VAVLSDAARK	KFEK-----	-----	-----	233	
Human	-KPVVGYALD	YNEYFRDLNH	VCVISETGKA	KYKA-----	-----	-----	218	
<i>T. foetus</i>	-RYIIGYGF	FHNKYRNLPV	IGILKESVYT	-----	-----	-----	183	
<i>T. cruzi</i>	-AFVIGYGLD	YDDTYRELRD	IVVLRPEVYA	EREAAQRKKQ	RAIGSADTDR	DAKREFHSKY	231	
<i>G. lamblia</i>	GSWLI GFGLD	DNGLRRGWAH	LFDINLSESE	VTEFRRRLTE	HIKGLNINGV	NRYQ-----	231	
<i>E. coli</i>	-----T WIEQ	PWDMGV	VFVPPISGR-	-----	-----	-----	152	

Figure 1.7: Sequence alignment of HGPRTs from different species. Alignment was performed using ClustalW

varies considerably with the smallest being the 150 amino acid long *E. coli* HPRT and the longest the 241 residue long *Leishmania donovanni* HPRT. Few residues are conserved across the purine phosphoribosyltransferases, the only recognisable motif being the PRPP loop (Fig. 1.7). The enzyme is active as an oligomer, with both dimeric and tetrameric forms reported. The only exceptions may be the *T. cruzi* (Focia et al., 1998a) and *T. foetus* (Somoza et al., 1996) where monomeric enzyme has been reported in solution.

1.3.2 Kinetic mechanism of HGPRTs

Kinetic analysis carried out on HGPRTs shows that it has an ordered Bi-Bi mechanism (Fig. 1.8). The first substrate to bind is PRPP, probably in complex with Mg^{2+} . This is followed by the binding of the purine (Xu et al., 1997). After product formation, pyrophosphate is released first followed by the release of the mononucleotide. Pre-steady state and steady state kinetic experiments carried out on human HGPRT show that the rate-determining step of the HGPRT reaction is not

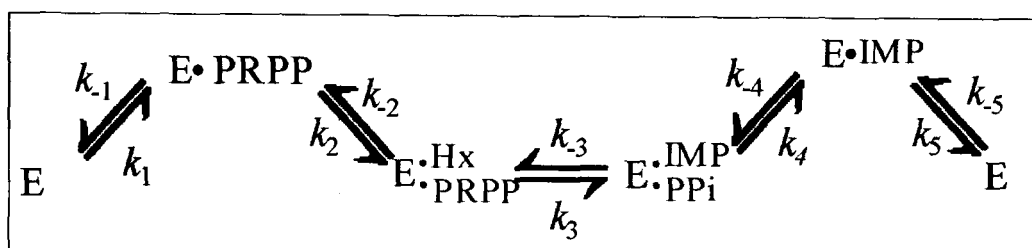


Figure 1.8: The ordered kinetic mechanism of HGPRTs.

product formation but the release of the mononucleotide. The K_d for the substrate PRPP is much lower than the K_m for this substrate. The human enzyme binds the purine base with millimolar K_d in the absence of PRPP. The K_d in the presence of PRPP is reduced 1000 fold with the K_m of the purine base being a few micromolar. In contrast, studies by Subbayya and Balaram, H. on the *P. falciparum* HGRRT have shown that this enzyme can bind the purine base in the absence of PRPP. This binding is non-productive and cannot be reversed by the addition of PRPP.

1.3.3 Substrate binding

Though the sequence identity even between HGPRTs from any two distantly related species is high, comparison of all available sequence data shows that only 11 residues are invariant. These residues are concentrated around the active site or are located in loop II (Craig & Eakin, 2001). The structure of HGPRTs in context of substrate binding and catalysis is discussed in this section.

Crystallographic studies have led to the identification of 5 flexible loops in HGPRTs that get ordered on substrate binding. These loop movements explain the ordered sequential mechanism of the enzyme (Heroux et al., 1999a). Loop I or the phosphate loop contains the cis peptide bond that is important for the binding of PRPP. Loop II undergoes dramatic movements, with one end of the loop moving as much as 20Å on substrate binding. This loop folds over the active site during catalysis. Loop III gets ordered on the recognition of the 5' phosphate group of PRPP and nucleotides. Loop III' is purported to play a role in the linking up of the

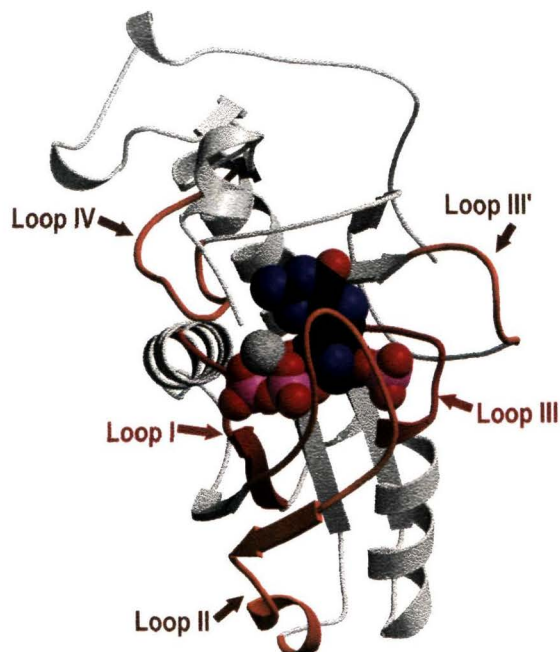


Figure 1.9: Flexible loops in HGPRTs. Ribbon representation of the human HGPRT structure in complex with Immucillin GP (1BZY). The five flexible loops implicated in HGPRT catalysis are indicated in red and Immucillin GP in space fill representation

hood and core domains after substrate binding. Loop IV is predominantly involved in the recognition of the purine base (Fig. 1.9). The availability of structures of different complexes of HGPRTs representing different stages of the catalysis allows speculation on the mechanism of the reaction and the motion of the reaction coordinate. These include structures of the 1) *T. gondii* (Heroux et al., 2000) and *T. foetus* HGPRTs with the purine analog 9-deazaguanine and the substrate PRPP representing the substrate bound state, 2) human and *P. falciparum* enzymes with immucillin HP and GP (transition state analogs of HGPRT)(Shi et al., 1999a, Shi et al., 1999b), respectively, representing the enzyme conformation during catalysis and 3) product bound forms of the enzyme from many species representing the conformation of the protein after product formation but before release (Eads et al., 1994, Somoza et al., 1996, Heroux et al., 1999a, Heroux et al., 1999b, Vos et al., 1998) and 4) the HGPRT apo enzyme from many species (Schumacher, 1996).

The purine base contacts with the protein are predominantly at the C terminus of

the protein. Structurally these residues are part of the hood domain of the protein. A feature common to all HGPRTs is the presence of an aromatic residue that stacks over the purine base. This corresponds to F197 in PfHGPRT and F184 in human HGPRT. In addition, an invariant aspartate (D148 in PfHGPRT) contacts the N7 of the purine base, an interaction believed to be important to catalysis. The purine contacts are discussed in detail in Chapter 2. PRPP is cradled between active site loops I and III which form an extensive network of hydrogen bonds with the phosphate and pyrophosphate groups, primarily through main chain atoms. One metal ion binding site is located on either side of the PRPP pyrophosphate group. A conserved non-proline cis peptide in loop I exposes the amide nitrogen to the active site so that the peptide bond between Leu67 and Lys68 contributes two adjacent hydrogen bonds to the PRPP-metal complex. The PRPP binding motif, also conserved among type I PRTs, contributes active site loop III which encircles the ribose-phosphate group (Focia et al., 1998b).

1.3.4 The HGPRT reaction

Based on the different complexes of HGPRT whose structures have been determined, Borhani and co-workers have proposed a sequence of events that occur during catalysis by HGPRTs (Heroux et al., 1999a). The binding of the apo-enzyme to PRPP, the first event in the catalytic process, is proposed to be aided by the isomerization of the peptide bond between a Lys and Gly in loop I (Lys89 and Gly90 in PfHGPRT) to its cis configuration. PRPP binding results in the organization of the purine binding pocket as loop I and loop IV are drawn together. Loop III is also ordered bringing in the catalytic aspartate into position for catalysis. The movement of loop III allows loop III' to approach the active site. Purine binding follows allowing the complete organization of loop III', followed by the closure of loop II over the fully occupied active site. Loop II closure probably brings the substrates bound in the active site closer together, leading to product formation. Fig. 1.9 shows these loops in the fully ordered conformation. Product formation

weakens the interaction of loop II resulting in its opening allowing pyrophosphate release. Borhani and co-workers propose that pyrophosphate release is assisted by the isomerization of the cis peptide bond formed at the beginning of the catalytic cycle back to the trans configuration. This inference is based on the observation of the peptide bond in both these conformations in different complexes of HGPRT. The other loop movements that occur as a consequence of PRPP binding probably are reversed culminating in the release of the newly formed nucleotide. The large movements of the protein that need to occur before product release may be responsible in making this step the rate determining step of HGPRT catalysis.

This proposed mechanism however, remains a matter of debate. In the absence of a structure with PRPP alone bound to the enzyme, the exact loop movements that occur due to PRPP binding remain conjectural. The cycling of the peptide bond in the P_{Pi}-loop between the cis and trans configurations within the timescales of the reaction remains a matter of speculation. Mutation of the Lys involved in the cis peptide bond to a proline in the *T. cruzi* enzyme does not affect enzyme activity suggesting that this cycling may not be important to catalysis (Canyuk et al., 2004). Catalysis in HGPRTs is proposed to be aided by Asp 148 (this aspartate is conserved across HGPRTs) that acts as a catalytic base and abstracts a proton from the N7 position of the purine base. This residue corresponds to an alanine in APRT. The catalytic base in this case is thought to be brought into the active site by the closure of loop II (Shi et al., 2001). Abstraction of the proton from the N7 position of the purine base generates a nucleophilic center on N9 (Xu & Grubmeyer, 1998). The two metal ions that are present in the active site probably facilitate the reaction, with their electron withdrawing potential activating P_{Pi} as the leaving group. Mutation of the catalytic aspartate to alanine however does not abolish catalysis with significant activity on the purine base, hypoxanthine being retained (Xu & Grubmeyer, 1998). Many HGPRTs also take up the purine analog, allopurinol that lacks the N7 nitrogen, as a substrate (Shivshankar et al., 2001). These observations question the importance of this catalytic base in the HGPRT

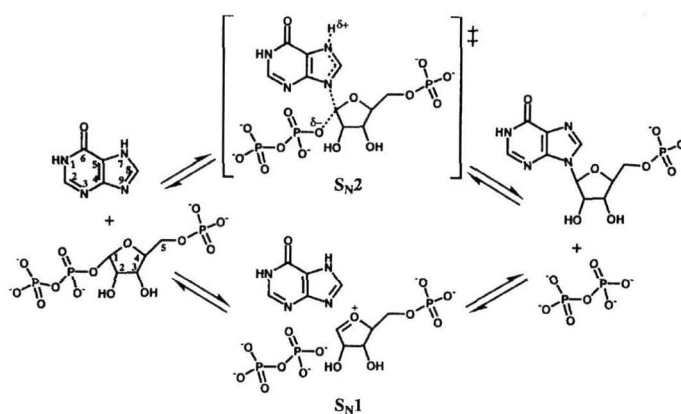


Figure 1.10: Proposed reaction mechanisms for the HGPRT catalyzed reaction

572
P06

reaction. pH activity profiles of the enzyme however, show a steady increase in activity of the enzyme with pH, showing that the ionization of the Asp148 does lead to an increase in activity of the enzyme (Xu & Grubmeyer, 1998). The possibility that the actual substrate for the reaction may be the anionic form of the substrate which would not require the base catalysis for generation of the nucleophile (Craig & Eakin, 2000) has also been raised. It has also been suggested that the enzyme may not contribute much to the fast rates for phosphoribosyl transfer beyond bringing the substrates in close proximity in the correct orientation for catalysis (Sinha & Smith, 2001).

1.3.5 The HGPRT reaction mechanism

Two schools of thought exist on the reaction mechanism: one proposing a dissociative S_N1 mechanism and the second an associative S_N2 mechanism (Craig & Eakin, 2000) (Fig. 1.10) Crystallographic evidence exists supporting both these schemes. The S_N1 mechanism has been proposed on the basis of the mechanism elucidated for the related enzymes, purine nucleoside phosphorylases where kinetic isotope effect measurements along with detailed kinetic analysis have unequivocally established a dissociative mechanism (Horenstein & Schramm, 1993). In the case of HGPRT, an S_N1 reaction would involve the formation of a labile ribooxocarbenium ion intermediate that would serve as a nucleophilic center for the next step of the

reaction (Li et al., 1999). Due to the susceptibility of this intermediate to hydrolysis by water, sequestration from the solvent would be necessary during catalysis. The closure of loop II over the active site observed in the substrate and transition state complexes, is thought to play a role in this sequestration (Shi et al., 1999a, Shi et al., 1999b). The slow onset, tight binding of the immucillin phosphate, designed to mimic the S_N1 transition state also lends credence to the S_N1 mechanism (Li et al., 1999).

However, considerable evidence also exists that favours the S_N2 mechanism. The closure of loop two does not completely exclude water from the active site. Water, sufficient to quench the reactive intermediate remains trapped in the active site after loop closure (Heroux et al., 1999b). In the substrate complexes of HGPRTs, the pyrophosphate is not cleaved from PRPP as would be expected in a dissociative mechanism (Focia et al., 1998b). The nature of the designed transition state inhibitor is such that it can bind to the protein even if the mechanism were to be S_N2 . The interaction of this analog with the protein in the malarial and human structures are also not indicative of the S_N1 mechanism. Stabilization in the case of an S_N1 mechanism would be expected to be through strong electrostatic interactions. Rather, the binding of the pyrophosphate in these complexes is stabilised by interaction with Mg^{2+} and by interactions resulting from the pucker of the ribose ring (Heroux et al., 1999a). Mutants of *T. foetus* HGPRT with loop II deleted retain significant though impaired activity (Lee et al., 2001). The literature thus remains inconclusive about the mechanism, though the evidence seems to favour an associative mechanism with bond breakage and bond formation occurring simultaneously.

Another question, the answer to which has remained elusive is the basis for the substrate specificity of HGPRTs. Of special interest is the xanthine specificity of many HGPRTs. This aspect forms the subject of the studies discussed in chapter 2 of this thesis. Mutagenesis and structural studies in literature that address this question are therefore, discussed in Chapter 2.

1.4 Adenylosuccinate synthetase (AdSS)

Adenylosuccinate synthetase follows HGPRT in the salvage pathway and *P. falciparum* AdSS (PfAdSS) forms the subject of the latter part of this thesis. AdSS catalyses the condensation of IMP with aspartate in a Mg^{2+} requiring reaction resulting in the formation of adenylosuccinate (ADS) (Lieberman, 1956). The reaction is accompanied by the hydrolysis of a molecule of GTP to GDP. ADS is then cleaved by a lyase to AMP. IMP also serves as a precursor for GMP. Conversion to GMP involves the enzymes IMP dehydrogenase (IMPDH) and GMP synthetase (GMPS). GMPS uses the hydrolysis of ATP to drive the transfer of the amino group from glutamine to XMP formed by the oxidation of IMP by IMPDH (Reyes et al., 1982). The AdSS reaction commits the fate of IMP to the synthesis of AMP and co-ordinate regulation of AdSS and GMPS is thought to play a role in the regulation of ATP/GTP ratios in a Cell (Borza et al., 2002). The pronounced A/T bias of the *P. falciparum* genome would require significantly skewed ATP/GTP ratios as compared to the human host. Study of *P. falciparum* AdSS therefore, gains importance. This section summarises the literature on AdSS.

1.4.1 Isozymes

Bacteria contain a single AdSS gene that is involved in both the *de novo* and salvage pathways for purine nucleotide synthesis (Stayton et al., 1983). This is also the case with yeast where a single *ade2* gene has been implicated, in addition to its role in nucleotide metabolism, to have a regulatory function. The yeast AdSS has been shown to bind ssDNA corresponding to the consensus sequence for the yeast autonomously replicating sequence. (Zeidler et al., 1993). Modelling studies on the yeast enzyme indicate the presence of a large positively charged surface on the molecule distinct from the active site of the enzyme (Sticht et al., 1997). The binding of DNA has also been shown to inhibit the activity of the enzyme. The substrate, IMP, GTP and aspartate however, do not affect the DNA binding property.

In vertebrates, two isozymes exist with distinct tissue distribution (Guicherit et al., 1994). The basic isozyme, also called the muscle isozyme, is predominant in muscle tissue including cardiac tissue and plays a role in the purine nucleotide cycle. This isozyme is involved in the maintenance of AMP pools in the muscle during intense contraction. The acidic isozyme which has a more general tissue distribution and lower expression acts in the *de novo* purine nucleotide biosynthetic pathway.

Comparison of the AdSS sequence from these different sources (Fig. 5.1) shows a high degree of similarity. The P-loop or the phosphate binding loop, common to all GTP binding proteins is present at the N-terminus of the protein. Other highly conserved sequence stretches correspond to regions that have been implicated in substrate binding and catalysis by biochemical and crystallographic studies.

1.4.2 AdSS Kinetics and Mechanism

The reaction catalysed by AdSS is illustrated in Fig. 1.11. Three mechanisms have been proposed for the reaction. The formation of labelled phosphate when the reaction was carried out with 6-¹⁸O-IMP as the substrate led Liberman (1956) to propose 6-phosphoryl-IMP as an obligatory intermediate in the reaction. Miller and Buchanan (19) suggested a concerted mechanism with three simultaneous bond formation and bond breaking steps. Markham and Reed proposed a mechanism in which aspartate adds on to C-6 of IMP forming a tetrahedral intermediate. The oxyanion of this intermediate was proposed to be eliminated after phosphorylation by GTP. Bass et al. (1984) demonstrated the exchange of ¹⁸O label from the $\beta - \gamma$ bridging position to a non-bridging position of GTP in the presence of AdSS and IMP but not in the absence of IMP or the enzyme. This would require the dissociation of the γ -phosphate of GTP for sufficiently large time scales to permit positional isomerization at the β -phosphate. This IMP dependent exchange lends credence to the phosphoryl-IMP intermediate proposed by Liberman. The presence of 6-phosphoryl-IMP in the crystals of both mouse and *E. coli* AdSS grown in

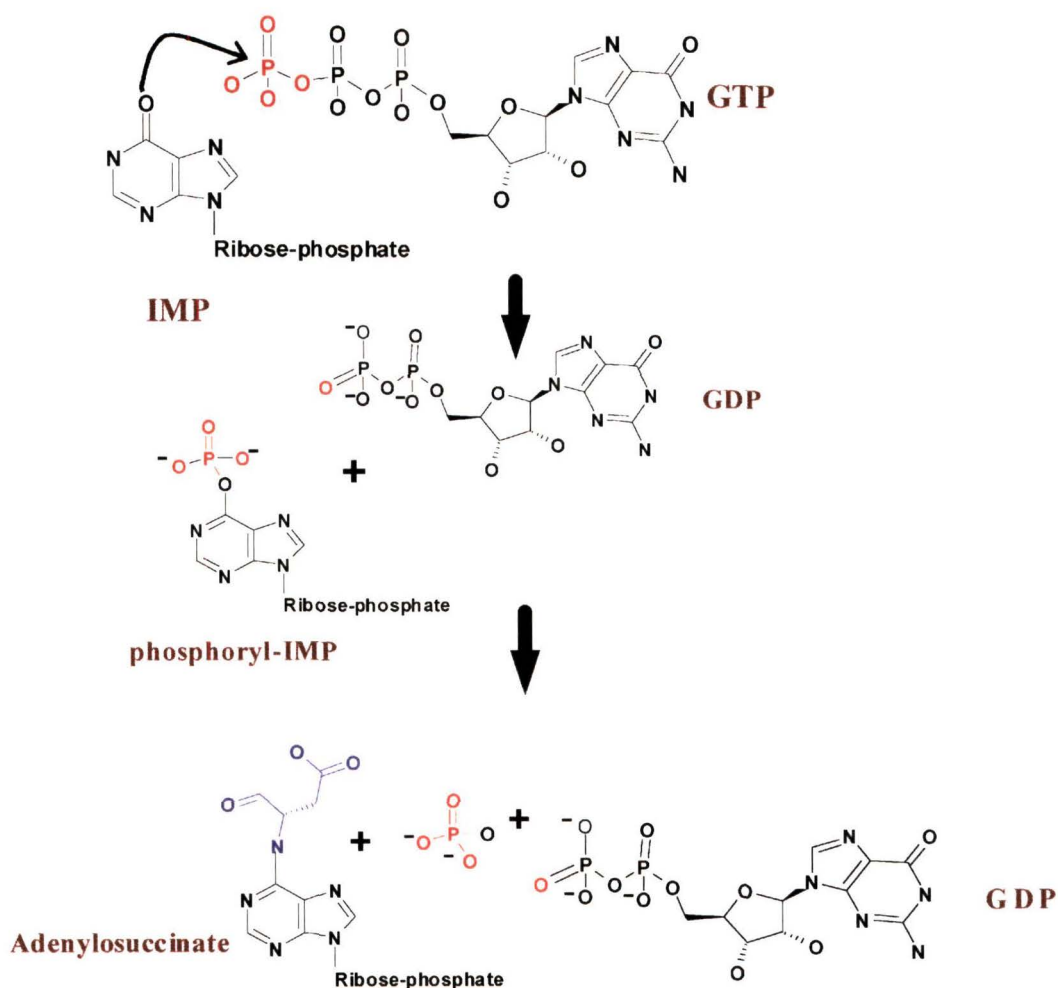


Figure 1.11: The reaction catalysed by adenylosuccinate synthetase.

the presence of IMP and GTP has conclusively established the formation of this intermediate (Inacu et al., 2002a, Choe et al., 1999).

The kinetic mechanism of all reported AdSS is rapid-equilibrium random sequential (Rudolph & Fromm, 1969). All the substrates of the reaction can bind to the enzyme independently though catalysis of the reaction that proceeds through a defined intermediate requires the presence of all the substrates together at the active site. The enzyme in most cases is a monomer-dimer equilibrium in dilute solution in the absence of ligands (Wang et al., 1997a, Kang et al., 1996). The active site of the enzyme lies at the dimer interface with residues from one subunit contributing to the IMP binding pocket of the other subunit (Honzatko et al., 1999, Honzatko

& Fromm, 1999). The dimer is therefore, stabilised by IMP binding. The maize AdSS has been reported to be monomer in solution as ascertained by gel filtration, but dynamic light scattering shows it to be a dimer which is most likely to be the active form (Prade et al., 2000).

1.4.3 Structure of AdSS and catalysis

E. coli and mouse AdSS have been studied extensively and various crystal structures of these enzymes including unligated (Silva et al., 1995, Inacu et al., 2001), partially ligated (Poland et al., 1997, Hou et al., 2002, Inacu et al., 2002a) and fully ligated (Poland et al., 1996a, Inacu et al., 2002a) structures are available. These allow a detailed interpretation of the catalytic process (Choe et al., 1999). The enzymes from both these sources are largely identical and the residue numbering corresponding to *E. coli* AdSS is used in this discussion.

The core of the protein is a β -sheet of 9 parallel strands and a 10th anti-parallel strand. These segments are connected by segments of the polypeptide that range in size from small loops to large sub-domains. The functional elements of the structure, including the regions that undergo large conformational changes on ligand binding, are largely contributed by these connecting segments. Six loops that undergo conformational changes on ligand binding have been identified from the structural analysis. All but one of these loops are organized by the binding of IMP.

Active site organization

The active site of AdSS is at the dimer interface, with residues from both subunits contributing to the two active sites. The cross subunit interaction primarily contributes to the IMP pocket and this substrate is known to stabilise the AdSS dimer. GTP can bind to the protein in the absence of IMP, but complete organization of the GTP pocket requires the presence of IMP (Poland et al., 1996b, Hou et al., 2002, Inacu et al., 2002a). The β and γ phosphates of GTP are not recognized when it binds to the protein in the absence of IMP. No aspartate bound crystal

structures of the enzyme are available. However, an aspartate analog hadacidin (Fig. 1.12) has been co-crystallised with both the *E. coli* (Poland et al., 1996a) and mouse enzymes. This analog co-ordinates Mg^{2+} through its N-formyl group, and

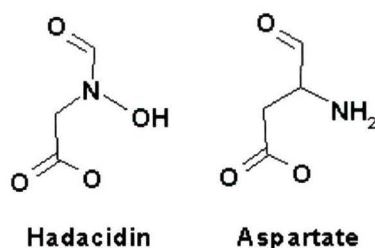


Figure 1.12: Structures of hadacidin and aspartate

H-bonds with Asp13 and Arg305 through its N-hydroxy group. The β -carboxylate interacts with Arg303 and Thr301. Poland et. al (1996a) have suggested on the basis of model building that the α -carboxylate of aspartate probably co-ordinates Mg^{2+} and hydrogen bonds to the backbone carbonyl of 38 and to its own β -carboxylate. Kinetic studies by Kang & Fromm (1995) implicate two Mg^{2+} ions in the AdSS reaction, one implicated in GTP binding and the other presumably in aspartate binding. However, only one has been found in all the crystal structures determined so far, coordinating both GTP and hadacidin (and presumably aspartate). The absence of the second Mg^{2+} has been attributed to the lower pH of the crystallisation and to the presence of the aspartate analog hadacidin and not aspartate itself in the crystals (Honzatko et al., 1999). The enzyme itself does not play a great role in the co-ordination of Mg^{2+} , with the predominant contacts of this metal ion being with the ligands. Only two of the 6 co-ordinations are through the protein. These are through the catalytic residues Asp13 and His41, the alteration of whose pK_a due to the co-ordination has a role in catalysis. Extensive mutagenesis and structural studies by Fromm and coworkers have led to an understanding of catalysis by AdSS.

The first reaction of the proposed two-step mechanism (Lieberman, 1956) requires only IMP, GTP, and Mg^{2+} . Asp13 putatively abstracts the proton from the N1 atom of IMP, forming the 6-oxyanion of IMP. Mg^{2+} and His41 stabilise charge development on the β -phosphoryl group of the guanine nucleotide, the former by

coordinating to the bridging oxygen atom between the $\beta - \gamma$ phosphoryl groups and the latter by hydrogen-bonding with a terminal oxygen of the γ -phosphoryl group of GTP. The three terminal oxygen atoms of the γ -phosphoryl group of GTP participate in numerous hydrogen-bonds which are essentially identical to those of the 6-phosphoryl group of 6-phosphoryl IMP. After formation of 6-phosphoryl IMP, Asp13 (now protonated) moves into the coordination sphere of the catalytic Mg^{2+} . As a consequence, Asp13 becomes a catalytic acid and re-protonates the N1 atom of 6-phosphoryl IMP, thereby generating the C6 cation of the intermediate. Binding of aspartate initiates the next step of catalysis. Nucleophilic attack by the α amino group of aspartate on the C6 of 6-phosphoryl IMP displaces the phosphate group leading to the formation of adenylosuccinate.

1.5 Inhibitors and substrate analogs of HGPRT and AdSS

Due to the central role of purine nucleotide metabolism in any actively metabolising cell, inhibition of HGPRT and AdSS is of importance and has attracted attention in therapeutics against cancers and infective diseases. Since the product of the HGPRT reaction serves as a substrate for the AdSS reaction, subversive substrates of the former may be used to target AdSS. Subversive substrates can also be channelled into the nucleotide pool of the cell and thereby used to retard cell growth. Inhibitors of both these enzymes are therefore discussed together here. The discussion here is restricted to non-physiological inhibitors of the enzyme.

1.5.1 HGPRT

Numerous molecules with inhibitory effects on HGPRTs have been identified (Queen et al., 1990, Eakin et al., 1997). Due to the similar structures of HGPRTs from various sources and the common mechanism, species specific inhibition is however, difficult to achieve. Inhibitors tried include transition state analogs, purine analogs and non-purine based compounds identified by structure based approaches.

The HGPRT reaction has been predicted to proceed through a ribooxocarbenium ion intermediate based on analogies with the transition state of the purine nucleoside phosphorylases (PNP) (Li et al., 1999). Immucillins are transition state analogs of PNPs with a nitrogen replacing the oxygen atom of the sugar ring, a carbon replacing N9 and a protonated N7 atom (Miles et al., 1998). Protonation of N1' leads to positive charge on the ring analogous to the sugar giving rise to a ribooxocarbenium ion like molecule. Immucillin phosphates, mimicking the transition state of HGPRTs have been shown to be inhibitors of the HGPRT reverse reaction (Li et al., 1999). The inhibition is slow onset tight binding with nM K_i s. These inhibitors have been crystallised with the human malarial and *Giardia* PRTs (Shi et al., 1999a, Shi et al., 1999b, Shi et al., 2000). The structures do not show electrostatic complementarity between the protein and the inhibitor, a feature characteristic of transition state analogs. The exact ionization state of the analog when it binds to the enzyme is also not clear (Craig & Eakin, 2000). It has been proposed that the form of Immucillin phosphates that bind to the enzyme is the neutral form based on pH dependent NMR studies. Slow conversion within the enzyme active site to the protonated ion increases binding affinity and is responsible for the slow on set tight binding inhibition (Li et al., 1999).

Selective competitive inhibitors of *T. foetus* HGPRT have been designed using the DOCK program based in the structure of this enzyme exploiting the differences seen in the product GMP binding pocket. 4-[N-(3,4-dichlorophenyl)carbamoyl]phthalic acid, a compound identified in this structure based rational screen had micromolar K_i s for the *T. foetus* enzyme with inhibition of the human enzyme seen only with mM concentrations of the inhibitor. Further virtual optimization followed by two rounds of screening of libraries created by combinatorial chemistry have identified an inhibitor with a K_i of 0.49mM with 30 fold greater specificity for the *T. foetus* enzyme. Both these inhibitors have low EC_{50} values on cultured *T. foetus* cells with the addition of excess purine reversing the inhibition (SOMazo et al., 1998, Aronov et al., 2000). Similar approaches have also been used to design potent

inhibitors of the *T. cruzi* (Freyman et al., 2000) and Giardia enzymes (Aronov et al., 2001)

Though a number of purine analogs are known to inhibit HGPRT, these remain non-viable alternatives *in vivo* as the K_m s for the purine base substrates that these would have to compete with are very low.

1.5.2 AdSS

Amino acids that serve as substrates for the AdSS reaction, with the exception of hydroxylamine, all have a functional group similar in charge to the β -carboxylate of aspartate. These include alanine-3-nitronate, cysteine sulphonate and L-alanosine. dGTP and GTP γ -S replace GTP as substrates. IMP analogs that serve as AdSS substrates include 2-deoxy-IMP and β -D-arabinosyl IMP (Stayton et al., 1983).

One of the most potent inhibitors of the enzyme is the fungal metabolite hadacidin (N-formyl-N-hydroxyglucine). This aspartate analog with micro molar K_i , isolated from the fermentation broths of *Penicillium frequentans*, is a highly specific inhibitor of AdSS. Analogs of hadacidin, N-acetyl-N-hydroxyglycine, N-formylglycine, N-hydroxyglycine, and N-actylglycine inhibit AdSS with much lower efficiency (Jahngen & Rossomando, 1984). L-alanosine (L(-)-2-amino-3-(hydroxynitrosamino)propionic acid) acts as an inhibitor of AdSS after being converted to L-alanosyl-5-amino-4-imidazolecarboxylic acid ribonucleotide by the *de novo* purine biosynthesis enzyme, AICAR synthetase (Tyagi & Cooney, 1980). Alanosine therefore, does not show any inhibition in most parasitic protozoa as they lack the enzymes for *de novo* purine nucleotide synthesis (Webster et al., 1984).

Hydantocidin, a spirocyclic hydantoin riboside, and a potent herbicide with low toxicity to mammals exerts its effect through AdSS (Siehl et al., 1996). This proherbicide requires phosphorylation of its 5'-OH to become active. Hydantocidin-5'-phosphate is an IMP analog with a K_i of 22 μ M in the presence of GDP, Mg^{2+} and aspartate (Walters et al., 1997). In crystal structures with the *E. coli*

AdSS, its interactions are identical to that of IMP except that it does not interact with Asp13 which is left free to co-ordinate with Mg^{2+} (Poland et al., 1996c). Hanessian and co-workers (Hanessian et al., 1999) synthesised hybrid molecules of hydantocidin phosphate and hadacidin and demonstrated the higher potency of this hybrid molecule in inhibiting AdSS. The crystal structure of *E. coli* AdSS in complex with this hybrid inhibitor showed that as expected, the inhibitor occupies both the IMP and aspartate binding sites of the enzyme.

1.5.3 Subversive substrates

The anti-leishmanial agent allopurinol owes its efficacy and specificity to its selective incorporation into the nucleotide pool of the organism after amination at the C6 position by the concerted action of both AdSS and ADS lyase of the parasite. The allopurinol riboside monophosphate that serves as the substrate for AdSS is generated by the action of adenosine kinase. Allopurinol riboside is in fact a better antileishmanial agent (Spector, 1984). 6-mercaptopurine, a drug used in the treatment of some cancers is converted into the nucleotide by the action of HGPRT. The product, 6-mercaptopurine ribonucleotide is an inhibitor of AdSS, binding to both the GTP and IMP sites of the mammalian enzyme (Bridger & Cohen, 1963). The inhibition of the *E. coli* enzyme is more potent and competitive with IMP alone (Stayton et al., 1983).

This thesis describes studies on *P. falciparum* hypoxanthine guanine phosphoribosyltransferase and adenylosuccinate synthetase. Since AdSS is a regulatory enzyme in purine nucleotide synthesis, inhibition by the products of the reaction adenylosuccinate and GDP and, by AMP and GMP is also significant (Honzatko et al., 1999). Studies on the inhibition by these nucleotides are discussed in chapter IV of this thesis.

Chapter 2

Studies on a xanthine active mutant of human hypoxanthine guanine phosphoribosyltransferase (HGPRT) generated by random mutagenesis.

A random mutagenesis approach used to obtain a xanthine active mutant of human HGPRT is described in this chapter. The randomly mutagenesised library used in this study was available in the laboratory at the time of initiation of these experiments.

2.1 Introduction

Hypoxanthine guanine phosphoribosyltransferases catalyse the Mg^{2+} dependent conversion of 6-oxopurine bases to their respective mononucleotides. The purine base specificity of this enzyme varies with the species it is derived from. The mammalian, yeast (Sloan et al., 1984), *Trypanosoma cruzi* (Allen and Ullman, 1994), *Leishmania donovani* (Allen et al., 1995) and *Schistosoma mansoni* (Dovey et al., 1996) PRTs recognize hypoxanthine and guanine while the enzyme from the parasites *Tritrichomonas foetus* (Beck & Wang, 1993), *Toxoplasma gondii* (Naguib et al., 1995) and *P. falciparum* (Queen et al., 1988) can recognize xanthine in addition. The enzyme from *Giardia lamblia* can phosphoribosylate guanine alone (Sommer et al., 1996). *E. coli* has two enzymes, a HPRT and a GXPRT (Vos et al., 1997). Comparison of the sequences of these enzymes does not reveal the basis

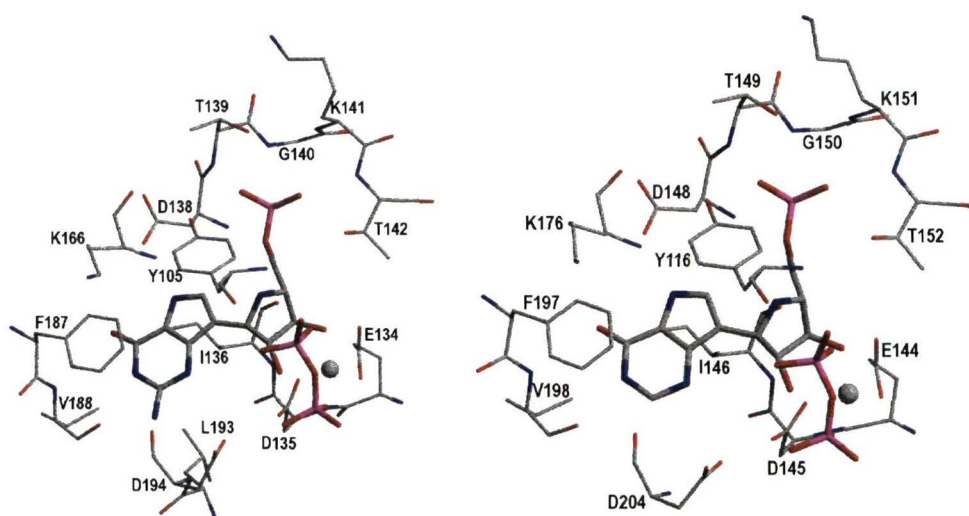


Figure 2.1: The contacts made by ImmucilinGP and ImmucillinHP in human (left) and *P. falciparum* (right) HGPRTs respectively, at a cutoff of 3.5Å. The PDB coordinates 1BZY (human) and 1CJB (*P. falciparum*) were used.

of these differences. The structures of a number of these enzymes have also been determined but the purine binding pockets have been found to be largely identical (Shi et al., 1999a, Shi et al., 1999b, Vos et al., 1997, Heroux et al., 1999a, Heroux et al., 1999b, Somoza et al., 1996, Eakin et al., 1997, Eriksen et al., 2000). The reasons for the differences in base specificity remain ambiguous.

2.1.1 Purine recognition in HGPRTs

The residues involved in the recognition of the purine base in *P. falciparum* and human HGPRTs are shown in Figure 2.1. The contacts are derived from the structures of these enzymes complexed to transition state analogs, Immucillins (Immucillin HP: (1S)-1(9-deazahypoxanthin-9-yl)1,4-dideoxy-1,4-imino-D-ribitol-5-phosphate). The G and H in the names of these analogs refers to the guanine and hypoxanthine equivalents of the analog, the P to the phosphorylated derivatives. Residue numbering for the human enzyme for the purpose of this discussion are with reference to the amino terminal Met taken as residue 1. As can be seen from the figure, the contacts made by the bases are identical in the two enzymes. Asp138 is thought to play the role as a catalytic base in abstracting a proton from

the N7 position leading to the generation of a negative charge at N9 aiding the attack of the ribose moiety. Phe187 stacks over the purine ring and is important for purine binding. Recognition of the amino group of guanine is through hydrogen bonding with the backbone carbonyl of Asp194 and this residue is conserved across HGPRTs.

Analysis of the crystal structures of *T. gondii* HGPRT in complex with the nucleotides IMP, GMP and XMP have led Heroux et al., (1999a, 1999b) to suggest that the purine recognition specificity does not lie in just a few residues but is a consequence of many subtle differences between enzymes. Examination of the structures highlights several differences between the human and *T. gondii* enzymes. Recognition of the N2 amino group in GMP in the human enzyme is through the peptide oxygens of Asp194 and Val188, residues that form part of Loop IV. Such an interaction would be unfavorable if the C2 substituent were to be a carbonyl group as in xanthine. The recognition of GMP in *T. gondii* is also similar with the backbone carbonyl of Asp206 hydrogen bonding to the amino group on guanine. However, in the XMP complex of the same enzyme, a shift of Loop IV allows the C2 carbonyl of xanthine to hydrogen bond to the Asp206 NH rather than to the peptide oxygen. A slight rotation of the purine ring also contributes to a reduction in the unfavorable interactions.

Other differences between the GMP and the XMP complexes of the *T. gondii* enzyme include a shift of Loop IV towards hypoxanthine and xanthine along with an alteration in the ϕ ψ angles of the residues C203 and C204 into favored regions of the Ramachandran plot. A similar shift in the GMP complex would be detrimental as the peptide NH and the N2 of GMP would be too closely apposed. The C-terminal α -helix of *T. gondii* HGPRT is also shifted closer to the active site in the IMP and XMP complexes. All these changes are accommodated by global changes in the hood domain residues of the enzyme and these observations seem to suggest that the additional specificity of some parasite enzymes may be a consequence of increased flexibility of the hood domain of the protein.

2.1.2 Altered specificity mutants of HGPRTs

Site-directed mutagenesis and chimeragenesis have been used to address the substrate specificity in HGPRTs. Though purine recognition residues lie at the C-terminus of the protein, substitution of the first 50 amino acids of human HGPRT with the corresponding residues of *P. falciparum* HGPRT results in an enzyme with additional specificity for xanthine (Sujoy Subbayya et al., 2000). Chimeric human and *T. gondii* HGPRTs with lack of activity on xanthine also find mention in literature (Heroux et al., 1999b). This chimera has the Loop IV residues 204-208 of the *T. gondii* enzyme substituted with the corresponding residues from the human enzyme. Both these observations support the interpretation from the crystal structures described above that Loop IV residues and hood domain reorganization play a role in xanthine recognition by HGPRTs.

Munagala and Wang (1998) have carried out extensive mutagenesis on the residues involved in purine recognition in the *T. foetus* enzyme. Mutation of the conserved Lys134 involved in the recognition of the 6-oxo group of the purine to Ser results in an enzyme with activity on adenine. The K_m s for hypoxanthine and guanine of this mutant increased.

In the *T. foetus* enzyme, Asp163 makes contacts with the exocyclic amino group of guanine. This residue, equivalent to D194 of human enzyme, is conserved among HGPRTs. Mutation of this residue to Asn resulted in an enzyme which no longer recognizes xanthine as a substrate. In the same study, mutation of R155 to E resulted in an increase in the K_m for xanthine alone. Mutation of the same residue to Lys resulted in elevated k_{cat} s on xanthine though the K_m was not altered.

Molecular dynamics simulations of different complexes of the human and *T. foetus* enzymes show differences in the Loop IV region of the enzymes (Pitera et al., 1999). The human GMP and *T. foetus* GMP complexes show low fluctuations in this region in the crystal structure. However, in the simulations, the parasite GMP and XMP complexes show much larger fluctuations while that of the human enzyme

remains low. The C2 pocket fluctuations of both the R155E and D163N mutations are also decreased compared to the wild-type *T. foetus* HGPRT.

A mutant of the *Salmonella typhimurium* enzyme (Thr at position corresponding to I193 of the human enzyme) with a 50 fold higher efficiency in the catalysis of guanine has been identified (Lee et al., 1998a). Site-directed mutation of Ile193 in the human enzyme to Thr however, did not alter substrate specificity while mutation of the same residue to Leu increased the K_m for guanine by a factor of 15 (Munagala et al., 2000). In another study, mutation of Ile193 to Phe in the human enzyme was shown to result in a 33 fold increase in the K_m for guanine. An analogous mutation in *G. lamblia* GPRT, L186F resulted in a 3.3 fold increase in the affinity for guanine. A triple mutant of the same enzyme, Y127I,K152R,L186F was found to have a greater affinity for guanine compared to the wildtype enzyme. In addition, this mutant was found to have the ability to phosphoribosylate hypoxanthine (Munagala et al., 2000). In *G. lamblia* GPRT K152 corresponds to K134 of the *T. foetus* enzyme described in context of the 6-oxo group recognition. This residue is further away from the C⁶ carbonyl and lengthening of its side chain by mutation to Arg improves purine binding.

In summary, mutagenesis studies to address the substrate specificity of HGPRTs remain largely inconclusive with analogous mutations in different enzymes leading to dramatically different effects on function. The purine base specificity seems to be a consequence of more than one factor with the global structure of the protein playing an important role. Understanding substrate specificity becomes important from the point of view of inhibitor design as it leads to the identification of parasite enzyme specific features. This chapter describes the attempts to explore this aspect by random mutagenesis of human HGPRT to expand its substrate specificity to include xanthine.

2.1.3 Random mutagenesis and directed evolution

The natural process of evolution through mutation, selection and amplification is slow. *In vitro* directed evolution strategies allow the mimicking of this process in the laboratory within acceptable timescales. These approaches are especially useful in systems where rational design is difficult or has failed. Mutants with desired properties that are obtained often have amino acid substitutions far away from the active site that cannot be predicted by the rational design approach (Shao & Arnold, 1996). Directed evolution studies have been carried out on numerous proteins and many reviews on the subject have been published (Arnold & Volkov, 1999, Tao & Cornish, 2002, Pluckthun, 1999, Powell et al., 2001). This section uses a few examples to highlight the potential of this method and is not an exhaustive summation of the existing volume of literature.

In vitro evolution requires a method for the generation of variants and a screen that would allow a rapid and efficient selection for desired properties. Random mutagenesis to generate variants may be achieved by use of mutator strains (Zhang et al., 1997), chemical mutagenesis or PCR based random mutagenesis of both whole genes (Zhou et al., 1991) or smaller segments. PCR based mutagenesis exploits the lack of proof reading activity of *Taq* DNA polymerase which makes it error prone. The error rate can be increased by modulation of reaction conditions for example by introduction of a dNTP bias or the inclusion of Mn^{2+} ions (Fromant et al., 1995). The potential for rapid generation of large libraries makes this the method of choice for random mutagenesis. The red fluorescent protein of *Discosoma* (DsRed) matures very slowly making it unsuitable for protein localization studies. Bevis and Glick (2002) have generated variants of DsRed that mature 15 times faster using a combination of directed and random mutagenesis with library sizes of the order of 10^3 to 10^5 . The variants were obtained after seven rounds of mutagenesis screened by high-throughput fluorescence.

DNA shuffling is a method for *in vitro* homologous recombination of pools

of selected mutant genes by random fragmentation and polymerase chain reaction (PCR) reassembly and can be described as *in vitro* sexual evolution. The greater flexibility of the approach allows generation of mutants with better success rates than random mutagenesis alone. Three cycles of shuffling and two cycles of backcrossing with wild-type DNA, to eliminate non-essential mutations, allowed the generation of β -lactamase mutants that have a 32,000 fold greater resistance to the antibiotic cefotaxime compared to the parent enzyme. Error prone PCR methodologies yielded only 16 fold increase in resistance (Stemmer, 1994). The *E. coli* aspartate aminotransferase was converted into an enzyme that accepts the branched amino acid valine and 2-oxo-valine with an efficiency five orders of magnitude greater than that of the parent while decreasing the activity on the natural substrate, aspartate 30 fold. This was achieved after five rounds of DNA shuffling and selection. The resultant mutants had six mutations, of which only one was found to be in the active site of the enzyme (Yano et. al., 1998). The approach has also been used to increase the stability of proteins, for example a 200 fold increase in the stability of subtilisin E at 65°C was achieved by a combination of error prone PCR and DNA recombination using the staggered extension process (StEP). (Zhao & Arnold, 1999, Zhao et al.,1998). Many variations of these procedures have been described that allow the generation of large libraries and are not described here.

The limiting factor in directed evolution approaches is the availability of a screen that allows rapid screening and selection of the large number of variants that the mutagenesis process can generate. The design of the screen is dependent on the protein being “evolved” and the property being selected for. For proteins that are essential for survival of an organism, a screen based on auxotrophic strains of preferably unicellular organisms like yeast and *E. coli* may be used. The selection process is improved further if the rate of growth varies with an improvement in the function. Wang et al (2001) have evolved the *Methanococcus jannaschii* tyrosyl-tRNA synthetase into an efficient O-methyl-L-tyrosine tRNA synthetase using positive selection for suppression of an amber stop codon in

the gene encoding chloramphenicol acyltransferase that allowed selection for chloramphenicol resistance. A negative screen to eliminate evolved variants with residual activity for tyrosine ensured that the evolved synthetase was selective for its intended substrate.

Phage display, which allows selection based on affinity, is a useful method for screening for variants (Spada et al., 1998). Many catalytic antibodies have been obtained by this method which involves the display of a protein on the surface of the phage (Takahashi et al., 2001). Affinity chromatography with the ligand of interest is used for selection. Selection is made easier since the phage displaying the protein itself harbors the DNA encoding the functional protein. Ponsard et al (2001) described a method using phage display and catalytic elution that allowed them to select for metallo- β -lactamase mutants active on benzylpenicillin. The phage displayed enzyme library was bound to magnetic beads coated with benzylpenicillin in the absence of zinc ions. Release of the phages displaying active enzyme from the magnetic beads by the addition of Zn^{2+} ions was then used to select for catalytic activity.

In vitro translation systems allow protein evolution in a cell free environment doing away with the interference of other cellular processes that may cloud the screen. Tawfik & Griffiths, (1998) described a water in oil emulsion system that compartmentalizes the genetic information with the expressed enzyme. Expression of a functional methyltransferase in such a compartment methylated the DNA protecting it from digestion by HaeIII endonuclease. This process allowed the selection of a HaeIII methyltransferase from a 10^7 fold excess of other DNA with two cycles of selection. Ribosome display methods which also couple the protein expressed to its own genetic material have also been used. Screening systems however, cannot be generalized and need to be tailored for each system.

Human HGPRT presents itself as an ideal target for directed evolution. Absence and reduced activity of this enzyme in humans causes Lesch-Nyhan syndrome

(Lesch & Nyhan, 1965) and gouty arthritis, respectively and a number of mutations that manifest as disease have been characterized (Jinnah et al., 2000). Mapping these mutations onto the structure of the enzyme shows that they are spread over the entire protein and not restricted to any specific region of the structure. This indicates that mutations that affect activity may not be restricted to the active site of the enzyme. In addition, the *E. coli* strain S ϕ 609 (*ara*, Δ *pro-gpt-lac*, *thi*, *hpt*, *pup*, *purH,J*, *strA*) (Jochimsen et al, 1975) is a convenient screen for xanthine active variants of the enzyme. This stain of *E. coli* lacks both the *de novo* and salvage pathways for purine nucleotides synthesis. As a consequence, growth of this mutant in minimal medium supplemented with a purine base is conditional to the expression of a functional PRT active on the purine in the medium. Selection for a xanthine active mutant of the enzyme would then involve selecting for growth in minimal medium containing xanthine after transformation with a mutagenized library. The characterization of a xanthine active mutant of human HGPRT generated by random mutagenesis is described in this chapter.

2.2 Materials and Methods

Restriction enzymes, *Taq* DNA polymerase, T₄ DNA ligase and other molecular biology reagents were purchased from Amersham Pharmacia, U.K., Bangalore Genei Pvt. Ltd., Bangalore, India or from MBI Fermentas. Lithuania and used according to the manufacturers' instructions. The *E. coli* strain S ϕ 609 (*ara*, Δ *pro-gpt-lac*, *thi*, *hpt*, *pup*, *purH,J*, *strA*) was gift from Dr. Per Nygaard, University of Copenhagen, Denmark. All chemicals used in the assays were from Sigma Chemical Company, USA and media components were from HiMedia Laboratories Ltd, Mumbai, India. Purine base stocks were made in 0.4 N NaOH and all other solutions in double distilled water.

2.2.1 Random mutagenesis and screening

Three sets of PCR conditions were used to generate the randomly mutagenized library of human HGPRT. In all the conditions, 10 ng of the template (human HGPRT gene PCR amplified from pTrc99A clone) and 150 ng of the primers

5'HPRT: 5' CCA CCA TGG CGA CCC GCA GCC CTG GC 3'

3'HPRT: 5' ACA GGA TCC TTA GGC TTT GTA TTT TGC TTT T 3'

were used for a 50 μ l reaction. The following three conditions were used for the generating the mutagenized library The amplified products from each PCR were

	1	2	3
dGTP	2.0 mM	0.2 mM	0.2 mM
dCTP	0.2 mM	2.0 mM	0.2 mM
dATP	0.2 mM	0.2 mM	0.2 mM
dTTP	0.2 mM	0.2 mM	0.2 mM
MnCl ₂	0.5 mM	0.3 mM	0.5 mM
MgCl ₂	3.0 mM	3.0 mM	3.0 mM

pooled, gel purified, restriction digested with Nco1 and BamH1 and ligated into the expression vector pTrc99A digested with the same enzymes. The ligation mix was disc dialysed and transformed into *E. coli* S ϕ 609 by electroporation. Xanthine positive human mutants were obtained by selecting for transformants with the ability to grow on minimal medium plates supplemented with xanthine.

2.2.2 Construction of single mutants

The mutant obtained by random mutagenesis was found to have lost the Nco1 cloning site in addition to the two mutation introduced at the protein level. The mutant HGPRT was therefore, amplified by PCR using human HGPRT primers (listed above), the amplified fragment digested with the enzymes Nco1 and BamH1

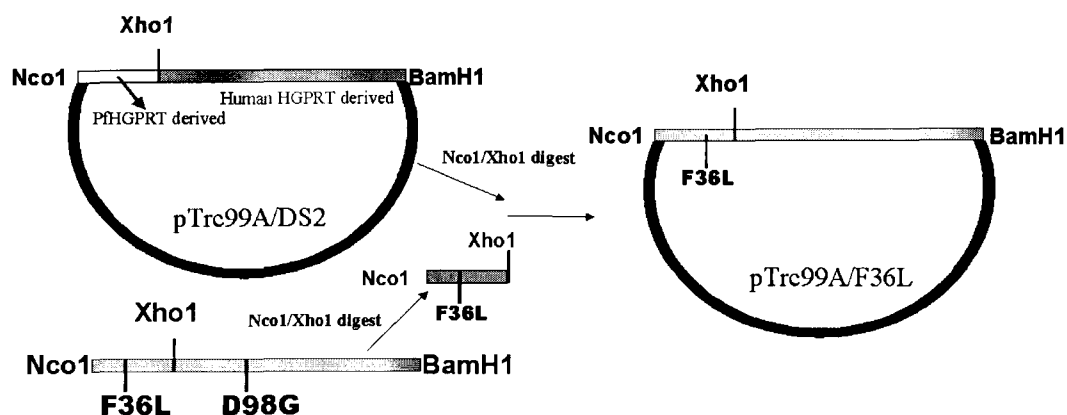


Figure 2.2: Schematic representation of the single mutant construction.

and ligated into the expression vector pTrc99A. The two mutations introduced by the random mutagenesis had a convenient restriction site, XhoI, separating them. This was exploited to create single mutants of the enzyme, F36L and D98G. To create the F36L mutant, the NcoI-XhoI fragment containing the F36L mutation was released from the parent plasmid and purified. This fragment was ligated into a pTrc99A vector fragment containing the remaining part of the human gene (Fig. 2.2). This vector fragment was generated by releasing the NcoI-XhoI fragment from a chimera of the human and *P. falciparum* HGPRTs already available in the laboratory. The D98G mutant was similarly constructed by ligating the XhoI-BamHI fragment into an appropriate vector fragment. The authenticity of all the mutants were verified by sequencing.

2.2.3 Site-directed mutagenesis

Site-directed mutagenesis was carried out by the megaprimer method (Sarkar & Sommer, 1990). The mutagenic primers used were:

F36G: 5'CC ATG AGG AAT tcc CAC CCT TTC C 3'

F36K: 5'CC ATG AGG AAT ctt CAC CCT TTC C 3'

F36E: 5'CC ATG AGG AAT etc CAC CCT TTC C 3'

F36W: 5'CC ATG AGG **AAT** cca CAC CCT TTC C 3'

F36A: 5'CC ATG AGG AAT **ggc** cAC CCT TTC C 3'

along with the 5'HPRT and 3'HPRT end primers. In addition to the desired mutation (lower case), these primers also contained restriction sites indicated in bold, incorporated by silent mutagenesis, in order to aid the selection of recombinants. The sites incorporated were EcoR1 in F36G, Hinf1 in F36K, F36E and F36W, and, HaeIII in F36A. The mutants were constructed in two steps. In the first step the mutagenic primer and the 5' end primer (5'HPRT) were used to amplify a 130 bp megaprimer. The PCR mix contained 200 ng of each primer, 20 ng of the template, 200 μ M of each dNTP and 5 units of *Taq* DNA polymerase for a 50 μ l reaction. The PCR cycle used was denaturation at 93°C for 30 s, annealing at 44°C for 30 sec and extension at 73°C for 1 min. The product obtained after 30 cycles of PCR was purified by elution from agarose gels and used as a 5'-megaprimer in a second round of PCR. The 3' primer used in the second PCR was 3'HPRT and the PCR conditions used were as described above. The full-length amplified product containing the desired mutation was purified, restricted with the enzymes Nco1 and Bam1 and ligated into the vector pTrc99A digested with the same enzymes. Recombinants were selected after transformation into the *E. coli* strain S ϕ 609 on basis of supercoiled plasmid mobility. The presence of the right insert was confirmed by restriction digestion with the enzymes, the sites for which were incorporated in the design of the mutagenic primers. All mutants were confirmed by sequencing (Fig. 2.3).

2.2.4 Functional complementation

Complementation studies were carried out using the *E. coli* strain S ϕ 609 (*ara*, Δ *pro-gpt-lac*, *thi*, *hpt*, *pup*, *purH,J*, *strA*) (Jochimsen et al, 1975) transformed with the expression plasmids carrying wildtype and mutant human HGPRT constructs in the expression vector pTrc99A. The cells grown overnight in LB medium with

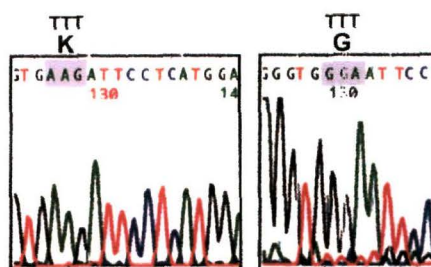


Figure 2.3: Sequencing chromatogram confirming incorporation of F36K (left) and F36G (right) mutations. The mutated codons are highlighted. The parent codon (F) is shown on top of the figures.

ampicillin and streptomycin, were washed with and resuspended in 1X M9 salt solution. A 1% inoculum of these cells was added to minimal medium containing 1X M9 salts, 1 mM MgSO₄, 0.1 mM CaCl₂, 1 mM thiamine hydrochloride, 1 mM proline, 0.2 % glucose, 0.3 mM IPTG, 25 µg/ml streptomycin, 100 µg/ml ampicillin and 0.5 mM hypoxanthine, guanine or xanthine. The cells were allowed to grow for 15 h at 37°C and A₆₀₀ was recorded. All experiments were repeated 3-5 times.

2.2.5 Protein expression and purification

The human HGPRT constructs do not hyper-express in the pTrc99A vector. All mutants were therefore subcloned into the expression vector pET23d under the control of the T7 promoter. Protein expression was carried out in the *E. coli* strain BL21(DE3). BL21(DE3) cells freshly transformed with the expression constructs were inoculated into terrific broth and grown to an A₆₀₀ of 0.6 at 37°C. The culture was cooled to a temperature of 20°C and protein expression induced by addition of IPTG to a concentration of 100 µM. Protein induction was allowed to proceed at 20°C for 18 h, cells harvested by centrifugation and stored at -70°C until further use.

Induced cells were thawed, resuspended in lysis buffer (50 mM Tris, pH7.5, 10 % glycerol, 0.1 µM PMSF and 1 mM DTT) and lysed by sonication. Cellular debris were removed by centrifugation and nucleotides precipitated by addition

of polyethyleneimine (PEI) to a concentration of 0.3 %. The protein was precipitated from the clarified supernatant obtained after centrifugation by addition of ammonium sulphate. The wildtype and mutant human HGPRTs precipitate between 40 to 65 % saturation of ammonium sulphate. The 40-65 % precipitate was dissolved in 1.2 M ammonium sulfate, 10 % glycerol, 20 mM Tris-HCl, pH 8.0, 1 mM DTT, 12 mM MgCl₂ and 0.1 mM EDTA. This solution was loaded onto a Phenyl sepharose column and eluted with a decreasing gradient of 1.2 M-0.0 M ammonium sulfate. Fractions containing HGPRT as monitored by SDS-PAGE were precipitated by adding ammonium sulfate to a concentration of 65 %. The resultant pellet was dissolved in 20 mM Tris-HCl, pH 8.0, 10 % glycerol and desalted on a G-25 column. The desalted material was loaded onto a Q-Sepharose column

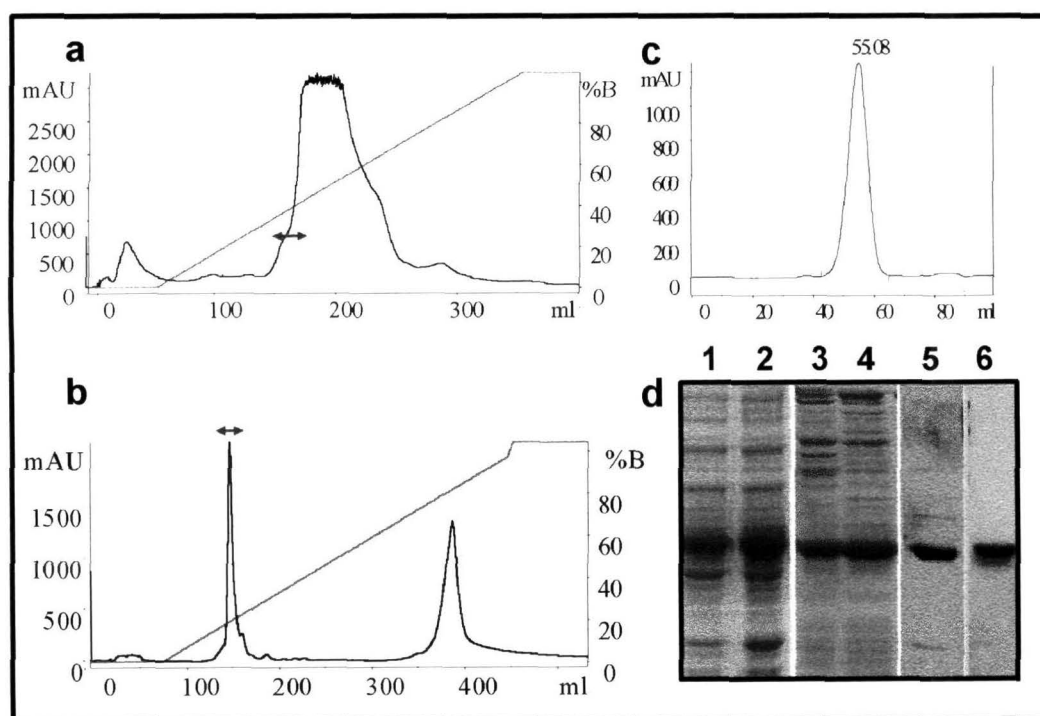


Figure 2.4: Purification profile of F36L human HGPRT. a) Phenyl sepharose elution profile, b) Elution profile from Q-Sepharose column, c) Elution profile from Sephacryl-S200 column, d) SDS-PAGE profile of purification. 1) Crude lysate, 2) 40-60 % ammonium sulphate fraction, 3,4) Fractions from phenyl sepharose column, 5) Protein after Q-Sepharose column, 6) Purified protein after gel filtration. Arrows indicate F36L.

(strong anion exchange resin) and eluted with a linear gradient of 0.0-1 M NaCl.

The fractions containing the protein were pooled and precipitated by addition of ammonium sulphate to a concentration of 65 %. The precipitated protein was dissolved in 10 mM potassium phosphate buffer, pH 7.0, 10 % glycerol, 1 mM DTT and subjected to gel filtration on a sephacryl-200 column equilibrated with the same buffer. The protein eluting from the gel filtration column was stored at 4°C for further use. All the mutants purified behaved identically during purification and representative traces and gels are shown in Fig. 2.4. Protein purity was checked by SDS-PAGE stained with Coomassie brilliant blue-R250 (Lammelli, 1970) and all preparations used were at least 90 % pure. Protein concentrations were determined by the Bradford's method (Bradford, 1976) using bovine serum albumin as a standard.

2.2.6 Enzyme assays and kinetics

Reactions carried out at room temperature (22-28°C) were monitored spectrophotometrically (Giacomello & Salerno, 1977) using either a Shimadzu UV 1601 or a Hitachi U2010 spectrophotometer. Assays at elevated temperatures were carried out on a Hitachi U2010 or a Perkin-Elmer-λ900 spectrophotometer equipped with a water jacketed cell holder. The standard assay condition was 100 mM Tris HCl, pH 7.4, 12 mM MgCl₂, 100 μM hypoxanthine or guanine or 200 μM xanthine and 1 mM PRPP and appropriate quantity of the enzyme (≈ 0.1-0.2 μg in 250 μl assays). Formation of IMP, GMP and XMP were monitored at 245, 257.5 and 255 nm, respectively. The Δε values used were 1900 M⁻¹cm⁻¹ (hypoxanthine to IMP), 5900 M⁻¹cm⁻¹ (guanine to GMP) and 3794 M⁻¹cm⁻¹ (xanthine to XMP) (Xu et al., 1997 and Keough et al., 1999). The final assay volumes were 250 μl. Reactions were initiated by the addition of enzyme. For the determination of kinetic constants, the purine base concentrations were varied between 2 μM and 100 μM in the case of hypoxanthine and guanine and between 25 μM and 300 μM in the case of xanthine with PRPP maintained constant at 1 mM. For the determination of PRPP K_ms, base concentrations were kept constant at 100 μM (hypoxanthine and guanine)

or 200 μM (xanthine) and PRPP concentration varied from 25 μM to 1 mM. At least 7 concentrations of the variable substrate were used. K_m s were determined by fitting to linear Michaelis-Menten kinetics after linear transformation. Data were also analysed by non-linear regression. The Graphpad Prism package was used in all analysis.

2.2.7 Temperature stability

For determination of temperature stability, proteins at a concentration of 0.1 mg/ml was incubated at various temperatures. Aliquots were withdrawn at different times and activity on the base hypoxanthine measured at room temperature using the standard assay.

2.2.8 Structure analysis

The PDB co-ordinate files used in the structural analysis presented are 1HMP (Human HGPRT GMP complex), 1BZY (Human HGPRT, Immucillin-GP, pyrophosphate complex) and 1CJB (*P. falciparum* HGPRT, Immucillin-HP, pyrophosphate complex). Contact analysis was performed using an in house program. Superpositions were done using Swiss-pdb viewer (Guex & Peitsch, 1997). Molecular representations shown in this chapter were generated using Molscript (Kraulis, 1991) and rendered using Raster3D (Merritt & Bacon, 1997).

2.3 Results

2.3.1 Screening for xanthine active mutants of human HGPRT

The randomly mutagenised library of human HGPRT in the expression vector pTrc99A was transformed into the *E. coli* strain S ϕ 609 by electroporation. The transformation mix was plated onto minimal medium plates supplemented with the purine base xanthine. Plasmids isolated from colonies that appeared were retransformed into the strain S ϕ 609 and two clones selected on the basis of the

faster growth of the retransformants on minimal medium plates containing xanthine (Fig. 2.5). Sequencing of these two clones showed the presence of three mutations,

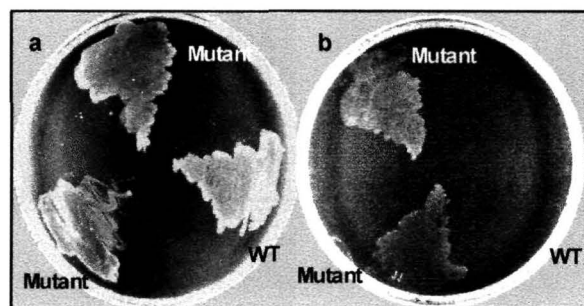


Figure 2.5: Growth of *Sφ609* transformed with wildtype and mutant human HGPRTs in pTrc99A on minimal medium plates supplemented with a) hypoxanthine and guanine, b) xanthine.

two of which resulted in amino acid substitutions, F36L and D98G. The third was a silent mutation at amino acid position 9 on the sequence. Surprisingly, the restriction site for *Nco*I, the enzyme used for the cloning was also mutated (Fig. 2.6). The mutated gene was therefore, amplified by PCR with end primers containing the restriction sites and cloned into pTrc99A. The two single mutants, F36L and D98G were generated using convenient restriction sites within the human HGPRT gene as described in Materials and Methods (2.2.2). The substrate specificity of the parent and the two single mutants was accessed semi-quantitatively by functional complementation in liquid medium (Fig. 2.7). As can be seen in the figure, wildtype human HGPRT complements the HGPRT deficiency in *Sφ609* only in the presence of hypoxanthine and guanine while the parent double mutant and the single mutant F36L can complement in the presence of xanthine also. This indicates that xanthine specificity is a consequence of the mutation of F36 to L and not due to the D98G mutation.

2.3.2 Functional complementation of site-directed mutants

Examination of the structure of human HGPRT complexed to a transition state analog shows that residue F36 does not lie close to the active site of

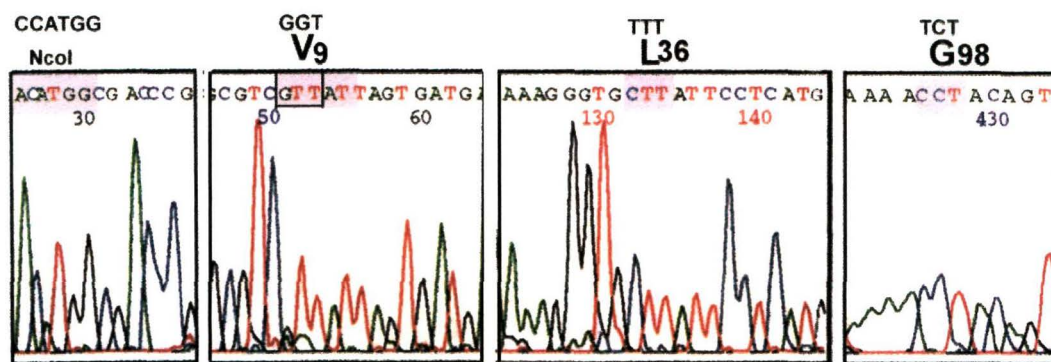


Figure 2.6: Sequencing chromatogram showing mutations generated in the xanthine active clone by random mutagenesis. The mutated codons are highlighted and the resultant amino acid and its position shown above the sequence. The original codons are also shown. The D98G mutation is shown on the complementary strand.

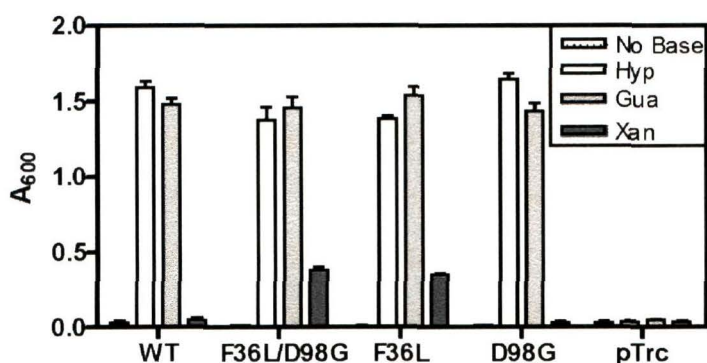


Figure 2.7: Functional complementation of single mutants, F36L and D98G. Experiment was performed as described in Materials and Methods (2.2.4).

the enzyme. This residue in fact lies in the hydrophobic core of the protein (Fig 2.14). Site-directed mutagenesis was therefore carried out to introduce 1) a cavity (F36G and F36A), 2) a positive charge (F36K), 3) a negative charge (F36E) and 4) a bulky residue (F36W) at this position. These mutants were created as described in Materials and Methods (2.2.3) and the substrate specificity analysed by functional complementation. Table 2.1 summarises the results of the functional complementation studies on these mutants in *S. cerevisiae*. The substrate specificity remained unaltered in all the mutants except F36K and F36G. Further studies with purified enzymes were therefore carried out on F36L, F36K and F36G only.

Table 2.1: Substrate specificity of human HGPRT mutants as determined by functional complementation in the *E. coli* strain S ϕ 609 .

Protein	H	G	X
HumanWT	✓	✓	X
F36L	✓	✓	✓
F36K	Weak	✓	X
F36G	X	X	X
F36A	✓	✓	X
F36E	✓	✓	X
F36W	✓	✓	X

✓ Complements, **X** Does not complement

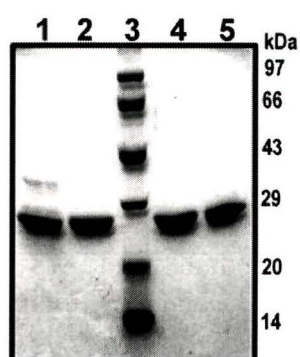


Figure 2.8: SDS-PAGE of purified human wildtype and mutant HGPRTs. 1) F36G, 2) F36K, 3) Marker, 4) F36L, 5) wildtype.

2.3.3 Enzyme purification

The wildtype and mutant HGPRTs do not hyper-express in *E. coli* S ϕ 609 . These were therefore cloned into the expression vector pET23d and expressed in the *E. coli* strain BL21(DE3). All the proteins could be purified to homogeneity using identical protocols as described in Materials and Methods(2.2.5). All proteins were judged at least 90 % pure by SDS-PAGE (Fig. 2.8).

Table 2.2: Kinetic parameters of human wildtype and mutant HGPRTs.

		K_m (μM)		k_{cat}/K_m ($\mu\text{M}^{-1}\text{s}^{-1}$)	
HPRT reaction					
Enzyme	k_{cat} (s^{-1})	Hypoxanthine	PRPP	Hypoxanthine	PRPP
Wildtype	7.1	1.0	32.9	7.1	0.21
F36L	5.4	2.0	43.5	2.7	0.12
F36K	3.4	1.7	07.2	2.0	0.47
F36G	3.1	2.9	12.0	1.0	0.26
GPRT reaction					
Enzyme	k_{cat} (s^{-1})	Guanine	PRPP	Guanine	PRPP
Wildtype	25.5	4.5	73.1	5.6	0.34
F36L	18.0	2.1	47.0	9.0	0.38
F36K	06.3	3.5	35.4	1.8	0,18
F36G	03.4	7.3	43.0	0.5	0.08
XPRT reaction					
Enzyme	k_{cat} (s^{-1})	Xanthine	PRPP	Xanthine	PRPP
Wildtype	0.007	-	-	-	-
F36L	0.037	393	$\approx 1-2$	0.01×10^{-2}	0.037
F36K	0.027	-	-	-	-
F36G	0.023	-	-	-	-

- : Value could not be determined

2.3.4 Kinetics

The kinetic parameters of the three mutants, F36L, F36G and F36K are compared to that of the wildtype human HGPRT in Table 2.2. The substrates specificities of the purified wildtpye and F36L mutant agree with that observed on functional complementation (Table 2.1). The wildtype enzyme catalyses the phosphoribosylation of hypoxanthine and guanine, while F36L shows activity on xanthine also (Fig. 2.9). The k_{cat} and K_m s for the purines, hypoxanthine and

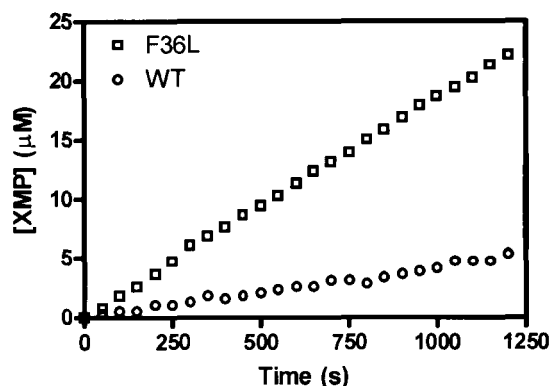


Figure 2.9: Xanthine phosphoribosylation by F36L and wildtype human HGPRTs monitored as described in Materials and Methods (2.2.6). Equal amounts of both proteins (3 μg) were added to initiate the reactions.

guanine, remain relatively unaltered. There is a disparity between the functional complementation and activity measurements on the purified proteins in the case of F36K and F36G. While, F36K shows only weak activity on hypoxanthine in the functional complementation, the activity measurements show that the k_{cat} for hypoxanthine is high. The F36G mutant shows large though reduced activity compared to the wildtype on all three substrates while it is inactive in the complementation assay. These discrepancies may be due to a variation in the expression of these mutants in *S*ϕ609 or due to a reduction in their stabilities. The K_m for PRPP of these two mutants for the hypoxanthine reaction is also lower compared to that of the wildtype. The PRPP K_m for xanthine phosphoribosylation by F36L is also very low and approaches the K_d determined for the wildtype enzyme.

2.3.5 Temperature stability

Human HGPRT has been documented to be highly resistant to high temperatures. The temperature stability of human wildtype and mutant HGPRTs was therefore investigated in order to study the effect of the mutation of core residues on stability. Both the wildtype and F36L were found to be remarkably stable to

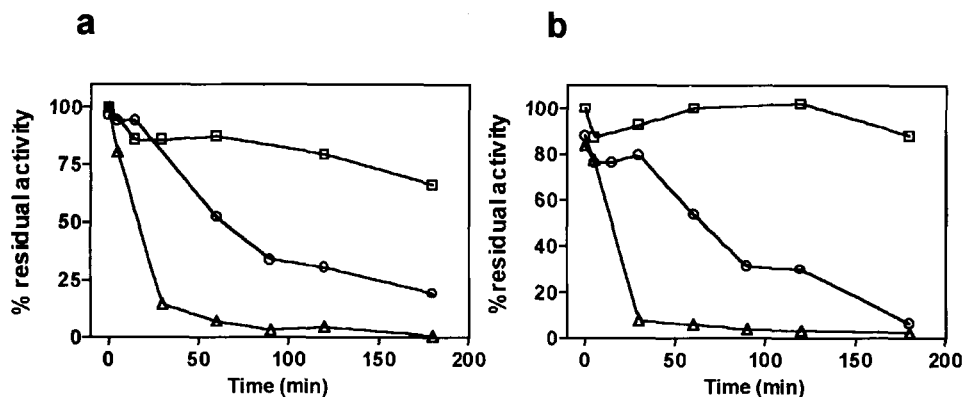


Figure 2.10: Residual activity of human (a) wildtype and (b) F36L HGPRTs after preincubation at 60°C - □, 70°C - ○ and 80°C - △

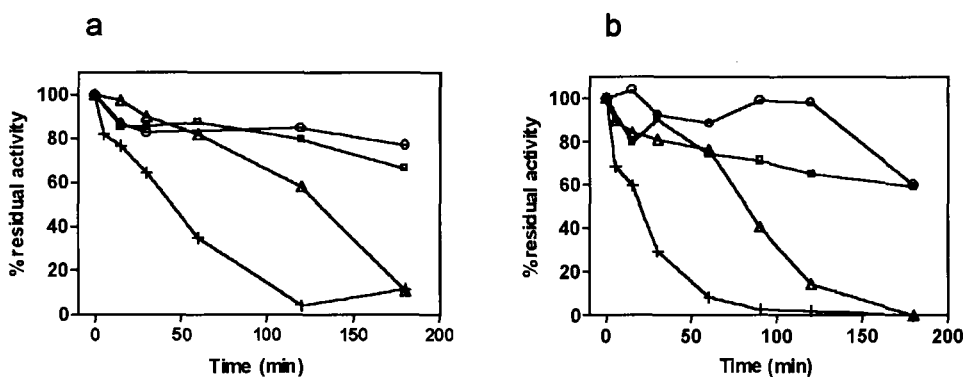


Figure 2.11: Residual activity after preincubation at (a) 60°C and (b) 65°C. Wildtype(□), F36L(○), F36K (△) and F36G(+).

temperature (Fig. 2.10) retaining more than 80% of their activity even after 3 h at 60°C. Activity was retained for about 0.5 h at 70°C. Fig. 2.11 shows the effect of preincubation at different temperatures on the activity of F36K and F36G. Though both these mutants are quite stable retaining a substantial amount of activity at 60°C, their stability is reduced compared to the wildtype and F36L mutant. This is more pronounced in the case of the F36G mutant. This reduced stability may result in the lack of expression/activity of the F36G mutant *in vivo* preventing complementation.

2.3.6 Activation energy for the reactions

All catalysts including enzymes work by lowering the activation energy of reactions. The activation energy of the reaction may be determined by measuring the rate of a reaction at different temperatures. This is feasible in the case of human HGPRT as the enzyme is exceptionally thermostable and reduction in reaction rates as a consequence of enzyme denaturation can be ruled out. Fig. 2.12A shows the increase in rate of phosphoribosylation catalysed by human wildtype and F36L HGPRTs as a function of temperature. As expected the activities increase linearly with temperatures as high as 65°C again highlighting the temperature stability of this enzyme. The Arrhenius plot for the determination of activation energies is shown in Fig. 2.12. The activation energies for the reaction by the two proteins are listed in Table 2.3. The table shows differences in the activation energies of the reaction catalysed by the two proteins. These differences may partly account for the differences in the k_{cat} s of the two enzymes and is discussed in section 3.12.

2.4 Discussion

2.4.1 Kinetics

The kinetic parameters of the three mutants are largely comparable to that of the wildtype enzyme. The k_{cat} s of hypoxanthine and guanine phosphoribosylation are marginally reduced, more so in the F36G mutant. The base (hypoxanthine & guanine) K_{m} s are also similar in the low micromolar range. Significantly, the xanthine phosphoribosylation activity is greater than that of the wildtype enzyme in all three mutants, the maximum activity being exhibited by F36L. The K_{m} for xanthine for this mutant is however, high. Interestingly, the PRPP K_{m} for the xanthine phosphoribosylation by F36L is much lower than the PRPP K_{m} of both F36L and the wildtype for the hypoxanthine and guanine reactions. The PRPP K_{m} of the F36K mutant for hypoxanthine phosphoribosylation is also low. It is interesting

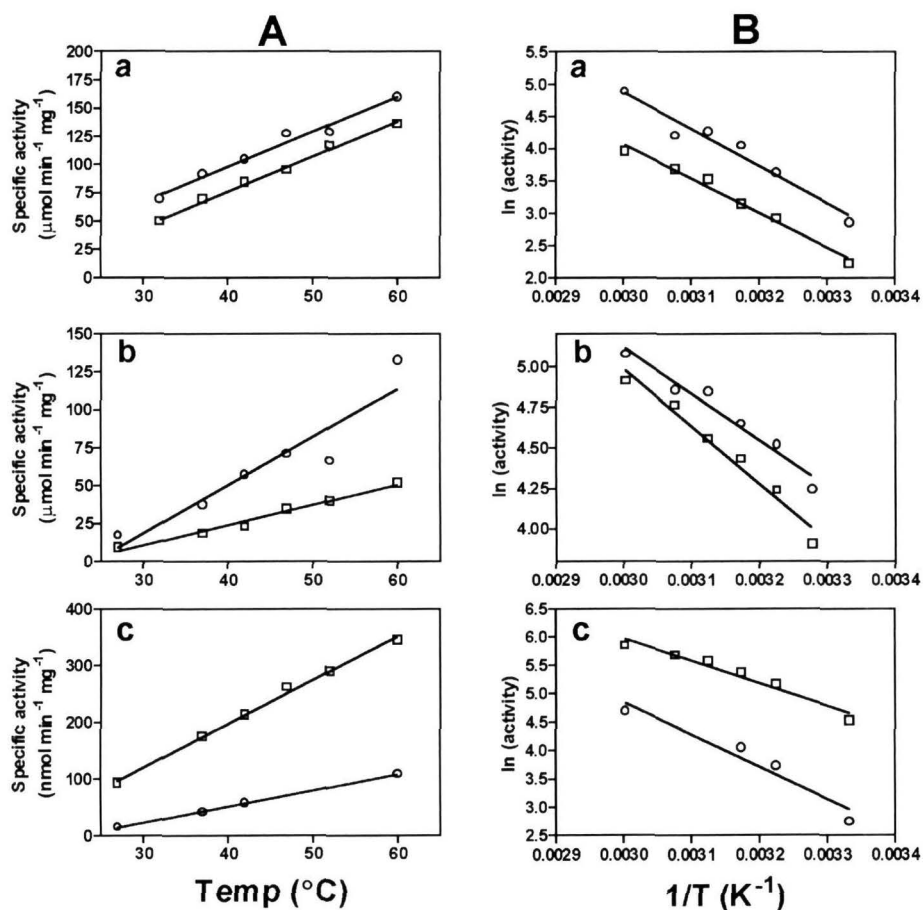


Figure 2.12: A) Activity of wildtype(○) and F36L(□) human HGPRTs at higher temperatures. B) Arrhenius plot for wildtype(○) and F36L(□) human HGPRTs. a) Hypoxanthine, b) Guanine, c) Xanthine.

Table 2.3: Activation energy for the HGPRT catalysed reactions

	Wildtype kJ mol ⁻¹	F36L kJ mol ⁻¹
Hypoxanthine	23.7±2.5	29.6±2.7
Guanine	47.8±5.3	44.3±3.0
Xanthine	47.3±8.6	32.9±3.6

to note that both these reactions have low k_{cat} s, a factor that may explain the lower PRPP K_{m} s.

The kinetics of human HGPRT has been studied in detail with both stopped-flow and steady state techniques (Xu et al., 1997). The reaction mechanism is ordered with PRPP binding preceding the binding of the purine base. The rate and dissociation constants for all the steps in the catalysis have been determined using pre-steady state kinetics, isothermal titration calorimetry and equilibrium gel filtration. The rate determining step of the reaction has been shown to be product release and not phosphoribosyl transfer. The greater k_{cat} s observed for the guanine reaction is a consequence of faster GMP release compared to IMP rather than the faster conversion of guanine to GMP. The K_{d} of the enzyme for PRPP is 1.3 μM while the K_{m} is 35 μM . The relationship between the K_{d} and K_{m} for PRPP has been found to be

$$K_{\text{m}[\text{PRPP}]} = \frac{k_{\text{cat}}}{k_{-1}} K_{\text{d}[\text{PRPP}]}$$

where k_{cat} , the rate of the forward reaction in the steady state and k_{-1} , the rate of dissociation of PRPP, which have been determined to be 13 s^{-1} and 0.24 s^{-1} , respectively. The K_{m} will therefore approach K_{d} as the rate of the reaction decreases. The low PRPP K_{m} with xanthine as the second substrate in the case of F36L could therefore be a reflection of the low k_{cat} of this mutant for xanthine phosphoribosylation. This may also be the case with the PRPP K_{m} of F36K with hypoxanthine as the second substrate.

2.4.2 Activation energies and xanthine activity

The activation energy for the reaction catalysed by human wildtype and F36L HGPRTs is plotted along with the k_{cat} for the reaction (Fig. 2.13). The increase in the k_{cat} for the xanthine reaction in F36L is associated with a decrease in the activation energy compared to the wildtype. The activation energies of the hypoxanthine and guanine reactions do not change significantly nor do the k_{cat} s. The ability of the F36L mutant to lower the activation energy for the xanthine reaction is probably a

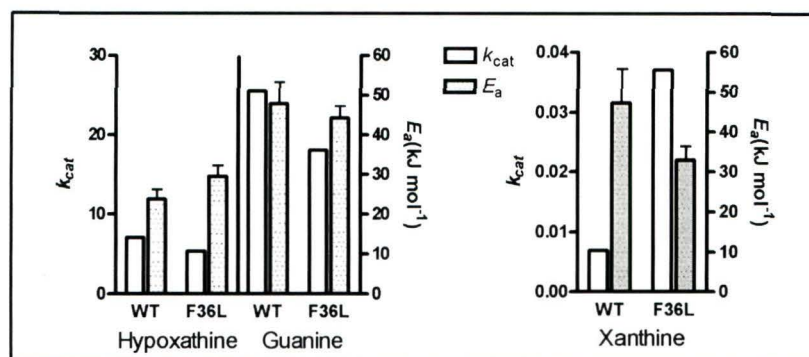


Figure 2.13: Comparison of k_{cat} with activation energy for phosphoribosylation by HGPRT

reflection of its ability to stabilise the transition state of the xanthine reaction better than the wildtype. Possible structural basis for this is presented in the following section.

2.4.3 Structural basis for xanthine activity

A number of crystal structures of HGPRTs from various sources in complex with various nucleotides are available. Heroux et al (1999a, 1999b) have determined the structure of *T. gondii* HGPRT in complex with the nucleotides IMP, GMP and XMP. Comparison of these structures with that of the human enzyme complexed with GMP allow rationalization of the purine binding specificities of these enzymes. The purine base contacts of the human enzyme are shown in Fig. 2.1. A hydrogen bonding interaction is present between the C2 amino group of GMP and the backbone oxygen of Asp194 (Asp200 in *T. gondii*) in both these enzymes. This interaction would be unfavorable if the C2 substituent were to be a carbonyl group as in xanthine. In the XMP complex of the *T. gondii* enzyme, a readjustment of Loop IV together with a rotation of the purine ring allows hydrogen bonding of the C2 carbonyl with the backbone amide of Asp206. Molecular dynamics simulations of the human and *T. foetus* HGPRTs in complex with various nucleotides by Pitera et al. (1999) show that the C2 pocket of this enzyme is far less rigid compared to the human enzyme which permits it to recognize both the amino group of GMP and

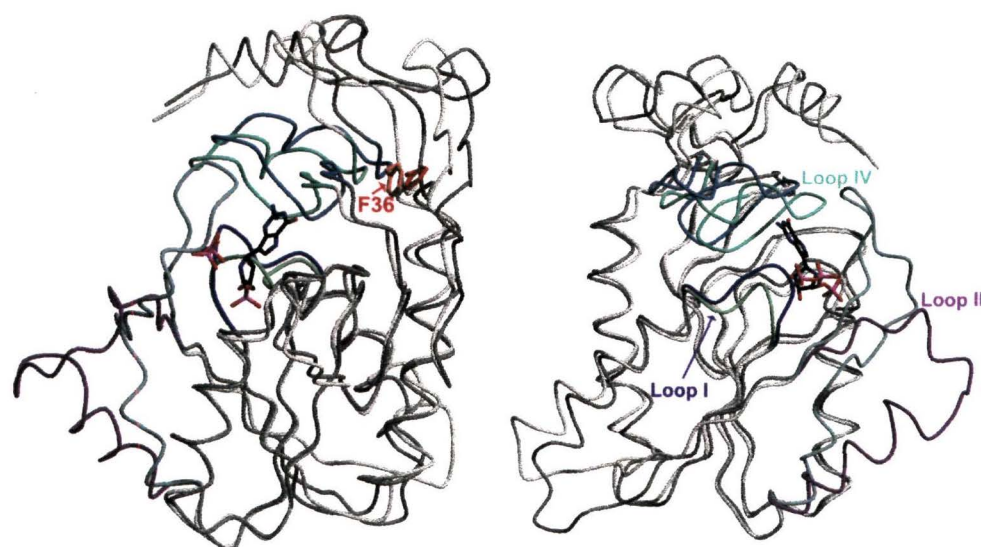


Figure 2.14: Superposition of structures of human HGPRT in complex with GMP (dark grey, 1HMP) and ImmucillinGP (light grey, 1BZY). Loops I, II and IV are coloured in different shades of blue. Lighter shades represent the Immucillin complex. The left panel shows the position of F36 relative to these loops. The right panel is included to illustrate the loop movements with greater clarity.

the carbonyl group of XMP.

The xanthine specificity seen in the F36L mutant of human HGPRT is consistent with these structural and theoretical explanations. Examination of the structure of human HGPRT shows that F36 does not lie in the active site of the enzyme (Fig. 2.14). However, it lies at the base of Loop IV making contact with residues on either end of this loop (Fig. 2.14, 2.15). Fig. 2.14 also shows the superposition of the structures of the human enzyme in complex with the product, GMP and in complex with the transition state analog, ImmucillinGP and pyrophosphate. Large regions of the protein are seen to be different between the two complexes. Prominent among these are loops I, II and IV. Loop IV dynamics have been proposed, as described above, to be important for purine recognition. Examination of the contacts made by F36 in the two structures shows a difference in the contacts, especially with residues at the base of Loop IV (Table 2.4).

Mutation of F36 most likely results in an enzyme in which this loop can

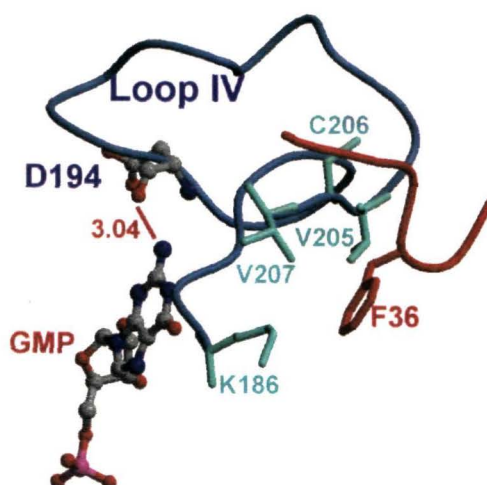


Figure 2.15: Contacts of F36L with Loop IV residues. Loop IV is shown in blue and the residues that make contact with F36 at a cutoff of 4.0Å are shown in cyan. The figure was generated using the PDB co-ordinate file 1HMP of the human enzyme in complex with GMP.

Table 2.4: Comparison of F36_i contacts in 1BZY and 1HMP.

		No. of contacts	
	Residue	1HMP	1BZY
1	Ile10	0	1
2	Glu14	0	2
3	Gly16	3	0
4	Pro184	0	3
5	Lys186	1	0
6	Val205	7	6
7	Cys206	2	1
8	Val207	2	1

rearrange to accommodate the C2 carbonyl of xanthine offsetting the repulsive interactions that would otherwise exist in the enzyme. This may also be the case with the F36G and F36K mutants which have a much greater xanthine activity than the parent wildtype enzyme. Excessive perturbation of interactions within the protein due to mutation of the bulky phenylalanine residue to a glycine may result in the destabilisation and reduced activity of the F36G mutant.

F36 in the human enzyme corresponds to L44 of *P. falciparum* HGPRT. Chapter 3 describes studies on an L44F mutant of PfHGPRT. The same mutation has also been made in three chimeras of human and *P. falciparum* HGPRT. In all these cases, activity on xanthine of the mutant is compromised (Table 3.7). The L44F mutant of the *P. falciparum* enzyme is also considerably destabilised. These observations are in agreement with the proposed role of F36 in human HGPRT in modulating substrate specificity probably by reorganization of Loop IV residues. A high resolution crystal structure of the F36L mutant in complex with XMP should provide insight on the determinants of substrate specificity in HGPRTs.

To summarise, a mutant of human HGPRT with the ability to phosphoribosylate xanthine in addition to its natural substrates, hypoxanthine and guanine, has been generated by random mutagenesis. The mutation, F36L, is in the hood domain of the protein. This is the first instance of a mutation in the hood domain of HGPRTs modulating substrate specificity. This mutant provides direct evidence for the proposed role of hood domain reorganization in accommodating purine bases in the active site of HGPRTs.

Chapter 3

Studies on the L44F mutant of PfHGPRT: Insights into the nature of the active form of the enzyme.

*This chapter describes studies on *P. falciparum* HGPRT and a mutant of the enzyme, L44F. Data presented here suggest that the activated form of PfHGPRT is less stable than the unactivated form of the enzyme.*

3.1 Introduction

HGPRT is a key enzyme in the purine salvage pathway of *P. falciparum* and flux through this enzyme serves as the sole source for purine nucleotides for the parasite. Human and *P. falciparum* HGPRTs share a sequence identity of 44 % and a similarity of 76 % (Fig.3.1). The structures of the two enzymes superpose with an RMSD of about 1.7 Å (Fig. 3.2, Shi et al., 1999a, Shi et al., 1999b). In spite of the similarity in sequence and structure, these enzymes differ significantly in their properties, the most prominent among these being the additional specificity of the parasite enzyme for the purine base, xanthine. In addition, while human HGPRT on purification from recombinant systems has very high activity, purified recombinant PfHGPRT has negligible activity. In fact, the low activity has raised questions on the importance of flux through HGPRT for the parasite despite its proven essentiality from inhibition studies. Previous studies in the laboratory have shown that PfHGPRT can be activated on incubation with the substrates, hypoxanthine and PRPP in low molarity potassium phosphate buffers, conditions under which the enzyme is a tetramer (Sujay Subbayya & Balaram, 2000a, Keough

The nature of the active form of PfHGPRT

<i>P. falciparum</i>	MPIPNNPGAG	ENAFDPVFK	DDDGYDLSF	MIPAHYKYL	TKVLVNGVI	KNRIEKLAYD	60
Human	MATRS-PGV-	-----VISD	DEPGYDLDF	CIPNHYAEDL	ERVFIPHGLI	MDRTERLARD	52
					↑		
<i>P. falciparum</i>	IKKVYNNEEF	HILCLLKGSR	GFFTALLKHL	SRIHNSAVE	MSKPLFGEHY	VRVKSVCNDQ	120
Human	VMKEMGGHHI	VALCVLKGYY	KFFADLLDYI	KALNRNS--D	RSIPMT-VDF	IRLKSVCNDQ	109
<i>P. falciparum</i>	STGTLEIVS-	EDLSCLKGKH	VLIVEDIIDT	GKTLVKFCEY	LKKFEIKTVA	IACLFIKRTP	179
Human	STGDIKVIIG	DDLSTLTGKN	VLIVEDIIDT	GKTMQTLLSL	VRQYNPKWYK	VASLLVKRTP	169
<i>P. falciparum</i>	LWNGFKAEFV	GFESIPDFVV	GYSLDYNEIF	RDLHCCLVN	DEGKKKYKAT	SL	231
Human	RSVGYKPDFV	GFEIPDKFVV	GYALDYNEYF	RDLNHVCVIS	ETGKAKYKA-	--	218

Figure 3.1: Sequence alignment of human and *P. falciparum* HGPRTs. Alignment was generated using ClustalW. The arrow indicates F36/L44 of human and *P. falciparum* HGPRT respectively.



Figure 3.2: Superposition of human (1BZY, red) and *P. falciparum* (1CJB, blue) HGPRT structures.

et al., 1999). About 10-20 fold increase in specific activity could be obtained. The studies also suggested that tetramerization is necessary but not sufficient for activation. The presence of the substrates is essential and probably brings about conformational changes necessary for the optimal activity of the enzyme. Reactions initiated with the unactivated enzyme show a lag phase followed by a linear phase though the reaction rates during the linear phase remain much lower than that of the activated enzyme. The duration of this reaction transient gradually decreases during the course of activation and disappears upon complete activation of the enzyme

(Sujay Subbayya, 2002). The presence of the reaction transient lends support to the suggestion that the enzyme undergoes a conformational change going from an inactive to an active form.

Examination of the sequence alignment of the *P. falciparum* and human enzyme shows that F36, that has a role in modulating the substrate specificity of the human enzyme (Chapter 2), corresponds to L44 in the *P. falciparum* sequence. A study of the effect of mutating L44 in the *P. falciparum* enzyme to F was therefore initiated. Investigations on this mutant have provided insights into the nature of the active form of the *P. falciparum* enzyme. However, experiments on the L44F mutant of the *P. falciparum* enzyme were limited by difficulties in obtaining reasonably pure enzyme. Some of the later studies presented in this chapter are therefore limited to the wildtype enzyme.

3.2 Materials and Methods

Enzyme assays were carried out on a Shimadzu UV 1601 or a Hitachi U2010 spectrophotometer. Reaction at specific temperatures were carried out using a Hitachi U2010 spectrophotometer or a Perkin-Elmer λ 900 spectrophotometer equipped with a water jacketed cell holder. Column chromatography was performed using a Akta Basic HPLC system from Amersham Pharmacia.

3.2.1 Site-directed mutagenesis

Site directed mutagenesis was carried out using the megaprimer PCR method (Sarkar & Sommer, 1990) in an identical manner to that described for creation of the site-directed mutants of human HGPRT (2.2.1). The primers used were:

Pff: 5' ACC AAG GTC TTT GTT CCA AAT **GGA GTC** ATA AAA AAC 3'

pETpf3: 5' CCA **GGA TCC** TTA TAA TGA AGT TGC TTT AT 3'

5'FPRT: 5' CCA **CCA TGG** CAA TAC CAA ATA ATC C 3'

The restriction sites are indicated in italics (*Hinf*I in Pflf, *Nco*I in 5'FPRT and *Bam*H1 in pETPf3) and the mutated codon in bold font. The *Hinf*I site in Pflf was incorporated by a silent mutation (bold italics). The first PCR used Pflf and pETpf3' to generate the megaprimer. The megaprimer and 5'FPRT were used as primers to generate the full-length sequence. The amplified full length gene was restriction digested with the enzymes *Nco*I and *Bam*H1 and ligated into the vector pTrc99A. S ϕ 609 cells transformed with the ligation mix were screened to obtain recombinants. The presence of the mutation was confirmed by digestion with *Hinf*I and by sequencing. (Fig. 3.3).

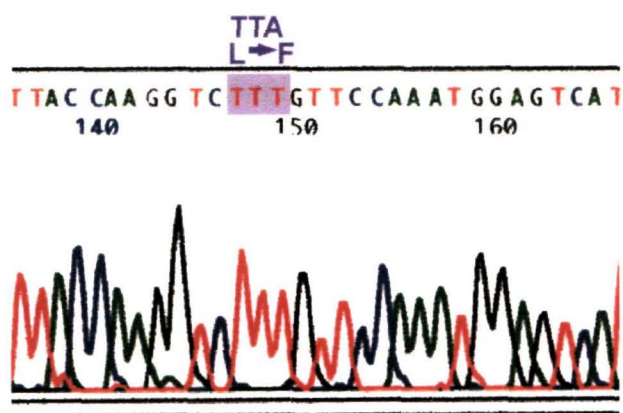


Figure 3.3: Section of the sequencing chromatogram confirming the incorporation of the L44F mutation. The mutated codon is highlighted and the same codon in the parent wildtype is shown above the sequence.

3.2.2 Functional complementation

Complementation studies were carried out using the *E. coli* strain S ϕ 609 (*ara*, Δ *pro-gpt-lac*, *thi*, *hpt*, *pup*, *purH,J*, *strA*) (Jochimsen et al., 1975) as described in 2.2.4. Expression constructs of WTPfHGPRT (wildtype *P. falciparum* HGPRT), P2A (P2A mutant of WTPfHGPRT) and L44F (L44F,P2A mutant of WTPfHGPRT) in pTrc99A were used for these studies.

3.2.3 Determination of *in vivo* stability.

For determination of the *in vivo* stability of P2A and L44F, S ϕ 609 cells containing the expression constructs of these mutations in pTrc99A were grown to OD₆₀₀ of 0.6 at 37°C, transferred to different temperatures and induced by addition of IPTG to a concentration of 1 mM. Protein translation was arrested by addition of chloramphenicol to a concentration of 300 μ g/ml after 4 h of induction. Aliquots were withdrawn periodically, cells precipitated by centrifugation and lysed by boiling in SDS-PAGE sample buffer for 10 min. Samples equivalent to 75 μ l of initial culture were resolved by SDS-PAGE, and transferred to PVDF membranes. Blots were probed with polyclonal anti-PfHGPRT raised in rabbit. Horse-radish peroxidase conjugated anti-rabbit-IgG was used as the secondary antibody and bands visualised using 3-amino-9-ethyl carbazole and hydrogen peroxide.

3.2.4 Enzyme purification

Wildtype PfHGPRT

Wildtype PfHGPRT (WTPfHGPRT) and the P2A mutant of PfHGPRT(P2A) from the *E. coli* strain S ϕ 609 were purified as described previously (Sujay Subbaya & Balaram, 2000). S ϕ 609 cells transformed with the respective pTrc99A constructs were grown in terrific broth to (OD)₆₀₀ of 0.6, protein expression was induced by the addition of 1 mM IPTG and cells allowed to grow for a further 18 h. Cells harvested by centrifugation were lysed by sonication in 50 mM Tris.HCl, pH 7.5, 10% glycerol, 0.1 mM EDTA. The lysates were clarified by centrifugation and nucleotides precipitated by addition of polyethylenimine (PEI) to a concentration of 0.03%. The 40-65% ammonium sulphate fraction containing the recombinant protein was dissolved and desalted into 10 mM Tris.HCl, pH 8.9 and purified by anion exchange chromatography. Protein eluted at about 100-150 mM NaCl was precipitated with ammonium sulphate, dissolved in 10 mM Tris.HCl, pH 6.9 and further purified by cation exchange chromatography. The cation exchange column was equilibrated with 10 mM Tris.HCl, pH 6.9 and protein eluted with a linear gradient of NaCl in the same buffer. Fractions containing the protein were

pooled, protein precipitated with ammonium sulphate and desalted by gel- filtration on a Superdex S-200 column equilibrated with 10 mM potassium phosphate buffer containing 2 mM DTT and 20% glycerol. Protein was stored under these conditions at a concentration of 2 mg/ml at 4°C.

L44F

Purification of the L44F mutant of PfHGPRT (hereafter referred to as L44F) however, proved to be difficult. This protein does not over-express in the *E. coli* strain S ϕ 609 . It was therefore subcloned in the expression vector pET23d and protein expressed in the *E. coli* strain BL21(DE3). BL21(DE3) cells freshly transformed with the construct were grown to an (OD)₆₀₀ of 0.6 at 20°C and protein expression induced at the same temperature by the addition of 50 μ M IPTG for 12 h. Cells were harvested by centrifugation and lysed in 50 mM Tris.HCl, pH 6.9, 100 mM KCl, 20 % glycerol and 10 mM DTT using a French press. Lysis supernatants were subjected to PEI precipitation and protein precipitated by addition of ammonium sulphate. The protein fraction (25-60 % saturation) was dissolved in the 20 mM Tris.HCl, pH 6.9, 100 mM KCl, 20 % glycerol, 2 mM DTT (Buffer A) and bound to a Cibacron Blue column equilibrated with the same buffer. A batch purification was carried out in the cold and protein eluted with a step gradient of increasing KCl in Buffer A. Protein containing fractions were pooled, concentrated by ultrafiltration and subjected to gel filtration on a Sephacryl-200 column (1.6 cm X 50 cm) equilibrated in Buffer A. The peak containing L44F was again concentrated, desalted in 20 mM Tris.HCl, pH8.9, 20 % glycerol and 1 mM DTT and purified by anion exchange chromatography (Q-sepharose column, batch purification) using a step gradient in the cold. Finally protein was buffer exchanged in 10 mM potassium phosphate buffer, pH 7.0, 20 % glycerol, 2 mM DTT on a Sephacryl-200 column and stored at 2 mg/ml in the same buffer until further use (Fig. 3.4).

3.2.5 Gel filtration

A Superdex-200 (300 x 10 mm) gel filtration column calibrated with β -Amylase (200 kDa), Alcohol dehydrogenase (150 kDa), Bovine serum albumin (66 kDa),

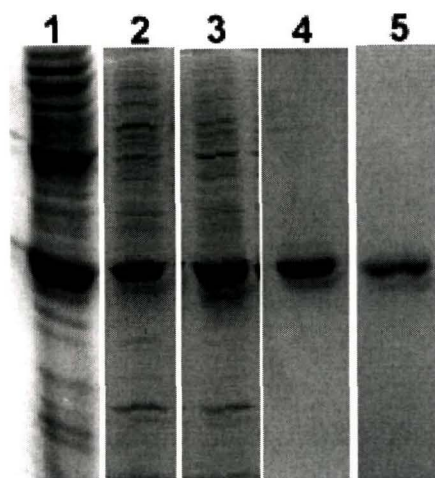


Figure 3.4: SDS-PAGE profile of L44F purification. Lane 1 : Crude lysate, 2: Cibacron Blue eluate, 3: S-200 fraction, 4: Q-sepharose eluate, 5: Purified protein.

Carbonic anhydrase (29 kDa) and Cytochrome C (12.4 kDa) was used for the analytical gel filtration studies. Gel-filtrations were done either in assay buffer (100 mM, Tris.HCl, pH 7.4, 12 mM $MgCl_2$, 1 mM DTT) or 10 mM phosphate buffer, pH 7.0, 20% glycerol, 1 mM DTT. PRPP concentration when used was 50 μM . Protein was at a precolumn concentration of 1 mg/ml. Enzymes were preincubated in 1 mM PRPP in the presence of 12 mM $MgCl_2$ for 30 min when the runs were carried in the presence of 50 μM PRPP.

3.2.6 Enzyme activation

All three of the above proteins have negligible activity on purification and need to be activated. Activations were carried out at a protein concentration of 30 μM with DTT concentration increased to 5 mM. Activation of the protein for all initial experiments was carried out with 200 μM PRPP and 60 μM hypoxanthine. Xanthine when used for the activation was at a concentration of 120 μM . IMP, XMP and GMP when used were at a concentration of 60 μM and magnesium at a concentration of 12 mM. Incubations were carried out at 4°C for at least 24 h unless otherwise specified.

3.2.7 Enzyme assays and kinetics

Enzyme assays were carried out as described in Chapter 2 (2.2.6). Kinetic parameters were determined by varying the concentration of one substrate keeping the other constant at a saturating value. Reactions were initiated by the addition of enzyme (1.6 μg in a 250 μl reaction). For the determination of purine K_m , the purine base concentrations were varied between 2 μM and 100 μM in the case of hypoxanthine and guanine or between 25 μM and 300 μM in the case of xanthine with PRPP maintained constant at 1 mM. For the determination of PRPP K_m s, base concentrations were kept constant at 100 μM (hypoxanthine and guanine) or 200 μM (xanthine) and PRPP concentration varied from 25 μM to 1 mM. At least 7 concentrations of the variable substrate were used. K_m s were determined by fitting to Michaelis-Menten kinetics after linear transformation. Data were also analysed by non-linear regression. The Graphpad Prism package was used in all analysis.

3.2.8 Circular dichroism

Circular dichroism measurements were carried out in 10 mM phosphate buffer, pH 7.0 at a protein concentration of 2.4 μM with unactivated proteins. Hypoxanthine, PRPP and xanthine concentrations were 33 μM , 100 μM and 66 μM , respectively when used. Measurements were carried out on a JASCO-715 spectropolarimeter equipped with a peltier heating system. Secondary structure was monitored as the ellipticity at 220 nm between a temperature of 25 and 90 $^{\circ}\text{C}$ with a heating rate of 1 $^{\circ}\text{C}/\text{min}$.

3.2.9 Paper chromatography

For determining slow product formation during activation, activation of WTPfHGPRT were set up with ^3H -hypoxanthine as described above. 10 μl aliquots were withdrawn after 6 and 48 h of activation, boiled for 5 min to denature protein, cold IMP and hypoxanthine added to a concentration of 2.5 mM each to allow visualization under UV. Samples were subjected to paper chromatography with 5 % potassium dihydrogen phosphate as the mobile phase. Spots were detected under

UV, cut out and radioactivity corresponding to IMP and hypoxanthine determined by liquid scintillation counting.

3.2.10 Temperature stability and activity

For determination of temperature stability, proteins were activated as described above for 24 h followed by incubation at various temperatures. Aliquots were withdrawn at different times and activity on the base xanthine measured at room temperature using the standard assay.

For the determination of the effect of temperature on activity, reactions were initiated by addition of enzyme activated for 24 h at 4°C, to assay buffer containing the appropriate substrates maintained at the requisite temperature. The assays were carried out at the same temperature in a thermostatted cell holder.

Temperature effects on the activation process were determined by carrying out the activation itself at different temperatures. The process was monitored by measuring the specific activity (for xanthine phosphoribosylation at room temperature) at different time points during the course of activation. The rate of activation determined from these measurements is the rate of increase in specific activity at each temperature calculated as the slope of the incubation time vs specific activity plots. Product formation during these activations was also determined by setting up activation with ³H-hypoxanthine and detecting the amounts of radiolabelled IMP and hypoxanthine at different time points during the activation process in the activation mix.

3.3 Results

3.3.1 Site-directed mutagenesis and functional complementation: Temperature sensitivity

The L44F mutant of PfHGPRT was generated by the megaprimer PCR method as described in Materials and Methods (3.2.1) and cloned into the expression vector pTrc99A. A P2A mutation was introduced in addition in order to facilitate cloning of

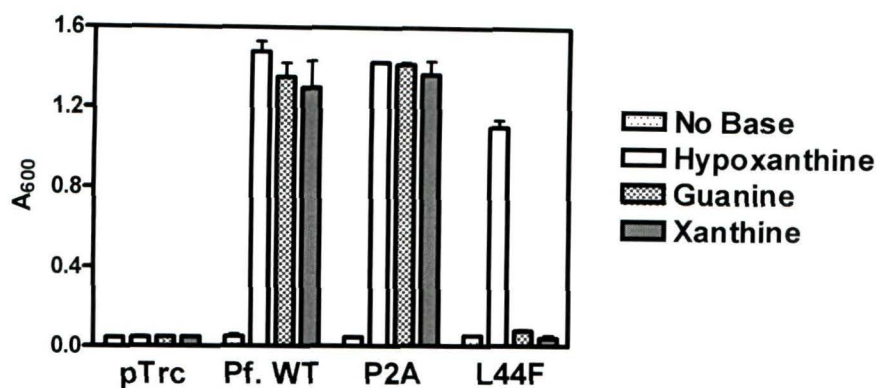


Figure 3.5: Substrate specificity of *P. falciparum* wildtype and mutant HGPRTs as determined by functional complementation. Growth of *S*ϕ609 cells transformed with the respective expression constructs in pTrc99A in minimal medium containing IPTG supplemented with the purine bases 16 h after inoculation was monitored as the absorbance at 600 nm.

the mutant. All control experiments described here were therefore carried out with the P2A mutant of PfHGPRT. The P2A mutant of the wildtype enzyme has been previously characterized in the lab and shown to be identical in its properties to the parent enzyme (Sujay Subbayya & Balaram, 2002). *E. coli* Sϕ609 cells transformed with this expression construct were used to determine the substrate specificity of this mutant by functional complementation (Fig. 3.5). While WTPfHGPRT and P2A support the growth of Sϕ609 in minimal medium supplemented with either hypoxanthine, guanine or xanthine, the L44F mutant complemented only with the purine base, hypoxanthine. Since, mutation at the same position in the human enzyme affects the stability of the enzyme (Fig. 2.11), functional complementation was also carried out at different temperatures. Fig. 3.6 shows the growth of Sϕ609 cells, transformed with either P2A or L44F, in the three purine bases at 20, 37 and 42 °C. Complementation by P2A is not temperature dependent with growth seen at all three temperatures in all three purine bases. L44F however, is temperature sensitive. This mutant does not support growth at 42°C on any of the three bases. At 37°C, growth is seen only in the presence of hypoxanthine. When the temperature is lowered to 20°C, feeble growth is observed in the presence of guanine and xanthine also, while growth on hypoxanthine is good.

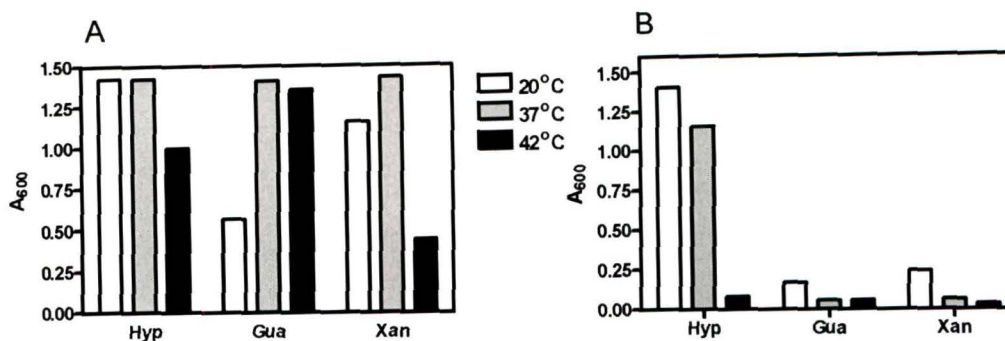

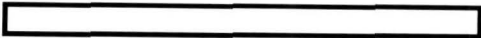









Figure 3.6: Growth of *E. coli* Sφ609 transformed with A) P2A and B) L44F at different temperatures monitored as absorbance at 600 nm. The measurements were made after 16 h of growth at 37 and 42° and 24 h of growth at 20°C.

Sφ609 (Jochimsen et al., 1975) lacks both the salvage and *de novo* pathways for purine nucleotide synthesis. In the presence of a functional HGPRT, AMP and GMP are synthesised as shown in Fig. 1.3. Hypoxanthine can be converted directly to IMP which can serve as a precursor for both AMP and GMP. Complementation in the presence of hypoxanthine is therefore most efficient. When the purine bases available are restricted to guanine or xanthine, GMP formation is direct. However, the formation of AMP would require first the conversion of GMP to IMP by the action of GMP reductase which can then be converted to AMP. GMP reductase in *E. coli* is induced only in the presence of large excess of GMP. Therefore, growth in the presence of guanine alone would require that GMP accumulate to levels high enough to induce the expression of GMP reductase (Zalkin & Nygaard, 1996). In addition the K_m of this enzyme for GMP is high, making the process of conversion to IMP rather inefficient until high levels of GMP accumulate (Zalkin & Nygaard, 1996). Good growth of Sφ609 on guanine and xanthine is therefore, observed only when large amounts of highly active HGPRTs are expressed. In the case of L44F, the temperature sensitivity of the enzyme results in much too low activity on guanine and xanthine at 37°C to allow complementation. At 20°C, sufficient enzymatic activity accumulates to allow weak growth on guanine and xanthine.

Construct	 PfHGPRT Human HGPRT	Substrate specificity		
		H	G	X
P2A(WT)		✓	✓	✓
P2AL44F		✓	✗	✗
DS1		✓	✓	✓
DS1L44F		✓	✗	✗
DS5		✓	✗	✗
DS5L44F		✗	✗	✗
DS7		✓	✓	✓
DS7L44F		✓	✓	✗

★ L44F mutation ✓ Supports growth of Sϕ609 ✗ Does not support growth

Figure 3.7: Substrate specificity of L44F mutants of chimeric HGPRTs as determined by functional complementation. The chimeric constructs are represented as bar diagrams.

3.3.2 Mutation of L44 to F in chimeric HGPRTs

Chimeric HGPRTs comprising of sequences from both *P. falciparum* and human HGPRTs had been previously constructed in the laboratory (Sujay Subbayya, 2002). Three of these chimeras comprising of N'terminal segments from PfHGPRT (Fig. 3.7) had been shown to be active. Chimera DS1 has the first 58 amino acids of the *P. falciparum* enzyme replacing the first 50 of the human enzyme, while in chimera DS7 the C terminal 58 amino acids are also from the *P. falciparum* enzyme. Chimera DS5 was constructed by replacing the C terminal 58 amino acids of the *P. falciparum* enzyme with that of the human enzyme (Sujay Subbayya, 2002). Leu at position 44 in these three chimeras was mutated to Phe and the substrate specificity evaluated by functional complementation. The L44F mutation was found to alter the ability to complement HGPRT deficiency in Sϕ609 in all three chimeras (Fig. 3.7). In addition, it was also found that the mutants of the chimeras do not

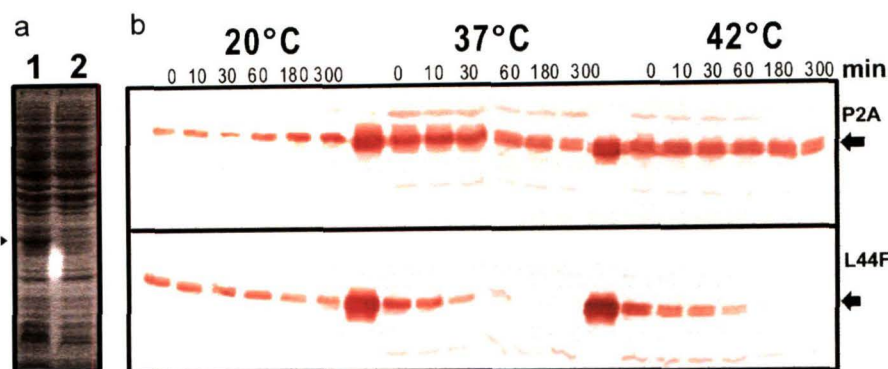


Figure 3.8: *In vivo* stability of P2A and L44F. a) SDS-PAGE analysis of *E. coli* S ϕ 609 cells transformed with 1. P2A and 2. L44F constructs 12 h after induction with IPTG. b) Western blot showing the residual levels of P2A and L44F in *E. coli* S ϕ 609 cells expressing the proteins, at different time points after translational arrest detected using anti-PfHGPRT antibodies. Arrows indicate the protein of interest.

express in S ϕ 609 while the parent constructs do. Though behavior on functional complementation is altered in all the three cases, it is not clear if the alteration is due to reduced stability or due to variation in expression levels. Only the L44F mutant of WTPfHGPRT was studied in detail.

3.3.3 Protein expression and *in vivo* stability

Both the wildtype and P2A PfHGPRT over-express in the *E. coli* strain S ϕ 609. However, expression of L44F cannot be detected by SDS-PAGE (Fig. 3.8a). This suggests that the temperature sensitivity of L44F (in S ϕ 609) could be a consequence of either the lack of expression of the enzyme or its lack of activity or stability with increase in temperature. The *in vivo* expression and stability of L44F at different temperatures was therefore examined. Protein expression was induced by addition of IPTG to cells transformed with constructs in pTrc99A, expression allowed to proceed at different temperatures for 4 h and protein translation arrested by the addition of chloramphenicol. The amount of P2A and L44F in aliquots withdrawn at various time points was determined by western blotting using PfHGPRT specific antibodies. The blots are shown in Fig. 3.8b. As can be seen, P2A is stable at all three temperatures with the level of protein remaining constant. L44F is remarkably

destabilised at both 37 and 42°C, with the protein getting completely degraded *in vivo* within 30 min. The stability at 20°C is considerably improved with almost no proteolysis at this temperature. This indicates the the *temperature sensitivity of L44F is a consequence of reduced stability and resultant proteolysis in vitro*. These observations are in agreement with the functional complementation studies.

3.3.4 Protein purification

P2A could be readily purified using protocols reported for the wildtype enzyme. L44F however, does not express in the *E. coli* strain S ϕ 609. Expression was therefore carried out in the *E. coli* strain BL21(DE3) after subcloning in the vector pET23d. Protein was found to go into inclusion bodies when cells were grown at 37°C before induction. The cultures when grown and induced at 20°C yielded soluble protein though the protein quality varied between batch. Purification of the enzyme also proved to be difficult. At least 100 mM KCl had to be maintained during the entire course of the purification to prevent non-specific aggregation with other *E. coli* proteins. All the purification steps were also carried out in the cold. Only a part of the protein was found to bind to the Cibacron Blue column. The unbound fraction could not be further purified. Purified protein recovery was also poor with the final yield of the protein varying between 300-500 μ g from 1 l of culture. The purity of the protein also varied between batches. After purification, the enzyme could be buffer exchanged into 10 mM potassium phosphate, pH 7.0, 2 mM DTT in the presence of 20 % glycerol and stored under these conditions without further precipitation. The spectroscopic measurements were carried out with protein that was at least 95 % pure as judged by SDS-PAGE (Fig. 3.9).

3.3.5 Oligomerization

Studies on WT PfHGPRT and P2A had shown that tetramerization is important for the activity of the enzyme (Sujay Subbayya & Balaram, 2002, Sujay Subbayya, 2002). This enzyme is a tetramer in low ionic strength phosphate buffer and a dimer under assay conditions in the absence of the substrate, PRPP. A shift towards a tetrameric species is seen in assay buffer in the presence of PRPP. Gel

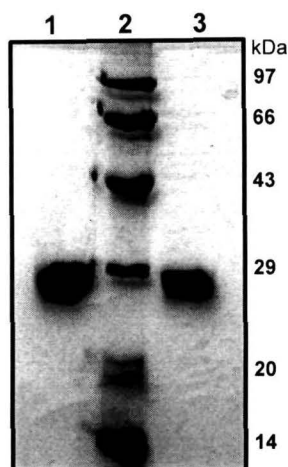


Figure 3.9: SDS-PAGE profile of L44F and P2A. 1) L44F, 2) Marker, 3) P2A.

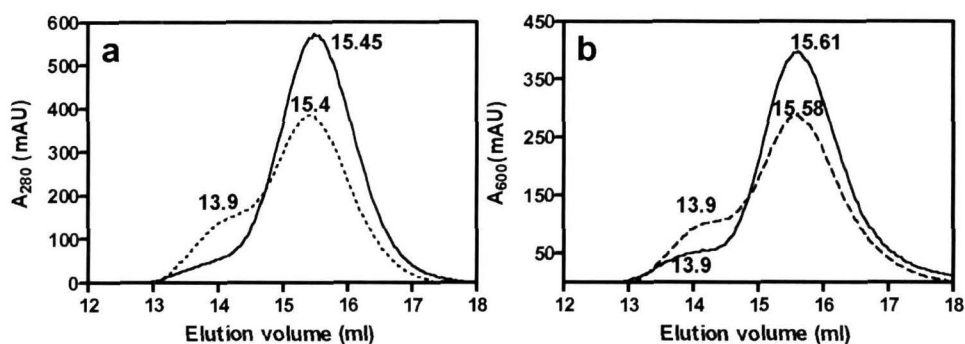


Figure 3.10: Gel filtration profile of a) P2A and b) L44F in a) Assay buffer with (dashed line) and without (solid line) PRPP. Gel filtration carried out as in Material and Methods (3.2.5).

filtration profiles of P2A and L44F in assay buffer in the presence and absence of PRPP are shown in Fig. 3.10. The precolumn concentrations of both the proteins were 1 mg/ml ($\approx 50 \mu\text{M}$ protein). Both these enzymes are tetrameric in 10 mM phosphate buffer. The elution profiles of L44F are similar to that of P2A under these conditions indicating that at high protein concentrations, the oligomerization of L44F is unaltered.

P2A and L44F however, behave differently at lower protein concentrations. The specific activity of unactivated L44F and P2A are plotted as a function of protein

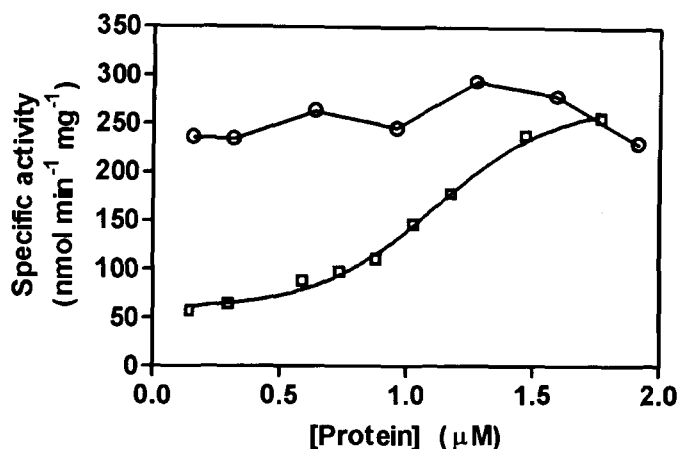


Figure 3.11: Concentration dependence of the activity of P2A(\circ) and L44F (\square). Assays were carried out with the unactivated enzyme. Plot is representative of two independent experiments.

concentration in the assay in Fig. 3.11. Over the concentration range studied, the specific activity of P2A is independent of protein concentration while that of L44F shows a distinct increase before plateauing at protein concentrations above $2.0 \mu\text{M}$. This indicates that the tetramer of L44F with a K_d of $1.12 \mu\text{M}$ in assay buffer in the presence of 1 mM PRPP, is weaker than that of P2A. However, both these proteins would be tetramers under activation conditions where the protein concentration is maintained at $30 \mu\text{M}$.

3.3.6 Activation and kinetic characterization

As mentioned earlier, PfHGPRT has negligible activity on purification and can be activated by incubation in the presence of substrates hypoxanthine and PRPP. This is also the case with L44F. Activation was also carried out in the presence of xanthine instead of hypoxanthine. The specific activities of the unactivated proteins are compared with the specific activities after activation in the presence of xanthine and hypoxanthine in Fig.3.12. As can be seen considerable increase in activity is observed only in the presence of hypoxanthine and not in the presence of xanthine. Maximal activity achieved after about 24 h at 4°C was stable for many days on storage under activation conditions. Kinetic properties were determined with these

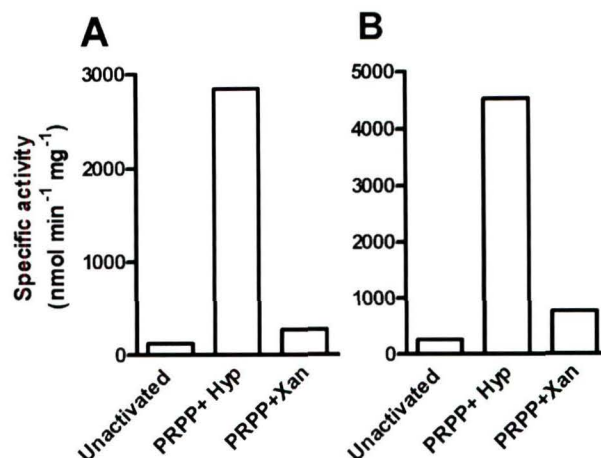


Figure 3.12: Activation of A) L44F and B) wildtype PfHGPRTs in the presence of hypoxanthine and xanthine. Note: This experiment compares L44F with WTPfHGPRT and not P2A. Numbers are representative of two replicates.

Table 3.1: Kinetic parameters of wildtype and mutant PfHGPRTs.

		K_m (μM)		k_{cat}/K_m ($\mu\text{M}^{-1}\text{s}^{-1}$)	
HPRT reaction					
Enzyme	k_{cat} (s^{-1})	Hypoxanthine	PRPP	Hypoxanthine	PRPP
P2A	1.13	≈ 0.65	22.0	1.7	0.05
L44F	0.94	< 1.0	44.0	> 0.94	0.02
GPRT reaction					
P2A	1.19	≈ 0.91	119	1.31	0.01
L44F	1.07	1.5	88.0	0.71	0.01
XPRT reaction					
P2A	2.9	410	84	0.04×10^{-1}	0.03
L44F	1.2	868	142	0.01×10^{-1}	0.01

activated preparations and are listed in Table 3.1.

Examination of the specific activities shows that the k_{cat} s and K_m s of both the enzymes on hypoxanthine are comparable while the activity on xanthine of the L44F mutant is 2 fold lower. The K_m of the mutant for xanthine is also increased. This is not surprising as a similar mutation in the human enzyme affects the ability of the

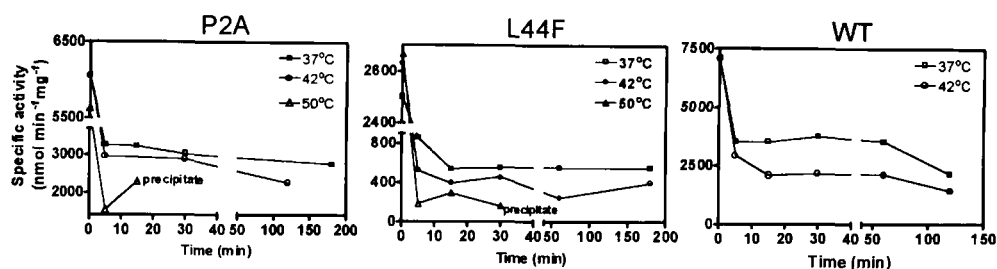


Figure 3.13: Temperature stability of wildtype and mutant PfHGPRTs. Enzymes after activation for 24 h at 4°C were incubated at the specified temperatures and residual activity on xanthine measured at different time points.

enzyme to catalyse xanthine phosphoribosylation.

3.3.7 Temperature stability

Since the complementation experiments indicated that the L44F mutant is temperature sensitive, the activity and stability of the enzymes at higher temperatures was examined. For the stability experiments protein under activation conditions was incubated for different times at higher temperatures and residual activity measured. Compared to the human enzyme that shows remarkable temperature stability, P2A and L44F lose considerable activity on incubation at higher temperatures. Fig. 3.13 shows the residual activity after incubation at different temperatures. The L44F mutant is considerably destabilised as compared to P2A. Another feature that emerges from the activity profiles is that the specific activity of the activated enzyme rapidly drops to a lower value on incubation at higher temperatures and is then stable at this lower value for at least 3 h. The value at which the activity stabilises decreases with increase in the temperature of incubation. This is indicative of *an equilibrium between an active and inactive form of the enzyme*, the populations of which vary with the temperature.

Fig. 3.14 shows the activity of P2A and L44F on the bases hypoxanthine and xanthine at different temperatures. These measurements involved initiation of reaction by addition of activated enzyme maintained on ice to preheated assay buffer containing PRPP and the respective purine base. Though the temperature instability

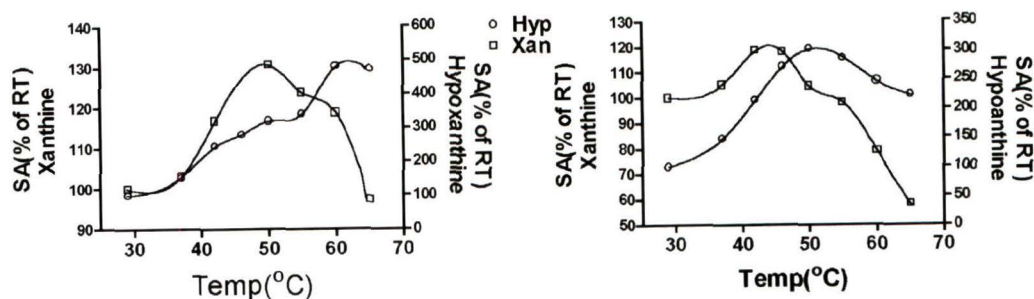


Figure 3.14: Activity of P2A (left panel) and L44F (right panel) at different temperatures. Activity is plotted as a percentage of activity at room temperature (RT). Reactions were carried out with activated enzyme. Note that the axis for hypoxanthine and xanthine are on different scales. Plots are representative of two independent measurements.

of P2A and L44F precludes the use of these values for the determination of activation energies for the phosphoribosylation, an interesting fact emerges from the temperature activity curves. As can be seen, the rate of phosphoribosylation by L44F starts to drop at temperatures lower than that of P2A in agreement to the observed thermal lability of this mutant. Surprisingly, the rates of phosphoribosylation of xanthine start to drop about 10°C before the rates on hypoxanthine in the case of both the enzymes. Since the enzymes preparations used are identical for both hypoxanthine and xanthine reactions, these observations raise the possibility of destabilisation of the enzymes by the substrates. The possible role of variation in substrate ionization with temperature in the rates of phosphoribosylation could be ruled out as the spectral properties of the bases do not change with increase in temperature (data not shown). The absorption spectra of these bases have been previously shown to be sensitive to the ionization state.

3.3.8 Effect of substrates on thermal stability: circular dichroism studies

To test the possibility that P2A and L44F are destabilised in the presence of the substrates, the denaturation of these enzymes with increase in temperature was monitored in the presence of the substrates by circular dichroism as described in materials and methods. Unactivated enzyme was used for these experiments as hypoxanthine from the activation mix would prevent determination of the effects of

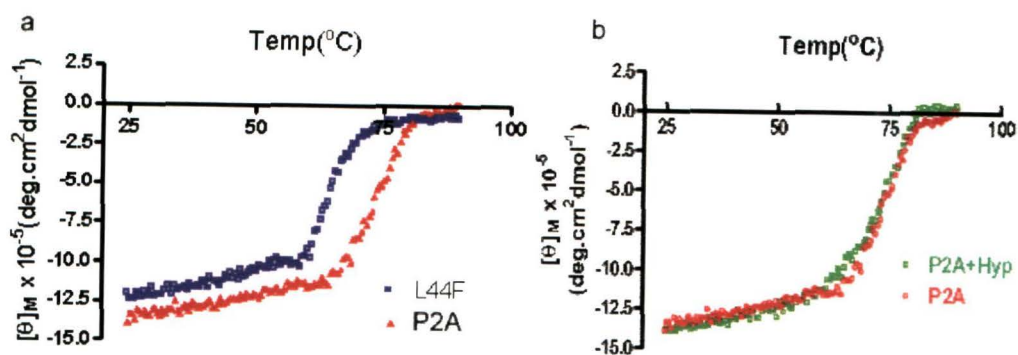


Figure 3.15: Denaturation of a) P2A and L44F b) P2A in the presence and absence of hypoxanthine, with increase in temperature monitored as ellipticity at 220 nm.

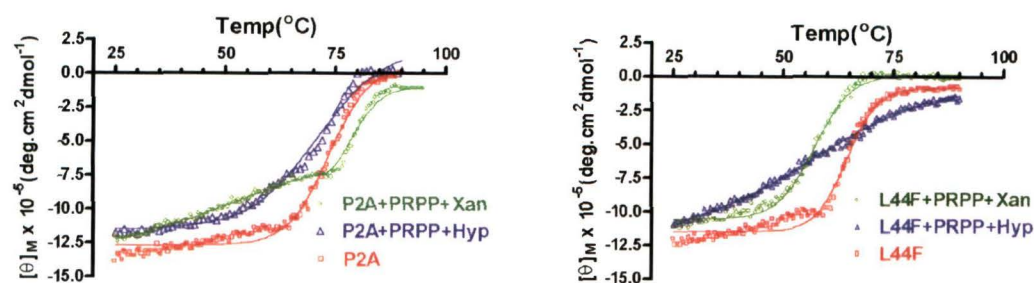


Figure 3.16: Effect of substrates on temperature denaturation of P2A and L44F monitored as ellipticity at 220 nm.

xanthine on stability. The measurements were carried out at a protein concentration of $2.4 \mu\text{M}$, in the presence of $100 \mu\text{M}$ PRPP and $33 \mu\text{M}$ hypoxanthine or $66 \mu\text{M}$ xanthine, conditions that are close to the activation conditions. The melting curves of P2A and L44F in the absence of substrates are shown in Fig. 3.15a. The loss in stability of L44F is again obvious with the mutant melting 6°C below P2A. The melting curves are not altered in the presence of either PRPP or hypoxanthine (Fig. 3.15b). Remarkably, the substrates when present together show a dramatic effect on the melting curves of the enzymes (Fig. 3.16). This effect is more obvious in the case of the L44F mutant as compared to P2A. In the case of P2A, presence of hypoxanthine and PRPP reduces the melting temperature by 2°C . The melting curves however, remain indicative of a cooperative two state transition as in the absence of substrates. Xanthine and PRPP alter the nature of the transition curve which is now indicative of an initial gradual denaturation to a state that then

Table 3.2: Melting temperatures and nature of transition for P2A and L44F under different conditions.

Enzyme & condition	$T_m(^{\circ}\text{C})$	Nature of transition
P2A	73.4	2 state
P2A+PRPP+Hyp	70.8	2 state
P2A+PRPP+Xan	-	Multi-state
L44F	64.3	2 state
L44F+PRPP+Hyp	56.1	Multi-state
L44F+PRPP+xan	57.0	2 state

undergoes cooperative melting. These effects are magnified in the melting of the L44F mutant. The two state transition of the protein transforms into a multistate transition in the presence of hypoxanthine and PRPP. In the presence of xanthine and PRPP, the transition remains two state but the melting temperature decreases by 7°C (Fig. 3.16, Table 3.2). It is indeed surprising that substrate induced conformational changes manifest as such drastic alterations at the level of the secondary structural stability of the protein. The melting curves also fit in with the observed temperature vs activity curves of the enzymes. The implications of these observation for the nature of the active form of the enzyme are dealt with in the discussion section of this chapter.

3.3.9 Activation of PfhGPRT: Product formation

The experiments described in this and the following sections were carried out with WT PfhGPRT. The activation of PfhGPRT is carried out in 10 mM phosphate buffer in the presence of the substrates, PRPP and hypoxanthine. Magnesium ions which are essential for catalysis were not added during the activation. The possibility that trace divalent metal ions may be present in the activation, either carried over with the protein during the purification or as a contaminant from one of the buffer components however, exists. Product formation would occur in such a scenario. Spectrometric measurement of product formation in the activation mix is

not feasible due to the lack of sensitivity and the large contribution of the protein to the absorption of the sample. Product formation was therefore detected by using ^3H -hypoxanthine in the activation. Hypoxanthine and IMP were then separated by paper chromatography (3.2.9) and the distribution of label between the two molecules determined. Table 3.3 compares the specific activity of the enzyme during the course of activation with the conversion to IMP. As can be seen from the table, the degree of activation correlates well with the amount of IMP formed during the activation. Indeed, activation was abolished in the presence of 1 mM EDTA. The possibility

Table 3.3: Product formation during activation of WTPfHGPRT at 4°C.

Condition of activation	Duration (hours)	Specific activity ^a (nmol min ⁻¹ mg ⁻¹)	$\frac{^3\text{H-Hyp}^b}{^3\text{H-IMP}}$
PRPP+Hyp, 4°C	6	1446.0	8.90
PRPP+Hyp, 4°C	48	5224.6	0.58
PRPP+Mg ²⁺ +Hyp, 4°C	3	11916.0	0.28

^a Specific activity for xanthine phosphoribosylation. This is distinct from the product formation in the activation mix.

^b Ratio of counts in hypoxanthine and IMP.

that the product formation seen during the assays is a consequence of carry over of product formed during the activation was also investigated. Assays carried out with the unactivated enzyme with IMP equivalent to that contributed from the activation mix failed to show the enhancement in activity that is seen during the activation process. It must be noted here that the all enzyme activity measurements involved continuous monitoring of product formation by spectrometry and therefore are a true measure of product formation during the assay. Any product added into the assay would not alter the specific activities determined.

The results described in the previous sections suggest that the activation process involves a conformational switch in the enzyme which destabilises the enzyme. The temperature dependence of the activation process was therefore investigated. These activations were carried out with ^3H -hypoxanthine in order to facilitate the measurement of product formation during the course of the activation. Fig. 3.17

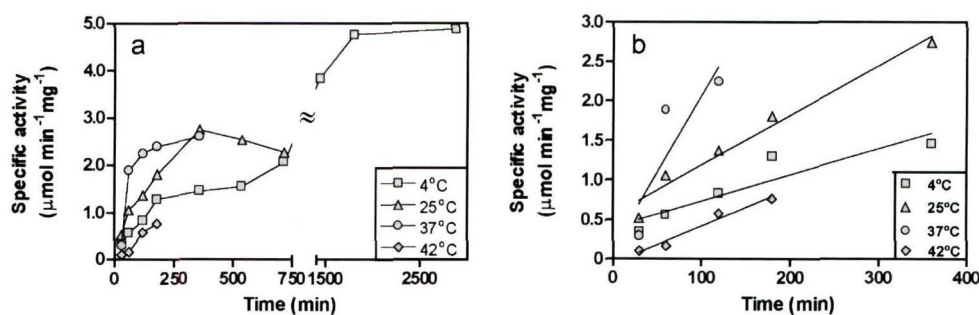


Figure 3.17: Effect of activation temperature on the activity of WTPfHGPRT. The time course of the activation at different temperatures monitored as the activity on xanthine is shown (a). The right panel (b) shows the linear region of the same graph. Activation was carried out with ^3H -hypoxanthine and PRPP.

shows the specific activity for xanthine phosphoribosylation of aliquots withdrawn at different time points from each activation. *The rate of activation (initial slopes of the time course) is much larger at higher temperatures. However, the maximal levels of activity achieved decrease with increase in temperature, in agreement with the preincubation studies described in 3.3.7.*

Aliquots were withdrawn after 6 h of activation at each temperature and the amount of hypoxanthine and IMP in the mixtures determined by paper chromatography. The rates of formation of IMP (amount of IMP formed/time) during the activation are plotted along with the rates of activation in Fig. 3.18. The rates of activation are the slopes of the curves in Fig. 3.17b. The rates of activation of PfhGPRT correlate very well with the rate of IMP formation. However, as mentioned earlier, the maximal activity achieved on activation decreases with increase in temperature. These experiments suggested that the conformational changes accompanying the activation process are brought about by the product of the reaction IMP and not the substrates themselves.

3.3.10 Activation by products

Fig. 3.19 compares the time course of the activation by IMP in the presence of Mg^{2+} and pyrophosphate (PPi) with that in the presence of hypoxanthine and PRPP

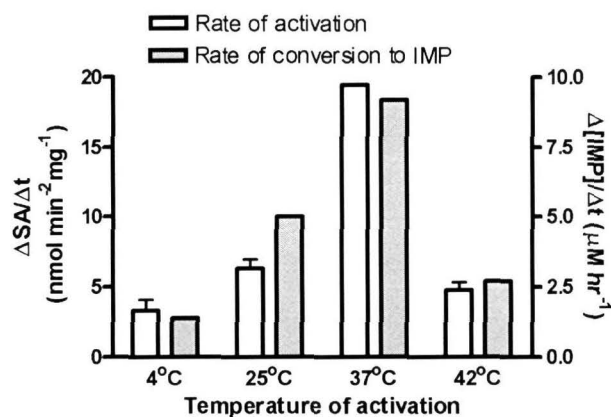


Figure 3.18: Rate of activation compared with the rate of IMP formation at different temperatures. The rates of activation of WTPfHGPRT were determined from the slopes in Fig. 3.17. The rates of product formation were determined using radiolabelled substrate as described in 3.2.9

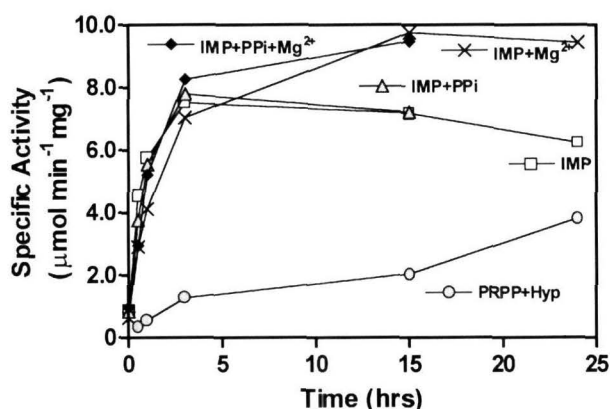


Figure 3.19: Activation of WTPfHGPRT by different combinations of products of the HGPRT reaction as indicated. Activation was followed by measuring xanthine phosphoribosylation.

(Fig. 3.19). As can be seen, IMP rapidly activates the enzyme to very high levels. Activation is maximum and most stable in the presence of IMP and Mg²⁺. Though IMP alone or IMP and PPi activate the enzyme rapidly, the activity is not stable and starts to drop after 24 h. This also raises the possibility that lack of activation in the presence of xanthine may be due to the lack of formation of XMP as the xanthine K_m of PfHGPRT is high. Incubation in the presence of XMP or GMP however, failed to activate the enzyme. Activations carried out at higher temperatures showed

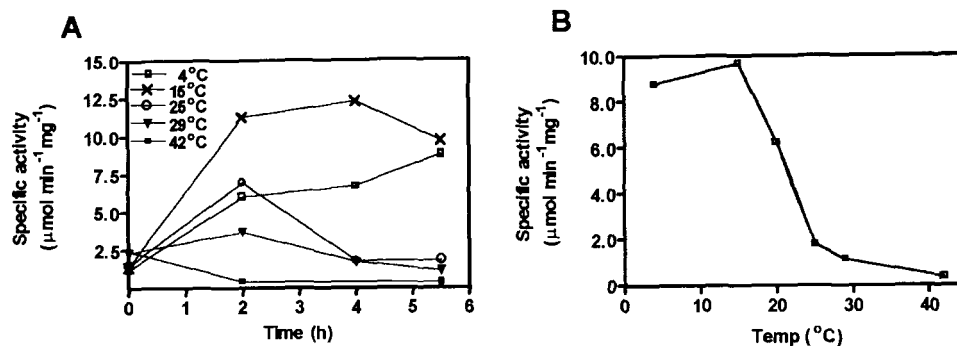


Figure 3.20: Time course of activation of WTPfHGPRT by IMP and Mg^{2+} at different temperatures(A). The left panel (B) shows the activity achieved after 5.5 h of activation at each temperature. The 0 time point is the activity measured immediately after the addition of the ligands to the enzyme pre-equilibrated to the requisite temperature. Specific activity on xanthine are indicated.

a similar trend as in the case of the activations with PRPP and hypoxanthine with *the activity being lower when the preincubations are at higher temperatures* (Fig. 3.20). Though these values reflect a combination of the degree of activation and enzyme stability, it is clear that the equilibrium between the active and inactive forms of the enzymes varies with the temperature.

3.4 Discussion

3.4.1 Core mutations and protein stability

Stability studies on the mutants of human HGPRT, F36L and F36G, suggested that mutation at this position in the core of the HGPRT structure can destabilise the protein (2.3.5). This is more obvious in the case of the L44F mutant of PfHGPRT. PfHGPRT is inherently less stable than the human counterpart. Preincubation studies with the human enzyme show that it retains a substantial amount of activity even at 80°C (Fig. 2.10). PfHGPRT on the other hand rapidly loses activity with increase in temperature. Mutation of the core residue L44 to F in context of the *P. falciparum* protein therefore, has a more dramatic effect on the stability resulting a temperature sensitive mutant. This is indeed fortunate as the substrate induced

changes manifest better in this mutant providing information on the nature of the active form of this enzyme.

The effect of core mutations on protein structure and stability are thought to be an interplay between packing and hydrophobicity. Generally, large to small substitutions that create or enlarge cavities are destabilising. Small to large substitutions that increase side chain size can result in overpacked variants which are destabilised due to unfavourable steric contacts, disruption of interactions with surrounding residues or the introduction of torsional strain. The effect of mutations are context and protein specific. For example, Eriksson et al., 1993, have shown that the mutation of F153 to L in the T4 lysozyme increases stability and mutation of L99 to F decreases protein stability marginally. The structure of the L99F mutant in this case shows substantial rearrangement of both side chains and backbones of residues around the mutation. The effect of these mutations do not correlate directly with the expectations from hydrophobicity considerations alone (Gromiha et al., 1999). It is therefore, not surprising that a mutation of a Leu to Phe in the core of PfHGPRT destabilises the structure.

3.4.2 Activation of PfHGPRT

Previous studies (Subbayya & Balaram, 2000, Keough et al., 1999) have demonstrated that PfHGPRT can be activated on preincubation with the substrates, PRPP and hypoxanthine. The results presented in this chapter show that activation is effected by the product of the reaction, IMP and not by the substrates themselves. It is surprising that the product of only one of the three alternate substrates enzyme, IMP, can activate the enzyme. This phenomenon is likely to be related to the mode of recognition of the three substrates by the enzyme. The inability of XMP and GMP to effectively activate the enzyme suggests that the contacts made by these purine moieties are not conducive for promoting the necessary conformational changes. As described in Chapter 2, studies on the *T. foetus* and *T. gondii* enzymes suggest the role of protein flexibility in the recognition of substrates. Potential unfavorable interactions of the enzyme with xanthine are offset by rearrangement of the protein structure, especially of residues in loop IV of the protein (Fig. 1.9). It is interesting

to note that L44 in PfHGPRT, like F36 in human HGPRT, lies at the base of loop IV making contacts with residues at either end of the loop in addition to a contacts with Val198 within the loop. This mutant of PfHGPRT shows a dramatic difference in stability between its activated and unactivated forms. Taken together, these factors suggest a role for loop IV mediated reorganization in the process of activation. This possibility however, needs further investigation. The presence of a Trp in loop IV of *T. gondii* HGPRT offers the possibility of constructing a similar mutant of PfHGPRT by replacement of the Phe at this position. This mutant may serve as a fluorescent reporter allowing monitoring of the activation process.

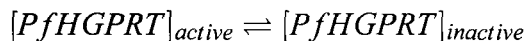
3.4.3 The active form of PfHGPRT is metastable

All the observations described above suggest that the conformation of the enzyme on purification is one of high stability albeit of low activity. Incubation with the substrates/ products alters the conformation to a less stable state. This state of lower stability, a metastable state, is the active form of the enzyme. The basis of this interpretation is presented below.

1. The temperature dependent denaturation of the proteins also shows that both hypoxanthine and xanthine destabilise the enzyme in the presence of PRPP (Fig. 3.16). The CD experiments have been carried out in the presence of substrates and not products as the process of activation was thought to be a consequence of substrate binding. The role of IMP formation in the process of activation was recognized only later (3.3.9). The circular dichroism measurements are however a reflection of the nature of the activated enzyme. The CD experiments were carried out after incubation of the proteins in the presence of base and PRPP on ice for 30 min, then at 25°C to raise the temperature to the start point of the measurement. Heating carried out a rate of 1°C per min allowed another 12 min for product formation during the experiment. Though these factors make the exact composition of the experimental solution an indeterminate quantity, sufficient product formation would have occurred to allow activation. In fact the activation with hypoxanthine and PRPP when carried out at elevated temperatures is

very rapid with significant activation achieved within 15 min (Fig. 3.17). The melting curves observed in the presence of hypoxanthine and PRPP therefore report on the activated form of the enzyme. The pronounced decrease in the stability under these conditions, especially in the case of the L44F mutant (Fig. 3.16, Table 3.2), *shows that the activated form of PfHGPRT is metastable.*

2. The effects of elevated temperatures on the activation (Fig. 3.17, 3.20) and stability (Fig. 3.13) also support this surmise. When activated enzyme preparations are incubated at elevated temperatures, the activity drops drastically to stabilise at a lower value (Fig. 3.13). The enzyme activity is restored to the value seen at 4°C when the samples are returned to this temperature after incubation at 25 or 37°C. The maximal levels of activity achieved also decreases with increase in temperature (Fig. 3.17, 3.20). This is suggestive of an *equilibrium between two form of the enzyme, one of higher activity and the other of lower activity.*



The population of each species at a particular temperature would then be determined by the energy barrier for conversion between the two states.

3. The activity vs temperature profiles of both P2A and L44F show differences with the substrate used in the assay (Fig. 3.14). The enzymes are destabilised in the presence of xanthine as compared to hypoxanthine. It must be noted here that similar measurements on wildtype and F36L mutants of human HGPRT show a continuous increase in activity upto temperatures as high as 65°C even though the K_m of these enzymes for xanthine are high (Fig. 2.12). The decrease in activity on xanthine observed with the *P. falciparum* enzymes is therefore a reflection of **substrate induced destabilisation** of the enzymes and not a consequence of differences in the K_m affecting activity with increase in temperature.

Taken together, these data allow a description of the energy landscape for the activation (Fig. 3.21). All evidence support the surmise that the activated state is less

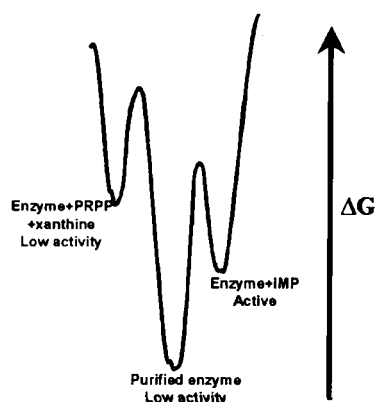


Figure 3.21: Proposed energy landscape for PfHGPRT

stable than the unactivated state. The enzyme in solution exists as an equilibrium between the two states. Binding of IMP provides sufficient energy to tide over the energy barrier between the two states, leading to activation. Since the inactive form is populated more at elevated temperatures, this is the form with the lower energy. The energy barrier for the conversion from the active form to the inactive form is smaller than the barrier for conversion from the inactive form to the active form. The active form of PfHGPRT can therefore be called a metastable state, attained by IMP binding.

The nature of the activated state is however, not clear. This state of reduced stability may well be the product bound form of the enzyme and points 2 and 3 above a reflection of equilibria between the ligand bound and free forms of the enzyme. The energy landscape proposed above should hold even if this were to be the case.

The process of ligand induced conformational change leading to activation also explains certain unusual observations in literature. Immuclin phosphates, transition state analogs of HGPRT, are potent inhibitors of the enzyme. Inhibition of the reverse reaction has been demonstrated with Immucillin-HP and Immucillin-GP (analogs of the hypoxanthine and guanine reaction transition states, respectively). Reversibility studies on human and *P. falciparum* HGPRT by Li et al., 1999 have demonstrated that activity returns on dilution of the inhibitor. Surprisingly, in the case of PfHGPRT the activity recovered after dilution of the inhibitor is higher than

that in the absence of the inhibitor. The authors however, work with an unactivated enzyme. Studies described above suggest that the incubation with the transition state analog would lead to a conformational switch in the enzyme to its active metastable state. This state would be at least partially retained even on removal of the activating agent leading to an apparent increase in activity after dilution of the inhibitor.

Metastable active states occur very infrequently in literature. Examples include the class of protease inhibitors, serpins which lose their inhibitory activity when stabilising mutations are introduced (Lee et al., 2000). In the case of the α -lytic protease the metastable active state is achieved with the aid of a pro-segment. Protein folding occurs in the presence of this segment, subsequent cleavage of which leads to trapping of the protease in this state due to a kinetic barrier. Denaturation and refolding in the absence of the pro-segment leads to the formation of a more stable but inactive state (Jaswal et al., 2002, Cunningham et al., 1999).

Perhaps of greater relevance to this study is the case of the glucose-3-phosphate dehydrogenase phosphoribulokinase multi-enzyme complex. The phosphoribulokinase component is in a metastable state and when released from the complex retains high activity. Relaxation into the stable form results in reduced activity (Graciet et al., 2002, Lebreton & Gontero, 1999). In most of the examples given above, the property of metastability is common to many proteins of common origin and function. PfHGPRT presents an unique example as this feature is not seen with homologs of identical function from other organisms. In addition, this state is achieved by product induced conformational changes. The *in vivo* implications of this phenomenon are not obvious. The absence of the *de novo* pathway in the malaria parasite entails a central role for this enzyme in the parasites' purine metabolism. The requirements of regulation and activity that this unique position would impose, especially in context of the AT bias of the *P. falciparum* genome, may necessitate novel modes for control of enzyme activity. It is possible that HGPRT exists as a complex with other enzymes allowing it to be maintained in this active state.

Chapter 4

Cloning, purification and kinetic characterization of *Plasmodium falciparum* adenylosuccinate synthetase.

This chapter discusses the cloning of full-length PfAdSS gene, recombinant expression of the protein and detailed kinetic characterization. Some results presented in this chapter are with a truncated clone of AdSS that was already available in the laboratory at the time of initiation of these experiments. A structural interpretation of the kinetic data in this chapter is presented in Chapter 6.

4.1 Introduction

Adenylosuccinate synthetase follows HGPRT in the purine salvage pathway and the reaction catalysed by this enzyme commits IMP to the AMP branch of the nucleotide biosynthetic pathway. The erythrocyte is the only tissue that lacks this essential enzyme (Webster and Whaun, 1981). This enzyme is important not just in dividing cells but also in the maintenance of cellular homeostasis. The *E. coli* and mouse AdSS have been expressed in recombinant systems and extensively characterized (Bass et al., 1987, Inacu et al., 2001). The enzyme from many other species has also been purified and kinetically characterized. These data are summarised here.

4.1.1 Sequence comparison

PfAdSS has previously been sequenced in this laboratory. The sequence is now also available from the *P. falciparum* genome database. Fig. 4.1 shows the alignment of AdSS representative of bacterial, yeast, protozoal, archeal, plant and mammalian sequences. The longest sequences are of the plant enzymes and the shortest of the archaea (*Pyrococcus*) (Bouyoub et al., 1996). The parasite AdSS exhibits highest similarity with the AdSS from *Dictyostelium discoideum* (70 %)(Wiesmuller et al., 1991) followed by the yeast (Lipps and Krauss, 1999) and human (Powell et al., 1992) enzymes showing a similarity of 67%. With the *E. coli* (Wolfe & Smith, 1988) enzyme, *P. falciparum* AdSS shows 62% similarity. Invariant residues primarily contribute to the substrate binding and include the GTP binding motif at the N terminal of the protein, residues involved in recognising the guanine base of GTP (TKLD), Arg155(*E. coli*) that makes cross subunit interactions and the catalytic residues Asp13 and His41 (*E. coli*).

4.1.2 Kinetics

The most extensive kinetic studies are those of Fromm and co-workers on the *E. coli* enzyme. Rudolph and Fromm (1969) established a methodology for the kinetic analysis of three substrate reactions involving the evaluation of the initial rate data with one variable substrate and the other two fixed at a constant ratio. This analysis, along with product and competitive inhibition studies allows the determination of the kinetic mechanism of a reaction. Kinetic studies on the *E. coli* enzyme show that the mechanism is rapid equilibrium random sequential. Studies by Markham and Reed (1977) on the enzyme purified from *Azotobacter vinelandii* have shown that the AdSS reaction has a random order of substrate binding in the reverse direction also. The enzyme has also been purified from human placenta (Van der Weyden & Kelly, 1974), *Trypanosoma cruzi* (Spector et al., 1982), *Schizosaccharomyces pombe* (Nagy et al., 1971), *Dictyostelium discoideum* (Wiesmuller et al., 1991),

```

MSLSLTLDS NPREFAVGGPY HRRYPPLHHP RSEFVCSAKR PAVSASLSVA ADSAATESIG RIGLSQVSG VL GCOWGDEG KGKLVDLAQ HFDIVARCOG GAN
-----
A. thaliana
D. discoideum
Mouseacidic
Mousebasic
S. cerevisiae
P. falciparum
E. coli

AGHTIYNSEG KKFALHLVPS GIINLDTTCV I GNGVVVHLP GLFKEIDGLE SNG---YSCK GRILVSDRAH LLFDFHQEVD GLRESELA- ----SFIGTT KRG
AGHTIVVD-G KIALHLIPS GIINLAKASI LGNGVVIHLP TFFKEVQGLQ DKG---INVK GRLVSDRAH LVFDLHQMID ANKEAELSNG TSN-DSIGTT KRG
Mouseacidic
AGHTVVVD-S KEYDFHLLPS GIINPNVTAI I GNGVVIHLP GLFEEAKNV QKGGLDGWE KRLIISDRAH LVDFDHOADV GQEQQR--Q EQAGKNIETT KKG
AGHTVVVD-G KEYDFHLLPS GIINTKAVSF I GNGVVIHLP GLFEEAKNE KKG--LKDWE KRLIISDRAH LVDFDHOADV GQEVQR--Q AQEGKNIETT KKG
S. cerevisiae
AGHTIVVD-G VKYDFHMLPS GIYNPNCQNL I GNGVVIHVP SFFKELETLE AKG--LKNAR SRLVSSRAH LVDFDHOAVT KLRLELSGR SKDCKNIETT GKG
P. falciparum
AGHTISVN-D KKYALHLLPC GVLYDNNISV I GNGMVIHVYK SLMEETESVG G-----KLL DRLYLSNKAH ILFDIHQIID SIQETKK--- LKEGKQIETT KRG
AGHTIVIN-G EXTVLHLIPS GILRENTVSI I GNGVVLSPA ALMKEMKELE DRG---IPVR ERLLSSEACP LILDYHVALD NAREKAR--- --GAKAIETT GRG
E. coli

IGPAYSSKVI RINGIRVGDIR HM-----DTL POKLDDLLSD A--AARQGFK YTPMLREEV EAYKRYADRLL EPHYT DTVHF INDSISQK-K KVLVEGQAT MLD
IGPCYSSKAS RGGLRVCDLY SP-----EHF RKTETRLVEN K-HRRFGSFE YD---VEAEL KRYQFAEML KPFVI DSVYV INQAFKDG-K KVLIEGAQST MLD
IRPVYSSKAA RSLRMCIDLIV SD---FDGF SERFKVLTNQ Y-KSIYPTLE ID---IEGEL QQLKGYMERI KPMVK DGVIY LYEALHGPPK KILVEGANAA LLD
Mousebasic
IGPYSSKAA RTGLRICDLL SD---FDEF SARFKNLAHQ H-QSMFPTLE ID---VEGQL KRLKGFARLI RMPVK DGVIY MTEALHGPPK KVLVEGANAA LLD
S. cerevisiae
IGPYSTRAS RSLRVHHLV NDQPGAWEEF VARYKRLIET R-RQRYGDPE YD---FEAKL AEYKRLREQL KPFVY DSVVF MHNAIKAK-K KILVEGANAA LLD
P. falciparum
IGPCYSTRAS RIGIRLGTAK NF-----ENF KMYSKLIDH L-MDLNITE YD---KKEKL NLFNYHLKLL RDRIV DVIISF MNTNIENN-K KVLIEGANAA MLD
IGPAYEDKVA RRGLRVGDIF DK-----ETF AEKLKVMVEY HNFQLVNYKY AEAVDYQKVL DDTMAVDAIL TSMVV DVSDL LDQARQRG-D FVMEGAQGT LLD

IDFGTYPFVT SSSPSAGGIC TGLGIAPSVV GDLI GVVKRAY TTRVSGSPPF TENIGTGDDL LRLAGQEFGT TTGRPRRCGW LDIVALKFSC QINGFASLNL TKL
LDFCYPIYVT SSASSVGGAC TGLGISPNKV VTQI GVVKRAY TTRVSGSPPF TEQNDHYGDS LRKAGSEFGT TTGRPRRCGW LDVAVLRYTS MINDFTRNL TKL
I DFGTYPFVT SSNCTVGGVC TGLGMPQNV GQVY GVVKRAY TTRVGI GAFP TEQDNEIGEL LQTRGREGV TTGRKRCRGW LDIVSLRYAH MINGETALAL TKL
I DFGTYPFVT SNTVGGVC TGLGIPQNI GQVY GVVKRAY TTRVGI GAFP TEQDNEIGEL LQNRGHEGV TTGRKRCRGW LDLMILRYAH MVNGFTALAL TKL
IDFGTYPFVT SNTGIGGVL TGLGIPRTI DEIY GVVKRAY TTRVGGPFP TEQDNEIGEL LQTRGHEGV TTGRKRCRGW LDIVLWLYST LINGTYSINI TKL
IDFGTYPFVT SACTVGGVF SGLGHHKLL NLVY GVVKRAY ITRVGGCPFL TELNDVYQY IREKQHYGT TTGRPRRCGW LDIVPMLLYVK CINSTEMINL TKL
IDHGTYPYVT SNTTAGGVA TSSGLGRYV DYVLGILKAY STRVAGPFP TELFDETFEFC LCKQNEFEGA TTGRRRRTGW LDIVAVTRAV QLNLSLGGFCL TKL

DVLSDNEIQ LGVAYKR-SD GTPVKS--FP GDLRLLEELH VEYVLPGMK SDISSVRNYS DLPKAAQQYV ERIEELVGPV IHYIGI GEGR DALIYK---- --
DVLSDFEIK IGVDYK--YK GETIKS--FP ASLETLAQCE VVYESFPGMK CDLSHVTEYD QLPFOAKNYI KRIEELVGPV IVYIGV GVER KNLIERKELI --
DILDMFTEIK VGVAEK--LD GETIPH--FP ANQEVINKVE VQKYLPGWN TDISNARTFK ELFVNAQNVY RFIEDELQIP VKWIGV GKSER ESMIQLF---- --
DILDVLEIK VGISYK--LN GKRIPI--FP ANQELIQKVE VEYETIPGMK ADTTGARKVE DLPFRPKATC ASWRITWVLQ SNGSAL G-SP ESP----- --
DVLDTFKEIP VGISYS--IQ GKKLDL--FP EDLNLGKVE VEYKVLPGWD QDITKINKYE DLPENAKKYL KYIEDVGVGPV VEWVGT GPAR ESMHKEIK-- --
DVLSGLEIL LCVNFNKKKT GELLEKCYP VEEISEEDE PVYKFSGMK EDISTCNEFD ELPENAKKYL LAIEKYLKTP IVWIGV GPNR KNMIVKKNFN LN
DVLVDGLKVK LCVAYR-MPD GREVTT--TP LAADDWKGVE PIYETMPGWS ESTEFGVKDRS GLPQAAINVI KRIEELTGVF IDIIST GPDR TETMLLRDPX DA
E. coli

```

Figure 4.1: Sequence alignment of AdSS from different species. Conserved residues are shaded.

Leishmania donovani (Spector et al., 1979), Yoshida sarcoma ascites cells (Matsuda et al., 1980), rat liver (Matsuda et al., 1977), rat muscle (Bass et al., 1984), rabbit muscle (Clark et al., 1977) and Novokoff ascites cells (Clark & Rudolph, 1976). Recombinant systems have also been used for the expression and purification of the *E. coli*, *Saccharomyces cerevisiae* and the mouse basic and acidic enzymes (Bass et al., 1987, Lipps & Krauss, 1999, Inacu et al. 2001, Borza et al., 2003). In many of these cases (human placenta, *S. pombe*, *A. vinelandii*), detailed kinetic characterization has been carried out and the results are in agreement with those observed with the *E. coli* enzyme. In all the enzymes studied, the competitive inhibitors of one substrate are non-competitive inhibitors of the other substrates.

The only exception may be the case of the maize enzyme. Inhibition studies with 5'-phosphohydantocidin show that it is a competitive inhibitor of IMP binding with slow onset inhibition (Walters et al., 1997). The slow onset can be abolished when the enzyme is preincubated with the inhibitor in the presence of GTP and aspartate. The reported plots of the inhibition with GTP as the variable substrate are almost parallel. GTP abolishes the slow onset nature of the inhibition at concentrations well below its K_m . The crystal structure of the *E. coli* enzyme with 5'-phosphohydantocidin in the absence of GTP have also been determined (Fonnester, 1996). The authors therefore, interpret the data to indicate synergism in the binding of the inhibitor and GTP with a random order of substrate binding. These data may also be taken to be indicative of the preferential binding of the inhibitor to the IMP binding site after GTP binding. Since 5'-phosphohydantocidin is competitive with respect to IMP, this may be an indication of the ordered binding of substrates to the maize enzyme, with GTP binding preceding IMP binding. Indeed, linear reactions can be obtained with the enzymes from *A. thaliana* and *Triticum aestivum* only on preincubation with GTP (Prade et al., 2000). The crystal structures may be misleading as they are of the *E. coli* enzyme and not the maize enzyme. Binding of this inhibitor to the *E. coli* enzyme in the absence of GTP could be due to the random substrate binding in this case.

The K_m s for the substrates, IMP and GTP, are in the low micro molar range and are presented in Table 4.3. The K_m for aspartate however, varies with many of the enzymes studied having a value of around 150-300 μ M. This is true of the bacterial enzymes and the mouse basic enzyme. The aspartate K_m for the mouse acidic enzyme and the yeast enzyme is much higher at 1.00 mM. Most of these enzymes show linear Michaelis-Menten kinetics with the exception of the *S. cerevisiae* enzyme that has been found to show weak negative co-operativity with the substrates GTP and aspartate. No co-operativity is seen with IMP.

4.1.3 Oligomerization

Both biochemical and crystallographic studies on the enzyme indicate that the enzyme is active as a dimer. The dissociation constant for the *E. coli* AdSS dimer has been determined to be close to 10 μ M in the absence of substrates, reducing to a negligible value in the presence of IMP (Honzatko & Fromm, 1999). Crystal structures show the requirement for dimerization to complete the active site of the enzyme. However, the existence of a monomer-dimer equilibrium as determined by ultracentrifugation shows that this association is dynamic and fast. Kang et al (1997) have exploited this fast equilibrium process to demonstrate with a set of structure based mutations that the *E. coli* enzyme is active as a dimer. They have created mutants of AdSS that are by themselves inactive but, when combined these mutants form hybrid dimers that have activity. Quantitation of the activity of these hybrids also established that the active wild type dimer has two functional active sites. Some reports of monomeric AdSS do exist but in view of the extensive crystallographic evidence from enzymes of varied origin, these probably represent the enzyme in its inactive monomeric form that dimerises in response to substrate.

4.1.4 Regulation of AdSS activity

AdSS plays two roles in metabolism - one in the purine nucleotide biosynthetic pathway and the other in the purine nucleotide cycle. The latter cycle involving in

addition, the enzymes ADS lyase and AMP deaminase leads to the net conversion of L-aspartate to ammonia and fumarate along with the hydrolysis of GTP to GDP. This cycle is thought to be present in tissues such as muscle, brain and kidney. This process may have a role to play in activating glycolysis as IMP, AMP and ammonia activate glycolytic enzymes and, in providing TCA cycle intermediates in tissues that lack pyruvate carboxylase (Goodman & Lowenstein, 1977). These two roles in mammalian systems are carried out by two different isozymes which differ in their response to regulatory molecules (Borza et al., 2003). This division of roles has however, been questioned as AMP deaminase deficiency does not affect the TCA cycle or the adenine nucleotide pools in muscle (Tarnopolsky et al., 2001).

AdSS is at the branch point between AMP and GMP in both the *de novo* and salvage pathways and is a point of regulation. Both product and feedback inhibition may play a role in the regulation of the enzyme. Inhibitors of physiological relevance include adenylosuccinate, GDP, AMP, GMP and the glycolytic intermediate, fructose-1,6-bisphosphate. Of the mammalian enzymes, the basic muscle isozyme has a higher IMP K_m and a lower K_m for aspartate compared to the acidic isozyme and is supposed to be involved in the purine nucleotide cycle. The acidic isozyme that has a very high K_m for aspartate, is less susceptible to inhibition by fructose-1,6-bisphosphate and is more strongly inhibited by nucleotides. This isozyme is implicated in the *de novo* biosynthetic pathway (Borza et al., 2003, Stayton et al., 1983).

The K_i s for the nucleotides GDP, GMP and adenylosuccinate are low (5-30 μ M) for all enzymes studied. The K_i s for AMP are much higher ranging from 10 to 3000 mM. AMP is a competitive inhibitor of the enzyme from most sources. Non-competitive inhibition patterns with both IMP and GTP has been found in some cases (Stayton et al., 1983) with AMP binding to both nucleotide sites. In crystalline complexes of the mouse basic isozyme, AMP binds only in the IMP binding pocket (Inacu et al., 2002b) though the inhibition is noncompetitive with IMP. The inhibition with the acidic isozyme is competitive (Borza et al., 2003).

This suggests that AMP probably inhibits IMP binding in the symmetry related monomer in the basic isozyme. In the case of the *E. coli* enzyme, studies by Kang and Fromm with hybrids of inactive mutants have shown the absence of cross-talk between the two subunits of the synthetase dimer. The K_i s of these molecules for AdSS from different sources are listed in Table 4.4 along with the values determined for PfAdSS as part of this study.

Substrate inhibition is also observed with the mouse basic isozyme at IMP concentrations above 1 mM, at saturating GTP concentrations. The acidic isozyme shows IMP inhibition only at sub-saturating GTP. The inhibition constant is high at 1 mM but is of physiological significance as the IMP concentration in working muscle can be very high. These observations with the mouse enzymes have led Borza et. al. (2003) to suggest that fluctuations in the relative concentrations of IMP and AMP would influence the activity of the acidic isozyme whereas the basic isozyme would be affected by AMP concentrations alone. These authors also conclude that it may not be possible to assign the isozymes to specific, defined roles. Weyden and Kelly (1974) also conclude on the basis of their studies on the human placental enzyme that AdSS may not be subject to specific molecular control *in vivo*. Nevertheless, since all the molecules listed above do affect the activity of the synthetase at physiologically significant concentrations, the concerted action of all these molecules *in vivo* would influence the regulation of this important metabolic pathway.

4.2 Materials and Methods

Restriction enzymes, *Taq* DNA polymerase, T_4 DNA ligase and other molecular biology reagents were procured from Amersham Pharmacia, U.K., Bangalore Genei Pvt. Ltd., Bangalore, India or from MBI Fermentas, Lithuania and used according to the manufacturers' instructions. *E. coli* strain H1238 was obtained from the *E. coli* Genetic Stock Center, Yale University. . Oligonucleotides were custom synthesised at Genemed Synthesis, Inc., CA, USA or at Microsynth, Switzerland.

4.2.1 *Plasmodium falciparum* culture and RNA isolation

In vitro culture of *P. falciparum* (clone T9/106) was maintained using the methodology described by Trager and Jenson, (1976). The parasites were propagated at 5 % hematocrit in human O⁺ erythrocytes in RPMI 1640 with 10 % human serum isolated from O⁺ human blood. Parasitemia of 10 % was routinely obtained. For total RNA isolation, intact free parasites were obtained by lysis of parasitised RBCs with saponin. Parasite cultures were harvested by centrifugation, and the resuspended in a 0.15 % solution of saponin in RPMI to lyse the erythrocytes. Lysis was allowed to proceed for 8 min on ice and excess RPMI added to arrest the lysis. Intact free parasites were harvested by centrifugation. The efficiency of the lysis was determined by examination of Giemsa stained thin smears of the parasites. RNA from the free parasites was isolated as reported (Triglia et al., 1988). cDNA synthesised by reverse transcription with oligo dT₁₈ was used as the template to amplify the AdSS gene.

4.2.2 Cloning of full-length AdSS

An N terminal truncated clone of *P. falciparum* AdSS (pTrcAd7) was cloned earlier in this laboratory. The full-length sequence of the *P. falciparum* AdSS gene was obtained from the *P. falciparum* genome sequence data generated at the Sanger Center, UK using this sequence for the search. Primers used for gene specific amplification of the *P. falciparum* gene from the cDNA were:

Adssfl: 5'ACACCATGGCCATATTTGATCATCAAATAAAAAAAT 3'

Adssc: 5'CCAGGTACCCTCGAGTTAGTTTAGGTTAAAATTCTT 3'

Constraints of primer design required the mutation of Asn at position 2 to Ala. A touch down PCR cycle involving reduction of annealing temperatures from 57°C to 45°C at the rate of 1°C per cycle was used for the initial amplification followed by 30 cycles with annealing at 45°C. The gel purified 1.4 kb amplicon was restriction digested with the enzymes Nco1 and Kpn1 and ligated into the vector pTrc99A

(Amman et al., 1988) digested with the same enzymes. The ligation mix was transformed into competent DH5 α cells and recombinants selected. One clone (pTrcAsfl) was selected and sequenced at an automated DNA sequencing facility.

4.2.3 Functional complementation

Complementation studies were carried out with the *E. coli* Strain H1238 (*argI61*, *argF58*, *thr25*, *purA54*, *tonA49*, *relA1*, *spoT1*) (Bouyoub et al., 1996) transformed with the AdSS expression constructs in pTrc99A. The cells, grown overnight in LB medium with 100 μ g/ml ampicillin, were washed with and resuspended in 1X M9 salt solution. A 1% inoculum of these cells was added to minimal medium containing 1X M9 salts, 1 mM MgSO₄, 0.1 mM CaCl₂, 1mM threonine, 1mM arginine, 0.2% glucose, 0.2 mM isopropyl- β -D-thiogalactopyranoside (IPTG), 100 μ g/ml ampicillin. The amino acids arginine and threonine were not included in the medium when casein hydrolysate was included at a concentration of 0.2%. The cells were allowed to grow for 24 h at 37°C and growth measured as the absorbance at 600 nm.

4.2.4 Protein expression

The full-length and truncated *P. falciparum* AdSS gene fragments were excised from pTrcASfl and pTrcAd7, respectively by NcoI and BamH1 digestion and ligated into the vector pET23d to generate the plasmids pETAsfl and pETAd7. The pET expression plasmids were freshly transformed into BL21(DE3) competent cells before each induction. Transformed BL21(DE3) cells were grown in Terrific Broth (TB) containing 100 μ g/mL ampicillin at 37°C with shaking to OD (600 nm) of 0.8. Cultures were either induced for 5 h at 37°C with 0.3 mM IPTG or were cooled to 20°C and induced by the addition of IPTG to a final concentration of 0.2 mM in the presence of 1 % ethyl alcohol (Stone et al., 1993). Low temperature inductions were carried out at 20°C for 12 h.

4.2.5 Protein purification

Cultures were induced at 20°C as described in the protein expression section for purification. Induced cultures were pelleted by centrifugation, resuspended in 50 mM Tris.HCl buffer, pH 7.5 containing 1 mM DTT, 10% glycerol and 0.1 μM PMSF. Cells were lysed using a french press and cellular debris removed by centrifugation at 20,000 g for 15 min at 4°C. The supernatant was treated with 0.3% polyethylenimine to precipitate nucleotides. Ammonium sulphate was added to 40% saturation, the resultant pellet discarded and the supernatant raised to 65% saturation of ammonium sulphate. The pellet was dissolved in 20 mM Tris, 10% glycerol, 1 mM DTT and desalted on a Sephadex-G25 column equilibrated with the same buffer. The desalted protein was loaded on a Q-Sepherose anion exchange column connected to an AKTA Basic HPLC. Protein was eluted with a linear salt gradient of 0 to 1 M NaCl in the same buffer. Fractions were analysed by SDS-PAGE and fractions containing the enzyme pooled. Protein was precipitated by addition of ammonium sulphate to 70% saturation. The protein pellet obtained after centrifugation was dissolved in storage buffer (20 mM Tris.HCl pH 6.9, 10% glycerol, 1 mM DTT and 1 mM EDTA) and loaded onto a Superdex-200 column (1 cm X 30 cm) equilibrated with the same buffer. The fractions containing the protein were pooled and stored as such at 4°C. SDS-PAGE analysis was performed using standard protocols (Laemmli, 1970).

4.2.6 Western blotting

The truncated AdSS clone in pET23d (pETAD7) was transformed into BL21(DE3), grown to OD (600nm) of 0.8 and induced at 37°C with 0.3 mM IPTG, to force the protein into inclusion bodies. The inclusion body preparation obtained after sonication was washed with 0.1% Triton X-100 solution and then subjected to preparative SDS-PAGE. The protein band was cut and electroeluted. This purified protein was used to raise polyclonal antisera in rabbit.

H1238 cells transformed with the pTrcAd7 or pTrcAsfl were grown in LB medium supplemented with 100 $\mu\text{g/ml}$ ampicillin at 37°C to a OD (600nm) of 0.6 and induced with 0.5 mM IPTG for 8 h at 37°C. Cells were pelleted by centrifugation, resuspended in SDS-PAGE sample loading buffer and subjected to SDS-PAGE separation. 250 μl culture equivalents were loaded in each well. Purified recombinant PfAdSS was also loaded as a positive control. The western blots, after transfer, were probed with polyclonal anti-AdSS antisera raised in rabbit. HRP conjugated goat anti-rabbit antibody was used as the secondary antibody and blots were developed with aminoethylcarbazole/ H_2O_2 substrate.

4.2.7 Analytical gel filtration

Analytical gel filtration was performed on a Superdex-200 column (1cm X 30cm) (Column 1, Apendix A) attached to an AKTA HPLC system. Runs were performed at a flow rate of 0.5 ml/min and protein elution monitored at a wavelength of 220 nm. The column was calibrated with β -Amylase (200 kDa), Alcohol dehydrogenase (150 kDa), Bovine serum albumin (66 kDa), Carbonic anhydrase (29 kDa) and Cytochrome C (12.4 kDa).

4.2.8 Enzyme assays and kinetics

All enzymes assays were performed in 30 mM sodium phosphate buffer, pH 7.5 and 5 mM Magnesium acetate at room temperature on a Simadzu (UV-1601) spectrophotometer or a Hitachi U2010 spectrophotometer. Reaction rates were monitored as an increase in absorbance at 280 nm or 290 nm due to the conversion of IMP to succinyl-AMP. A $\Delta\epsilon$ value of 11300 $\text{M}^{-1}\text{cm}^{-1}$ and 3390 $\text{M}^{-1}\text{cm}^{-1}$ at 280 and 290 nm respectively, were used to calculate reaction velocities (Bass et al., 1987). Substrate concentrations when saturating were 250 μM IMP, 150 μM GTP and 5 mM aspartate. IMP concentrations were varied between 250 μM and 20 μM , GTP between 150 μM and 5 μM and, aspartate between 10 mM and 750 μM for determination of kinetic constants. Inhibitor concentrations used for

specific experiments are indicated in the figure legends. For the inhibition studies, two substrates were held constant at saturating concentrations and initial rates determined at 5-7 concentrations of the third substrate, at various concentration of each inhibitor. Reactions were initiated by the addition of 2-3 μg of enzyme. Reaction volumes were 300 μl .

4.2.9 Kinetic data analysis

Kinetic constants were determined from Lineweaver-Burk plots of the initial velocity data by weighted linear regression after linear transformation. The equations used were,

$$v = \frac{V_{max}S}{[K_m(1 + \frac{I}{K_i}) + S]} \quad \text{for competitive inhibition}$$

$$v = \frac{V_{max}S}{[K_m(1 + \frac{I}{K_i}) + S(1 + \frac{I}{K_i})]} \quad \text{for noncompetitive inhibition}$$

$$v = \frac{V_{max}S}{[K_m + S(1 + \frac{I}{K_i})]} \quad \text{for uncompetitive inhibition}$$

All initial velocity data were also analysed by non-linear regression fit to the Michaelis-Menten equation and found to agree with the interpretation from the linear regression analysis. The Graphpad Prism software was used in all analysis.

4.3 Results

4.3.1 Cloning of PfAdSS

A truncated cDNA sequence of the PfAdSS gene was previously obtained in the laboratory. A BLAST search of the genome database with this sequence yielded an unannotated sequence identical to the search sequence. Comparison of this genomic segment with the cDNA sequence indicated the presence of a 73 bp intron at position 1092 of the gene. The truncated clone was found to be missing only 5 amino acids in the N-terminal on comparison with a translation of the genomic sequence. The fragments coding for the truncated and full-length proteins were amplified, restricted

and cloned into the expression vector pTrc99A to obtain the plasmids pTrcAd7 and pTrcASfl having the truncated and full length clones, respectively. The full-length clone differed from the deduced protein sequence obtained by translation of the genomic sequence entry in having an Ile at position 203 instead of Leu. The truncated clone in addition to the missing 5 N-terminal amino acids differed at two positions from the genomic entry: these are I156M and K175E.

4.3.2 Functional complementation

The truncated and full-length constructs in the expression vector pTrc99A were analysed for production of functional protein by complementation in the *E. coli* strain H1238 (*argI61*, *argF58*, *thr25*, *purA54*, *tonA49*, *relA1*, *spoT1*). This strain is a pur A mutant and grows in minimal medium, only when complemented by a functional AdSS gene (Bouyoub et al., 1996). Fig. 4.2a shows the growth of pTADS7/H1238 in minimal medium supplemented with the amino acids Arg and Thr at different concentrations of isopropyl β -D-thiogalactopyranoside (IPTG). Induction of the PfAdSS gene, which is under the control of the Trc promoter in pTADS7, produces functionally active AdSS as seen by increase in growth of cells with increase in IPTG concentration (Fig. 4.2a). Effect of hadacidin, an analogue of aspartate and a competitive inhibitor of AdSS, was monitored using the complementation assay. IPTG induced cultures of pTADS7/H1238, upon treatment with 50 μ M hadacidin, showed greater than 85% suppression of cell growth (Fig. 4.2b). Recovery of cell growth was seen when adenine was added to cells treated with hadacidin (Fig. 4.2b), as AMP formation is now brought about by bacterial adenine phosphoribosyltransferase. Though the truncated clone was found to complement AdSS deficiency in *E. coli* H1238 in minimal medium supplemented with the amino acids Arg and Thr alone, for which H1238 is auxotrophic, the full-length clone showed growth only in the presence of casein hydrolysate in the medium (Fig 4.3).

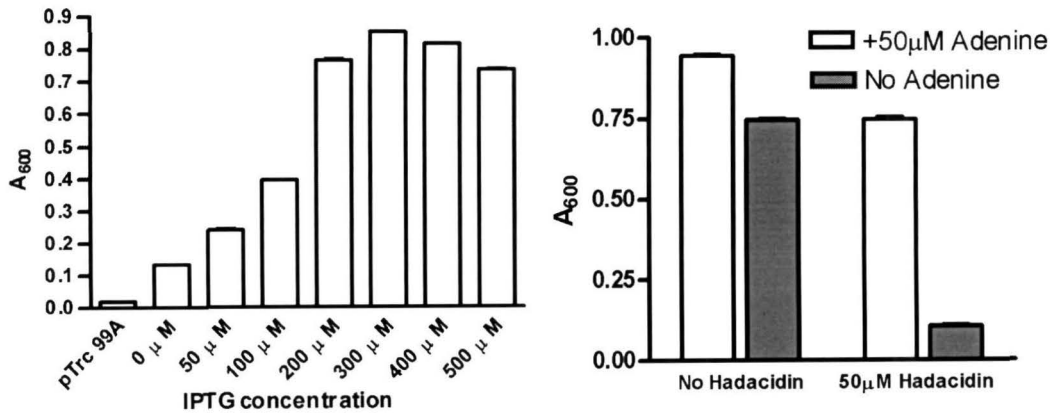


Figure 4.2: Effect of IPTG concentration (left) and hadacidin (right) on functional complementation of AdSS deficiency by truncated PfAdSS in H1238.

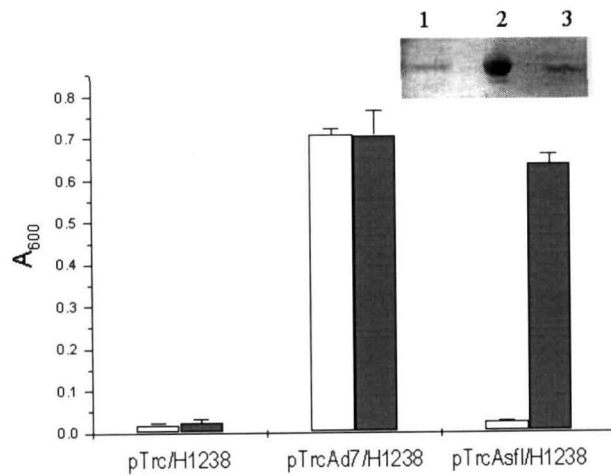


Figure 4.3: Functional complementation in *E. coli* H1238 by full-length and truncated AdSS in the presence (■) and absence (□) of 0.2% casein hydrolysate. The data represent a mean of three experiments. Inset: expression of the truncated and full-length clones in H1238 detected by western blotting with anti-PfAdSS antibodies. Lane 1, pTrcAd7/H1238, lane 2, purified recombinant *P. falciparum* AdSS, lane 3, pTrcAsfI/H1238.

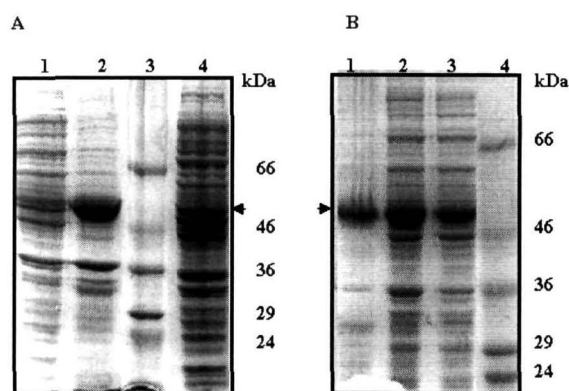


Figure 4.4: SDS-PAGE analysis of PfAdSS induction in BL21(DE3) carried out at (A) 37°C (lane 1, soluble fraction, lane 2, insoluble fraction, lane 3, marker, lane 4, whole cell), (B) 20°C (lane 1, insoluble fraction, lane 2, whole cell, lane 3, soluble fraction, lane 4, marker). Arrows indicate expressed protein.

4.3.3 Hyper-expression of PfAdSS in *E.coli*

Expression levels with the pTrc constructs were low and could be detected only in western blots probed with polyclonal antisera (Fig. 4.3, Inset). The full-length clone was therefore, excised from the pTrc vector and cloned into the expression vector pET23d and protein expressed in the *E. coli* strain BL21(DE3). Hyper-expression of a protein corresponding to 50 kDa on SDS-PAGE gels could be obtained when induction was carried out both at 20°C and 37°C. The protein, however, was predominantly in inclusion bodies when induction was done at 37°C (Fig. 4.4A). Soluble protein could be obtained on induction at 20°C with the recombinant protein constituting about 10 -15% of the total soluble protein (Fig. 4.4B).

4.3.4 Purification of recombinant PfAdSS and stabilisation of activity

Recombinant AdSS was induced and purified as described in the Methods section (4.2.5). The protein after ammonium sulphate fractionation was loaded on a quaternary ammonium based anion exchange column. In the absence of DTT in the buffers, the protein elution was spread over a wide range of salt concentration. All

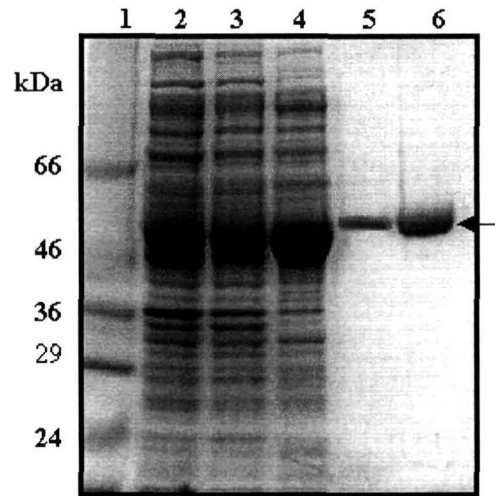


Figure 4.5: SDS-PAGE analysis of recombinant PfAdSS. Lane 1, marker, lane 2, crude lysate, lane 3, PEI supernatant, lane 4, ammonium sulphate fraction, lane 5, Q-Sepharose purification, lane 6, Superdex 75. Arrow indicates recombinant *P. falciparum* AdSS.

Table 4.1: Purification table of recombinant PfAdSS.

Purification step	Total protein (mg)	Total activity (mUnits)	Specific activity (mUnits/mg)	Purification (fold)	Yield (%)
Crude lysate	323	27179	83.9	1.0	100
PEI supernatant	140.4	27178	193.5	2.3	99
Ammonium sulphate 40-60% fraction	129.4	19865	158.6	1.9	73
Q-sepharose	9.6	10291	1072.0	12.8	38
Superdex-75	8.9	9648	1143.0	13.8	36

Note: Data were obtained from 1.5 l culture.

Experimental conditions as described in Materials and Methods.

protein fractions were found to be inactive. Activity could not be recovered even after addition of DTT to the purified protein. The enzyme eluted as a sharp peak at a salt concentration of about 100 mM, on the anion exchange (Q-sepharose, Fig. 4.5) column, when all the purification steps were carried out in the presence of 1 mM DTT. The protein after this step was 90% pure as analysed by SDS-PAGE (Fig 4.5, Table 4.1). Enzyme stored under conditions of elution from the anion exchange

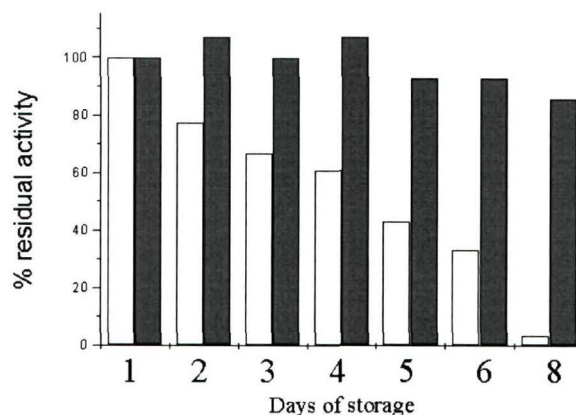


Figure 4.6: Stabilization of PfAdSS activity by EDTA. Residual activity of enzyme stored in 20 mM Tris.HCl, pH 8.0, 10% glycerol, 1 mM DTT (□) 20 mM Tris.HCl, pH 6.90, 10% glycerol, 1 mM DTT and 1 mM EDTA (■).

column (20 mM Tris.HCl, pH 8.0, 1 mM DTT, 10% glycerol, \approx 100 mM NaCl) was found to lose activity with time. Reduction of the pH to 7.0 slowed down the rate of loss in activity. Complete stabilisation of activity could be achieved in the presence of 1 mM EDTA in the storage buffer (Fig. 4.6). The protein containing fractions from the anion exchange column were therefore pooled, EDTA added to a concentration of 1 mM and protein precipitated by addition of ammonium sulphate to 70% saturation. The protein was dissolved in 20 mM Tris.HCl, pH 6.9, 1 mM DTT, 1 mM EDTA, 10% glycerol and loaded on a Superdex 75 gel filtration column equilibrated with the same buffer. The enzyme eluted as a single peak after the void volume of the column. The enzyme activity was found to be stable for at least 3 weeks under these buffer conditions at 4°C (Fig.4.6). EDTA could not be included in the anion exchange step as this resulted in elution of all protein loaded as a single peak without any purification.

4.3.5 Oligomerization

Recombinant PfAdSS shows a molecular weight of 50 kDa on SDS-PAGE. The oligomerization of the protein, as studied by gel filtration on a Superdex-200 column

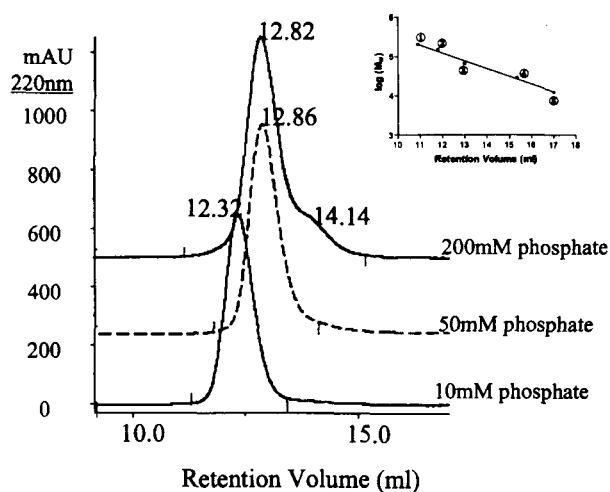


Figure 4.7: Analytical gel filtration of recombinant PfAdSS on a prepacked Superdex 200 column under different buffer conditions. Buffers were of the indicated phosphate concentration, pH 7.5 with 5mM MgCl₂ and 1mM DTT. Inset (top right): Calibration of the column with standard molecular weight markers. 1. β -Amylase (200kDa), 2. Alcohol dehydrogenase (150kDa), 3. Bovine serum albumin (66kDa), 4. Carbonic anhydrase (29kDa), 5. Cytochrome C (12.4kDa).

(Column 1, Appendix A), was found to be extremely sensitive to the ionic strength of the buffer used (Fig.4.7). The protein eluted as a dimer (105 kDa) in 10 mM phosphate buffer pH 7.5, 5 mM MgCl₂. The peak shifted to a region corresponding to a molecular weight of 82 kDa in a buffer containing 50 mM phosphate, pH 7.5, 5 mM MgCl₂. A small peak corresponding to a monomer (46.3 kDa) appeared when the phosphate concentration was increased to 200 mM. A similar elution profile, with a small monomer peak, was obtained when gel filtration was carried out in 10mM phosphate buffer containing 500 mM NaCl, 5 mM MgCl₂, and 1 mM DTT. No shift in elution volume was observed over a range of precolumn concentrations of 1.5 to 30 μ M of the monomer. Elution volumes did not alter in the presence of either 150 μ M IMP or 150 μ M GTP in the buffer. The elution at a molecular weight corresponding to 82 kDa is indicative of rapid monomer-dimer equilibration in buffers of high ionic strength. This equilibrium shifts towards the monomer with increasing ionic strength of the buffer.

4.3.6 Kinetic characterization

The enzyme activity was found to be maximum in 50 mM sodium phosphate buffer, pH 7.5 as compared to 50 mM HEPES buffer (82% of activity in phosphate) and 50 mM Tris buffer (45% of activity in phosphate) at the same pH. The enzyme activity was maximal in a pH range of 6.8 to 7.5. More than half-maximal activity was retained even at a low pH of 5.8 and higher pH of 8.8. All subsequent reactions were therefore, carried out in 30 mM sodium phosphate buffer, pH 7.5.

The K_m s for the three substrates GTP, IMP, aspartate were found to be 4.8 μ M, 22.8 μ M and 1.4 mM respectively. The Lineweaver-Burk plots for all three substrates, at saturating concentrations of the other two substrates, were linear indicating the absence of any co-operativity in the enzyme. Negative co-operativity has been reported in the case of the *Saccharomyces cerevisiae* enzyme for aspartate and GTP (Lipps & Krauss, 1999).

4.3.7 Inhibition studies

Inhibition by adenylosuccinate

The double reciprocal plots at various concentrations of adenylosuccinate, a product of the reaction, with IMP as the variable substrate have equal intercepts on the $1/v$ axis indicating competitive inhibition (Fig. 5.1,I a). Adenylosuccinate showed non-competitive inhibition with respect to the other two substrates, GTP and aspartate, at saturating concentrations of IMP (Fig. 5.1,I b,c).

Competitive inhibitors of GTP

Fig. 5.1II b shows that GMP is a competitive inhibitor of GTP binding to the enzyme. Inhibition with respect to aspartate, as in the case of all other AdSS in literature, was non-competitive (Fig. 5.1,II c). Surprisingly, GMP was found to be an uncompetitive inhibitor of IMP, with both the apparent V_{max} and K_m going down

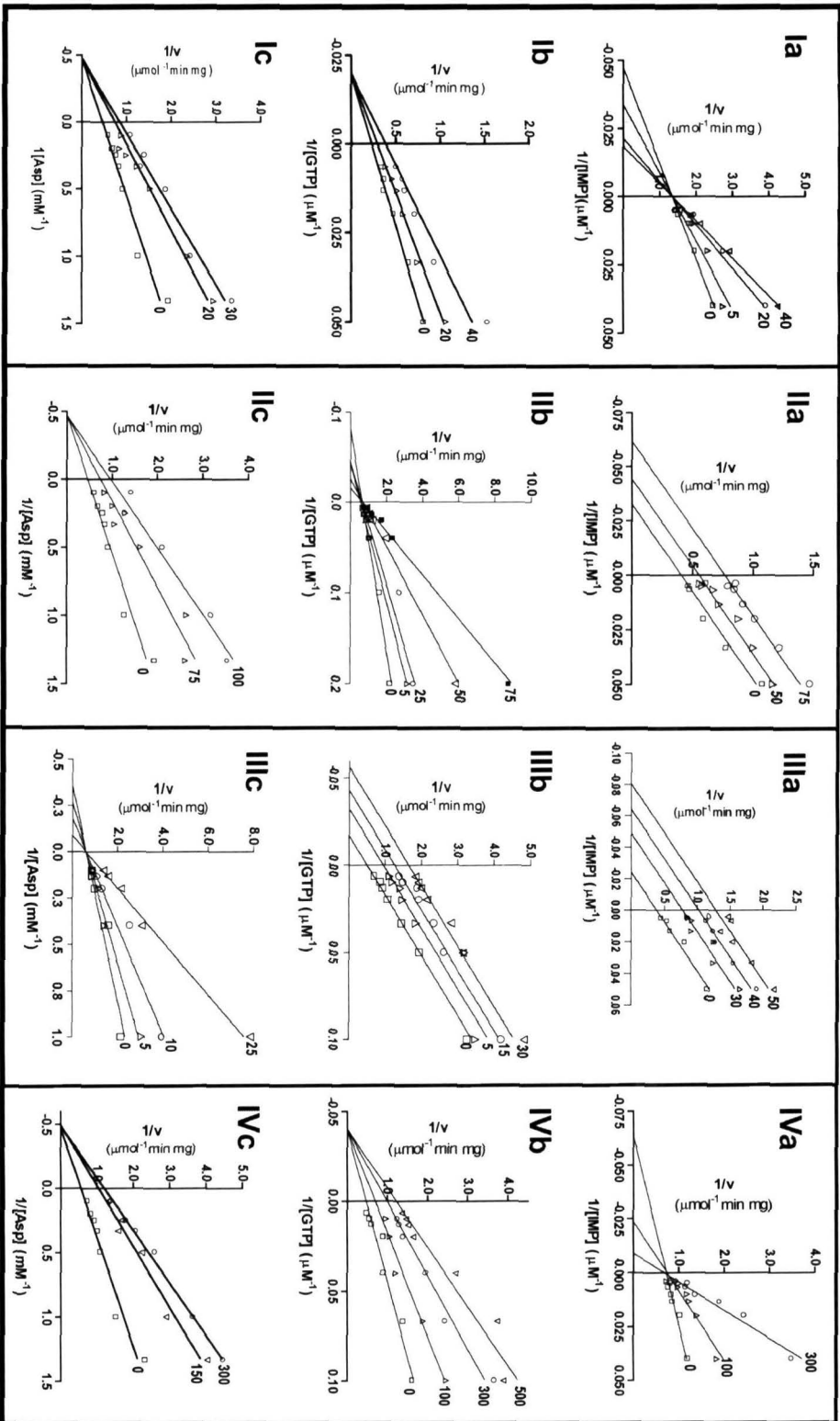


Figure 4.8: Lineweaver-Burk plots of the inhibition of PfAdSS by I) adenylosuccinate (ADS), II) GMP, III) Hadacidin and IV) AMP. a) Variable IMP, b) Variable GTP, c) Variable aspartate. The concentrations of the inhibitors in μM are indicated beside each line. Substrate concentrations when constant were $250 \mu\text{M}$ IMP, $150 \mu\text{M}$ GTP and 5 mM aspartate. GTP was at $50 \mu\text{M}$ in IV a and IMP at $75 \mu\text{M}$ in IV b.

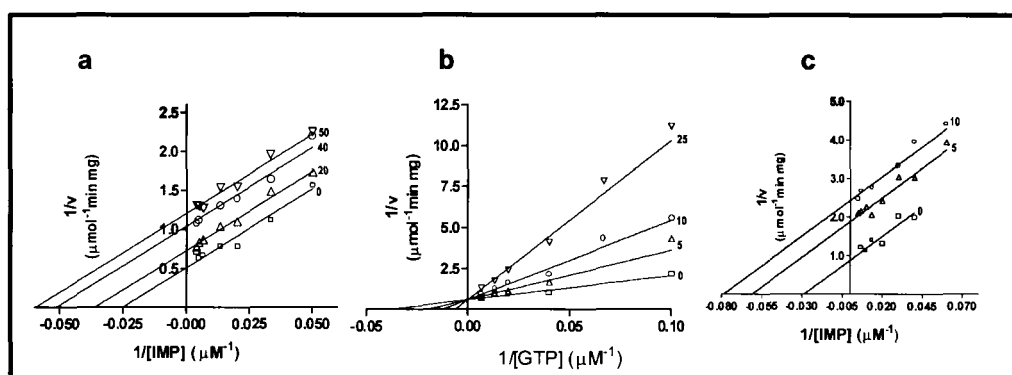


Figure 4.9: Lineweaver-Burk plots of inhibition of PfAdSS by GDP. The numbers beside each line indicate the concentration of GDP in μM . a) Variable IMP, GTP at $150 \mu\text{M}$, b) Variable GTP, IMP at $250 \mu\text{M}$ and c) Variable IMP with GTP at $50 \mu\text{M}$.

without change in slope of the double reciprocal plots, with increase in concentration of the GMP (Fig. 5.1,II a). A similar pattern of inhibition was also seen with GDP. Inhibition studies were also done at sub-saturating GTP and the plots obtained were similar to the ones at high GTP concentrations (Fig.4.9).

Hadacidin as a competitive inhibitor of aspartate

Hadacidin (N-formyl-N-hydroxyglycine), is a potent inhibitor of all known AdSS. It binds to the aspartate binding site of AdSS and is competitive with respect to aspartate (Fig. 5.1,III c). PfAdSS is also potently inhibited by hadacidin with a K_i of $5.6 \mu\text{M}$, giving a K_m to K_i ratio of ≈ 300 . The double reciprocal plots at various concentrations of hadacidin yielded parallel lines when the variable substrates were IMP or GTP (Fig. 5.1,III a,c). The inhibition with respect to both IMP and GTP was uncompetitive, indicating that hadacidin binds only to the enzyme-IMP-GTP- Mg^{2+} complex.

Inhibition by AMP

AMP is an end product of the nucleotide biosynthetic pathway and probably plays a role in regulation of the enzyme. AMP inhibited IMP binding competitively,

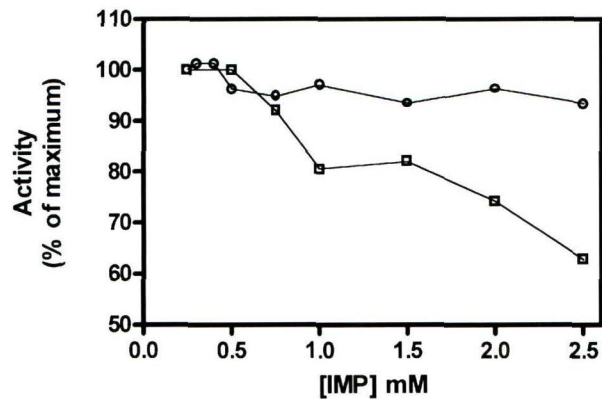


Figure 4.10: Inhibition of PfAdSS by IMP. 150 μM GTP (○), 50 μM GTP (□)

the K_i being 80 μM (Fig. 5.1,IV a). Inhibition with aspartate and GTP as the variable substrates was non-competitive (Fig. 5.1,IV b,c).

Substrate inhibition

Figure 6 shows the rates of the AdSS reaction at saturating and subsaturating concentrations of GTP with increasing concentrations of IMP. While no inhibition is seen in the presence of high concentrations of GTP, the reaction is inhibited by IMP when GTP is limiting (Fig. 4.10).

4.4 Discussion

Initial functional complementation studies were carried out with an N-terminal truncated construct, pTrcAd7. *P. falciparum* genes are highly AT rich and tend to excise themselves from cloning vectors in *E. coli* (McFadden & Roos, 1999). The truncated clone was obtained as a consequence of such an event during attempts to clone 5' end of the AdSS gene. The growth of H1238 transformed with this expression construct indicated that the truncated AdSS codes for a functional AdSS protein the activity of which could be inhibited by hadacidin, an aspartate analog and specific inhibitor of AdSS. However, the full-length clone did not complement AdSS deficiency in minimal medium unless the medium was supplemented with

casein hydrolysate.

The strain H1238, in addition to lacking a functional *purA* gene, is also a *relA1*, *spoT1* mutant. *relA* is induced during amino acid starvation leading to the stringent response and codes for a guanosine-3',5' bis(pyrophosphate) (ppGpp) synthetase while *spoT* codes for a ppGpp phosphorylase (Hernandez & Bremer, 1991, Cashel et al., 1987). *RelA1* is a transposon-induced mutation that leads to the synthesis of two truncated *relA* fragments that associate into an active protein with residual ppGpp synthetic activity (Metzger et al., 1989). ppGpp formed cannot be degraded in H1238 due to the absence of SpoT activity. This would lead to the accumulation of ppGpp in H1238 under conditions of amino acid starvation. An elevated basal level of ppGpp in *relA1*, *spoT203* (SpoT null) double mutants is implicated in the slow growth of these double mutants (Metzger et al., 1989).

ppGpp is a GTP analog and a potent inhibitor of AdSS (Stayton & Fromm, 1979). The truncated clone but not the full-length clone complements AdSS deficiency in the absence of casein hydrolysate in the medium (amino acid starvation), while both complement in the presence of casein hydrolysate (relieves amino acid starvation) (Fig. 1). These results indicate that ppGpp inhibits the full-length protein but not the truncated protein. The GTP binding loop of AdSS lies at the amino terminus of the protein (Silva et al., 1995). The truncation of the protein by 5 amino acids probably gives an enzyme that can no longer be inhibited by ppGpp, while retaining its capacity to bind GTP, permitting complementation even under conditions of amino acid starvation. The full-length clone is inhibited by ppGpp and cannot complement the AdSS deficiency in H1238 in the absence of casein hydrolysate.

Sequencing of the full-length and truncated AdSS genes showed that in addition to the 5 amino acid missing at the N terminus, the truncated clone differed at three positions from the full-length clone, a significant change being the presence of a Met at position 156 instead of the Ile found in the full-length protein. At the N

terminus of the AdSS protein is the P-loop that is involved in the recognition of the phosphate groups of GTP. Since the truncation in pTrcAd7 is at the N-terminal, it is possible that the recognition of GTP analogs is affected in the truncated clone without compromising GTP binding. This might result in different responses of the two proteins to ppGpp. The other factor that may contribute to differential inhibition by ppGpp may be the L156M mutation in the truncated clone. This residue lies at the dimer interface of the protein and is adjacent to Arg155, which makes contacts with IMP bound in the active site of the other subunit of the dimer (Chapter 6). Since the active site of the enzyme is at the junction of the two monomers, alteration of this residue may affect the dimer interface of the protein leading to altered binding of ligands.

ppGpp is an effector of the stringent response in prokaryotes and is produced during nutrient starvation. It is an inhibitor of many cellular processes including transcription, translation, and nucleotide biosynthesis and an activator of amino acid biosynthesis (Chatterji & Oha, 2001). Till recently, this molecule was thought to be important exclusively in prokaryotic systems. However, *relA/spoT* homologs have recently been found in *Arabidopsis* (van der Biezen, 2000) and *Chlamydomonas* (Kasai, et al., 2002). In *Arabidopsis*, two homologs have been identified and a role in response to pathogens and other stresses proposed. In *Chlamydomonas reinhardtii*, the ppGpp synthase has been found to localize to the chloroplast and probably reflects the conservation of the stringent response in evolution (Kasai, et al., 2002). These observations raise the possibility that such a process may be present in other eukaryotes including *P. falciparum*. A cursory search of the *P. falciparum* genome does not reveal any sequence with obvious homology to RelA, though sequence divergence cannot be ruled out. Indeed, 60% of the ORFs identified in the genome are annotated as hypothetical proteins. It is also possible that the proposed inhibition of PfAdSS by ppGpp may be an incidental consequence of it being a substrate analog and not a reflection on parasite physiology.

4.4.1 Protein Stability

The reducing agent, DTT is required during purification for the recovery of active enzyme. The enzyme is inactive if purified in the absence of DTT. Spreading of the protein on the anion exchange column during elution in the absence of DTT is probably due to the formation of variously oxidised species with different affinities for the anion exchange resin. Activity once lost cannot be recovered on addition of reducing agent indicating that the loss of activity due to oxidation is irreversible. The requirement for EDTA in the storage buffer suggests the role trace metal ions contaminating the buffer, in the inactivation of the enzyme. The bacterial (Bass et al., 1987) and plant enzymes are stable in solution in the absence of EDTA (Prade et al., 2000, Walters et al., 1997), while the human enzyme is reported to require the presence of EDTA for stability (Van der Weyden & Kelly, 1974). The stabilisation of activity with reduction in pH and by the addition of EDTA is indicative of the involvement of cysteines in the inactivation of the enzyme. Investigations on this aspect of the protein form the basis of the studies reported in chapter 5.

4.4.2 Kinetic characterization

The kinetic parameters of PfAdSS are presented along with those of enzymes from other species in Table 4.3. The K_m s for IMP and GTP are comparable to that of the other homologs. The aspartate K_m is however, much higher than that of the *E. coli* and mouse muscle enzymes. It is comparable to that of the acidic mouse enzyme, the isozyme that is thought to be involved in purine nucleotide biosynthesis.

Chapter 6 of this thesis presents the crystal structure of PfAdSS in complex with the intermediate, 6-phosphoryl-IMP, GDP, hadacidin and Mg^{2+} . This structure, representing the fully occupied AdSS active site, rules out the ping-pong mechanism. If the mechanism were to be ping-pong, a complex with the product of the first step of the reaction, GDP, and the substrate analog of the next step of catalysis, hadacidin, would not be bound at the active site simultaneously. Similar complexes have

also been reported for the *E. coli* and mouse muscle AdSS. Among the sequential mechanisms, a distinction needs to be made between random, partially ordered and fully ordered substrate binding.

Inhibition data can be used to determine the kinetic mechanism of a reaction. In a fully random mechanism, a competitive inhibitor of one substrate would show non-competitive inhibition with the other two substrates. This has been shown to be the case with all AdSS reported thus far including the human (Van der Weyden & Kelly, 1974), mouse muscle (Inacu et al., 2001), yeast (Lipps & Krauss et al., 1999), *Azotobacter* (Markham & Reed, 1977) and *E. coli* (Rudolph & Fromm, 1969) enzymes. In case of partially random and fully ordered mechanisms, competitive inhibitors of one substrate would act as uncompetitive inhibitors of one or both of the other substrates the binding of which is obligatory for the binding of inhibitor (and presumably the substrate that it competes with). The pattern of inhibition may be used to distinguish between the two mechanisms and would also reveal the order of substrate binding (Fromm, 1979a). These interpretations are valid under the assumption that the binding of the inhibitor to the enzyme or enzyme substrate complex leads to the formation of a dead end complex without catalytic activity albeit in a reversible way. The inhibition experiments need to be carried out at sub-saturating concentrations of the substrate that a particular inhibitor is competitive with.

In this study, adenylosuccinate has been used as a competitive inhibitor with respect to IMP, GDP and GMP as competitive inhibitors of GTP binding and hadacidin as the competitive inhibitor of aspartate. Sub-saturating concentrations of the substrate have been achieved by increasing the concentration of the inhibitor rather than by reduction of the concentration of the substrate. Some of the inhibition studies have also been carried out at sub-saturating substrate.

The results of the inhibition experiments are summarised in Table 4.2. Examination of the pattern of inhibition with respect to each substrate shows

Table 4.2: Summary of AdSS inhibition kinetics

Substrate Inhibitor	Type of inhibition		
	IMP	GTP	Aspartate
Adenylosuccinate	COMPETITIVE	Non-competitive	Non-competitive
GDP/GMP	Uncompetitive	COMPETITIVE	Non-competitive
Hadacidin	Uncompetitive	Uncompetitive	COMPETITIVE
AMP	COMPETITIVE	Non-competitive	Non-competitive

that the substrate binding in PfAdSS is ordered. The uncompetitive inhibition of IMP by GDP and GMP indicates that these inhibitors bind to the GTP binding site only subsequent to IMP binding. Uncompetitive inhibition of both IMP and GTP by hadacidin shows that hadacidin and hence, aspartate bind only the enzyme-IMP-GTP complex. It is however, not clear if aspartate binds subsequent or prior to the first step of catalysis, the formation of 6-phosphorylIMP. Even in the case of the *E. coli* and mouse enzymes where substrate binding is random, the transfer of the phosphoryl group from GTP to IMP can occur in the absence of aspartate (Inacu et al., 2002a, Choe et al., 1999). Isotope equilibrium studies on the rat basic isozyme show that aspartate preferentially binds to the enzyme-IMP-GTP complex though the mechanism is random (Cooper et al., 1986).

Initial rate experiments of enzymes with preferred modes of binding can sometimes be misleading indicating apparent ordering even though substrate binding is random. Initial rate experiments on inosine monophosphate dehydrogenase (IMPDH) suggest that reaction is ordered in the forward reaction (Xiang et al., 1996) while kinetic isotope effect studies show that substrate binding is random (Xiang & Markham, 1997). The discrepancy in these studies arises due to the greater “stickiness” of IMP as compared to the other substrate, NAD^+ . The dissociation constant and the K_m for the substrate NAD^+ , however are $340 \mu\text{M}$ and $150 \mu\text{M}$ respectively, indicating that the binding of IMP does facilitate NAD^+ binding (Digits & Hedstrom). In addition, product inhibition studies can be misleading

Table 4.3: Kinetic constants for AdSS from different species

Enzyme	k_{cat} (s^{-1})	K_m (μM)		
		IMP	GTP	Asp
<i>P. falciparum</i> ¹	1.1	22.8	18.4	1800
<i>E. coli</i> ²	1.37	20	10	350
Mouse(basic) ³	5.4	12.0	12.0	140
Mouse (acidic) ³	4.2	45.0	15.0	950
<i>S. cerevisiae</i> ⁴	0.21	200	80	1650
Human placental ⁵	-	37-70	31-72	950-1160
<i>A. vinelandii</i> ⁶	2.2	13	15	500

¹This study, ²Rudolph & Fromm, 1969, ³Borza et al., 2003,

⁴Bass et al., 1987, ⁵Weyden & Kelly, 1974. ⁶Nagy et al., 1973

- data not available

in IMPDH as product release is indeed ordered. This also raises the question as to whether a reaction should be called random or ordered when preferred binding modes can be identified. In spite of these considerations, the inhibition kinetics of PfAdSS is different from that of the enzyme from other species under similar conditions of assay indicating differences in substrate binding.

4.4.3 Regulation of PfAdSS

The kinetic and inhibition constants for PfAdSS are summarised in Table 4.3, 4.4 along with the values for the mouse acidic and basic isozymes from the literature (3).

Comparison of the kinetic constants of these enzymes shows that PfAdSS is similar to the acidic mouse enzyme. In addition to the high aspartate K_m s of both PfAdSS and mouse acidic AdSS, the two enzymes have similar K_i s for the nucleotide AMP. AMP seems to bind only to the IMP pocket in PfAdSS. This nucleotide has been found to bind to both the IMP and GTP binding sites in some cases (Stayton et al., 1983). Both these enzymes show inhibition by the substrate IMP only when

Table 4.4: Inhibition constants for AdSS from different species

Enzyme	K_i (μM)				
	AMP	GDP	GMP	ADS	Hadacidin
<i>P. falciparum</i> ¹	66	5.3	18.9	28.7	5.6
Mouse(basic) ³	700	19	12	21	-
Mouse (acidic) ³	59	30	14	16	-
Human placental ⁵	170	45	10	57	-

^{1-3,5} as in Table 4.3

- data not available

GTP is limiting (Fig. 4.10), unlike the basic mouse isozyme which is inhibited by high concentrations of IMP even when GTP is saturating. Borza et al., 2003 have suggested that the acidic isozyme would therefore, be regulated by the relative levels of IMP and AMP while the basic isozyme would be regulated by IMP alone. These observations are in accordance to the proposed role of the acidic mouse isozyme in *de novo* purine biosynthesis. Though *P. falciparum* lacks the *de novo* biosynthetic pathway, flux through AdSS is the only mode of biosynthesising AMP. AdSS would therefore, play a role similar to that of the acidic isozyme within the parasite, rather than a role in the purine nucleotide cycle as has been proposed for the basic isozyme.

The AT content of the *P. falciparum* genome is much greater than that of *E. coli* and mouse (Weber et al., 1987). The AMP requirement of the parasite will therefore be much higher than its GMP requirement. Since, AdSS is one of the regulatory points of purine nucleotide synthesis, it would be expected that inhibition of this enzyme in the parasite would be different compared to the enzyme from other species with a more balanced AT to GC ratios in their genomes. The low K_i s for GDP and GMP do therefore, seem counterintuitive, but may be important to prevent further depletion of the already low GTP levels in the parasite. Regulation of metabolite pools in a cell is a complex process involving a network of many different mechanisms. Though a one to one correlation between the inhibition by

these inhibitors is not apparent, it does allow the maintenance of requisite nucleotide ratios.

It is not unusual to see variation in the kinetic mechanism of the same enzyme from different species. The purine salvage enzyme, adenine phosphoribosyltransferase is one such example with the *L. donovoni* enzyme showing an ordered mechanism (Bashor et al., 2002) while substrate binding in the *G. lamblia* enzyme is random (Sarver & Wang, 2002). Exactly why two similar enzymes catalysing identical reactions with identical central enzyme substrate complexes should exhibit different pathways for enzyme substrate interactions is not clear. Catalytically, neither the random nor the ordered mechanisms have an advantage (Fromm, 1979). The order of substrate binding may however, play a role in the regulation of enzyme activity *in vivo*. Ordered binding of GTP ensures that it binds only to a productive complex, an important factor in a parasite maintaining relatively low levels of guanine nucleotides. Aspartate binding to a productive complex may offer an additional advantage to an organism that has no amino acid biosynthetic capability and depends on hemoglobin degradation for them (Francis et al., 1997).

To summarise the results, PfAdSS is different from all known AdSS in having an ordered mechanism of substrate binding. The K_i s for the inhibitors of physiological significance are not different from those of the other enzymes in literature. The ordered binding of substrates means that aspartate can bind only to the enzyme-IMP-GTP complex unlike the mammalian enzymes where it binds to the enzyme alone. Aspartate analogs designed to bind to such a complex would then preferentially bind the parasite enzyme, and would be all the more potent due to the high K_m for aspartate. Since aspartate can bind the host apo-enzyme, inhibition would be much less in this case. PfAdSS thus presents aspects that can be exploited for species specific inhibitor design.

Chapter 5

Studies on interface cysteine mutants of *Plasmodium falciparum* adenylosuccinate synthetase.

This chapter presents work done as a continuation of the observation that EDTA protects PfAdSS from inactivation during storage. The results presented highlight the unique properties of interface cysteines in PfAdSS. Relevant literature on cysteine modifications is presented.

5.1 Introduction

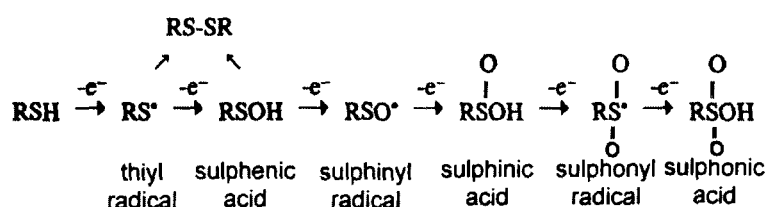
As described in Chapter 4, *P. falciparum* adenylosuccinate synthetase (PfAdSS) required storage with EDTA for activity to be maintained during storage. This implicates metal ions in the inactivation of AdSS in solution. Absence of the reducing agent DTT also led to irreversible loss of activity within a short span of time. Enzyme purified in the absence of any reducing agent was completely inactive, implicating cysteines in the inactivation process. Literature is replete with examples of metal-catalysed inactivation of enzymes. Cysteine due to its property of undergoing ready oxidation, not just to disulphides but also to other oxidised species like sulphenic acids, is implicated in many such processes.

5.1.1 Metal catalysed oxidation systems

Transition metals when provided with suitable reducing agents are capable of catalysing the activation of O₂ to various reactive oxygen species (ROS) (Stadtman, 1993). These ROS can readily attack biomolecules resulting in their oxidation.

Metal catalysed oxidation (MCO) of proteins has a role to play during oxidative stress, aging and is also of importance in biotechnological manufacturing of proteins. The levels of free transition metal ions is very low as they remain sequestered by molecules like transferrin, ferritin, ceruloplasmin, transcuperin and albumin. MCO however, becomes important in pathological conditions that lead to the presence of large concentrations of transition metal ions. Diseases associated with MCO systems include Alzheimer's disease (Multhaup et al., 1997), Parkinson's and other neurodegenerative disorders (Stadtman & Oliver, 1991).

These reactions are typically catalysed by redox active metal ions that can readily interconvert between different oxidation states like Cu^{2+} and Fe^{2+} in the presence of molecular oxygen (Stadtman, 1993). In addition, MCO systems require electron donors such as thiols, ascorbate, NADH etc or an enzymatic source of electrons. The electron donor plays a role in the reduction of the metal ion and in the production of H_2O_2 by the reduction of O_2 . The H_2O_2 then disproportionates via Fenton chemistry to a hydroxyl radical (OH) and an hydroxyl ion with the regeneration of the of the oxidised metal ion (Stadtman, 1993). The hydroxyl radical is responsible for the oxidative damage of proteins. These reactions are usually site specific in proteins with cysteine residues being most frequently affected (Stadtman & Oliver, 1991). Progressive oxidation of cysteine by single electron transfers has been proposed to take the following course (Park & Bauerle, 1999) : Other residues



that are susceptible to oxidative damage are histidines, methionines and tyrosines. Oxidation frequently leads to the loss of protein function often accompanied by aggregation.

5.1.2 Improving protein stability

Improving the stability of proteins is desirable as it allows greater ease in their purification and study. Increased half life holds special relevance to commercially important proteins. Mutagenesis, both random and site-directed, is one of the approaches adopted towards this goal (Lee & Vasmatzis, 1997). It is not always possible to predict the outcome of a mutation and many efforts at increasing stability have adopted the random mutagenesis approach (Chirumamilla et al., 2001). Rational approaches to alter protein stability have also met with some success. With respect to cysteines, both removal and addition of cysteine residues can improve stability. Introduction of well placed cysteines at the sub-unit interfaces of oligomeric proteins followed by oxidation to disulphide bonded dimers has been shown to improve the stability of many proteins (Velanker et al., 1999). However, the high reactivity of cysteine residues also makes them undesirable in many cases. Cysteines are highly susceptible to oxidation not only to oxygenated cysteine derivatives like sulphenic, sulphinic and sulphonic acids but also to disulphides, both intramolecular and intermolecular. This leads to disruption of protein structure and activity in many cases. Mutation of cysteines to other residues therefore does result in stabilisation of proteins. Cysteines most often are mutated to Serines due to the similarity in the side chains of these amino acids or to Ala or Val. Many examples of such mutations exist in literature and quite often improve stability without significant alterations in function (Amaki et al., 1994, Takagi et al., 2000). The most prominent exceptions are the cases where the cysteine environment alters its pK_a allowing ionization at physiological pH. Replacement with serine which cannot ionize therefore proves to be detrimental to protein function (Vatsis et al., 2002).

5.1.3 Oxidized cysteines in proteins

Oxidation-reduction or redox modulation of protein function is recognized as an important mechanism for controlling cellular activities. Such processes have been documented to be mediated by cofactors such as FAD, iron-sulphur centers, heme

prosthetic groups and redox-active disulphides. These redox processes with fast on/off mechanisms allow the rapid sensing of oxidative stress in the environment (Yeh & Claiborne, 2002). Examples include the OxyR transcription factor in *E. coli*, peroxide oxidation of which leads to the formation of disulphide bonds and results in transcriptional activation of antioxidant defence genes (Aslund et al., 1999). The SoxR protein in *E. coli* performs a similar function and has a iron-sulphur cluster that oxidises leading to the activation of transcription of several downstream genes (Pomposiello & Demple, 2001). Cysteine sulphenic acids (R-SOH) have now emerged as important modifications in both enzyme catalysis and regulation (Claiborne et al., 2001, Claiborne et al., 1999). Other oxidised forms of cysteines include the sulphinic acids (R-SO₂H) and sulphonic acids (R-SO₃H). Of these the sulphonic acids are most stable followed by the sulphinic acids. The sulphenic acids are highly labile and hard to detect (Yeh & Claiborne, 2002). Sulphenic acids are stable only under specialized conditions of isolation from other reactive groups. Though not simple to achieve in small molecules, cysteines in proteins can be placed in such ideal environments that stabilise sulphenic acids. The absence of other Cys-SH groups in the vicinity and association with microenvironments with restricted solvent access are two major criteria for the stabilisation of Cys-SOH in proteins. The greater stability of ionized sulphenate compared to the sulphenic acid has also been documented (Claiborne et al., 2001, Claiborne et al., 1999).

The use of cryogenic conditions for crystallographic data collection have allowed this detection of these labile moieties in proteins (Yeh & Claiborne, 2002). Cysteine sulphenates have also been detected after derivatization with reagents such as diamedione or 7-chloro-4-nitrobenz-2-oxa-1,3-diazole (Ellis & Poole, 1997). The oxygen on the thiol group is retained during these reactions and can be detected by mass spectrometry. Higher oxidation states of the thiol group can be readily detected without need for derivatization.

Functional roles of cysteine sulphenic acids include that of a catalytic modification in redox enzymes such as NADH-oxidase and also in some mutant enzymes where catalytic aspartates or glutamates have been replaced by cysteine (Claiborne et al., 2001, Claiborne et al., 1999). Reversible cysteine oxidation has been found to

have role in the regulation of signaling proteins such as tyrosine phosphatases (Lee et al., 1998b).

5.1.4 Protein-protein interactions

Protein-protein interactions play an important role in the functioning of many proteins. These interactions may be between different proteins leading to the formation of hetero-multimers or between identical polypeptides forming homo-multimers. Examples of hetero-multimers include large complexes like the ribosome, the photosystems and the ATP-synthase complex where many different proteins associate to form the functional complex. Such association is not restricted to large complexes. Consecutive enzyme in biochemical pathways associate allowing efficient substrate channelling to successive enzymes. Transient associations between receptors and their ligands are important regulators of cellular function.

An enormous number of enzymes, carrier proteins, scaffolding proteins, transcription regulatory factors etc function as homo-oligomers. Formation of homo-oligomers has many advantages. Oligomers often lead to greater stability like in the case of the *Pyrococcus furiosus* ornithine carbamoyltransferase. This thermostable enzyme exists as a tetramer of trimers while its mesophilic counterparts function as trimers. Disruption of the association of the tetramers leads to loss of stability (Clantin et al., 2001). Oligomerization also allows co-operativity and allostery in ligand binding, hemoglobin, though not a true homo-oligomer being a classic example. This tetrameric molecule shows co-operativity in oxygen binding and is allosterically modulated by protons and organic phosphates that bind at the interface and disrupt sub-unit interactions (Hobish & Powers, 1986). Regulatory properties can also be linked to sub-unit interactions as protein function can be related to protein concentration. Such control can be positive or negative with the oligomer or monomer having higher activity.

In many cases the active site is itself constituted on assembly of the oligomer. The active site of the HIV-protease is at the interface of this homodimeric protein.

Most other proteases of the same class are single polypeptides with two highly similar domains that suggest a gene duplication event (DiIanni et al., 1990). The homodimeric HIV-protease allows the virus economy in the genetic information that is required to code for the activity. Scaffolding proteins like the viral coat protein and the cytoskeletal proteins like tubulin and actin are functional in a polymeric state.

5.1.5 The AdSS dimer interface

Most characterized adenylosuccinate synthetases (AdSSs) are homodimers in solution at high concentration. The K_d for dissociation of the *E. coli* AdSS dimer has been determined to be 10 μ M reducing to a negligible quantity in the presence of substrates (Honzatko & Fromm, 1999). In the case of plant AdSS, gel filtration studies indicate a monomeric species while dynamic light scattering shows dimers. Since the crystal structure of the plant enzymes show interaction between the active sites of the dimer, this enzyme is also likely to be active as a dimer (Prade et al., 2000).

Extensive studies carried out on the *E. coli* enzyme have established the importance of dimerization in catalysis. The dimeric form of the enzyme has been demonstrated by MALDI-TOF MS (Wang et al., 1997a). The wildtype enzyme in the presence of active site ligands exists exclusively as a dimer. Mutation of residues important for interfacial interactions, R143 and D231, leads to change in the dissociation constant of the dimer. The K_m s for the substrates, IMP and GTP are also elevated but k_{cat} is not affected. *E. coli* AdSS most probably exists as a monomer at low concentrations (Kang et al., 1996). The enzyme is activated by dimerization induced by substrates and this may represent a control mechanism of adenylosuccinate biosynthesis.

Kang et al. (1996) showed by means of subunit complementation using site directed mutants that the active site of AdSS lies at the dimer interface. Crystallographic studies show that R143 in the *E. coli* enzyme projects into the active site of the juxtaposed subunit. Asp13 and His41 are catalytically important

residues in the synthetase and mutation to Ala leads to complete loss of activity. Dimerization is however, not affected in these active site mutants. Mutation of R143 to Leu results in increased K_m s for IMP and GTP but does not affect catalysis though the activity under standard assay conditions (substrate concentrations lower than K_m of mutants) is low. Mixing of the R143L and the D13A or H41A mutants leads to an increase in activity under standard assay conditions. This improvement is due to the formation of hetero-dimers as illustrated in Fig. 5.1. The R143L mutant is

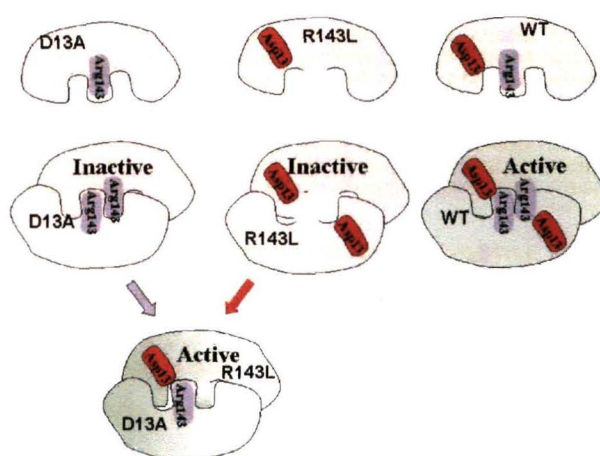


Figure 5.1: Subunit complementation in *E. coli* AdSS. Hetero-dimer formation results in active enzyme. Figure adapted from Kang et al. (1996).

a dimer in solution and heterodimer formation in the presence of D13A could be demonstrated by gel filtration studies. These observations show that only the dimer of the *E. coli* AdSS is active.

The crystal structure of *E. coli* AdSS validates the studies with the mutants (Poland et al., 1996b). The only residue that makes direct contact with the substrates from across the subunit is R143. This residue however, does not play a role in catalysis and its interactions with the 5'-phosphoryl group of IMP are important for substrate binding only. The interface in *E. coli* AdSS is extensive with dimerization burying an area of 5270 Å². Interface contacts involve two different regions that are almost entirely separated except for one hydrogen bond between the two segments. The interacting residues are highlighted in Fig. 5.2. As can be seen from the figure, both hydrophobic and hydrophilic interactions contribute to dimer

modified only in the presence of 3.5 M urea. Though not directly important for activity, refolding of the partially denatured protein is affected on modification of Cys344. The remaining two cysteines are modified only after complete denaturation in the presence of 8 M urea (Dong et al., 1990). None of these cysteines lie at the dimer interface in the structure of the enzyme. AdSS from Yoshida sarcoma ascites tumor cells has been shown to be inactivated by Hg^{2+} ions. This inhibition could be reversed by DTT (Matsuda et al., 1980). The rabbit skeletal enzyme was completely inactivated on incubation with the thiol modifying agent, DTNB (Muirhead & Bishop, 1974)

This chapter describes the results on three interface cysteine to serine mutants of PfAdSS which suggest the involvement of charge on these cysteines in maintaining dimer integrity in this parasite enzyme.

5.2 Materials and Methods

5.2.1 Enzyme assays

Enzyme assays were performed as described in Chapter 4 (4.2.8). Protein concentrations were estimated by the Bradford's method with bovine serum albumin as a standard.

5.2.2 Fluorescence

Fluorescence emission spectra were recorded on a Perkin-Elmer LS-55B or a Hitachi F2500 spectrofluorimeter. The protein sample was excited at 280 nm and emission spectra recorded from 300 nm to 400 nm. Protein concentration was 1.0 μM . Excitation and emission band pass were 7.5 nm and 5.2 nm, respectively for measurements on the Perkin Elmer machine. For the urea denaturation experiments, protein at a concentration of 4.0 μM was incubated for 30 min at the desired urea concentration in 50 mM Tris, pH 7.4 and fluorescence spectra recorded after excitation at 280 nm on a Hitachi F2500 spectrofluorimeter. Excitation and emission band pass were 10 and 20 nm, respectively.

5.2.3 Cysteine modification

The pH of protein at 2 mg/ml in 20 mM Tris.HCl, pH 6.9, 10 % glycerol, 1 mM DTT and 1 mM EDTA was increased to 8.0 by addition of Tris pH 8.0 to 40 mM and then treated with 20 mM iodoacetate and the modification allowed to proceed for 15 min on ice. Reaction was stopped by the addition of sodium acetate, pH 5.2 to a concentration of 60 mM. Unreacted iodoacetate was removed by passing through a Sephadex G-25 column equilibrated with the protein storage buffer without DTT. The residual activity of the samples was measured using the standard assay(4.2.8). The controls were also taken through the same procedure except that iodoacetate was excluded from the reaction. Iodoacetamide and IAEDANS modifications were also performed identically.

5.2.4 Size-exclusion chromatography

Two Superdex-200 (300 x 10 mm) gel filtration columns (referred to as column 1 and 2) independently calibrated with β -Amylase (200 kDa), Alcohol dehydrogenase (150 kDa), Bovine serum albumin (66 kDa), Carbonic anhydrase (29 kDa) and Cytochrome C (12.4 kDa) were used for the analytical gel filtration studies (Calibration shown in Appendix A). Size exclusion chromatography of the metal ion inactivated protein samples were carried out on a prepacked column (Column 1) equilibrated with 50 mM sodium phosphate buffer, pH 7.5, 5 mM Mg_2Cl_2 . Gel filtrations of the iodoacetate modified proteins were carried out on a Superdex-200 (300 x 10 mm) column packed in the lab (column 2) equilibrated with 20 mM Tris.HCl, pH 6.9, 10 % glycerol and 1 mM EDTA. Iodoacetate treatments were performed as above and the modified protein injected into the column immediately after acidification to arrest the reactions. Controls were treated identically except that iodoacetate was excluded from the reaction, before analysis by gel filtration. Sample volumes were 100 μ l in all runs and elution was carried out at a flow rate of 0.5 ml/min.

5.2.5 Site-directed mutagenesis.

Site-directed mutagenesis was carried by the megaprimer PCR method. The primers used were

Asfl 5'-ACA **CCATGG** CCATATTTGATCATCAAATAAAAAATG-3'

AdSSc 5'-CCAGGTACC **CTCGAG** TTAGTTTAGGTTAAAATTCTT-3'

C328S 5'-ATTATATGTTAA *ATCGAT* TAATAGTATTG-3'

C368S 5'-GAAAAG *GGATTC* TACCCTGTTGAAG-3'

In addition to the desired mutation, these primers also contained restriction sites indicated in bold, incorporated by silent mutagenesis, in order to aid the selection of recombinants. The sites incorporated were *Clal* in C328S and *Bam*H1 in C368S. The mutated codon is shown in italics. The pETAsfl plasmid containing the wildtype PfAdSS gene was used as a template for the construction of the two single mutants, C328S and C368S. Briefly, the mutagenic primer (C328S or C368S) was used along with the C terminal primer (AdSSc) to generate the megaprimer containing the mutation. The PCR mix contained 200 ng of each primer, 20 ng of the template, 200 μ M of each dNTP and 5 units of *Taq* DNA polymerase for a 50 μ l reaction. The PCR cycle used was denaturation at 93°C for 30 s, annealing at 44°C for 30 s and extension at 73°C for 1 min. The product obtained after 30 cycles of PCR was purified by elution from agarose gels and used as a megaprimer in a second round of PCR. The other primer used in the second PCR was Asfl and the PCR conditions used were as described above. The full-length amplified product containing the desired mutation was purified, restricted with the enzymes *Nco*1 and *Xho*1 and ligated into the vector pET23d digested with the same enzymes. Recombinants were selected after transformation into the *E. coli* strain DH5 α on basis of supercoiled plasmid mobility. The presence of the right insert was confirmed by restriction digestion with the enzymes the sites for which were incorporated in the design of the mutagenic primers.

The double mutant was constructed using the same procedure with the C368S mutant in pET23d as the template. The primers C328S and AdSSc were used for the first round of mutagenesis in this case. The presence of the mutations was confirmed by sequencing (Fig. 5.3). The C328S and C328S, C368S mutants were found to be free of PCR introduced errors. However, the C368S mutant was found harbor a point mutation within the sequence of the N terminal primer used in the mutagenesis leading to the conversion of F4 to L. This mutation was not carried over to the double mutant, even though C368S was used as the template to generate this mutant.

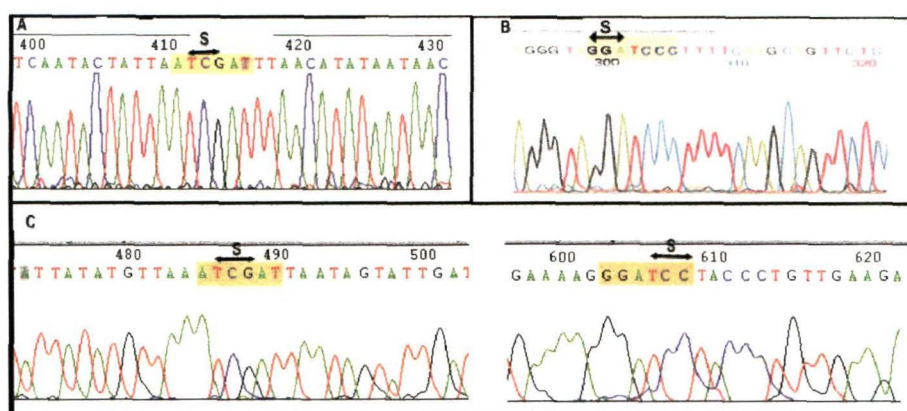


Figure 5.3: Sequencing chromatograms confirming incorporation of mutations. a) C328S, b) C368S, c) C328S,C368S. The restriction sites introduced are highlighted and the mutated codons are denoted by arrows and the amino acid is indicated.

5.2.6 Protein expression, purification and enzyme assays

BL21(DE3) cells were freshly transformed with the pET23d constructs of wildtype and mutant PfAdSS for protein expression. These freshly transformed cells were inoculated into terrific broth and grown to OD(600 nm) of 0.6 at 37°C, cooled to 25°C and protein expression induced by the addition of IPTG to a concentration of 100 μM. Induction was carried out at 25°C for 12 h. Protein purification protocols were identical to those described for wildtype PfAdSS in Chapter 4 (4.2.5). Purified proteins were stored at a concentration of 2 mg/ml in 20 mM Tris.HCl, pH 6.9, 10 % glycerol, 2 mM DTT and 1 mM EDTA at 4°C. All proteins behaved identically during purification and representative chromatograms and SDS-PAGE profiles are shown in Fig. 5.4.

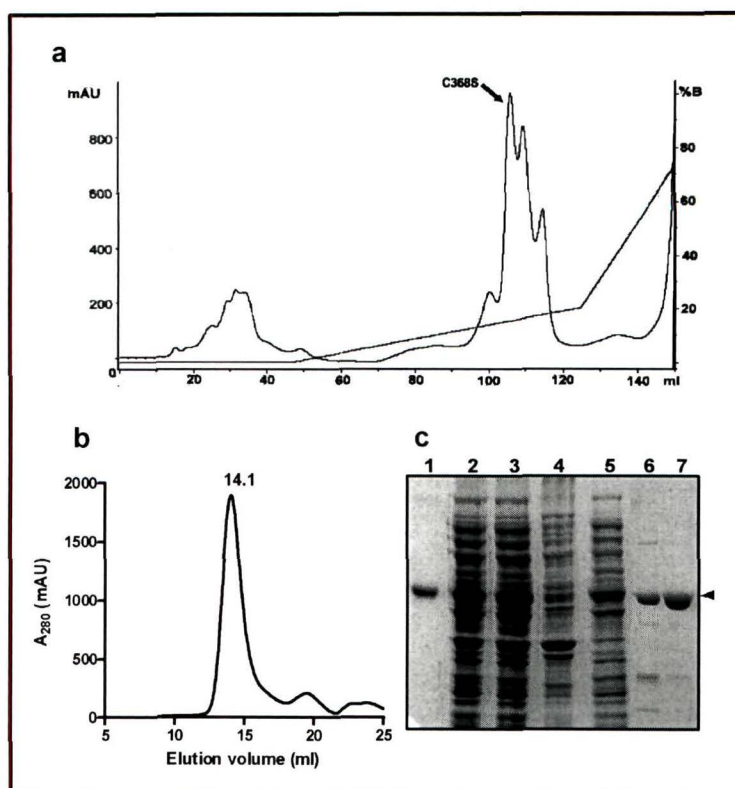


Figure 5.4: Purification of C360S: Elution profile of C368S on a) anion exchange (Q-Sepharose-HP) HPLC. Arrow indicates the C368S peak. b) Superdex-200 gel filtration column. c) Purification profile of C368S. 1) Marker (wildtype) PfAdSS, 2) Crude lysate, 3) PEI supernatant 4) 40 % ammonium sulphate pellet, 5) 40-65 % ammonium sulphate pellet, 6) Q-Sepharose eluate, 7) purified C368S.

5.3 Results

5.3.1 Effect of metal ions on PfAdSS

Activity

The requirement of EDTA for enzyme stability indicated the role of metal ions in the inactivation of PfAdSS. The effect of two metal ions, Mn^{2+} and Cu^{2+} , on PfAdSS were therefore investigated. As removal of DTT or EDTA led to loss of activity, the incubations were carried out in the presence of 1 mM of each compound. Shown in Fig. 5.5a is the residual activity of the protein on addition of 5 mM $MnCl_2$ which shows that the activity does not drop in the presence of manganese ions.

Addition of CuCl_2 to a concentration of 5 mM resulted in immediate precipitation of the protein. Addition of only 0.5 mM CuCl_2 resulted in complete loss of activity within 48 h (Fig. 5.5b). This was surprising, as the concentration of EDTA during the incubation was 1 mM, 2 fold in excess of the Cu^{2+} added. Presence of the substrate, IMP, protected the enzyme from inactivation by the metal ion (Fig. 5.5c)

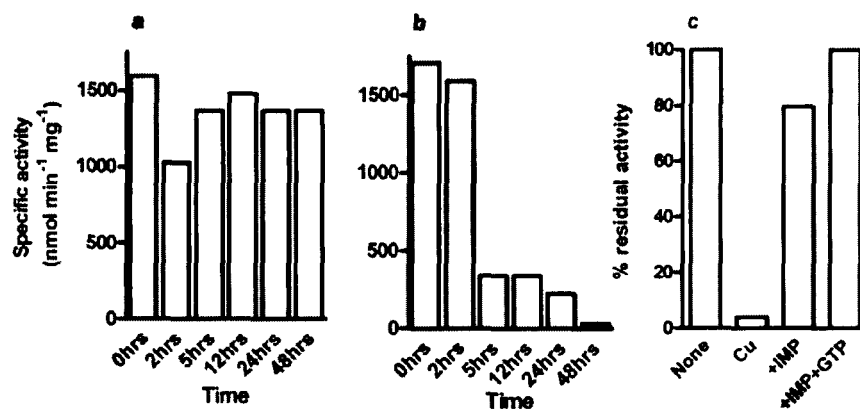


Figure 5.5: Effect of metal ions on activity on PfAdSS. Protein incubated in presence of a) 5 mM Mn^{2+} b) 0.5 mM Cu^{2+} c) 0.5 mM Cu^{2+} and substrates as indicated (IMP 250 μM , GTP 150 μM .)

Oligomerization

Gel filtration analysis of the protein inactivated by copper showed that the oligomeric status of the enzyme shifts towards the dimer. A small peak corresponding to an aggregated species also appears (Fig.5.6a). The enzyme in the absence of any treatment is a monomer dimer equilibrium. Reducing and non-reducing SDS-PAGE showed that the inactivation was accompanied by the appearance of disulphide bonded species (Fig.5.6c). Inactivation was also accompanied by a drop in the intrinsic tryptophan fluorescence of the protein (Fig.5.6b). The intensity of fluorescence of the inactivated protein improved when the measurements were made in the presence of 5 mM DTT. Treatment with Mn^{2+} does not lead to any of these changes in the properties of the enzyme and it retains as much activity as the untreated enzyme. Presence of IMP during the incubation with Cu^{2+} prevented the above changes in the properties of the enzyme.

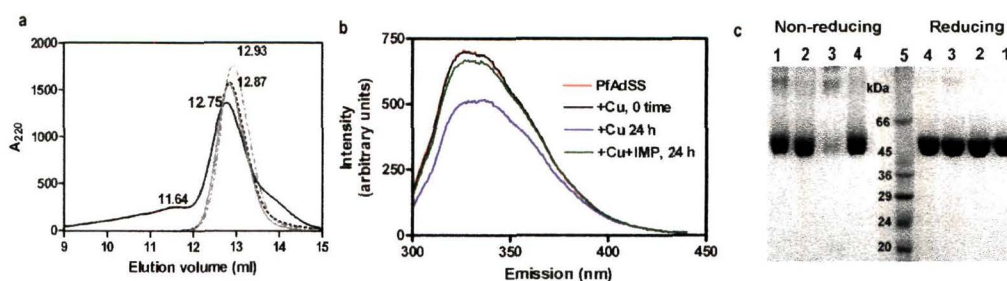


Figure 5.6: a) Gel filtration profiles (column 1 used) of native PfAdSS (dotted grey line, 12.93 ml), PfAdSS incubated with Mn^{2+} (solid grey, 12.87 ml), PfAdSS incubated with Cu^{2+} (solid black, 12.75 ml) and PfAdSS incubated with Cu^{2+} and 150 μM IMP (solid light grey, 12.87 ml). Elution volumes are indicated. b) Fluorescence spectra of PfAdSS, PfAdSS immediately (0 time) and 24 h after addition of Cu^{2+} , and, PfAdSS incubated with Cu^{2+} in the presence of 150 μM IMP. c) SDS-PAGE profile of PfAdSS 1) incubated with Cu^{2+} and 150 μM IMP, 2) incubated with Mn^{2+} , 3) incubated with Cu^{2+} and 4) untreated under reducing and non-reducing conditions.

5.3.2 Effect of cysteine modifying agents on activity

The results shown above implicate cysteines in the inactivation of the enzyme. The effect of cysteine modifying agents on the activity and oligomerization of the wildtype enzyme was therefore monitored. In the absence of substrates, treatment with iodoacetate led to almost complete loss of activity within 15 min at 4°C. This inactivation could be prevented by the presence of IMP (Fig. 5.7). Size-exclusion chromatography of the modified protein showed that the inactivation was accompanied by a shift (Fig. 5.8a). The effect of modification with iodoacetamide was also evaluated. This modifying agent led to complete loss of activity. Gel filtration analysis of the iodoacetamide modified protein failed to give defined peaks indicating the distribution of the protein over different oligomeric states in this case (Fig. 5.8b). These observations together indicated that the cysteine that is modified is at the interface of the protein.

5.3.3 Rationale for generation of cysteine mutants

All initial attempts at crystallisation of wild type PfAdSS resulted in precipitation. The observations detailed above suggested that the reason might be the

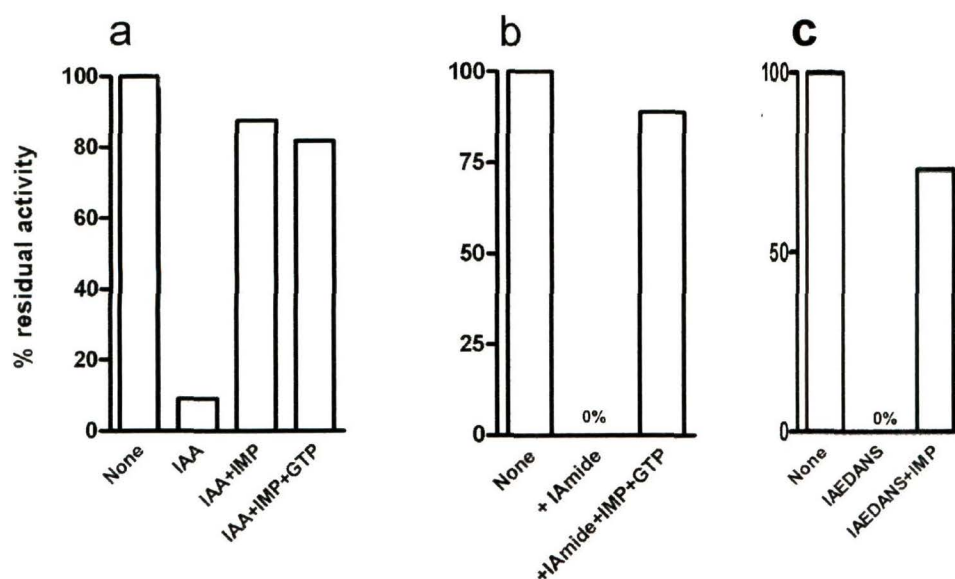


Figure 5.7: Effect of cysteine modifying agents on activity of PfAdSS. a) Iodoacetate (IAA) treatment b) Iodoacetamide (IAmide) treatment c) IAEDANS treatment. Activity is shown as a % of the control. Modifications were carried out as detailed in materials and methods.

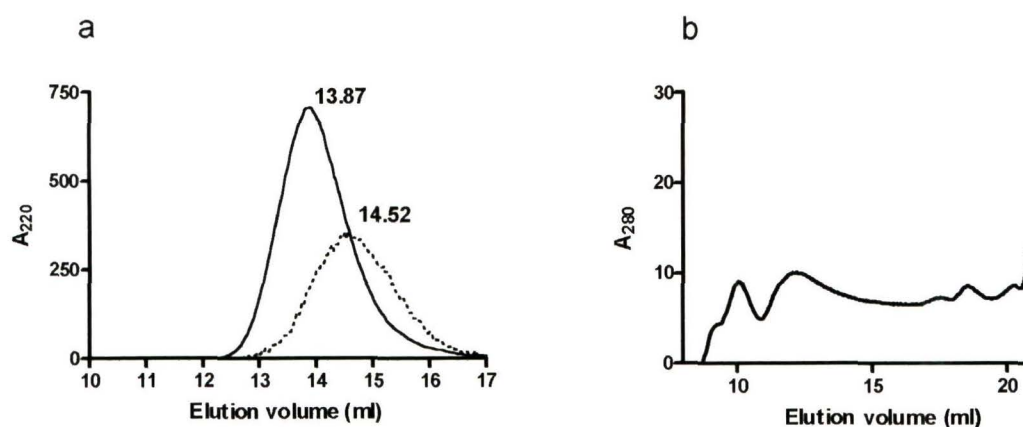


Figure 5.8: Gel filtration (column 2) profiles of wildtype PfAdSS a) modified with iodoacetate (dotted line) and without modification (solid line). b) modified with iodoacetamide. Note: Elution is monitored at 220 nm in (a) and at 280 nm in (b).

oxidation of the protein during crystallisation. It was therefore reasoned that the mutation of interface cysteines to serine would give a protein of greater stability and make it more amenable to crystallisation. Shown in Fig. 5.2 is the sequence alignment of PfAdSS with the *E. coli* and mouse muscle enzymes, for which

structures were available at the time of these experiments. The residues that contribute to the dimer interface in the two structures are highlighted. On the basis of this alignment, two cysteines, C328 and C368 were found to correspond to residues that lie at the interface of the protein and are not conserved. These cysteines were therefore mutated to serine as described in materials and methods and purified. The mutants constructed were 1. C328S 2. C368S and 3. C328S,C368S hereafter referred to as the double mutant.

5.3.4 Expression and purification of interface cysteine mutants of AdSS

The three Cys mutants generated by the megaprimer PCR method (Sarkar & Sommer, 1990) were cloned into the pET23d vector and the recombinant proteins expressed in the *E. coli* strain BL21(DE3). The purification protocol used for all the three mutants was identical to that used for the wildtype enzyme (4.2.5). Representative chromatograms are shown in the section on Materials and Methods. The SDS-PAGE profiles of the expressed and the purified proteins are shown in Fig. 5.9. All proteins used for this study were at least 95 % pure as judged by SDS-PAGE.

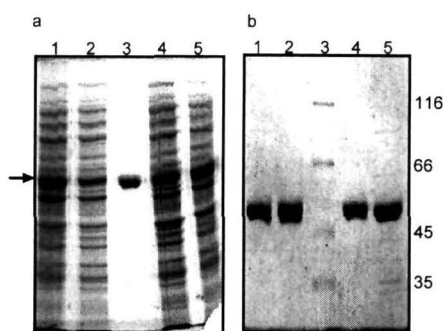


Figure 5.9: SDS-PAGE profile of PfAdSS mutants. a) Induction of recombinant protein in *E. coli* BL21(DE3). 1: C328S, 2: C328SC368S, 3: purified WTPfAdSS, 4: C368S, 5: wildtype PfAdSS. b) Purified proteins 1: C328S, 2: C328SC368S, 3: Marker, 4: C368S, 5: Wildtype PfAdSS.

5.3.5 Kinetic characterization cysteine mutants

The kinetic properties of the mutants are compared to that of the wildtype enzyme in Table 5.1. The K_m s for the nucleotides, IMP and GTP are very similar to that of the wildtype protein. Variation appears in the Michaelis constant for aspartate, which is comparable to the wild type in the case of the C328S mutant, is 4 fold lower in the case of the double mutant and is higher in the case of the C368S mutant.

Table 5.1: Kinetic parameters of wildtype and mutant PfAdSS.

Protein	k_{cat}	K_m		
		IMP (μ M)	GTP (μ M)	Asp (mM)
Wildtype	0.52 ^a	22.8	18.4	1.80
C328S	0.52	23.7	27.5	1.83
C368S	0.51	24.8	20.6	3.20
C328S,C368S	0.53	19.7	17.2	0.40

^aThis value varied between 0.52 and 1.16 between preparations.

5.3.6 Oligomeric status

Since the residues mutated were at the subunit interface of the enzyme, the oligomerization of the protein was evaluated by gel filtration. Fig. 5.10 shows the elution profiles of the proteins from a S-200 column. The wildtype protein elutes at a volume of 13.85 ml (89 kDa) indicative of a monomer-dimer equilibrium with the dimer predominating. The elution of the C368S mutant is also identical to the wildtype. Surprisingly, the C328S mutant eluted as a broad peak at 14.17 ml indicating a shift of the equilibrium towards the monomer. The oligomerization of the double mutant was more drastically affected with the appearance of a small peak close to a monomeric species.

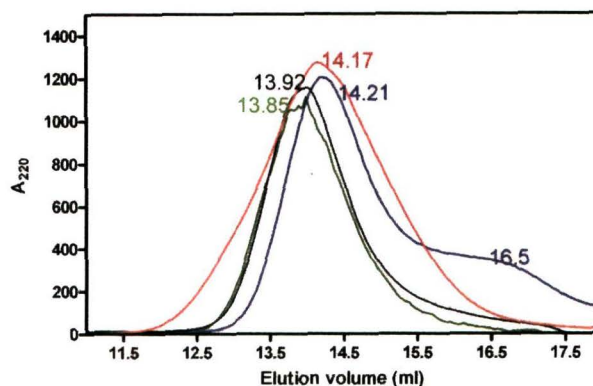


Figure 5.10: Gel filtration profile (Column 2) of wildtype and mutant PfAdSS. Wildtype (green), C368S (black), C328S (red), C328SC368S (blue) (Column 2). Elution volumes in ml are indicated.

5.3.7 Stability

The relative stabilities of wild type AdSS and the three mutants were evaluated under unfolding conditions. Unfolding was monitored in terms of shift in fluorescence emission maxima on excitation at 280 nm after denaturation at different concentrations of urea. Fig. 5.11 shows the emission maxima of these four proteins at different concentrations of urea. The curves for the wild type and C368S are superimposable indicating that the two have identical stabilities. The emission maxima of C328S and the double mutant are red shifted by 3 nm in the absence of urea. The curves however, superimpose at higher urea concentrations. After an initial increase in the emission maximum up to a concentration of 2 M urea, the curve plateaus till a concentration of 6.5 M urea. However, in the case of all the proteins, the emission maximum is at only 244 nm even at urea concentrations of 8 M indicating that the proteins are not fully unfolded. The difference in the emission maximum of the proteins in the absence of urea may be a reflection of the differences in the oligomerization of the proteins seen on gel filtration. However, effect of mutation on tertiary structure cannot be ruled out.

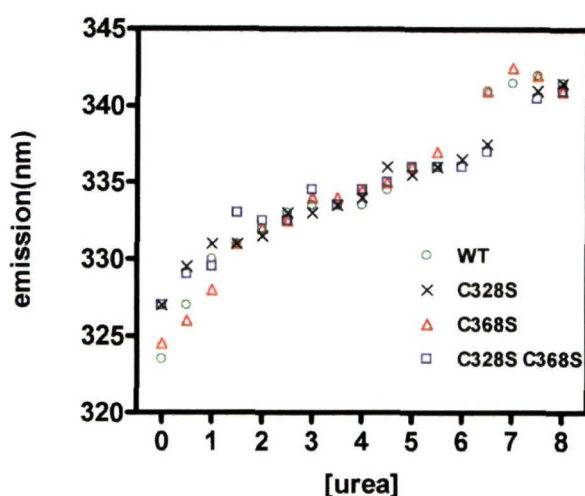


Figure 5.11: Equilibrium unfolding of PfAdSS wildtype and mutants monitored as the change in emission maximum after excitation at 280 nm.

5.3.8 Effect of iodoacetate treatment on the mutants

Effect on activity

The interface cysteine mutants were constructed as a consequence of the observation that the iodoacetate treatment of the wildtype enzyme led to loss of activity. The specific activities of the wildtype and mutants with and without modification with iodoacetate is shown in Table 5.2. Examination of the effect of this cysteine modifying agent on the activity of the mutants showed that replacement of interface cysteines affords partial protection to inactivation by iodoacetate. Maximum protection is seen with the double mutant. The loss of activity in the double mutant indicates that one or more cysteines other than those mutated are involved in the inactivation process.

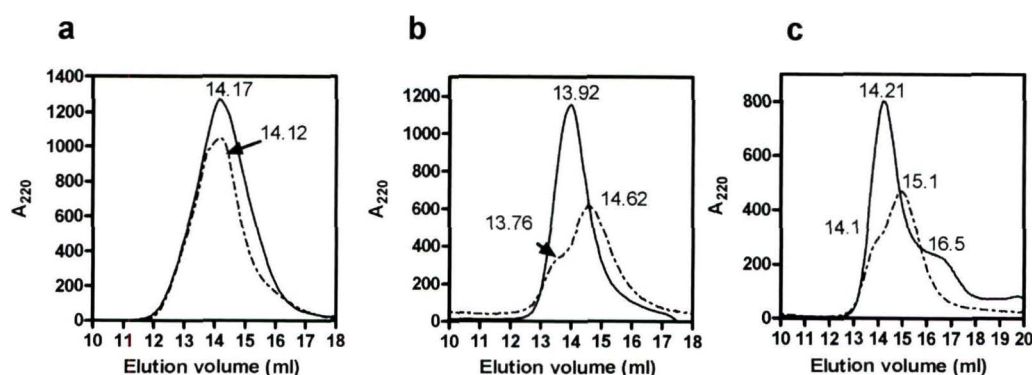
Effect on oligomerization

The gel filtration profiles of all three mutants before and after iodoacetate modification are shown in Fig. 5.12. Unlike the wildtype which gives a single peak shifted towards a monomer on modification (Fig. 5.8, C368S is partially protected giving two peaks, one corresponding to the parent unmodified peak and

Table 5.2: Effect of iodoacetate (IAA) treatment on activity of wildtype and mutant PfAdSS

Protein	Specific activity (nmol min ⁻¹ mg ⁻¹)		% residual activity
	Unmodified	IAA modified	
Wildtype	622	89	9.3
C328S	623	266	42.7
C368S	613	291	47.5
C328S,C368S	630	434	69.0

the other shifted towards the monomer (Fig. 5.12b). Surprisingly, the C328S mutant which forms an inherently less stable dimer does not alter in its oligomerization after modification (Fig. 5.12a). Though both these cysteines are absent in the double mutant, the gel filtration profiles alter after modification (Fig. 5.12c). These observations indicate that modification of C328 (in C368S) results in the disruption of the dimer in the wildtype protein. The loss of activity and change in subunit association seen in the case of the double mutant is most probably a consequence of modification of a third cysteine in this case. This cysteine probably becomes exposed and therefore available for modification as a consequence of the disruption of the dimer interface in the double mutant.

**Figure 5.12:** Gel filtration (column 2) profiles of a) C328S, b) C368S, c) C328S,C368S, before and after modification with iodoacetate. Solid lines represent unmodified protein and broken lines the proteins after modification with iodoacetate

5.3.9 Oxidation of C328

The crystal structure of PfAdSS shows additional electron density around C328 that is suggestive of oxidation this residue (Fig. 6.8). This further shows that the reactivity of Cys328 is high. The enzyme is also able to tolerate oxidation at this position without loss of activity as the protein used for the crystallisation has high specific activity and so do the crystals of the protein (Fig. 6.9). Mass spectral analysis of tryptic digests (Appendix A, A2)) show the presence of a peptide with a mass 16amu greater than that of the unmodified fragment containing the C328 though the these experiments remain preliminary.

5.4 Discussion

5.4.1 Metal catalysed inactivation of PfAdSS

The inactivation of PfAdSS by Cu^{2+} ions but not Mn^{2+} ions indicates the involvement of a redox system in the process. Mn^{2+} is a relatively stable ion while Cu^{2+} can readily interconvert between the +1 and +2 oxidation states. Cu^{2+} is has been implicated in a number of redox processes leading to the inactivation of proteins by oxidation (Cecconi et al., 1998, Khosravi et al., 2000). Cysteines represent one of the residues most susceptible to such oxidative processes. It is therefore, not surprising that PfAdSS, with 10 cysteines is rapidly inactivated by oxidation in the presence of Cu^{2+} ions, and forms disulphide linked oligomeric species. Cu^{2+} catalysed disulphide bond formation is well documented in literature. For example, Cu^{2+} has been shown to lead to the formation of disulphide-linked dimers of the S100B protein resulting in the formation of the biologically active form that can simulate the proliferation of primary astrocytes (Lee et al., 2000).

What is surprising is that the inactivation takes place even in the presence of a two fold molar excess of EDTA. This may be due to one of two reasons. 1. Cu^{2+} catalysed oxidation processes can take place at very low concentration of the metal ion with concentrations in the nanomolar range being reported for this process (Stadtman, 1993). Even though a two fold molar excess of EDTA is present in these

studies, low concentrations of unchelated Cu^{2+} ions may be present in the system in equilibrium with the chelated metal ion. These concentrations may be sufficient to drive the process which is catalytic. However, metal catalysed oxidations in many systems is prevented by the presence of a chelator at concentrations equal to or greater than the amount of metal ion present. 2. Examples also exist in literature of proteins where the oxidation is either simulated or completely dependent on EDTA (Stadtman, 1993, Maier et al., 1996). The possibility that PfAdSS is one such example exists. This aspect could not be investigated as this enzyme is rapidly inactivated unless stored in the presence of EDTA, even in the absence of externally added metal ion. The protection afforded by EDTA however, does suggest that it is the metal ion itself and not the EDTA-metal complex that is responsible for the inactivation. If the metal-EDTA complex were to be essential, inactivation would take place even without the addition of additional Cu^{2+} .

Non-reducing gels of the Cu^{2+} inactivated protein show the formation of disulphide bonded dimers. Examination of the crystal structure of PfAdSS (Chapter 6) does not reveal any two cysteines at disulphide bonding distance of each other at the interface. This indicates that the formation of the disulphide bonded species in the presence of Cu^{2+} may be accompanied by a distortion of the structure of the protein.

5.4.2 Kinetic properties of interface mutants

The K_m s of the mutants for the substrates IMP and GTP remain unaltered compared to the wildtype enzyme. However, a significant variation is seen in the aspartate K_m s of two of the mutants. While the aspartate K_m of C368S goes up to 3.2 mM, there is a sharp drop in the value for the double mutant to 400 μM . Both the residues modified do not lie near the aspartate binding site of the protein. The only major difference between these mutants and the wildtype is in the association into dimers. The gel filtration profiles indicate that in the double mutant, the monomer-dimer equilibrium is shifted towards the monomer. This raises the possibility that binding of aspartate is influenced by the oligomerization of the protein. The active form of AdSS is a dimer, with residues from both subunits contributing to each

of the two active sites in the dimer. Since substrate binding in PfAdSS is ordered (Chapter 4) and, the IMP binding site comprises of residues from both subunits (Chapter 6), it is possible that interference with the dimerization alters the binding of the other substrates of the enzyme. The Lineweaver-Burk plots for the mutants are however, linear, and do not indicate co-operativity in either wildtype or mutant PfAdSS. The only report of co-operativity in AdSS is in the case of the *S. cerevisiae* enzyme where negative co-operativity has been documented with the substrates GTP and aspartate (Lipps & Krauss, 1999). Inacu et al.(2002a) have suggested, on the basis of inhibition of the mouse basic isozyme by the substrate IMP even in the presence of saturating concentrations of GTP, that there might be cross talk between the AdSS sub-units.

5.4.3 Importance of C328 and C368 in PfAdSS

The activity and gel filtration profiles of the mutants indicates that modification of both C328 and C368 contributes to loss of activity. Mutation of these cysteines to serines affords only partial protection to inactivation by iodoacetate indicating the role of one or more cysteines in the inactivation process. Modification of C328 (in C368S) leads to disruption of the dimer, so does the mutation of C328 to Ser. Modification of the C328S mutant by iodoacetate does not lead to further change in the oligomerization, implying that C368 modification does not affect the oligomerization. These observations indicate that C328 is of greater importance for the maintenance of dimer integrity than C368. Though both the cysteines are mutated to serine in the double mutant, modification with iodoacetate does lead to alteration in the association of the dimer. Since the single mutant C328S is not affected by iodoacetate treatment, this is contrary to expectation. This may be because of the modification of a third cysteine, which might be exposed to the modifying agent due to the weakening of the dimer in the double mutant.

5.4.4 Is a charged cysteine necessary for maintaining dimer integrity?

The results presented in this chapter raise the possibility that the presence of a charged cysteine at the interface of PfAdSS may be necessary for the dimerization

of the protein. Firstly, iodoacetate treatment of the protein leads to complete loss of activity and is accompanied by the destabilisation of the dimer. However, the protein continues to be present as an equilibrium between a monomer and a dimer. Treatment with iodoacetamide, which is not charged, leads to distribution of the enzyme over a wide range on gel filtration, suggesting that presence of a charge on the modifying agent helps preserve subunit association.

Second, the mutation of C328 to Ser leads to disruption of the dimer. Cys to Ser mutations are routinely introduced into proteins in order to stabilise them to oxidation (Cecconi et al., 2002). Since these two amino acids are largely similar, this substitution does not normally alter the properties of the mutant. The side chains of these amino acids however, differ in their ionization abilities. The thiol group of Cys can readily ionize to a thiolate resulting in a charged species. It can also oxidise to sulphinic, sulphenic and sulphonic acids resulting in upto three negative charges on the residue. Ser side chains on the other hand ionize only at very high pH; neither can they get oxidised to charged species. The interactions of this residue are restricted to hydrogen bonding both as a donor and an acceptor through the OH group.

Thirdly, complete inactivation of the enzyme by both iodoacetate and iodoacetamide within 15 min at 4°C even in the presence of 1 mM DTT indicates the presence of very highly reactive cysteines in the enzyme. This factor also suggests that the cysteine, the modification of which affects subunit association, may be in its ionized form.

Finally, C328 in the active wildtype protein may be modified probably by oxidation to a sulphenic acid. This is in spite of the presence of 10 mM DTT in the storage buffer of the enzyme. The crystal structure of PfAdSS solved to a resolution of 2Å reveals extra electron density on C328 that corresponds to more than one oxygen indicating that this residue is indeed modified, at least in the crystal.

Taken together, these factors indicate that a charge on the cysteines at the interface is necessary to maintain the dimer of PfAdSS. The presence of oxidised cysteines at the interface however, is a matter of debate as the modifications

seen could be artifacts of the enzyme preparation and crystallographic structure determination. Examination of the cysteine thiolates in literature indicates that a positively charged residue, frequently a histidine, near the cysteine plays a role in decreasing the pK_a and leads to ionization (Plou et al., 1996). Examination of the structure of PfAdSS (Chapter 6) shows that the interface of this protein is positively charged. The environment around Cys328 includes two Lys and one His residues. These observations indicate that the environment around C328 favours ionization to a thiolate. Increased reactivity of the cysteine resulting from the ionization may result in its oxidation, at least *in vitro*.

Unusual pK_a s for cysteines residues have been observed in many proteins. The thiol-imidazole ion pair is frequently encountered in the active site of enzymes which have cysteines in their active site. The resultant alteration of the pK_a of cysteine results in a highly reactive thiolate in the active site of these enzymes. Examples include cysteine proteases like papain (Shipton & Brocklehurst, 1977) and polyketide synthases ($pK_a = 5.5$) (Jez & Noel, 2000). Altered pK_a of non-active site cysteines has also been reported. In the human placental glutathione transferase Pi, Cys 47 has been shown to exist as a thiolate anion with a pK_a of about 4.0. This cysteine is not in the active site of the enzyme and mutation to serine results in a decrease in affinity for glutathione but does not affect catalysis (Lo Bello et al., 1995). Cysteines involved in metal coordination are frequently found as thiolates and ionization is necessary for metal binding (Simonson & Calimet, 2002).

Though cysteine sulphenic acids are extremely labile, many examples of such species in proteins exist. They have now been demonstrated by both chemical and crystallographic studies. In enzymes such as NADH-peroxidase, NADH-oxidase, nitrile hydratase and some proxiredoxins, Cys-SOH have been shown to have a functional role in the native protein (Claiborne et al., 1999). In the enzymes involved in redox processes, the oxidised cysteine is catalytically important, while in nitrile hydratase, it serves to bind iron and NO (Claiborne et al., 2001). In the case of tyrosine phosphatases and glutathione reductases, the Cys-SOH form has been suggested to play a role in the reversible inhibition of these enzymes during signal transduction (Denu & Tanner, 2002) and nitrosative stress (Claiborne et al.,

1999), respectively. Reversible cysteine oxidation is now emerging as mechanism for cellular response to oxidative stress. A regulatory role of sulphenic acids in glycolysis has also been proposed on the basis of the observation that mild oxidation of glyceraldehyde-3-phosphate dehydrogenase converts it to an acylphosphatase (Dan'shina et al., 2003). Oxidized cysteines can also replace carboxyl functional groups in proteins. In glucoamylase, Glu-400 serves as a catalytic base. A E400C mutant of this enzyme was found to regain catalytic activity when the cysteine was oxidised to a sulphenic acid (Mirgorodskaya et al., 1999). Similar restoration of activity has also been observed after periodate oxidation of cysteine in phosphoribulokinase, an enzyme with aspartate in the active site (Runquist & Miziorko, 2002). The existence of such an oxidised cysteine PfAdSS and its role in maintaining the active dimer needs to be examined.

To summarise, the attempts to create mutants of PfAdSS with improved stability have led to the identification of unusual properties of the PfAdSS subunit interface. Mutation studies highlight the importance of charged cysteines at the interface in the maintenance of dimer integrity. Replacement of C328 at the interface with serine, a residue that cannot ionize, leads to disruption of inter-subunit interactions. Mass spectral analysis of tryptic digests of wildtype PfAdSS raise the possibility that C328 at the dimer interface may be present in the oxidised form in the active protein. Crystallographic evidence for the oxidation of C328 is presented in Chapter 6 of this thesis.

Chapter 6

Structure of *P. falciparum* AdSS: Insights into function.

This chapter presents the crystal structure of P. falciparum AdSS solved to a resolution of 2 Å. The structure explains the unique features of PfAdSS presented in the previous two chapters. The structure was solved as a collaboration with Prof. M.R.N.Murthy's lab at Molecular Biophysics Unit, IISc., Bangalore. The details of the data collection and structure solution are included in this chapter for completeness.

6.1 Introduction

6.1.1 Structure of *E. coli* and mouse AdSS

Extensive studies have been carried out by the groups of Fromm and Honzatko on both the *E. coli* and mouse AdSS. The structures of both these enzymes in the unliganded form and in complex with various combinations of substrate and substrate analogs have been determined and allow an understanding of the functioning of this enzyme. The first structure of AdSS defined a previously unobserved protein fold (Poland et al., 1993). The key features of the enzyme that these structures highlight include the oligomeric state of the active enzyme, the catalytic residues and their role in the reaction, the identity of the reaction intermediate and the numerous loop movements that occur on substrate binding. All crystal structures show the presence of a dimer with both subunits contributing residues to the binding of the substrate, IMP. The asymmetric unit in the structures is either a dimer or a monomer with the dimer axis coincident with a crystallographic

axis of symmetry. Cross subunit interaction with the substrate primarily involves Arg143 (*E. coli* AdSS) which contributes to the recognition of the 5'-phosphoryl group of IMP bound in the other subunit (Poland et.al, 1996a). Attempts at crystallising the synthetase in the presence of the substrates IMP and GTP have resulted in structures which show that the first step of the catalysis has occurred (Choe et al., 1999, Inacu et al., 2002). These structures which have 6-phosphoryl IMP and GDP bound in the active site of the enzyme establish that the reaction intermediate indeed involves the transfer of the γ -phosphate of GTP to O6 of IMP as proposed by the kinetic and isotope exchange studies on the enzyme (Lieberman, 1956, Cooper et al., 1986, Bass et al., 1984). This enzyme has infact been called a thermodynamic sink for this intermediate as all attempts to crystallise the synthetase in the presence of either the substrates or the products resulted in the formation of this molecule (Inacu et al.,2002a).

Asp13 and His41 have been proposed to be the catalytic residues based on the structures of this enzyme and mutagenesis studies. Choe et al., 1999 have proposed that His41 plays a dual role in catalysis. In the first step, it binds to the β -phosphoryl group of GDP and donates a proton to the leaving group acting as an acid catalyst. After protonation of the leaving group, it dissociates from the leaving group, gets reprotonated, undergoes a 90° rotation about its $C\beta-C\gamma$ bond and hydrogen bonds to the 6-phosphoryl group of the intermediate. The crystal structure of a mutant of the *E. coli* enzyme, R303L in complex with 6-phosphoryl IMP shows that the aspartate binding pocket is occupied by 3 water molecules. In this complex, His41 continues to bind the β -phosphoryl group of GDP and not the 6-phosphoryl group on IMP. This suggests that the rotation of His41 is conditional to aspartate binding ensuring the existence of a mechanism for full activation of the 6-phosphoryl group only after the binding of aspartate. The loss of activity on mutation of Asp13 to Ala indicates the importance of this residue in catalysis. Asp13 hydrogen bonds with N1 of IMP in the IMP, GDP, NO_3^- , Mg^{2+} complex of the enzyme (Poland et. al., 1996a) but does not co-ordinate Mg^{2+} . This is consistent with its role as a catalytic base in abstracting a proton from the N1 of IMP. Subsequent coordination to Mg^{2+} after intermediate formation transforms this side chain into a potent acid allowing

the transfer of the proton back to N1 of IMP, generating an electrophilic center on C6 preparing it for the next step of the reaction. Nucleophilic attack by the aspartate on C6 then leads to the displacement of the phosphoryl group. The identity of the residue abstracting the proton from aspartate has been a matter of debate with a role suggested for the β carboxyl group of aspartate. A comparison of the unligated and the variously complexed structures of the synthetase show 6 dynamic elements that respond to substrate binding (Fig. 6.16, Table 6.2)(Inacu et al., 2001, Inacu et al., 2002a, Poland et al., 1996b). The unligated structures define the loop open conformations (Silva et al., 1995, Inacu et al., 2001) and the 6-phosphoryl IMP, GDP, hadacidin, Mg^{2+} complex the ligated conformation of these loops (Choe et al., 1999, Inacu et al., 2002). Of these, the GTP loop alone responds to the binding of GTP. The structure of the mouse enzyme in complex with IMP has all the loops in the ligated conformation in one subunit and the Val and Asp loops in the unligated conformation in the other. In the 6-phosphoryl IMP, GDP complex, all the loops except the Asp loop in one subunit are in the ligated conformation. Both the subunits are completely ordered in the 6-phosphoryl IMP, GDP, hadacidin complex (Choe et al., 1999, Inacu et al., 2002a).

Structures of the mouse and *E. coli* enzyme in complex with AMP (Fonnester et al., 1996, Inacu et al., 2002b) and of the mouse enzyme in complex with the product adenylosuccinate (ADS) (Inacu et al., 2002b) provide insight into the mechanism of product release and feedback inhibition. The AMP binding mode in the complex along with GDP, Mg^{2+} and sulphate is similar to that seen for ADS in the product complex (ADS, GDP, Mg^{2+} , sulphate complex). However, in the complex of the enzyme with AMP alone, the binding mode is similar to that seen for IMP though the pre-Switch loop is oriented in a non-productive mode. This conformation of the pre-switch loop allows the binding of Mg^{2+} IMP to the GTP binding pocket. The product ADS (ADS, GDP, Mg^{2+} , sulphate complex) binds to the enzyme with the base moiety tilted by an angle of 30° compared to the base in 6-phosphoryl IMP. In addition, the base also deviates from planarity with an obvious displacement of C6 from the plane defined by N1, N6 and C5. The distorted conformation of ADS that is seen in the structure also suggests that the

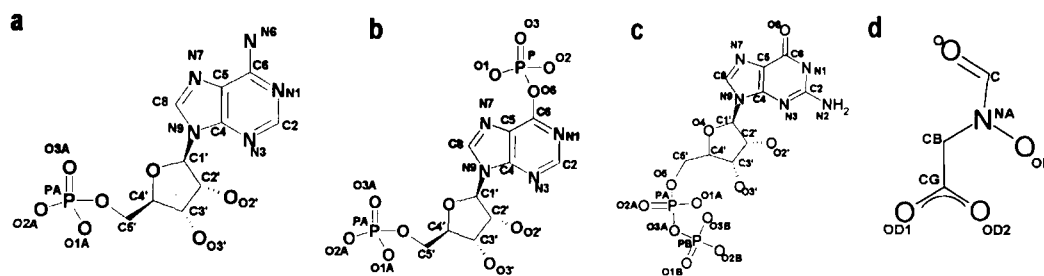


Figure 6.1: Structures showing atom labelling as used in the text for a) AMP/ADS, b) 6-phosphoryl-IMP, c) GDP and d) hadacidin.

tautomer stabilised by the synthetase may be different from that in solution. The C6-N6 torsion angle in the structure reduces the bond order between these two atoms as the tautomer with a double bond between C6-N6 cannot form. This may enhance the basicity of the N6 atom and lead to its protonation. This has led these authors to suggest that the synthetase probably stabilises a protonated form of ADS in the active site and that the second step of the catalysis, the displacement of the 6-phosphoryl group on IMP by aspartate does not require proton abstraction.

The similarity between the structures and mechanism of the *E. coli* and mouse synthetases and the high level of similarity between the sequences of all known synthetases suggests that the structure and mechanism would be largely conserved among these enzymes. However, differences may exist that tailor this enzyme to the specific needs of an organism as it lies at a regulatory point in purine nucleotide synthesis. This chapter describes the structure of *P. falciparum* adenylosuccinate synthetase (PfAdSS) solved by Prof. M.R.N. Murthy and K. Eaazhisai as part of this study to a resolution of 2 Å in a collaborative effort. The structure is of the enzyme in complex with the reaction intermediate 6-phosphoryl IMP, GDP and the aspartate analog, hadacidin. A comparison of the PfAdSS structure with the *E. coli* and mouse enzymes is presented and features that explain the properties of the enzyme described in the previous two chapters are discussed.

6.2 Materials and Methods

All reagents were of high quality and were purchased from Sigma, USA. Hadacidin was a generous gift from Dr. Bruce F. Cooper, Rice University, USA. The plates used for the hanging drop crystallisation were from Tarsons, India and the microbatch plates were from Grainer.Bio one, Germany.

6.2.1 Structure analysis

All the structural alignments of PfAdSS, *E. coli* AdSS and mouse AdSS were carried out using the program ALIGN (Cohen, 1997) or with Swiss-PdbViewer (Guex & Peitsch, 1997). RMSD calculations for the loop regions and analysis of the conformational changes due to ligand binding were carried out by comparative analyses of structures of mouse, *E. coli* and *P. falciparum* AdSSs using ALIGN. All the interactions were evaluated using an in house program. NACCESS (Hubbard & Thornton, 1993) was used for the surface area calculations. The interface residues were identified by recognizing the residues of one monomer which were in direct contact with the residues from the other monomer within a cut-off distance of 4 Å. All molecular representations presented in this chapter were generated using Molscrip (Kraulis, 1991) and rendered using Raster3D (Merritt & Bacon, 1997).

6.3 Results and Discussion

6.3.1 Protein crystallisation

Initial attempts at crystallising PfAdSS were carried out by the hanging drop method. About 30 mg of protein was used in these crystallisation trials carried out both in the presence and absence of substrates and resulted almost entirely in precipitation. The conditions tried included many from the hampton screens constituted in the lab in addition to variations of those already reported for *E. coli* and mouse AdSS. Biochemical studies carried out along side these crystallisation attempts indicated that the PfAdSS was unusually susceptible to oxidation even in the presence of high concentrations of the reducing agent DTT. Since the

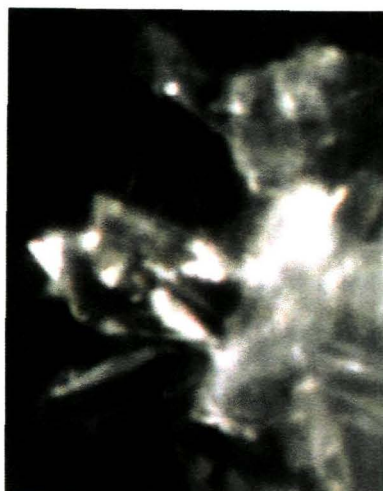


Figure 6.2: Crystal of PfAdSS grown in the presence of IMP and GTP

experiments described in Chapter 5 also suggested that these reactive cysteines were at the interface of the protein, three cysteine to serine mutants of the enzyme were also created. These mutants were however not used for crystallisation as single crystals of the wildtype protein were obtained while these mutants were being purified. Crystallization of the enzyme was also attempted by the microbatch method as the oil overlay as it was brought to our notice that this setup can reduce protein oxidation. The DTT concentration in protein solutions was also raised to 10 mM. The first crystals of the wild type protein were obtained with equal volume mixture of the protein (7.5 mg/ml in 20 mM Tris.HCl, pH 6.9, 20 % glycerol, 10 mM DTT and 1 mM EDTA) incubated with 5 mM each of IMP and GTP and, the precipitant solution comprising of 50 mM sodium acetate, 1 M ammonium sulphate, 50 mM magnesium acetate and 100 mM HEPES, pH 7.5 after 15 days of evaporation through the oil layer (Fig. 6.2). This crystal of PfAdSS, though not a clean single crystal was mounted and found to diffract to a resolution of 4 Å. Only 4 frames of data could be collected on this crystal. Repeated attempts at obtaining good quality crystals under similar conditions by the hanging drop method were completely unsuccessful.

Subsequent crystallisation attempts were restricted to the microbatch method and were carried out at Prof. M.R.N. Murthy's lab at I.I.Sc. Crystals were obtained by mixing 10 μ l of the protein (9 mg/ml in 20 mM Tris, pH 6.9, 1 mM EDTA,

Table 6.1: Data collection and refinement statistics of PfAdSS complex

Space group	C222 ₁
Cell parameters	a=91.58 Å
	b=117.12 Å
	c=80.42 Å
R_{free} & R_{cryst} (initial) %	59.2 & 57.0
R_{free} & R_{cryst} (final) %	24.2 & 19.9
Rmsd in bond length (Å)	0.005
Rmsd in bond angle (°)	1.331
Average B values (Å ²) ^b	
Protein atoms (3352)	24.52
Ligands Mg(1);IMO(28);HAD(9);	20.09;18.26;19.49;
GDP(29);Water(283)	30.61; 32.16

^b The number in parenthesis is the number of atoms

10 mM DTT, 5 mM each of IMP, GTP and hadacidin and, 50 mM magnesium acetate) with 2-5 μ l of a solution containing 100 mM sodium cacodylate (pH 6.5) and 20-25 % PEG4000. Plate like crystals appeared in 3 days and grew to a maximum size of 0.3 mm x 0.2 mm x 0.1 mm in a week. Data was collected on a crystal mounted in a cryo loop at 110K on a on a MAR300 image plate detector system mounted on a Rigaku RU-200 rotating anode X-ray generator. The crystal diffracted to resolution better than 2.0 Å and final data were collected to 2.0 Å. The structure was solved by molecular replacement using the structures of *E. coli* and mouse AdSS. Model building and refinement of the protein residues followed by addition of the ligand and water molecules resulted in a final R-value of 20 % (R-free=24 %). The space group was identified as C222₁ with unit cell parameters a=91.6 Å, b=117.1 Å, c=80.4 Å. Final data-statistics are listed in Table 6.1.

6.3.2 Structure of *P. falciparum* AdSS

The asymmetric unit of the crystal is a monomer (Fig. 6.3). The biologically relevant form of the enzyme is a dimer the molecular axis of symmetry coinciding



Figure 6.3: Ribbon representation of the PfAdSS monomer showing sub-domain organization. The central β sheet is represented in red. Sub-domains I to IV are represented in yellow, cyan, brown and green, respectively and secondary structural elements that do not belong to any sub-domain are coloured purple.

with a crystallographic axis along the a axis (Fig. 6.4). In the final map, the electron density is of good quality for most of the protein residues and for the ligands. The first 13 residues at the N terminus and 6 residues at the C terminus are disordered. Around ten residues appeared to possess alternate conformations. A total of 262 water molecules were found in the crystallographic asymmetric unit. The structure has acceptable stereo chemical parameters (Table 1). The program PROCHECK (Laskowski et al., 1993) indicates that more than 91 % of the residues are in the most favoured region of the Ramachandran map. Only Ser331 is in the disallowed region. Ser331 of PfAdSS corresponds to Gly355 and Ser323 in mouse and *E. coli* synthetases, respectively, where these residues lie well within the fully allowed regions of the Ramachandran plot. The unusual conformation of Ser331 in the present structure is stabilised by hydrogen bonding interactions with Lys327, Asn330 and Ile332. The residues, Gln23 and Asn232, which possess generously allowed conformations in *E. coli* (Choe et al., 1999) and mouse synthetases (Inacu

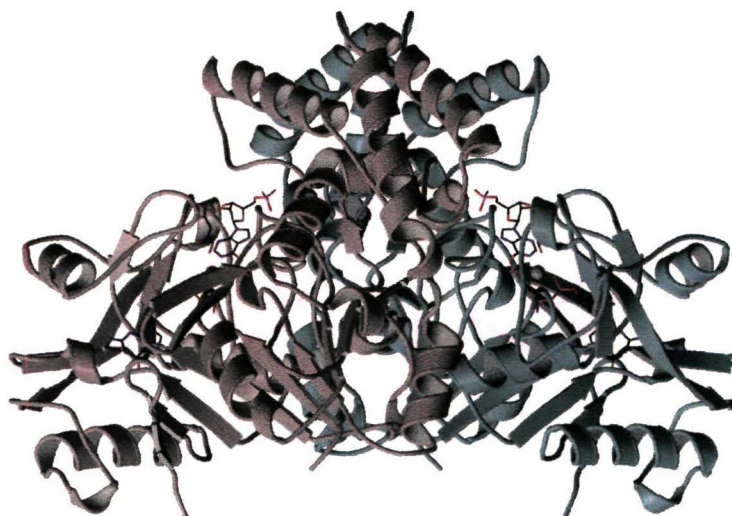


Figure 6.4: Ribbon representation of the PfAdSS dimer. The two sub-units are coloured differently.

et al., 2002a), are in similar conformations in the PfAdSS complex also. The conformation of Gln23 is stabilised by hydrogen bonding interactions with Met235 and Glu27. The positioning of Glu27, which also occurs in the generously allowed region of the Ramachandran map ($\phi = -80^\circ$, $\psi = -16^\circ$), is crucial for the interactions of the polypeptide with the ligands. The active site residue, Asn232, interacts with 6-phosphoryl-IMP. This residue has been reported to be in the fully allowed region in the unligated *E. coli* (PDB code 1ADE)(Poland et al., 1996b) and mouse AdSS (PDB code 1J4B) (Inacu et al., 2001) and undergoes a transition to the generously allowed region upon ligand binding. Mutations at this position in the *E. coli* enzyme reduce catalytic rates by 10-1000 fold without affecting K_m of IMP (Wang et al., 1997b). Asn232 presumably plays a catalytic role by facilitating the nucleophilic attack of O6 of IMP on the γ -phosphate of GTP. The distorted main chain conformation of this residue may be essential to orient its side chain for ideal catalysis.

The secondary structure and the polypeptide fold of PfAdSS are similar to those of AdSS from other organisms (Fig. 6.5). The insertions and deletions in *P. falciparum* synthetase occur mainly in the loop regions and lead only to local conformational changes. Superposition of the C_α atoms of PfAdSS complex against



Figure 6.5: Superposition of PfAdSS (purple) with mouse (left) and *E.coli* (right) AdSS.

the structurally equivalent 407 and 398 C_{α} atoms of *E. coli* and mouse AdSS complexes (Fig. 6.5), respectively, yields RMSD values of 1.10 Å and 1.01 Å. The RMSD for the superposition of the liganded PfAdSS complex with the unliganded *E. coli* AdSS is slightly larger (1.84 Å). Each subunit consists of 19 strands (β 1- β 19), 12 α -helices and seven 3_{10} helices. Starting from the N-terminus, helices are numbered from α 1 through α 19. Nine parallel β -strands (β 9, β 7, β 5, β 2, β 10, β 1, β 11, β 15 and β 18) along with a tenth anti-parallel strand (β 19) form a central sheet. The sheet is bordered by four sub-domains (Figure 4). The small sub-domain I (Residues 54-65) comprises of only two β -strands (β 3 and β 4) and has the appearance of a finger-like extension of the segment between β 2 and β 5 of the central β -sheet. Sub-domain II (Residues 114-206) forms bulk of the inter-subunit interface. The majority of the residues for the ligand binding pocket are contributed by sub-domains III (Residues 278-302) and IV (Residues 339-418). There are four helices (α 1- α 4) which do not belong to any domain and line the central β sheet. Besides sub-domain II, helices α 11- α 13 also form part of the inter-subunit interface.

6.3.3 Dimer interface

The RMSD values for the superposition of the structurally equivalent C_{α} atoms of PfAdSS complex against the unligated and fully ligated mouse and *E. coli* synthetases are 2Å and 1Å, respectively. Only sub-domain I and III have a

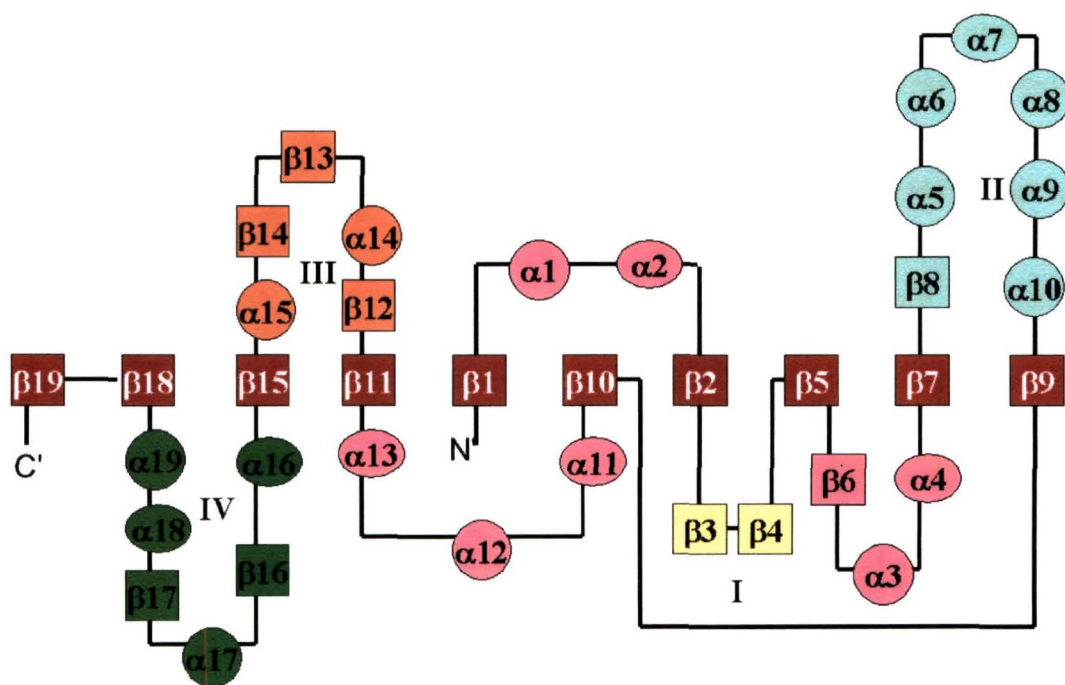


Figure 6.6: Topology diagram of PfAdSS. Squares represent β strands, circles α helices and ellipses 3_{10} helices. The sub-domains are numbered and colour coding is as in Fig. 6.3.

rigid structure while sub-domain II and IV are variable. Sub-domain II, which comprises secondary structures $\beta 8$ and $\alpha 5$ - $\alpha 9$ and contributes to the interface, differs significantly in its orientation from the other two AdSS complexes. The average B-factor of this domain is not significantly different from that of the entire protein and hence, the observed changes in this domain are unlikely to be due to disorder. Part of sub-domain IV consisting of residues 355-379 contributing to the dimer interface also shows marked differences in orientation. Thus most of the segments with significant structural differences from the other two complexes belong to the dimer interface. Therefore, the dimer formation and stability in PfAdSS is likely to be substantially different from the other two synthetases.

As in the other homologs, the dimer interface is extensive with contribution from many segments of the polypeptide chain. There is extensive complementarity in the surface features of the two monomers at the interface. The surface accessible area buried on dimerization is 4823 \AA^2 . Stretches of residues that largely contribute to the interface are 149-159, 243-270 and 325-333. Both hydrophobic and hydrophilic

interactions are involved in the association of monomers (Fig 6.7). The interface does not have a single hydrophobic surface, but instead consists of several small hydrophobic patches. 21 water molecules that occur in the interface also contribute to the stability of the PfAdSS dimer. Large number of water molecules are seen in *E. coli* and mouse AdSS complexes also (Choe et al., 1999, Inacu et al., 2002a). There are four salt-bridges across the interface (cut-off value of 4 Å) including the one between Lys152 and Asp239 which is conserved in all the known AdSS structures. In contrast, the *E. coli* AdSS complex has 16 salt bridges while mouse AdSS complex has 4 connecting the two subunits of the dimer (Inacu et al., 2001). The PfAdSS interface is stabilised by 18 direct hydrogen bonds (cut-off value of 3.5 Å), which includes some short strong hydrogen bonds (between NZ of Lys112 and OH of Tyr325 (2.52 Å) and between O of Gly157 and OH of Tyr243 (2.55 Å)). The contribution of hydrogen bonding to the stabilisation of the dimer is less in PfAdSS when compared to the other two synthetases. Substrate binding also contributes to dimer stability, with Arg155 making direct as well as water-mediated hydrogen bonding interactions with the 5'-phosphate of IMP from the symmetry related monomer.

The most striking feature of the interface in the PfAdSS structure is the preponderance of positively charged residues (Fig. 6.7), 22 positive residues (Lys, Arg and His) against 6 negatively charged residues (Asp and Glu)). Two regions that are prominent involve Lys130 and Lys131 and a cluster involving His263, His264 and Lys265. In contrast, a more balanced set of charged residues occur at the interface of *E. coli* and mouse AdSS. In spite of the clustering of positive charges at the interface, the PfAdSS dimer is stable. Gel filtration studies on the *P. falciparum* enzyme in increasing concentrations of phosphate show the appearance of a minor monomer peak only at high concentrations of phosphate (200 mM) (Fig. 4.7).

Although three cysteine residues (Cys250, Cys328 and Cys368) occur at the interface of PfAdSS, the subunits are not covalently linked by disulfide bonds. Cys250 gets partially buried upon dimerization. In contrast, Cys328 and Cys368 appear to be more completely buried on dimerization. The solvent accessibility of C328 and C368 reduce from 72.3% and 42.8% to 15.4% and 13.3% on dimerization.

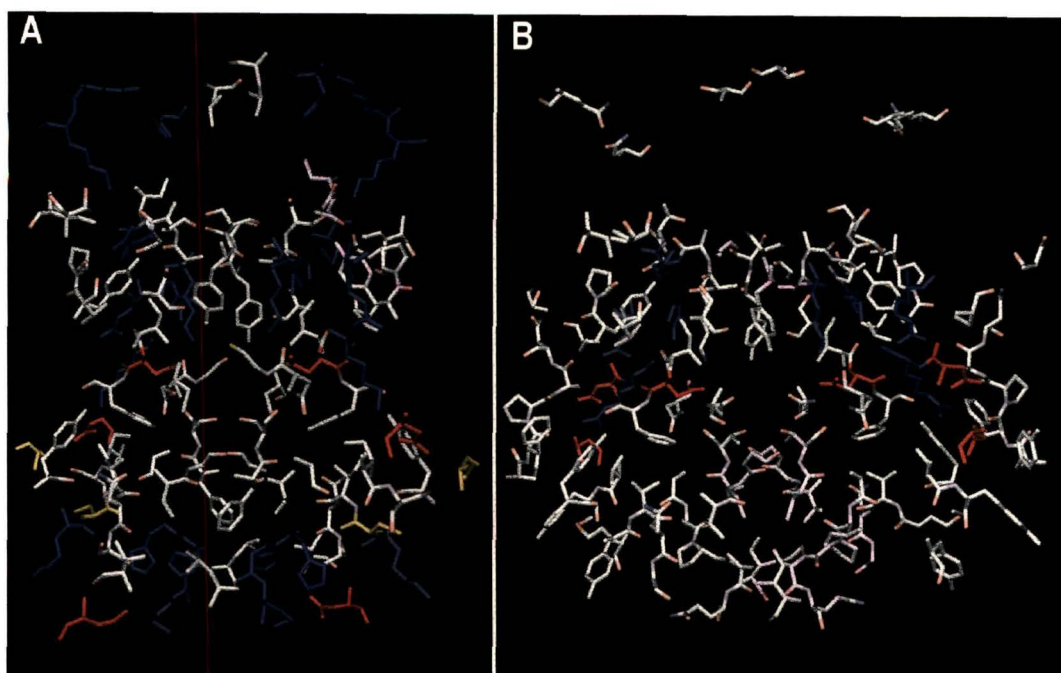


Figure 6.7: Residues at the subunit interface of *P. falciparum* (A) and mouse (B) AdSS. Residues are coloured according to charge. Blue, red and grey represent positive, negative and uncharged residues respectively. Water molecules at the interface are not shown.

These two residues appear to be chemically modified in PfAdSS, although the precise nature of modification cannot be deduced from the electron density map (Fig. 6.8). As discussed in Chapter 5, mutation of these cysteines to Ser disrupts the dimer. Crystals of AdSS, when dissolved, show measurable activity despite the cysteines being modified (Fig. 6.9). These observations suggest that these cysteine residues, either in their oxidised form or ionized to a cysteine thiolate, contribute to dimer stability. Fig. 6.10 shows the environment around C328 at the interface. As can be seen, the residues surrounding this cysteine are predominantly positively charged. Though the contacts of these basic residues are at large distances, these may be relevant as the extra electron density around the cysteine thiol has not been modelled. These basic residues could lower the pK_a of the cysteine considerably and lead to its ionization at physiological pH. This interaction is reminiscent of the enzymes where a cysteine thiolate has a role in catalysis and is maintained in the ionized form due to the presence of a His residue in close proximity (Plou et al., 1996).

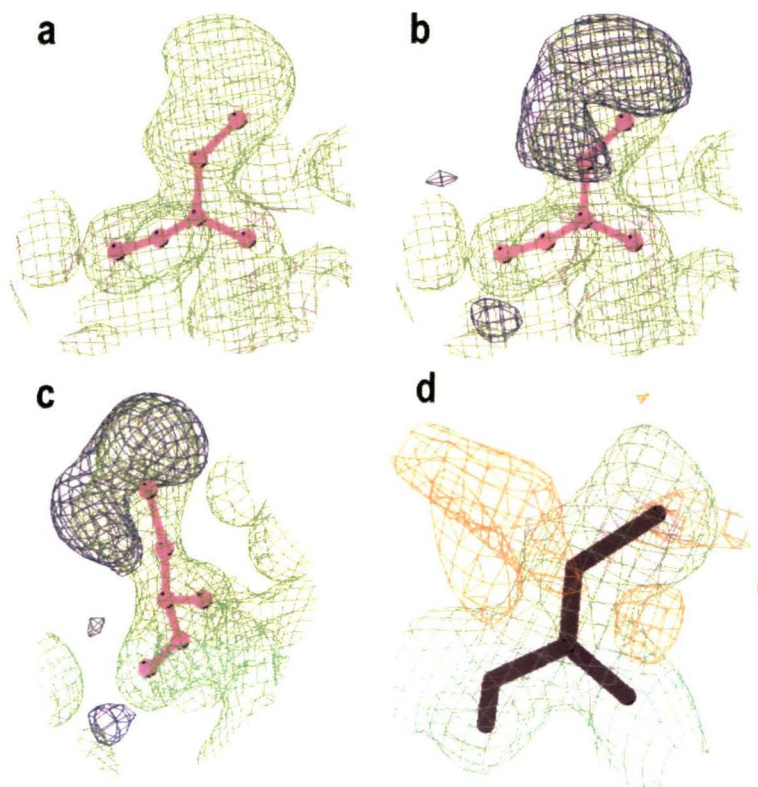


Figure 6.8: Electron density around C328 (a-c) and C368 (c) in PfAdSS. The continuous density represents the $2F_o-F_c$ map contoured a 1.0σ and the broken density F_o-F_c map contoured at 2.5σ

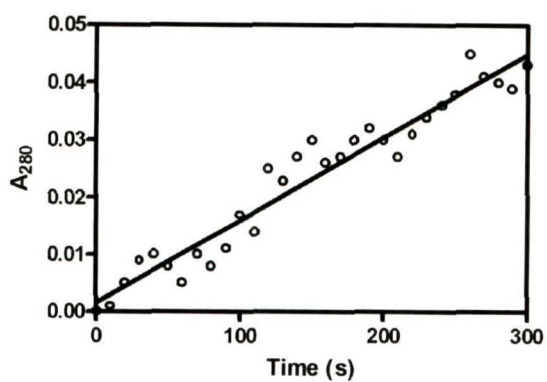


Figure 6.9: Activity of dissolved crystals of PfAdSS. The increase in absorption at 290 nm due to formation of adenylosuccinate was monitored. The reaction was performed in the presence of the substrates and inhibitors carried over with the crystal.

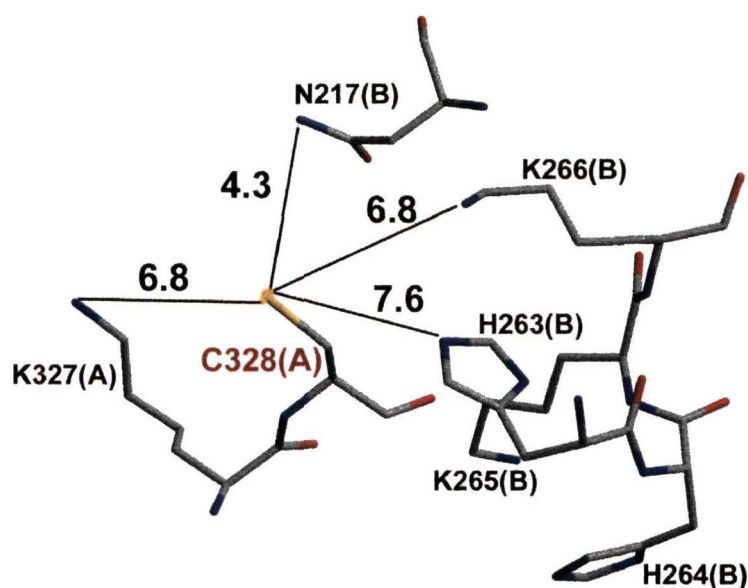


Figure 6.10: C328 environment in the PfAdSS crystal structure. The numbers indicate distances in Å. The subunits contributing the residues are indicated within parenthesis. Contacts as high as 7 Å are marked as the extra electron density on the cysteine thiol have not been modelled.

Though the cellular environment is reducing, oxidised cysteines have been implicated both in catalysis and in regulation of protein function (Claiborne et al., 1999)). Whether such a process is indeed operative in *P. falciparum* or our observation of oxidised cysteines in PfAdSS is an artefact of the enzyme preparation needs investigation. The positively charged environment of the interface may also alter the pK_a of the cysteines favouring ionization to a thiolate. Our mutagenesis studies do suggest that a charge at C328 is necessary for maintenance of dimer integrity (5.4.3).

6.3.4 Active site pocket

6-phosphoryl-IMP binding

The orientation and geometry of the 6-phosphoryl IMP in the PfAdSS complex comply with the allowed conformations for nucleotides. The ribose is in C2'-*endo* envelope (2E) form with a pseudo rotation angle of 162° . The orientation of O5' about the exocyclic C4'-C5' bond is (*gauche*, *gauche*) with a γ value of

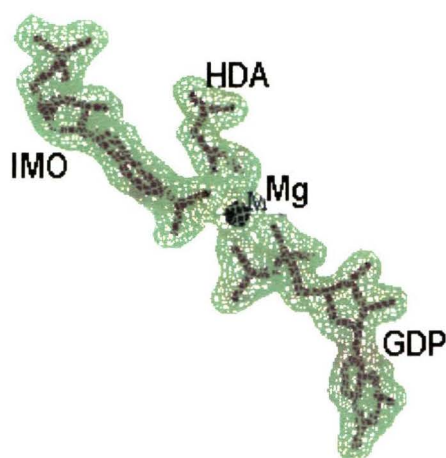


Figure 6.11: $2F_o - F_c$ map corresponding to the bound ligands in PfAdSS, contoured at 1.0σ

43° . The base is oriented with a torsion angle of $\chi = -141^\circ$ with respect to the sugar, representing *anti* conformation. Contacts through 5'-phosphoryl group of IMP contribute principally to the binding of IMP to the protein. These include contacts with Thr141, Asn51 and Thr247 from the same subunit and, Arg155 of the symmetry related subunit (Fig. 6.12). The cross subunit interaction through Arg143 in *E. coli* AdSS (Arg155 in PfAdSS) is important for the formation of dimers (Kang et al., 1998). Interestingly, three water molecules that are hydrogen bonded to the oxygen atoms of the 5'-phosphoryl group are conserved in *E. coli* and mouse synthetases and hence, are presumably important for IMP binding.

The electron density map clearly shows that the first step of the catalytic reaction, which results in the formation of 6-phosphoryl IMP with the concomitant conversion of GTP to GDP, has occurred (Fig. 6.11). This intermediate is stabilised by various direct and water mediated interactions with the protein (Fig. 6.12). The 6-phosphoryl group interacts with the residues Asp26, Lys29, Gly53, His54 and Asn232. Asp26 is believed to participate in the abstraction of a proton from the N-1 atom of IMP, facilitating the formation of the 6-oxyanion of the nucleotide. This aids the transfer of the γ -phosphate of GTP to IMP. Once protonated and coordinated to Mg^{2+} , this aspartate is believed to act as a catalytic acid creating a cationic center on C-6 of IMP, facilitating the next step of the reaction (Choe et al., 1999).

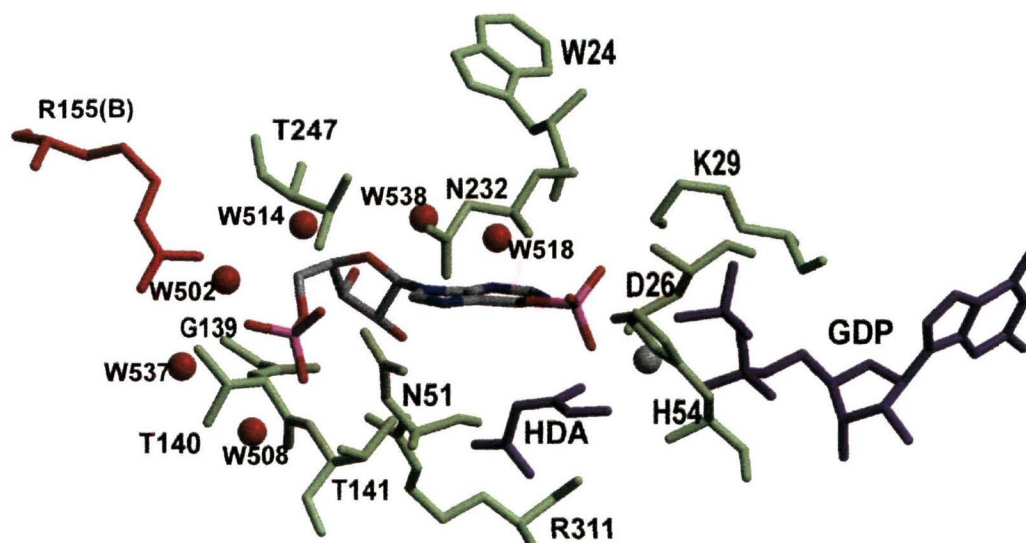


Figure 6.12: Contacts made by phosphoryl-IMP in PfAdSS. Residues within 3.5 Å of this ligand are shown. R155 from the other subunit is shown in red, ligands other than phosphoryl-IMP(cpk) are shown in violet and the residues from the same subunit in green. Water molecules (W) =labelled in smaller font are shown as red balls.

In the present structure, OD1 of Asp26 is hydrogen bonded to N1 atom of IMP (2.96 Å). An interesting feature at the active site is the occurrence of a short, strong hydrogen bond between NE2 of His54 and O2 of 6-phosphoryl IMP (2.54 Å). This hydrogen bond is present in the mouse synthetase complex also (2.46 Å). Cleland and Kreevoy (1994) have suggested that such short hydrogen bonds, termed 'Low Barrier Hydrogen Bonds (LBHB)', are key interactions that stabilise the transition state of enzymatic reactions and reduce the energy barrier for proton transfer. This is in agreement with the proposed role of His54 as a catalytic acid in the second step of the reaction, the nucleophilic displacement of the 6-phosphoryl group by aspartate. His54 is purported to play a role in the protonation of the leaving group, phosphate, in the second step (Choe et al., 1999). Interactions of His54 with the GDP-β-phosphoryl group are similar to those observed in the other AdSS structures. The interactions between Asn232 and IMP are also similar to those in the *E. coli* and mouse AdSS complexes.

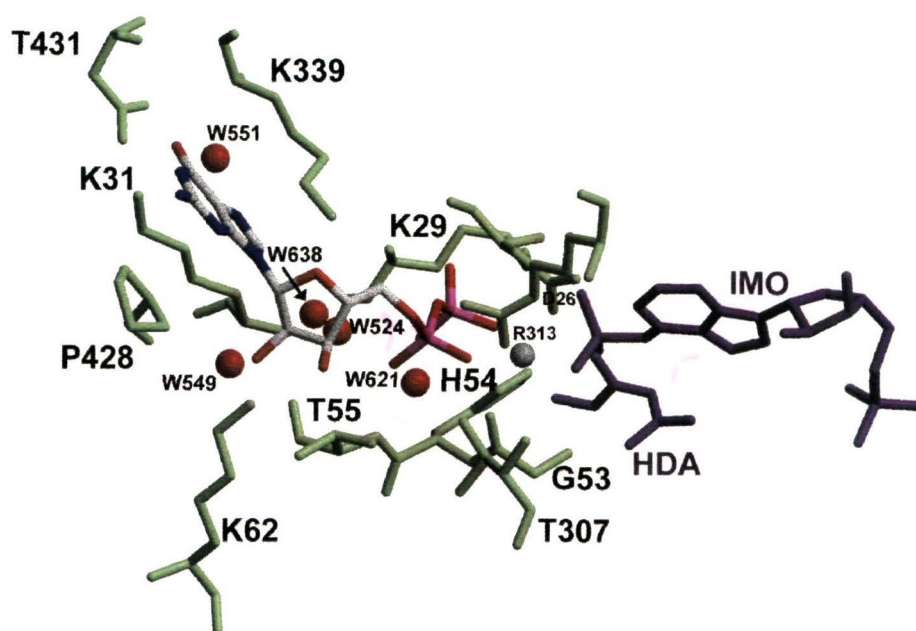


Figure 6.13: GDP contacts in PfAdSS. GDP is represented in cpk, the other ligands in violet and the protein residues in green. Water molecules (W) shown as red balls are labelled in smaller font.

GDP binding

As anticipated from the presence of 6-phosphoryl IMP, the final $2F_o-F_c$ map reveals densities only for GDP (Fig. 6.11). Density corresponding to the γ -phosphate of GTP is absent. This is consistent with the observation that the first step of catalysis is phosphoryl transfer from GTP to IMP. The sugar ring in GDP is in C2'-*endo* form with its O5' in the (*trans*, *gauche*) conformation. The pseudo rotation angle of the ribose moiety is 156° . The χ -value of -94° reflects the high-anti orientation of the base with respect to the sugar.

Fig. 6.13 shows the interactions of GDP with the protein residues. Though the active site of PfAdSS is largely identical to the *E. coli* and mouse synthetases, significant variation is seen in the interactions of GDP with the polypeptide. One of the differences is at residue 425 which is Gly in PfAdSS and Ser (residue 414) in *E. coli* AdSS. Ser414 in *E. coli* AdSS is believed to be responsible for the recognition of the 6-oxo group of the guanine base through the interaction of the side-chain hydroxyl with the nucleotide (Poland et al., 1996a). The cavity created by

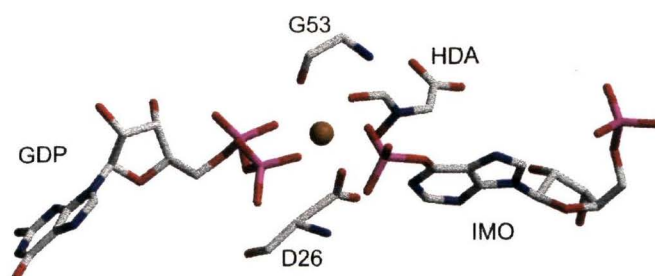


Figure 6.14: Mg^{2+} co-ordination in PfAdSS.

the Ser to Gly substitution in PfAdSS is occupied by a water molecule (551 O). This molecule, hydrogen bonding to both N7 and O6 of GDP, mimics OG of Ser414 of *E. coli* AdSS. In mouse AdSS also, this residue is a Gly, although a water molecule has not been reported. The PfAdSS complex has additional hydrogen bonds not observed in the other two AdSS complexes. The amino group of Lys31, a conserved residue, is shifted towards the guanine base and is hydrogen bonded to O6. OG of Thr307 (Val in mouse AdSS and Ala in *E. coli* AdSS) forms a hydrogen bond with O2A of GDP. However, this substitution does not lead to significant conformational changes in the vicinity of residue 307. Similarly, Lys62 forms hydrogen bonds in PfAdSS complex with the ribose hydroxyls of GDP, an interaction that is absent in the other AdSS. Additionally, Lys29 is involved in many contacts with GDP, including a LBHB between the backbone N and O3B of GDP. The sidechain amino group of this residue is hydrogen bonded to both O2B and O3B of GDP. These interactions probably stabilise the negative charge developed on the β -phosphoryl group on removal of the γ -phosphoryl group.

Mg^{2+} and hadacidin binding pockets:

Mg^{2+} is octahedrally coordinated to OD1 of Asp26, O of HDA, O2A of GDP, O2B of GDP, O of Gly53 and O1 of IMO (Fig. 6.14). The identities and conformations of the residues coordinated to the metal ion in the PfAdSS complex are identical to those in the *E. coli* and mouse synthetase complexes.

The nitrogen atom of hadacidin has a planar geometry. The conformation of the molecule is stabilised by various hydrogen bonding interactions with the protein

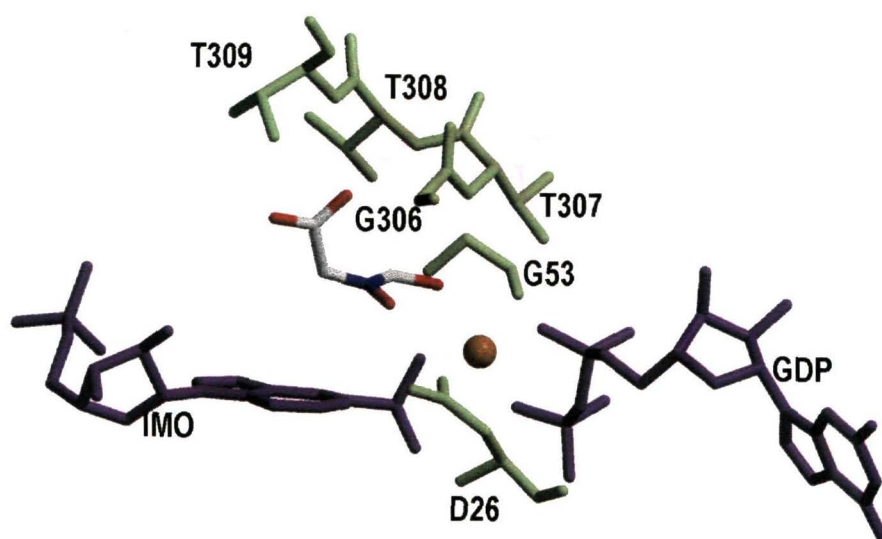


Figure 6.15: Hadacidin binding in PfAdSS. Hadacidin is represented in cpk, the other ligands in blue and the protein residues in green. Contacts illustrated are with residues within 3.5 Å of hadacidin.

residues (Fig. 6.15). The major contributions are from Asp26, Thr307, Thr308, Thr309, Arg311 and Arg313. Residues 307-308 form part of the Asp loop, which in the mouse and *E. coli* enzymes, gets ordered in response to aspartate binding (Hou et al., 2002, Inacu et al, 2002a). OG of Thr307 is hydrogen bonded to O of hadacidin. This interaction is absent in both the mouse and *E. coli* complexes, where Thr307 is replaced by Val and Ala, respectively. Presumably this hydrogen bond will also hold L-aspartate in PfAdSS. In spite of this additional hydrogen bonding, the K_m for L-aspartate is higher in PfAdSS than in AdSS from other sources. Examination of the structure of PfAdSS complex does not suggest structural reasons for the higher K_m of the enzyme for aspartate. This may result from the slow formation of 6-phosphoryl IMP suggested by the lower k_{cat} value of PfAdSS when compared to other synthetases.

6.3.5 Conformation of dynamic loops: Implication for an ordered mechanism

Large regions in the *E. coli* and mouse synthetases get ordered on substrate binding (Fig. 6.16). Since, efforts to crystallise unligated PfAdSS have so far been

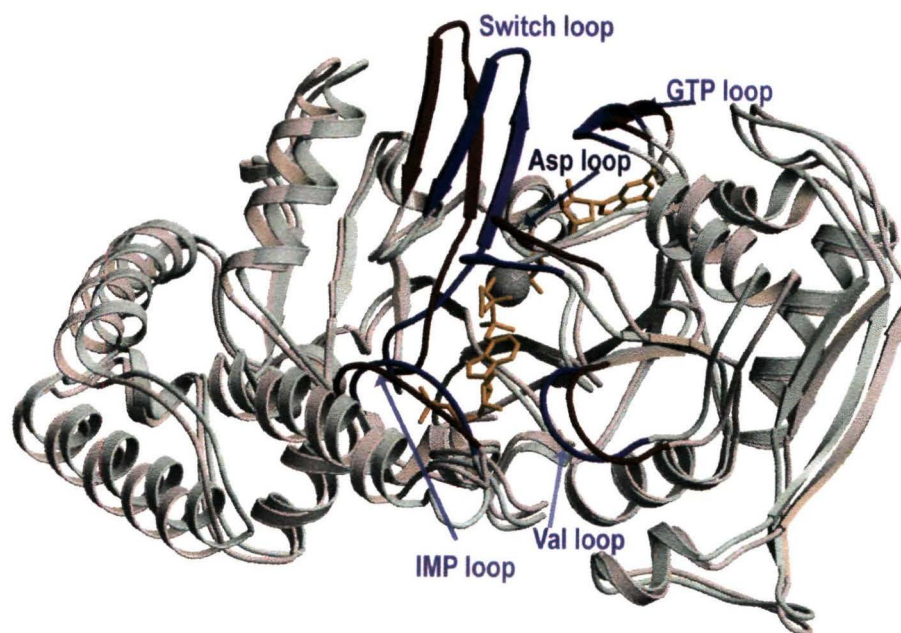


Figure 6.16: Superposition of the fully ligated and unligated mouse AdSS. The shades of red/pink represent the unligated structure and the shades of blue the ligated structure(1LON). The loops that undergo conformational changes on ligand binding are highlighted in darker shades.

Table 6.2: Dynamic loops in AdSS

Loops	<i>P. falciparum</i>	Mouse	<i>E. coli</i>
Pre-switch loop	48-52	65-69	33-37
Switch loop	53-66	70-83	40-53
IMP loop	138-146	160-168	126-134
Val loop	280-286	304-410	270-278
Asp loop	306-312	330-336	298-304
GTP loop	428-433	448-452	417-412

unsuccessful suggesting conformational heterogeneity in the absence of active site ligands, it is likely that similar structural changes occur in the *P. falciparum* enzyme also. In the following discussion on the dynamic loops in the synthetases, we follow the nomenclature proposed by Iancu et al.(2002a) for these loops (Table 6.2, Fig. 6.16). Extensive studies by the groups of Fromm and Honzatko have shown that almost all conformational changes are brought about by IMP binding, perhaps aided by anions in the GTP phosphate binding pocket (Hou et al., 2002, Inacu et al., 2002a). In the plant enzymes, the complex with guanine nucleotides alone has a conformation similar to the IMP ligated structures (Prade et al., 2000). In contrast, guanine nucleotides alone cannot organise the active site in the case of the mouse and *E. coli* complexes, though GTP binding occurs in the absence of IMP (Poland et al., 1996b, Inacu et al., 2002a).

In the present structure, all the loops are in their fully ligated conformations. The most pronounced conformational change between the unligated and ligated mouse and *E. coli* enzymes is in the Switch loop (Residues 53-66). This loop undergoes a displacement of around 9 Å on ligand binding in the *E. coli* and mouse enzymes (Poland et al., 1996a, Inacu et al., 2002a). However, an overlap of this loop of PfAdSS complex against that of *E. coli* and mouse synthetases in their fully ligated conformations (1CG0 and 1LON; Fig. 6.5) results in an RMSD of 0.99Å and 1.53Å, respectively, implying an overall similarity of the switch loop in all the three AdSS. The orientations of the two catalytic residues, Asn51 and His54 that form part of this loop are not different between the three structures. However, differences exist between the structures at the closed-end of this loop (Ser57-Lys62). Superimposition of the fully ligated PfAdSS complex with similar complexes of mouse and *E. coli* shows that this loop is positioned further towards GDP in PfAdSS (Fig. 6.17). This inward movement is restricted to the closed end of the loop. As a consequence, residues at the closed end make hydrogen bonding interactions that are not seen in the other AdSS structures. The most prominent of these is the H-bonding between NZ of Lys62 and the ribose hydroxyls of GDP. The corresponding residues in mouse and *E. coli*, Glu79 and Lys49, respectively, do not come within H-bonding distance of GDP. This conformation of the Switch loop seems to be enforced by H-


```
P.fal 100 GGKL LD----RLYL110  
Mouse  EKKG LKDWEKRLII  
E.coli  EDRG IP-VREERLLL
```

Figure 6.18: Sequence alignment showing 4 residue deletion in PfAdSS

Interestingly, in structures of *Arabidopsis thaliana* and *Triticum aestivum* AdSS in complex with GDP, Thr in the Switch loop (corresponding to Lys62 of PfAdSS) interacts with the ribose hydroxyls. In the plant enzymes, incubation with GTP is required for obtaining stable activity and GDP alone is sufficient for organising the active site (Prade et al., 2000).

GDP in the PfAdSS structure also H-bonds with Thr307, the corresponding residues in mouse and *E. coli* being Val331 and Ala299. This Thr is in the aspartate loop (Inacu et al., 2001) that gets ordered in response to aspartate in the other AdSS (Hou et al., 2002). Perhaps in PfAdSS, GTP binding brings about this loop movement. Hadacidin in the structure interacts with Thr307 and also co-ordinates Mg^{2+} . Since Mg^{2+} binding to the enzyme is thought to follow GTP binding, these two factors, together, could lead to the ordering of aspartate binding.

6.4 Conclusion

The structure of the fully ligated PfAdSS reported here is largely identical to the fully ligated structures reported for the mouse and *E. coli* enzymes. The differences observed in the kinetic behaviour of PfAdSS can be attributed to small structural variations seen in the GTP binding pocket. Residues in the Switch loop, which respond to IMP binding, have additional hydrogen bonding interactions with the ribose hydroxyls of GDP and also, with residues in the GTP loop. GDP also makes additional hydrogen bonds with Thr307 in the aspartate loop. These interactions may account for the ordered binding of substrates that is observed in PfAdSS. However, in the absence of unligated and partially ligated structures of PfAdSS, these inferences drawn from the available *E. coli* and mouse structures remain conjectural. The kinetic and structural data highlight the difficulty in extrapolating from structure to mechanism with subtle structural differences having significant

mechanistic implications.

As only the salvage pathway is operative in *P. falciparum*, AdSS represents an important drug target. It is interesting to note that allopurinol ribonucleoside phosphate (ARP) is a substrate for *L. donovonii* AdSS (LdAdSS) and only a weak inhibitor of the mammalian basic isozyme (Spector et al., 1984). Succinylation of ARP by LdAdSS and subsequent incorporation into the parasite's nucleotide pool is responsible for the selective toxicity of this IMP analogue to the parasite. The structure of *P. falciparum* AdSS reported here opens up the possibility of exploiting differences in protein-ligand interactions between the parasite and host enzyme for species-specific inhibitor design.

Appendix A

Column calibration and mass spectrometry

Calibration curves for gel filtration columns used in study

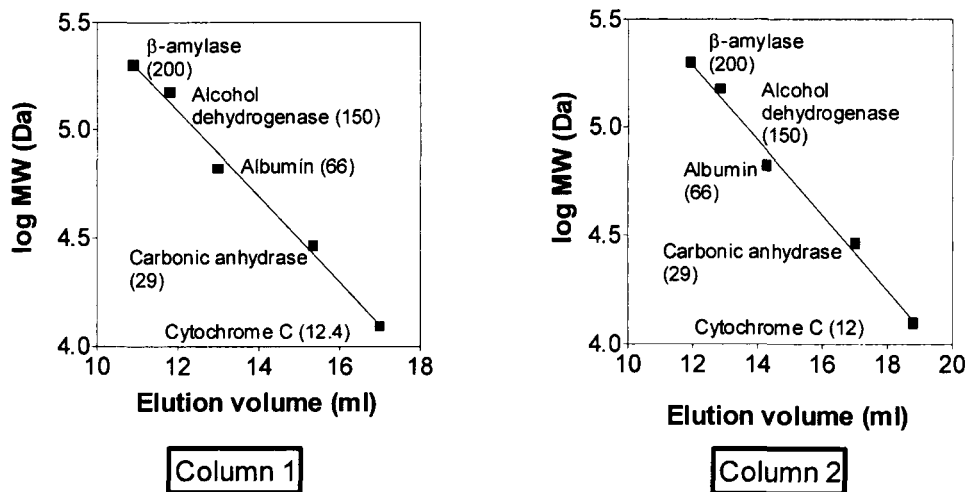


Figure A.1: Calibration curves for a) column 1 and Column 2 used in studies gel filtration analysis in chapters 3,4 and 5. Column runs were performed in 20 mM Tris HCl, pH 7.0, 100 mM KCl.

Mass spectral analysis of wildtype PfAdss

Wildtype PfAdSS was subjected to partial digestion by trypsin, the peptides obtained separated by reverse phase HPLC and their masses determined by electrospray ionization mass spectrometry. Fig. 3 shows the HPLC trace of the tryptic digest of AdSS. The mass profile of the section indicated by the arrow shows the

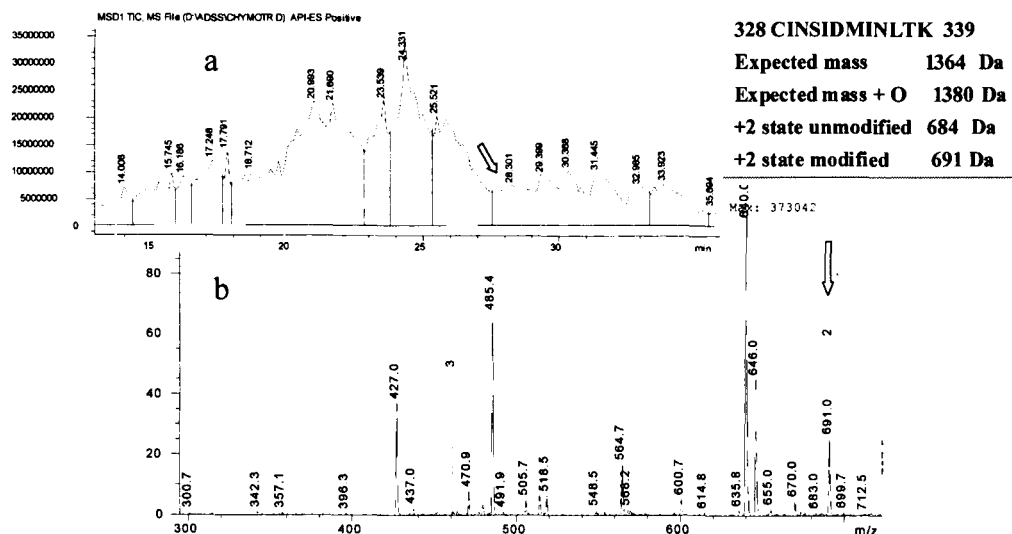


Figure A.2: LC-MS analysis of tryptic digests of wildtype PfAdSS. a) HPLC profile of the tryptic digest. b) m/z profile of the region marked by the arrow in the HPLC trace. Solid arrow shows the peak corresponding to an m/z value of 691. Top right inset shows the expected masses of the tryptic fragment containing C328

presence of a peptide with an m/z ratio of 691, which could correspond to a peptide containing C328 if it were to be modified to a cysteine sulphenic acid. The expected masses of this peptide with and without an additional oxygen are shown as an inset to Fig. 2. It is indeed surprising that such a species representing a cysteine sulphenic acid is detected on mass spectrometry as sulphenic acids are highly unstable. They are readily oxidized to higher states or readily reduced in the presence of reducing agents like DTT to the free thiol. In fact, detection of these species which are quite often transient requires trapping as derivatives of molecules such as diamedione followed by mass spectrometry.

References

1. Allen TE & Ullman B. (1994) Molecular characterization and overexpression of the hypoxanthine-guanine phosphoribosyltransferase gene from *Trypanosoma cruzi*. *Mol Biochem Parasitol.* 65:233-45.
2. Allen TE, Hwang HY, Jardim A, Olafson R & Ullman B. (1995) Cloning and expression of the hypoxanthine-guanine phosphoribosyltransferase from *Leishmania donovani*. *Mol Biochem Parasitol.* 73:133-43.
3. Amaki Y, Nakano H & Yamane T (1994). Role of cysteine residues in esterase from *Bacillus stearothermophilus* and increasing its thermostability by the replacement of cysteines. *Appl Microbiol Biotechnol.* 40:664-8.
4. Amann, E., Ochs, B. & Abel, K-J. (1988) Tightly regulated *tac* promoter vectors useful for expression of unfused and fused proteins in *Escherichia coli*. *Gene.* 69, 301-315.
5. Arnold FH, Volkov AA. (1999) Directed evolution of biocatalysts. *Curr Opin Chem Biol.* 3:54-9. Review
6. Aronov AM, Munagala NR, Kuntz ID & Wang CC. (2001) Virtual screening of combinatorial libraries across a gene family: in search of inhibitors of *Giardia lamblia* guanine phosphoribosyltransferase *Antimicrob Agents Chemother.* 45:2571-6.
7. Aronov AM, Munagala NR, Ortiz De Montellano PR, Kuntz ID & Wang CC. (2000) Rational design of selective submicromolar inhibitors of *Tritrichomonas foetus* hypoxanthine-guanine-xanthine phosphoribosyltransferase. *Biochemistry.* 39:4684-91.
8. Aslund F, Zheng M, Beckwith J & Storz G. (1999) Regulation of the OxyR transcription factor by hydrogen peroxide and the cellular thiol-disulfide status. *Proc Natl Acad Sci U S A.* 96:6161-5.
9. Bahl A, Brunk B, Coppel RL, Crabtree J, Diskin SJ, Fraunholz MJ, Grant GR, Gupta D, Huestis RL, Kissinger JC, Labo P, Li L, McWeeney SK, Milgram AJ, Roos DS, Schug J & Stoeckert CJ Jr. (2002) PlasmoDB: the Plasmodium genome resource. An integrated database providing tools for accessing, analyzing and mapping expression and sequence data (both finished and unfinished). *Nucleic Acids Res.* 30:87-90.
10. Banerjee, R., Liu, J., Beatty, W., Pelosof, L., Klemba, M. & Goldberg, D. E. (2002) Four plasmepsins are active in the *Plasmodium falciparum* food vacuole, including a protease with an active-site histidine. *Proc Natl Acad Sci U S A.* 99:990-5.
11. Bannister L & Mitchell G. (2003) The ins, outs and roundabouts of malaria. *Trends Parasitol.* 19:209-13.
12. Basco, L. K. Marquet, F., Makler, M. M. & Le Bras, J. (1995) *Plasmodium falciparum* and *Plasmodium vivax*: lactate dehydrogenase activity and its application for in vitro drug susceptibility assay. *Exp. Parasitol.*, 80, 260-271.

References

13. Bashor C, Denu JM, Brennan RG & Ullman B. (2002) Kinetic mechanism of adenine phosphoribosyltransferase from *Leishmania donovani*. *Biochemistry*.41:4020-31.
14. Bass MB, Fromm HJ & Rudolph FB. (1984) The mechanism of the adenylosuccinate synthetase reaction as studied by positional isotope exchange. *J Biol Chem*. 259: 12330-3.
15. Bass MB, Fromm HJ & Stayton MM. (1987) Overproduction, purification, and characterization of adenylosuccinate synthetase from *Escherichia coli*.*Arch Biochem Biophys*. 256 :335-42.
16. Beck JT & Wang CC. (1993) The hypoxanthine-guanine-xanthine phosphoribosyltransferase from *Tritrichomonas foetus* has unique properties. *Mol Biochem Parasitol*.60:187-94.
17. Bera AK, Smith JL & Zalkin H. (2000) Dual role for the glutamine phosphoribosylpyrophosphate amidotransferase ammonia channel. Interdomain signaling and intermediate channeling. *J Biol Chem*. 275:7975-9.
18. Berman PA, Human L & Freese JA. (1991) Xanthine oxidase inhibits growth of *Plasmodium falciparum* in human erythrocytes in vitro. *J Clin Invest*. 88:1848-55.
19. Bevis BJ & Glick BS. (2002) Rapidly maturing variants of the *Discosoma* red fluorescent protein (DsRed). *Nat Biotechnol*. 20: 83-7.
20. Borza T, Iancu CV, Pike E, Honzatko RB & Fromm HJ. (2003) Variations in the response of mouse isozymes of adenylosuccinate synthetase to inhibitors of physiological relevance. *J Biol Chem*. 278:6673-9.
21. Bouyoub A, Barbier G, Forterre P & Labedan B. (1996) The adenylosuccinate synthetase from the hyperthermophilic archaeon *Pyrococcus* species displays unusual structural features. *J Mol Biol*. 261:144-54.
22. Bozdech Z, Llinás M, Pulliam BL, Wong ED, Zhu J, et al. (2003) The transcriptome of the intraerythrocytic developmental cycle of *Plasmodium falciparum*. *PLoS Biology* 1: e5.
23. Bridger WA & Cohen LH. (1963) The mechanism of inhibition of adenylosuccinate lyase by 6-mercaptopurine nucleotide (thioinosinate). *Biochim Biophys Acta*. 73:514-6.
24. Canyuk B, Focia PJ & Eakin AE. (2001) The role for an invariant aspartic acid in hypoxanthine phosphoribosyltransferases is examined using saturation mutagenesis, functional analysis, and X-ray crystallography. *Biochemistry*. 40:2754-65.
25. Canyuk B, Medrano FJ, Wenck MA, Focia PJ, Eakin AE & Craig SP. (2004) Interactions at the Dimer Interface Influence the Relative Efficiencies for Purine Nucleotide Synthesis and Pyrophosphorolysis in a Phosphoribosyltransferase. *J Mol Biol*. 335:905-921.
26. Cashel, M., Gentry, D.R., Hernandez, J.V. & Vinella, D. (1987) The stringent response. in *Escherichia coli* and *Salmonella*: Cellular and Molecular Biology

- (Neidhardt, C.F. ed.), American Society for Microbiology, Washington, D.C. Vol. 1, pp 1496-1458.
27. Cecconi I, Moroni M, Vilardo PG, Dal Monte M, Borella P, Rastelli G, Costantino L, Garland D, Carper D, Petrash JM, Del Corso A & Mura U. (1998) Oxidative modification of aldose reductase induced by copper ion. Factors and conditions affecting the process. *Biochemistry*. 37:14167-74.
 28. Cecconi I, Scaloni A, Rastelli G, Moroni M, Vilardo PG, Costantino L, Cappiello M, Garland D, Carper D, Petrash JM, Del Corso A & Mura U. (2002) Oxidative modification of aldose reductase induced by copper ion. Definition of the metal-protein interaction mechanism. *J Biol Chem*. 277:42017-27.
 29. Chatterji D & Ojha AK. (2001) Revisiting the stringent response, ppGpp and starvation signaling. *Curr Opin Microbiol*. 4:160-5.
 30. Chen C & Zheng X. (1992) Development of the new antimalarial drug pyronaridine: a review. *Biomed Environ Sci*. 5:149-60.
 31. Chen Q, Schlichtherle M & Wahlgren M. (2000) Molecular aspects of severe malaria. *Clin Microbiol Rev*. 13:439-50.
 32. Chirumamilla RR, Muralidhar R, Marchant R & Nigam P. (2001) Improving the quality of industrially important enzymes by directed evolution. *Mol Cell Biochem*. 224:159-68.
 33. Choe JY, Poland BW, Fromm HJ & Honzatko RB. (1999) Mechanistic implications from crystalline complexes of wild-type and mutant adenylosuccinate synthetases from *Escherichia coli*. *Biochemistry*. 38: 6953-61.
 34. Claiborne A, Mallett TC, Yeh JI, Luba J & Parsonage D. (2001) Structural, redox, and mechanistic parameters for cysteine-sulfenic acid function in catalysis and regulation. *Adv Protein Chem*.58:215-76.
 35. Claiborne, A., Yeh, J.I., Mallett, C., Luba, J., Crane. E.J., Charrier, V. & Parsonage, D. (1999) Protein-sulphenic acids: Diverse roles of an unlikely player in enzyme catalysis and redox regulation. *Biochemistry* 47, 15407-15416
 36. Clantin B, Tricot C, Lonhienne T, Stalon V & Villeret V. (2001) Probing the role of oligomerization in the high thermal stability of *Pyrococcus furiosus* ornithine carbamoyltransferase by site-specific mutants. *Eur J Biochem*. 268:3937-42.
 37. Clark AW & Rudolph FB. (1976) Regulation of purine metabolism. Adenylosuccinate synthetase from Novikoff ascites tumor cells. *Biochim Biophys Acta*. 437:87-90.
 38. Clark SW, Berry SA, Ewing R & Rudolph FB. (1977) Regulation of purine metabolism: a comparative study of the kinetic properties of adenylosuccinate synthetases from various sources. *Comp Biochem Physiol B*. 58:63-5.
 39. Cleland, W. W. & Kreevoy, M. M. (1994). Low-barrier hydrogen bonds and enzymic catalysis. *Science* 264, 1887-1890.
 40. Cohen, G. E. (1997). ALIGN: a program to superimpose protein coordinates accounting for insertions and deletions. *J. Appl. Cryst.* 30, 1160-1161.

References

41. Cooper BF, Fromm HJ & Rudolph FB. (1986) Isotope exchange at equilibrium studies with rat muscle adenylosuccinate synthetase. *Biochemistry*. 25:7323-7.
42. Crabb BS, Cooke BM, Reeder JC, Waller RF, Caruana SR, Davern KM, Wickham ME, Brown GV, Coppel RL & Cowman AF. (1997) Targeted gene disruption shows that knobs enable malaria-infected red cells to cytoadhere under physiological shear stress. *Cell*. 89:287-96.
43. Craig SP 3rd & Eakin AE. Purine phosphoribosyltransferases. (2000) *J Biol Chem*. 275:20231-4.
44. Cunningham EL, Jaswal SS, Sohl JL & Agard DA. (1999) Kinetic stability as a mechanism for protease longevity. *Proc Natl Acad Sci U S A*. 96:11008-14.
45. Dan'shina PV, Schmalhausen EV, Arutiunov DY, Pleten' AP & Muronetz VI. (2003) Acceleration of glycolysis in the presence of the non-phosphorylating and the oxidized phosphorylating glyceraldehyde-3-phosphate dehydrogenases. *Biochemistry (Mosc)*. 68:593-600.
46. de Koning-Ward TF, Janse CJ & Waters AP. (2000) The development of genetic tools for dissecting the biology of malaria parasites. *Annu Rev Microbiol*. 54:157-85.
47. Denu JM & Tanner KG. (2002) Redox regulation of protein tyrosine phosphatases by hydrogen peroxide: detecting sulfenic acid intermediates and examining reversible inactivation. *Methods Enzymol*. 348:297-305.
48. Digits JA & Hedstrom L. (1999) Kinetic mechanism of *Tritrichomonas foetus* inosine 5'-monophosphate dehydrogenase. *Biochemistry*. 38:2295-306.
49. DiIanni CL, Davis LJ, Holloway MK, Herber WK, Darke PL, Kohl NE & Dixon RA. (1990) Characterization of an active single polypeptide form of the human immunodeficiency virus type 1 protease. *J Biol Chem*. 265:17348-54.
50. Dong Q, Soans C, Liu F & Fromm HJ. (1990) Identification of different classes of nonessential sulfhydryl groups in *Escherichia coli* adenylosuccinate synthetase. *Arch Biochem Biophys*. 276:77-84.
51. Dovey HF, McKerrow JH, Aldritt SM & Wang CC. (1986) Purification and characterization of hypoxanthine-guanine phosphoribosyltransferase from *Schistosoma mansoni*. A potential target for chemotherapy. *J Biol Chem*. 261:944-8.
52. Dunn, C. R., Banfield, N. J., Barker, J. J., Higham, C. W., Moreton, K. M., Turgut-Balik, D., Brady, R. L. & Holbrook, J. J. (1996) The structure of lactate dehydrogenase from *Plasmodium falciparum* reveals a new target for anti-malarial design *Nat. Struct. Biol.*, 3, 912-915.
53. Dyson HJ, Jeng MF, Tennant LL, Slaby I, Lindell M, Cui DS, Kuprin S & Holmgren A. (1997) Effects of buried charged groups on cysteine thiol ionization and reactivity in *Escherichia coli* thioredoxin: structural and functional characterization of mutants of Asp 26 and Lys 57. *Biochemistry*. 36:2622-36.

54. Eads JC, Scapin G, Xu Y, Grubmeyer C & Sacchettini JC. (1994) The crystal structure of human hypoxanthine-guanine phosphoribosyltransferase with bound GMP. *Cell*. 78:325-34.
55. Eakin AE, Guerra A, Focia PJ, Torres-Martinez J & Craig SP 3rd. (1997) Hypoxanthine phosphoribosyltransferase from *Trypanosoma cruzi* as a target for structure-based inhibitor design: crystallization and inhibition studies with purine analogs. *Antimicrob Agents Chemother*. 41: 1686-92.
56. Eakin AE, Nieves-Alicea R, Tosado-Acevedo R, Chin MS, Wang CC & Craig SP 3rd (1995) Comparative complement selection in bacteria enables screening for lead compounds targeted to a purine salvage enzyme of parasites. *Antimicrob Agents Chemother*. 39:620-5.
57. Ellis HR & Poole LB. (1997) Novel application of 7-chloro-4-nitrobenzo-2-oxa-1,3-diazole to identify cysteine sulfenic acid in the AhpC component of alkyl hydroperoxide reductase. *Biochemistry*. 36:15013-8.
58. Eriksen TA, Kadziola A, Bentsen AK, Harlow KW & Larsen S. (2000) Structural basis for the function of *Bacillus subtilis* phosphoribosylpyrophosphate synthetase. *Nat Struct Biol*. 7:303-8.
59. Eriksson AE, Baase WA & Matthews BW. (1993) Similar hydrophobic replacements of Leu99 and Phe153 within the core of T4 lysozyme have different structural and thermodynamic consequences. *J Mol Biol*. 229:747-69.
60. Fitzpatrick, T., Ricken, S., Lanzer, M., Amrhein, N., Macheroux, P. & Kappes, B. (2001) Subcellular localization and characterization of chorismate synthase in the apicomplexan *Plasmodium falciparum*. *Mol. Microbiol.*, 40, 65-75.
61. Florens L, Washburn MP, Raine JD, Anthony RM, Grainger M, Haynes JD, Moch JK, Muster N, Sacci JB, Tabb DL, Witney AA, Wolters D, Wu Y, Gardner MJ, Holder AA, Sinden RE, Yates JR & Carucci DJ. (2002) A proteomic view of the *Plasmodium falciparum* life cycle. *Nature*. 419: 520-6.
62. Flores, M. V., O'Sullivan, W. J. & Stewart, T. S. (1994) Characterisation of the carbamoyl phosphate synthetase gene from *Plasmodium falciparum*. *Mol. Biochem. Parasitol.*, 68, 315-318.
63. Flores, M.V., Atkins, D., Wade, D., O'Sullivan, W. J. & Stewart, T. S. (1997) Inhibition of *Plasmodium falciparum* proliferation *in vitro* by ribozymes. *J. Biol. Chem*. 272, 16940-16845.
64. Focia PJ, Craig SP 3rd & Eakin AE. (1998b) Approaching the transition state in the crystal structure of a phosphoribosyltransferase. *Biochemistry*. 37: 17120-7.
65. Focia PJ, Craig SP 3rd, Nieves-Alicea R, Fletterick RJ & Eakin AE. (1998a) A 1.4 Å crystal structure for the hypoxanthine phosphoribosyltransferase of *Trypanosoma cruzi*. *Biochemistry*. 37: 15066-75.
66. Fonne-Pfister R, Chemla P, Ward E, Girardet M, Kreuz KE, Honzatko RB, Fromm HJ, Schar HP, Grutter MG & Cowan-Jacob SW. (1996) The mode of action and the structure of a herbicide in complex with its target: binding of activated hydantocidin to the feedback regulation site of adenylosuccinate synthetase. *Proc Natl Acad Sci U S A*. 93: 9431-6.

References

67. Foth BJ, Ralph SA, Tonkin CJ, Struck NS, Fraunholz M, Roos DS, Cowman AF & McFadden GI. (2003) Dissecting apicoplast targeting in the malaria parasite *Plasmodium falciparum*. *Science*. 299: 705-8.
68. Francis SE, Sullivan DJ Jr & Goldberg DE. (1997) Hemoglobin metabolism in the malaria parasite *Plasmodium falciparum*. *Annu Rev Microbiol*. 51:97-123..
69. Freymann DM, Wenck MA, Engel JC, Feng J, Focia PJ, Eakin AE & Craig SP. (2000) Efficient identification of inhibitors targeting the closed active site conformation of the HPRT from *Trypanosoma cruzi*. *Chem Biol*. 7: 957-68.
70. Fromant M, Blanquet S & Plateau P. (1995) Direct random mutagenesis of gene-sized DNA fragments using polymerase chain reaction. *Anal Biochem*. 224:347-53.
71. Fromm HJ. (1979a) Use of competitive inhibitors to study substrate binding order. *Methods Enzymol*. 63:467-86.
72. Fromm HJ. (1979b) Summary of kinetic reaction mechanisms. *Methods Enzymol*. 63:42-53.
73. Gardiner DL, Skinner-Adams TS, Spielmann T & Trenholme KR. (2003) Malaria transfection and transfection vectors. *Trends Parasitol*. 19: 381-3.
74. Gardner, M. J., Hall, N., Fung, E. et al., (2002) Genome sequence of the human malaria parasite *Plasmodium falciparum*. *Nature* 419:498-511.
75. Gardner, M. J., Shallom, S. J., Carlton, J. M. et al., (2001) Sequence of *Plasmodium falciparum* chromosomes 2, 10, 11 and 14. *Nature* 419:531-4.
76. Gero A. M., Brown G. V. & O'Sullivan W. J. (1984) Pyrimidine *de novo* synthesis during the life cycle of the intraerythrocytic stage of *Plasmodium falciparum*. *J. Parasitol.*, 70, 536-541.
77. Giacomello A & Salerno C. (1977) A continuous Spectrophotometric assay for hypoxanthine-guanine phosphoribosyltransferase. *Anal Biochem*. 79:263-7.
78. Giao PT & de Vries PJ. (2001) Pharmacokinetic interactions of antimalarial agents. *Clin Pharmacokinet*. 40:343-73.
79. Goodman MN & Lowenstein JM. (1977) The purine nucleotide cycle. Studies of ammonia production by skeletal muscle in situ and in perfused preparations. *J Biol Chem*. 252:5054-60.
80. Graciet E, Lebreton S, Camadro JM & Gontero B. (2002) Thermodynamic analysis of the emergence of new regulatory properties in a phosphoribulokinase-glyceraldehyde 3-phosphate dehydrogenase complex. *J Biol Chem*. 277:12697-702.
81. Gromiha MM, Oobatake M, Kono H, Uedaira H & Sarai A. (1999) Role of structural and sequence information in the prediction of protein stability changes: comparison between buried and partially buried mutations. *Protein Eng*. 12:549-55.
82. Guddat LW, Vos S, Martin JL, Keough DT & de Jersey J. (2002) Crystal structures of free, IMP-, and GMP-bound *Escherichia coli* hypoxanthine phosphoribosyltransferase. *Protein Sci*. 11:1626-38.

83. Guex, N. & Peitsch, M.C. (1997) SWISS-MODEL and the Swiss-PdbViewer: An environment for comparative protein modeling. *Electrophoresis* 18, 2714-2723. <http://www.expasy.org/spdbv/>
84. Guicherit OM, Cooper BF, Rudolph FB & Kellems RE. (1994) The muscle and nonmuscle isozymes of adenylosuccinate synthetase are encoded by separate genes with differential patterns of expression. *Adv Exp Med Biol.* 370:585-90.
85. Hall, N., Pain, A., Berriman, M., Churcher, C. et al., (2002) Sequence of *Plasmodium falciparum* chromosomes 1, 3-9 and 13. *Nature* 419:527-31.
86. Hanessian S, Lu PP, Sanceau JY, Chemla P, Gohda K, Fonne-Pfister R, Prade L & Cowan-Jacob SW. (1999) An Enzyme-Bound Bisubstrate Hybrid Inhibitor of Adenylosuccinate Synthetase. *Angew Chem Int Ed Engl.* 38: 3159-3162.
87. Hannon GJ. RNA interference. (2002) *Nature.* 418: 244-51. Review.
88. Hernandez, J.V. & Bremer, H., (1991). *Escherichia coli* ppGpp synthetase II activity requires *spoT*. *J. Biol. Chem.*, 266, 5991-5999.
89. Heroux A, White EL, Ross LJ & Borhani DW. (1999b) Crystal structures of the *Toxoplasma gondii* hypoxanthine-guanine phosphoribosyltransferase-GMP and -IMP complexes: comparison of purine binding interactions with the XMP complex. *Biochemistry.* 38: 14485-94.
90. Heroux A, White EL, Ross LJ, Davis RL & Borhani DW. (1999a) Crystal structure of *Toxoplasma gondii* hypoxanthine-guanine phosphoribosyltransferase with XMP, pyrophosphate, and two Mg(2+) ions bound: insights into the catalytic mechanism. *Biochemistry.* 38:14495-506.
91. Heroux A, White EL, Ross LJ, Kuzin AP & Borhani DW. (2000) Substrate deformation in a hypoxanthine-guanine phosphoribosyltransferase ternary complex: the structural basis for catalysis. *Structure Fold Des.* 8: 1309-18.
92. Hitchings, G. H. (1971) Folate antagonists as antibacterial and antiprotozoal agents. *Ann. N. Y. Acad. Sci.*, 186, 444-451.
93. Hobish MK &, Powers DA. (1986) pH dependence of 2,3-diphosphoglycerate binding to human hemoglobin A0 at 21.5 degrees C. *Proteins.* 1:164-75.
94. Hoffman SL, Subramanian GM, Collins FH & Venter JC. (2002) Plasmodium, human and Anopheles genomics and malaria. *Nature.* 415702-9.
95. Holt, R. A., Subramanian, G. M., Halpern, A. et al., (2002) The genome sequence of the malaria mosquito *Anopheles gambiae*. *Science* 298:129-49.
96. Honzatko RB & Fromm HJ. (1999) Structure-function studies of adenylosuccinate synthetase from *Escherichia coli*. *Arch Biochem Biophys.* 370:1-8..
97. Honzatko RB, Stayton MM & Fromm HJ. (1999) Adenylosuccinate synthetase: recent developments. *Adv Enzymol Relat Areas Mol Biol.* 73:57-102, ix-x.
98. Hou, Z., Wang, W., Fromm, H. J. & Honzatko, R. B. (2002). IMP alone organizes the active site of adenylosuccinate synthetase from *Escherichia coli*. *J. Biol. Chem.* 277, 5970-5976.

References

99. Hubbard, S. J. & Thornton, J. M. (1993). 'NACCESS', Computer program, Department of Biochemistry and Molecular Biology, University College, London.
100. Hyde JE.(2002) Mechanisms of resistance of *Plasmodium falciparum* to antimalarial drugs. *Microbes Infect.* 4:165-74,
101. Hyman, R. W., Fung, E., Conway, A., Kurdi, O., Mao, J., Miranda, M., Nakao, B., Rowley, D., Tamaki, T., Wang, F. & Davis, R. W. (2002) Sequence of *Plasmodium falciparum* chromosome 12. *Nature* 419:534-7.
102. Iancu CV, Borza T, Choe JY, Fromm HJ & Honzatko RB. (2001) Recombinant mouse muscle adenylosuccinate synthetase: overexpression, kinetics, and crystal structure. *J Biol Chem.* 276: 42146-52.
103. Iancu CV, Borza T, Fromm HJ & Honzatko RB. (2002a) IMP, GTP, and 6-phosphoryl-IMP complexes of recombinant mouse muscle adenylosuccinate synthetase. *J Biol Chem.* 277: 26779-87.
104. Iancu CV, Borza T, Fromm HJ, Honzatko RB. (2002b) Feedback inhibition and product complexes of recombinant mouse muscle adenylosuccinate synthetase. *J Biol Chem.* 277: 40536-43.
105. Isokpehi RD, Hide WA. (2003) Integrative analysis of intraerythrocytic differentially expressed transcripts yields novel insights into the biology of *Plasmodium falciparum*. *Malar J.* 2:38.
106. Ittarat, I., Asawamahasakda, W. & Meshnick, S. R. (1994) The effects of antimalarials on the *Plasmodium falciparum* dihydroorotate dehydrogenase. *Exp. Parasitol.*, 79, 50-56.
107. Jahngen EG & Rossomando EF. (1984) Adenylosuccinate synthetase from *Dictyostelium discoideum*: effects of hadacidin analogs and binding of [14C]hadacidin. *Arch Biochem Biophys.* 229:145-54
108. Jaswal SS, Sohl JL, Davis JH & Agard DA. (2002) Energetic landscape of alpha-lytic protease optimizes longevity through kinetic stability. *Nature.* 415:343-6.
109. Jez JM & Noel JP. (2000) Mechanism of chalcone synthase. pKa of the catalytic cysteine and the role of the conserved histidine in a plant polyketide synthase. *J Biol Chem.* 275:39640-6.
110. Jiang, L., Lee, P. C., White, J. & Rathod, P. K. (2000) Potent and selective activity of a combination of thymidine and 1843U89, a folate-based thymidylate synthase inhibitor, against *Plasmodium falciparum*. *Antimicrob. Agents Chemother.*, 44, 1047-1050.
111. Jinnah HA, De Gregorio L, Harris JC, Nyhan WL & O'Neill JP. (2000) The spectrum of inherited mutations causing HPRT deficiency: 75 new cases and a review of 196 previously reported cases. *Mutat Res.* 463:309-26.
112. Jochimsen B, Nygaard P & Vestergaard T. (1975) Location on the chromosome of *Escherichia coli* of genes governing purine metabolism. Adenosine deaminase (add), guanosine kinase (gsk) and hypoxanthine phosphoribosyltransferase (hpt). *Mol Gen Genet.* 143:85-91.

113. Kang C & Fromm HJ. (1995) Identification of an essential second metal ion in the reaction mechanism of *Escherichia coli* adenylosuccinate synthetase. *J Biol Chem.* 270:15539-44.
114. Kang C, Kim S & Fromm HJ. (1996) Subunit complementation of *Escherichia coli* adenylosuccinate synthetase. *J Biol Chem.* 271:29722-8.
115. Kasai K, Usami S, Yamada T, Endo Y, Ochi K &, Tozawa Y. (2002) A RelA-SpoT homolog (Cr-RSH) identified in *Chlamydomonas reinhardtii* generates stringent factor in vivo and localizes to chloroplasts in vitro. *Nucleic Acids Res.* 30:4985-92.
116. Keough DT, Ng AL, Winzor DJ, Emmerson BT & de Jersey J. (1999) Purification and characterization of *Plasmodium falciparum* hypoxanthine-guanine-xanthine phosphoribosyltransferase and comparison with the human enzyme. *Mol Biochem Parasitol.* 98:29-41.
117. Khosravi M, Shire SJ & Borchardt RT. (2000) Evidence for the involvement of histidine A(12) in the aggregation and precipitation of human relaxin induced by metal-catalyzed oxidation. *Biochemistry.* 39:5876-85.
118. Kicska GA, Tyler PC, Evans GB, Furneaux RH, Schramm VL & Kim K. (2002b) Purine-less death in *Plasmodium falciparum* induced by immucillin-H, a transition state analogue of purine nucleoside phosphorylase. *J Biol Chem.* 277:3226-31.
119. Kicska, G. A., Tyler, P. C., Evans, G. B., Furneaux, R. H., Kim, K. & Schramm, V. L. (2002a) Transition state analogue inhibitors of purine nucleoside phosphorylase from *Plasmodium falciparum*. *J. Biol. Chem.* 277:3219-25.
120. Kim C, Xuong NH, Edwards S, Madhusudan, Yee MC, Spraggon G & Mills SE. (2002) The crystal structure of anthranilate phosphoribosyltransferase from the enterobacterium *Pectobacterium carotovorum*. *FEBS Lett.* 523: 239-46.
121. Kim, H., Certa, U., Dobeli, H., Jakob, P. & Hol, W. G. (1998) Crystal structure of fructose 1-6-bisphosphate aldolase from human malarial parasite *Plasmodium falciparum*. *Biochemistry* 37, 4388-4396.
122. Krahn JM, Kim JH, Burns MR, Parry RJ, Zalkin H & Smith JL. (1997) Coupled formation of an amidotransferase interdomain ammonia channel and a phosphoribosyltransferase active site. *Biochemistry.* 36: 11061-8.
123. Kraulis, P. J. (1991). MOLSCRIPT: A Program to Produce Both Detailed and Schematic Plots of Protein Structures. *J. Appl. Cryst.* 24, 946-950.
124. Krungkrai, J. (1995) Purification, characterization and localization of mitochondrial dihydroorotate dehydrogenase in *Plasmodium falciparum*, human malaria parasite. *Biochim. Biophys. Acta.* 1243, 351-360.
125. Krungkrai, J., Cerami, A. & Henderson, G. B. (1990) Pyrimidine biosynthesis in parasitic protozoa: Purification of a monofunctional dihydroorotase from *Plasmodium bergeri* and *Crithidia fasciculata*. *Biochemistry* 29, 6270-6275.
126. Krungkrai, J., Cerami, A. & Henderson, G. B. (1991) Purification and characterization of dihydroorotate dehydrogenase from the rodent malaria parasite *Plasmodium berghii*. *Biochemistry* 30, 1934-1939.

References

127. Kumar R, Adams B, Oldenburg A, Musiyenko A & Barik S. (2002) Characterisation and expression of a PP1 serine/threonine protein phosphatase (PfPP1) from the malaria parasite, *Plasmodium falciparum*: demonstration of its essential role using RNA interference. *Malar J.* 1:5.
128. Laemmli, U.K. (1970) Cleavage of structural proteins during the assembly of the head of bacteriophage T4. *Nature.* 227, 680-685.
129. Lander, E. S., Linton, L. M., Birren, B. et al., (2001) Initial sequencing and analysis of the human genome. *Nature* 409:860-921.
130. Lanners, H, N. (1991) Effect of the 8-aminoquinoline primaquine on culture-derived gametocytes of the malaria parasite *Plasmodium falciparum*. *Parasitol. Res.* 77, 478-481.
131. Laskowski, R. A., Moss, D. S. & Thornton, J. M. (1993). Main-chain bond lengths and bond angles in protein structures. *J. Mol. Biol.* 231, 1049-1067.
132. Lasonder E, Ishihama Y, Andersen JS, Vermunt AM & Pain A, Sauerwein RW, Eling WM, Hall N, Waters AP, Stunnenberg HG, Mann M. (2002) Analysis of the *Plasmodium falciparum* proteome by high-accuracy mass spectrometry. *Nature.* 419:537-42.
133. Le Roch KG, Zhou Y, Blair PL, Grainger M, Moch JK, Haynes JD, De La Vega P, Holder AA, Batalov S, Carucci DJ & Winzeler EA. (2003) Discovery of gene function by expression profiling of the malaria parasite life cycle. *Science.* 301:1503-8.
134. Lebreton S & Gontero B. (1999) Memory and imprinting in multienzyme complexes. Evidence for information transfer from glyceraldehyde-3-phosphate dehydrogenase to phosphoribulokinase under reduced state in *Chlamydomonas reinhardtii*. *J Biol Chem.* 274:20879-84
135. Lee B & Vasmatzis G. Stabilization of protein structures. (1997) *Curr Opin Biotechnol.* 8:423-8.
136. Lee C, Park SH, Lee MY & Yu MH. (2000) Regulation of protein function by native metastability. *Proc Natl Acad Sci U S A.* 97:7727-31.
137. Lee CC, Craig SP 3rd & Eakin AE. (1998a) A single amino acid substitution in the human and a bacterial hypoxanthine phosphoribosyltransferase modulates specificity for the binding of guanine. *Biochemistry.* 37:3491-8.
138. Lee CC, Medrano FJ, Craig SP 3rd & Eakin AE. (2001) Investigation of the functional role of active site loop II in a hypoxanthine phosphoribosyltransferase. *Biochim Biophys Acta.* 1537:63-70.
139. Lee SR, Kwon KS, Kim SR & Rhee SG. (1998b) Reversible inactivation of protein-tyrosine phosphatase 1B in A431 cells stimulated with epidermal growth factor. *J Biol Chem.* 273:15366-72.
140. Lesch M & Nyhan WL. (1964) A familial disorder of uric acid metabolism and central nervous system function. *Am J Med.* 36:561-70.
141. Li CM, Tyler PC, Furneaux RH, Kicska G, Xu Y, Grubmeyer C, Girvin ME & Schramm VL. (1999) Transition-state analogs as inhibitors of human and

- malarial hypoxanthine-guanine phosphoribosyltransferases. *Nat Struct Biol.* 6:582-7.
142. Lieberman, I. (1956) Enzymatic synthesis of adenosine-5'-phosphate from inosine-5'-phosphate. *J. Biol. Chem.* 223, 327-339.
143. Lipps G & Krauss G. (1999) Adenylosuccinate synthase from *Saccharomyces cerevisiae*: homologous overexpression, purification and characterization of the recombinant protein. *Biochem J.* 341 :537-43.
144. Lo Bello M, Battistoni A, Mazzetti AP, Board PG, Muramatsu M, Federici G & Ricci G. (1995) Site-directed mutagenesis of human glutathione transferase P1-1. Spectral, kinetic, and structural properties of Cys-47 and Lys-54 mutants. *J Biol Chem.* 270:1249-53.
145. Luebke RW, Andrews DL, Copeland CB, Riddle MM, Rogers RR & Smialowicz RJ. (1991) Host resistance to murine malaria in mice exposed to the adenosine deaminase inhibitor, 2'-deoxycoformycin. *Int J Immunopharmacol.* 13:987-97.
146. Maier KL, Hinze H, Meyer B & Lenz AG. (1996) Metal-catalyzed inactivation of bovine glucose-6-phosphate dehydrogenase -- role of thiols. *FEBS Lett.* 396:95-8.
147. Makobongo, M. O., Riding, G., Xu, H., Hirunpetcharat, C., Keough, D., de Jersey, J., Willadsen, P. & Good, M. F. (2003) The purine salvage enzyme hypoxanthine guanine xanthine phosphoribosyl transferase is a major target antigen for cell-mediated immunity to malaria. *Proc Natl Acad Sci U S A.* 100:2628-33.
148. Malhotra P, Dasaradhi PV, Kumar A, Mohammed A, Agrawal N, Bhatnagar RK & Chauhan VS. (2002) Double-stranded RNA-mediated gene silencing of cysteine proteases (falcipain-1 and -2) of *Plasmodium falciparum*. *Mol Microbiol.* 45:1245-54.
149. Matsuda Y, Ogawa H, Fukutome S, Shiraki H & Nakagawa H. (1977) Adenylosuccinate synthetase in rat liver: the existence of two types and their regulatory roles. *Biochem Biophys Res Commun.* 78:766-71.
150. Matsuda Y, Shimura K, Shiraki H & Nakagawa H. (1980) Purification and properties of adenylosuccinate synthetase from Yoshida sarcoma ascites tumor cells. *Biochim Biophys Acta.* 616:340-50
151. Matsui Lee IS, Suzuki M, Hayashi N, Hu J, Van Eldik LJ, Titani K & Nishikimi M. (2000) Copper-dependent formation of disulfide-linked dimer of S100B protein. *Arch Biochem Biophys.* 374:137-41
152. McConkey, G. A. (2000) *Plasmodium falciparum*: isolation and characterisation of a gene encoding protozoan GMP synthase. *Exp. Parasitol.* 94, 23-32.
153. McFadden, G. I. & Roos, D. S. (1999) Apicomplexan plastids as drug targets. *Trends Microbiol.* 7, 328-332.
154. McLeod R, Muench SP, Rafferty JB, Kyle DE, Mui EJ, Kirisits MJ, Mack DG, Roberts CW, Samuel BU, Lyons RE, Dorris M, Milhous WK & Rice DW.

References

- (2001) Triclosan inhibits the growth of *Plasmodium falciparum* and *Toxoplasma gondii* by inhibition of apicomplexan Fab I. *Int J Parasitol.* 31:109-13.
155. McRobert L & McConkey GA. (2002) RNA interference (RNAi) inhibits growth of *Plasmodium falciparum*. *Mol Biochem Parasitol.* 119: 273-8.
156. Medana IM, Chaudhri G, Chan-Ling T &, Hunt NH. (2001) Central nervous system in cerebral malaria: 'Innocent bystander' or active participant in the induction of immunopathology? *Immunol Cell Biol.* 79:101-20.
157. Merritt, E. A. & Bacon, D. J. (1997). Raster3D: Photorealistic Molecular Graphics. *Methods Enzymol.* 277, 505-524.
158. Meshnick, S. R. (1997) Why Does Quinine Still Work After 350 Years of Use? *Parasitol. Today* 13, 89-90.
159. Metzger, S., Schreiber, G., Aizenman, E., Cashel, M. & Glaser, G., (1989) Characterization of the *relA1* mutation and a comparison of *relA1* with new *relA* null alleles in *Escherichia coli*. *J. Biol. Chem.*, 264, 21146-21152.
160. Miles RW, Tyler PC, Furneaux RH, Bagdassarian CK & Schramm VL. (1998) One-third-the-sites transition-state inhibitors for purine nucleoside phosphorylase. *Biochemistry.* 37:615-21.
161. Miller RW, Buchanan JM. (1962) Biosynthesis of the purines. 28. Mechanism of action of adenylosuccinase. *J Biol Chem.* 237:491-6.
162. Mirgorodskaya E, Fierobe HP, Svensson B & Roepstorff P. (1999) Mass spectrometric identification of a stable catalytic cysteine sulfinic acid residue in an enzymatically active chemically modified glucoamylase mutant. *J Mass Spectrom.* 34:952-7.
163. Muirhead KM & Bishop SH. (1974) Purification of adenylosuccinate synthetase from rabbit skeletal muscle. *J Biol Chem.* 249:459-64.
164. Multhaup G, Ruppert T, Schlicksupp A, Hesse L, Behr D, Masters CL & Beyreuther K. (1997) Reactive oxygen species and Alzheimer's disease. *Biochem Pharmacol.* 54:533-9.
165. Munagala N, Sarver AE & Wang CC. (2000) Converting the guanine phosphoribosyltransferase from *Giardia lamblia* to a hypoxanthine-guanine phosphoribosyltransferase. *J Biol Chem.* 275:37072-7.
166. Munagala NR & Wang CC. (1998) Altering the purine specificity of hypoxanthine-guanine-xanthine phosphoribosyltransferase from *Tritrichomonas foetus* by structure-based point mutations in the enzyme protein. *Biochemistry.* 37:16612-9.
167. Nagaraj, G., Uma, M. V., Shivayogi, M. S. & Balaram, H. (2001) Antimalarial activities of peptide antibiotics isolated from fungi. *Antimicrob. Agents Chemother.* 45, 145-149
168. Naguib FN, Iltzsch MH, el Kouni MM, Panzica RP & el Kouni MH. (1995) Structure-activity relationships for the binding of ligands to xanthine or guanine phosphoribosyl-transferase from *Toxoplasma gondii*. *Biochem Pharmacol.* 50:1685-93.

169. Nagy M, Djembo-Taty M & Heslot. (1973) Regulation of the biosynthesis of purine nucleotides in *Schizosaccharomyces pombe*. 3. Kinetic studies of adenylosuccinate synthetase. *Biochim Biophys Acta*. 309:1-10.
170. Newton CR, Taylor TE & Whitten RO. (1998) Pathophysiology of fatal falciparum malaria in African children. *Am J Trop Med Hyg*. 58:673-83.
171. Ozturk DH, Dorfman RH, Scapin G, Sacchettini JC & Grubmeyer C. (1995) Structure and function of *Salmonella typhimurium* orotate phosphoribosyltransferase: protein complementation reveals shared active sites. *Biochemistry*. 34:10764-70.
172. Park OK & Bauerle R. (1999) Metal-catalyzed oxidation of phenylalanine-sensitive 3-deoxy-D-arabino-heptulosonate-7-phosphate synthase from *Escherichia coli*: inactivation and destabilization by oxidation of active-site cysteines. *J Bacteriol*. 181:1636-42.
173. Parker, W.B. & Cheng, Y.C. (1990) Metabolism and mechanism of action of 5-fluorouracil. *Pharmacol. Ther.* 48, 381-395.
174. Pitera JW, Munagala NR, Wang CC & Kollman PA. (1999) Understanding substrate specificity in human and parasite phosphoribosyltransferases through calculation and experiment. *Biochemistry*. 38:10298-306.
175. Plasterk RH & Ketting RF. (2000) The silence of the genes. *Curr Opin Genet Dev*. 10: 562-7.
176. Plou FJ, Kowlessur D, Malthouse JP, Mellor GW, Hartshorn MJ, Pinitglang S, Patel H, Topham CM, Thomas EW, Verma C & Brocklehurst K. (1996) Characterization of the electrostatic perturbation of a catalytic site (Cys)-S-/(His)-Im+H ion-pair in one type of serine proteinase architecture by kinetic and computational studies on chemically mutated subtilisin variants. *J Mol Biol*. 257:1088-111.
177. Poland BW, Bruns C, Fromm HJ & Honzatko RB. (1997) Entrapment of 6-thiophosphoryl-IMP in the active site of crystalline adenylosuccinate synthetase from *Escherichia coli*. *J Biol Chem*. 272: 15200-5.
178. Poland BW, Fromm HJ & Honzatko RB. (1996a) Crystal structures of adenylosuccinate synthetase from *Escherichia coli* complexed with GDP, IMP hadacidin, NO₃⁻, and Mg²⁺. *J Mol Biol*. 264: 1013-27.
179. Poland BW, Hou Z, Bruns C, Fromm HJ, Honzatko RB. (1996b) Refined crystal structures of guanine nucleotide complexes of adenylosuccinate synthetase from *Escherichia coli*. *J Biol Chem*. 271:15407-13.
180. Poland BW, Lee SF, Subramanian MV, Siehl DL, Anderson RJ, Fromm HJ & Honzatko RB. (1996c) Refined crystal structure of adenylosuccinate synthetase from *Escherichia coli* complexed with hydantocidin 5'-phosphate, GDP, HPO₄⁽²⁻⁾, Mg²⁺, and hadacidin. *Biochemistry*. 35:15753-9.
181. Poland BW, Silva MM, Serra MA, Cho Y, Kim KH, Harris EM & Honzatko RB. (1993) Crystal structure of adenylosuccinate synthetase from *Escherichia coli*. Evidence for convergent evolution of GTP-binding domains. *J Biol Chem*. 268: 25334-42.

References

182. Pollack, Y., Shemer, R., Metzger, S., Spira, D. T. & Golenser, J. (1985) *Plasmodium falciparum*: expression of the adenine phosphoribosyltransferase gene in mouse L cells. *Exp. Parasitol.* 60, 270-275.
183. Pomposiello PJ & Demple B. (2001) Redox-operated genetic switches: the SoxR and OxyR transcription factors. *Trends Biotechnol.* 19:109-14.
184. Powell KA, Ramer SW, Del Cardayre SB, Stemmer WP, Tobin MB, Longchamp PF & Huisman GW. (2001) Directed Evolution and Biocatalysis. *Angew Chem Int Ed Engl.* 40:3948-3959.
185. Powell SM, Zalkin H & Dixon JE. (1992) Cloning and characterization of the cDNA encoding human adenylosuccinate synthetase. *FEBS Lett.* 303:4-10.
186. Prade L, Cowan-Jacob SW, Chemla P, Potter S, Ward E & Fonne-Pfister R. (2000) Structures of adenylosuccinate synthetase from *Triticum aestivum* and *Arabidopsis thaliana*. *J Mol Biol.* 296: 569-77.
187. Price, R. N. (2000) Artemisinin drugs: novel antimalarial agents. *Expert Opin Investig Drugs.* 9:1815-27.
188. Queen SA, Vander Jagt D & Reyes P. (1988) Properties and substrate specificity of a purine phosphoribosyltransferase from the human malaria parasite, *Plasmodium falciparum*. *Mol Biochem Parasitol.* 30: 123-33.
189. Queen, S. A., Jagt, D. L. & Reyes, P. (1990) *In vitro* susceptibilities of *Plasmodium falciparum* to compounds which inhibit nucleotide metabolism. *Antimicrob. Agents Chemother.* 34, 1393-1398.
190. Queen, S. A., Van der Jagt, D. L. & Reyes, P. (1989) Characterization of adenine phosphoribosyltransferase from the human malaria parasite, *Plasmodium falciparum*. *Biochim. Biophys. Acta.* 996, 160-165.
191. Rathod , P. K., Khatri, A., Hubbert, T. & Milhous, W. K. (1989) Selective activity of 5-fluoroorotic acid against *Plasmodium falciparum in vitro*. *Antimicrob. Agents Chemother.* 33, 1090-94.
192. Read, J. A., Wilkinson, K. W., Tranter, R., Sessions, R. B. & Brady, R. L. (1999) Chloroquine binds in the cofactor-binding site of *Plasmodium falciparum* lactate dehydrogenase. *J. Biol. Chem.* 274, 10213-18.
193. Reyes, P., Rathod, P. K., Sanchez, D. J., Mrema, J. E. K., Reickmann, K. L. & Heidrich, H. G. (1982) Enzymes of purine and pyrimidine metabolism from the human malaria parasite, *Plasmodium falciparum*. *Mol. Biochem. Parasitol.* 5, 275-290.
194. Ridley, R. G. (2002) Medical need , scientific opportunity and the drive for antimalarial drugs. *Nature* 415:686-93.
195. Roberts, F., Roberts, C. W., Johnson, J. J., Kyle, D. E., Krell, T., Coggins, J. R., Coombs, G. H., Milhous, W. K., Tzipori, S., Ferguson, D. J., Chakrabarti, D. & McLeod, R. (1998) Evidence for the shikimate pathway in apicomplexan parasites. *Nature* 393, 801-805.
196. Rosenthal, PJ & Meshnick, SR. (1998) Hemoglobin processing and the metabolism of amino acids, heme and iron. In *Malaria, parasite biology*,

- pathogenesis and protection* Sherman, I. W. Ed, ASM Press Washington D. C. pp145-158.
197. Roth, E. Jr. (1990) *Plasmodium falciparum* carbohydrate metabolism: a connection between host cell and parasite. *Blood Cells* 16, 453-466.
198. Rudolph FB & Fromm HJ. (1969) Initial rate studies of adenylosuccinate synthetase with product and competitive inhibitors. *J Biol Chem.* 244:3832-9.
199. Runquist JA & Miziorko HM. (2002) Anionic substitutes for catalytic aspartic acids in phosphoribulokinase. *Arch Biochem Biophys.* 405:178-84.
200. Salas, F., Fichmann, J., Lee, G. K., Scott, M. D. & Rosenthal, P. J. (1995) Functional expression of falcipain, a *Plasmodium falciparum* cysteine proteinase, supports its role as a malarial hemoglobinase. *Infect. Immun.* 63:2120-2125.
201. Sarkar G & Sommer SS. (1990) The "megaprimer" method of site-directed mutagenesis. *Biotechniques.* 8:404-7.
202. Sarver AE & Wang CC. (2002) The adenine phosphoribosyltransferase from *Giardia lamblia* has a unique reaction mechanism and unusual substrate binding properties. *J Biol Chem.* 277:39973-80.
203. Schumacher MA, Carter D, Ross DS, Ullman B & Brennan RG. (1996) Crystal structures of *Toxoplasma gondii* HGXPRTase reveal the catalytic role of a long flexible loop. *Nat Struct Biol.* 3: 881-7.
204. Schumacher, M. A., Scott, D. M., Mathews, I. I., Ealick, S. E., Roos, D. S., Ullman, B. & Brennan, R. G. (2000) *Toxoplasma gondii* adenosine kinase: expression, purification, characterization, crystallization and preliminary crystallographic analysis. *Acta Crystallogr. D Biol. Crystallogr.* 56, 76-78.
205. Sergio, A., Luo, U. S., Moreno, S. N. J. & Docampo, R. (2000) Oxidative phosphorylation, Ca²⁺ transport, and fatty acid-induced uncoupling in malaria parasites mitochondria. *J. Biol. Chem.* 275, 9709-15.
206. Seymour, K. K., Lyons, S. D., Phillips, L., Rieckmann, K. H. & Christopherson, R. I. (1994) Cytotoxic effects of inhibitors of *de novo* pyrimidine biosynthesis upon *Plasmodium falciparum*. *Biochemistry* 33, 5268-5274.
207. Shao Z & Arnold FH. (1996) Engineering new functions and altering existing functions. *Curr Opin Struct Biol.* 6:513-8.
208. Sharma V, Grubmeyer C & Sacchettini JC. (1998) Crystal structure of quinolinic acid phosphoribosyltransferase from *Mycobacterium tuberculosis*: a potential TB drug target. *Structure.* 6: 1587-99.
209. Shenai, B. R., Sijwali, P. S., Singh, A. & Rosenthal, P. J. (2000) Characterization of native and recombinant falcipain-2, a principal trophozoite cysteine protease and essential hemoglobinase of *Plasmodium falciparum*. *J. Biol. Chem.* 275:29000-10.
210. Sherman, I. W. (1998) A brief history of malaria and discovery of the parasites lifecycle. In *Malaria, parasite biology, pathogenesis and protection* Sherman, I. W. Ed, ASM Press Washington D. C. pp 135 -144.

References

211. Sherman, I. W. (1979) Biochemistry of *Plasmodium* (Malarial parasites). *Microbiol. Rev.* 43, 453-495.
212. Shi W, Li CM, Tyler PC, Furneaux RH, Cahill SM, Girvin ME, Grubmeyer C, Schramm VL & Almo SC. (1999a) The 2.0 Å structure of malarial purine phosphoribosyltransferase in complex with a transition-state analogue inhibitor. *Biochemistry.* 38: 9872-80.
213. Shi W, Li CM, Tyler PC, Furneaux RH, Grubmeyer C, Schramm VL & Almo SC. (1999b) The 2.0 Å structure of human hypoxanthine-guanine phosphoribosyltransferase in complex with a transition-state analog inhibitor. *Nat Struct Biol.* 6: 588-93.
214. Shi W, Tanaka KS, Crother TR, Taylor MW, Almo SC & Schramm VL. (2001) Structural analysis of adenine phosphoribosyltransferase from *Saccharomyces cerevisiae*. *Biochemistry.* 40:10800-9.
215. Shipton M & Brocklehurst K. (1977) Benzofuroxan as a thiol-specific reactivity probe. Kinetics of its reactions with papain, ficin, bromelain and low-molecular-weight thiols. *Biochem J.* 167:799-810.
216. Shivashankar K, Subbaya IN & Balaram H. (2001) Development of a bacterial screen for novel hypoxanthine-guanine phosphoribosyltransferase substrates. *J Mol Microbiol Biotechnol.* 3:557-62
217. Siehl DL, Subramanian MV, Walters EW, Lee SF, Anderson RJ & Toschi AG. (1996) Adenylosuccinate synthetase: site of action of hydantocidin, a microbial phytotoxin. *Plant Physiol.* 110:753-8.
218. Sijwali, P. S., Shenai, B. R., Gut, J., Singh, A. J. & Rosenthal P. J. (2001) Expression and characterization of the *Plasmodium falciparum* haemoglobinase falcipain-3. *Biochem. J.* 360:481-489.
219. Silva MM, Poland BW, Hoffman CR, Fromm HJ & Honzatko RB. (1995) Refined crystal structures of unligated adenylosuccinate synthetase from *Escherichia coli*. *J Mol Biol.* 254:431-46.
220. Silva, A. M., Lee, A. Y., Gulnik, S. V., Majer, P., Collins, J., Bhat, T. N., Collins, P. J., Cachau, R. E., Luker, K. E., Gluzman, I. Y., Francis, S. E., Oksman, A., Goldberg, D.E. & Erickson, J. W. (1996) Structure and inhibition of plasmepsin II, a hemoglobin-degrading enzyme from *Plasmodium falciparum*. *Proc. Natl. Acad. Sci. U S A.* 93:10034-39.
221. Simonson T & Calimet N. (2002) Cys(x)His(y)-Zn²⁺ interactions: thiol vs. thiolate coordination. *Proteins.* 49:37-48.
222. Sinha SC & Smith JL. The PRT protein family. (2001) *Curr Opin Struct Biol.* 11:733-9.
223. Sinha, K. M., Ghosh, M., Das, I. & Datta, A. K. (1999) Molecular cloning and expression of adenosine kinase from *Leishmania donovani*: identification of unconventional P-loop motif. *Biochem. J.* 339, 667-673.
224. Sinha, K. M., Ghosh, M., Das, I. & Datta, A. K. (2000) Crystal structures of *Toxoplasma gondii* adenosine kinase reveal a novel catalytic mechanism and prodrug binding. *J. Mol. Biol.* 298, 875-893.

225. Sloan DL, Ali LZ, Picou D & Joseph A Jr. (1984) Studies of the catalytically-active form of hypoxanthine-guanine phosphoribosyltransferase from yeast. *Adv Exp Med Biol.* 165: 45-50.
226. Smith JL, Zaluzec EJ, Wery JP, Niu L, Switzer RL, Zalkin H & Satow Y. (1994) Structure of the allosteric regulatory enzyme of purine biosynthesis. *Science.* 264: 1427-33.
227. Sommer JM, Ma H & Wang CC. (1996) Cloning, expression and characterization of an unusual guanine phosphoribosyltransferase from *Giardia lamblia*. *Mol Biochem Parasitol.* 78: 185-93.
228. Somoza JR, Chin MS, Focia PJ, Wang CC & Fletterick RJ. (1996) Crystal structure of the hypoxanthine-guanine-xanthine phosphoribosyltransferase from the protozoan parasite *Trichomonas foetus*. *Biochemistry.* 35: 7032-40.
229. Somoza JR, Skillman AG Jr, Munagala NR, Oshiro CM, Knegt RM, Mpoke S, Fletterick RJ, Kuntz ID & Wang CC. (1998) Rational design of novel antimicrobials: blocking purine salvage in a parasitic protozoan. *Biochemistry.* 37: 5344-8.
230. Spada S, Honegger A & Pluckthun A. (1998) Reproducing the natural evolution of protein structural features with the selectively infective phage (SIP) technology. The kink in the first strand of antibody kappa domains. *J Mol Biol.* 283:395-407.
231. Spector T, Berens RL & Marr JJ. (1982) Adenylosuccinate synthetase and adenylosuccinate lyase from *Trypanosoma cruzi*, Specificity studies with potential chemotherapeutic agents. *Biochem Pharmacol.* 31:225-9.
232. Spector T, Jones TE & Elion GB. (1979) Specificity of adenylosuccinate synthetase and adenylosuccinate lyase from *Leishmania donovani*. Selective amination of an antiprotozoal agent. *J Biol Chem.* 254:8422-6.
233. Spector, T., Jones, T. E., LaFon, S. W., Nelson, D. J., Berens, R. L. & Marr, J. J. (1984). Monophosphates of formycin B and allopurinol riboside. Interactions with leishmanial and mammalian succino-AMP synthetase and GMP reductase. *Biochem. Pharmacol.* 33, 1611-1617.
234. Srivastava, I. K., Rottenberg, H. & Vaidya, A. B. (1997) Atovaquone, a broad spectrum antiparasitic drug, collapses mitochondrial membrane potential in a malarial parasite. *J. Biol. Chem.* 272, 3961-3966.
235. Stadtman ER & Oliver CN. (1991) Metal-catalyzed oxidation of proteins. Physiological consequences. *J Biol Chem.* 266:2005-8.
236. Stadtman ER. (1993) Oxidation of free amino acids and amino acid residues in proteins by radiolysis and by metal-catalyzed reactions. *Annu Rev Biochem.* 62:797-821.
237. Stayton MM, Rudolph FB & Fromm HJ. (1983) Regulation, genetics, and properties of adenylosuccinate synthetase: a review. *Curr Top Cell Regul.* 22:103-41.
238. Stayton, M.M. & Fromm, H.J. (1979) Guanosine 5'-diphosphate-3'-diphosphate inhibition of adenylosuccinate synthetase. *J. Biol. Chem.* 254, 2579-2581

References

239. Stemmer WP. (1994) Rapid evolution of a protein in vitro by DNA shuffling. *Nature*. 370:389-91.
240. Sticht H, Gallert KC, Krauss G & Rosch P. (1997) Homology modeling of adenylosuccinate synthetase from *Saccharomyces cerevisiae* reveals a possible binding region for single-stranded ARS sequences. *J Biomol Struct Dyn*. 14: 667-75.
241. Stone, R.L., Zalkin, H. & Dixon, J.E. (1993) Expression, purification, and kinetic characterization of recombinant human adenylosuccinate lyase. *J. Biol. Chem.* 268, 19710-19716.
242. Sujay Subbayya (2002) Investigations on the *Plasmodium falciparum* human and chimeric hypoxanthine guanine phosphoribosyltransferase. PhD Thesis
243. Sujay Subbayya IN & Balaram H. (2000) Evidence for multiple active states of *Plasmodium falciparum* hypoxanthine-guanine-xanthine phosphoribosyltransferase. *Biochem Biophys Res Commun*. 279:433-7.
244. Sujay Subbayya IN & Balaram H. (2002) A point mutation at the subunit interface of hypoxanthine-guanine-xanthine phosphoribosyltransferase impairs activity: role of oligomerization in catalysis. *FEBS Lett*. 521:72-6.
245. Sujay Subbayya IN, Sukumaran S, Shivashankar K & Balaram H. (2000) Unusual substrate specificity of a chimeric hypoxanthine-guanine phosphoribosyltransferase containing segments from the *Plasmodium falciparum* and human enzymes. *Biochem Biophys Res Commun*. 272:596-602.
246. Suplick K, Akella R, Saul A & Vaidya AB. (1988) Molecular cloning and partial sequence of a 5.8 kilobase pair repetitive DNA from *Plasmodium falciparum*. *Mol Biochem Parasitol*. 30: 289-90.
247. Surolia N & Surolia A. (2001) Triclosan offers protection against blood stages of malaria by inhibiting enoyl-ACP reductase of *Plasmodium falciparum*. *Nat Med*. 7:167-73.
248. Takagi H, Hirai K, Wada M & Nakamori S. (2000) Enhanced thermostability of the single-Cys mutant subtilisin E under oxidizing conditions. *J Biochem (Tokyo)*. 128:585-9.
249. Takahashi N, Kakinuma H, Liu L, Nishi Y & Fujii I. (2001) In vitro abzyme evolution to optimize antibody recognition for catalysis. *Nat Biotechnol*. 19:563-7.
250. Tao H & Cornish VW. (2002) Milestones in directed enzyme evolution. *Curr Opin Chem Biol*. 6:858-64
251. Tarnopolsky MA, Parise G, Gibala MJ, Graham TE & Rush JW. (2001) Myoadenylate deaminase deficiency does not affect muscle anaplerosis during exhaustive exercise in humans. *J Physiol*. 533:881-9.
252. Tawfik DS & Griffiths AD. (1998) Man-made cell-like compartments for molecular evolution. *Nat Biotechnol*. 16:652-6.
253. Trager W & Jensen JB. (1976) Human malaria parasites in continuous culture. *Science*. 193:673-5

254. Triglia T, Peterson MG & Kemp DJ. A procedure for in vitro amplification of DNA segments that lie outside the boundaries of known sequences. *Nucleic Acids Res.* 1988 Aug 25;16(16):8186.
255. Triglia, T., Menting, J. G. T., Wilson, C. & Cowman, A. F. (1997) Mutations in dihydropteroate synthase are responsible for sulfone and sulfonamide resistance in *Plasmodium falciparum*. *Proc. Natl. Acad. Sci. USA* 94, 13944 -13949.
256. Triglia, T., Wellems, TE. & Kemp, DJ. (1992) Towards a high resolution map of the *Plasmodium falciparum* genome. *Parasitol. Today.* 8:225-9.
257. Tyagi AK & Cooney DA. (1980) Identification of the antimetabolite of L-alanosine, L-alanosyl-5-amino-4-imidazolecarboxylic acid ribonucleotide, in tumors and assessment of its inhibition of adenylosuccinate synthetase. *Cancer Res.* 40:4390-7.
258. van der Biezen EA, Sun J, Coleman MJ, Bibb MJ & Jones JD. (2000) Arabidopsis RelA/SpoT homologs implicate (p)ppGpp in plant signaling. *Proc Natl Acad Sci U S A.* 97:3747-52.
259. Van der Weyden MB & Kelly WN. (1974) Human adenylosuccinate synthetase. Partial purification, kinetic and regulatory properties of the enzyme from placenta. *J Biol Chem.* 249:7282-9.
260. Vatsis KP, Peng HM & Coon MJ. (2002) Replacement of active-site cysteine-436 by serine converts cytochrome P450 2B4 into an NADPH oxidase with negligible monooxygenase activity. *J Inorg Biochem.* 91:542-53.
261. Velanker SS, Gokhale RS, Ray SS, Gopal B, Parthasarathy S, Santi DV, Balaram P & Murthy MR (1999) Disulfide engineering at the dimer interface of *Lactobacillus casei* thymidylate synthase: crystal structure of the T155C/E188C/C244T mutant.. *Protein Sci.* 8:930-3.
262. Velanker, S. S., Ray, S. S., Gokhale, R. S., Suma, S., Balaram, H., Balaram, P. & Murthy, M. R. N. (1997) Triosephosphate isomerase from *Plasmodium falciparum*: the crystal structure provides insights into antimalarial drug design. *Structure* 5, 751-761.
263. Venter, J. C., Adams, M. D., Myers, E.W. et al., (2001) The sequence of the human genome. *Science* 291:1304-51.
264. Versees W, Decanniere K, Pelle R, Depoorter J, Brosens E, Parkin DW & Steyaert J. (2001) Structure and function of a novel purine specific nucleoside hydrolase from *Trypanosoma vivax*. *J Mol Biol.* 307: 1363-79.
265. Vos S, de Jersey J & Martin JL. (1997) Crystal structure of *Escherichia coli* xanthine phosphoribosyltransferase. *Biochemistry.* 36: 4125-34.
266. Vos S, Parry RJ, Burns MR, de Jersey J & Martin JL. (1998) Structures of free and complexed forms of *Escherichia coli* xanthine-guanine phosphoribosyltransferase. *J Mol Biol.* 282: 875-89.
267. Walters EW, Lee SF, Niderman T, Bernasconi P, Subramanian MV & Siehl DL. (1997) Adenylosuccinate synthetase from maize. Purification, properties, and mechanism of inhibition by 5'-phosphohydantocidin. *Plant Physiol.* 114:549-55.

References

268. Wang W, Gorrell A, Honzatko RB & Fromm HJ. (1997a) A study of *Escherichia coli* adenylosuccinate synthetase association states and the interface residues of the homodimer. *J Biol Chem.* 272:7078-84.
269. Wang, W., Hou, Z., Honzatko, R. B. & Fromm, H. J. (1997b). Relationship of conserved residues in the IMP binding site to substrate recognition and catalysis in *Escherichia coli* adenylosuccinate synthetase. *J. Biol. Chem.* 272, 16911-16916.
270. Warhurst, D. C. (1998) Antimalarial drug discovery: development of inhibitors of dihydrofolate reductase active in drug resistance *Drug Disc. Today* 3, 538-546.
271. Waterkeyn JG, Crabb BS & Cowman AF. (1999) Transfection of the human malaria parasite *Plasmodium falciparum*. *Int J Parasitol.* 29: 945-55.
272. Waters AP, Thomas AW, van Dijk MR & Janse CJ. (1997) Transfection of malaria parasites. *Methods.* 13: 134-47.
273. Weber JL. (1987) Analysis of sequences from the extremely A + T-rich genome of *Plasmodium falciparum*. *Gene.* 52:103-9.
274. Webster H. K. & Whaun J. M. (1982) Antimalarial properties of bredinin. *J. Clin. Invest.* 70, 461-469.
275. Webster HK & Whaun JM. (1981) Purine metabolism during continuous erythrocyte culture of human malaria parasites (*P. falciparum*). *Prog Clin Biol Res.* 55:557-73.
276. Webster HK, Whaun JM, Walker MD & Bean TL. (1984) Synthesis of adenosine nucleotides from hypoxanthine by human malaria parasites (*Plasmodium falciparum*) in continuous erythrocyte culture: inhibition by hadacidin but not alanosine. *Biochem Pharmacol.* 33:1555-7.
277. Wellems, T. E. & Plowe, C. V. (2001) Chloroquine-resistant malaria. *J Infect Dis.* 184:770-6
278. White NJ & Olliaro P. (1998) Artemisinin and derivatives in the treatment of uncomplicated malaria. *Med Trop .* 58: 54-6.
279. WHO (1999) The World Health Report. Making a difference. *World Health Organisation,*
280. Wiesmuller L, Wittbrodt J, Noegel AA & Schleicher M. (1991) Purification and cDNA-derived sequence of adenylosuccinate synthetase from *Dictyostelium discoideum*. *J Biol Chem.* 266:2480-5
281. Wilairatana P, Krudsood S, Treeprasertsuk S, Chalermrut K & Looareesuwan S. (2002) The future outlook of antimalarial drugs and recent work on the treatment of malaria. *Arch Med Res.* 33: 416-21.
282. Wilson RJ, Denny PW, Preiser PR, Rangachari K, Roberts K, Roy A, Whyte A, Strath M, Moore DJ, Moore PW & Williamson DH. (1996) Complete gene map of the plastid-like DNA of the malaria parasite *Plasmodium falciparum*. *J Mol Biol.* 261:155-72.
283. Wilson, R. J. & Williamson, D. H. (1997) Extrachromosomal DNA in the Apicomplexa. *Microbiol. Mol. Biol. Rev.* 61, 1-16.

284. Wolfe SA & Smith JM. (1988) Nucleotide sequence and analysis of the purA gene encoding adenylosuccinate synthetase of *Escherichia coli* K12. *J Biol Chem.* 263:19147-53.
285. Xiang B & Markham GD. (1997) Probing the mechanism of inosine monophosphate dehydrogenase with kinetic isotope effects and NMR determination of the hydride transfer stereospecificity. *Arch Biochem Biophys.* 348:378-82.
286. Xiang B, Taylor JC & Markham GD. (1996) Monovalent cation activation and kinetic mechanism of inosine 5'-monophosphate dehydrogenase. *J Biol Chem.* 271:1435-40.
287. Xu Y & Grubmeyer C. (1998) Catalysis in human hypoxanthine-guanine phosphoribosyltransferase: Asp 137 acts as a general acid/base. *Biochemistry.* 37:4114-24.
288. Xu Y, Eads J, Sacchettini JC & Grubmeyer C. (1997) Kinetic mechanism of human hypoxanthine-guanine phosphoribosyltransferase: rapid phosphoribosyl transfer chemistry. *Biochemistry.* 36:3700-12.
289. Yano T, Oue S & Kagamiyama H. (1998) Directed evolution of an aspartate aminotransferase with new substrate specificities. *Proc Natl Acad Sci U S A.* 95:5511-5.
290. Yeh JI & Claiborne A. (2002) Crystal structures of oxidized and reduced forms of NADH peroxidase. *Methods Enzymol.* 353:44-54.
291. Yoshioka, A., Tanaka, S., Hiraoka, O., Koyama, Y., Hirota, Y., Ayusawa, D., Seno, T., Garrett, C. & Wataya, Y. (1987) Deoxyribonucleoside triphosphate imbalance. 5-Fluorodeoxyuridine-induced DNA double strand breaks in mouse FM3A cells and the mechanism of cell death. *J. Biol. Chem.* 262, 8235-41.
292. Yuan L, Wu CS, Craig SP 3rd, Liu AF & Wang CC. (1993) Comparing the human and schistosomal hypoxanthine-guanine phosphoribosyltransferases by circular dichroism. *Biochim Biophys Acta.* 1162:10-6.
293. Yuvaniyama J, Chitnumsub P, Kamchonwongpaisan S, Vanichtanankul J, Sirawaraporn W, Taylor P, Walkinshaw MD & Yuthavong Y. (2003) Insights into antifolate resistance from malarial DHFR-TS structures. *Nat Struct Biol.* 10:357-65.
294. Zeidler R, Hobert O, Johannes L, Faulhammer H & Krauss G. (1993) Characterization of two novel single-stranded DNA-specific autonomously replicating sequence-binding proteins from *Saccharomyces cerevisiae*, one of which is adenylosuccinate synthetase. *J Biol Chem.* 268:20191-7.
295. Zhang JH, Dawes G & Stemmer WP. (1997) Directed evolution of a fucosidase from a galactosidase by DNA shuffling and screening. *Proc Natl Acad Sci U S A.* 94:4504-9.
296. Zhao H & Arnold FH. (1999) Directed evolution converts subtilisin E into a functional equivalent of thermitase. *Protein Eng.* 12:47-53.

References

297. Zhao H, Giver L, Shao Z, Affholter JA & Arnold FH. (1998) Molecular evolution by staggered extension process (StEP) in vitro recombination. *Nat Biotechnol.* 16:258-61.
298. Zhou YH, Zhang XP & Ebright RH. (1991) Random mutagenesis of gene-sized DNA molecules by use of PCR with Taq DNA polymerase. *Nucleic Acids Res.* 19:6052.